Department of Electrical Engineering
Technion – Israel Institute of Technology

MICROWAVES – #46216

LECTURE NOTES

based upon lectures delivered by

Prof. L. Schächter

October 2009

CONTENTS

Chapter 1: Transmission Lines

In this chapter we shall first recapitulate some of the topics learned in the framework of the course ``Waves and Distributed Systems'' and then we shall extend the analysis to topics that are of importance to microwave devices. But first a few examples:
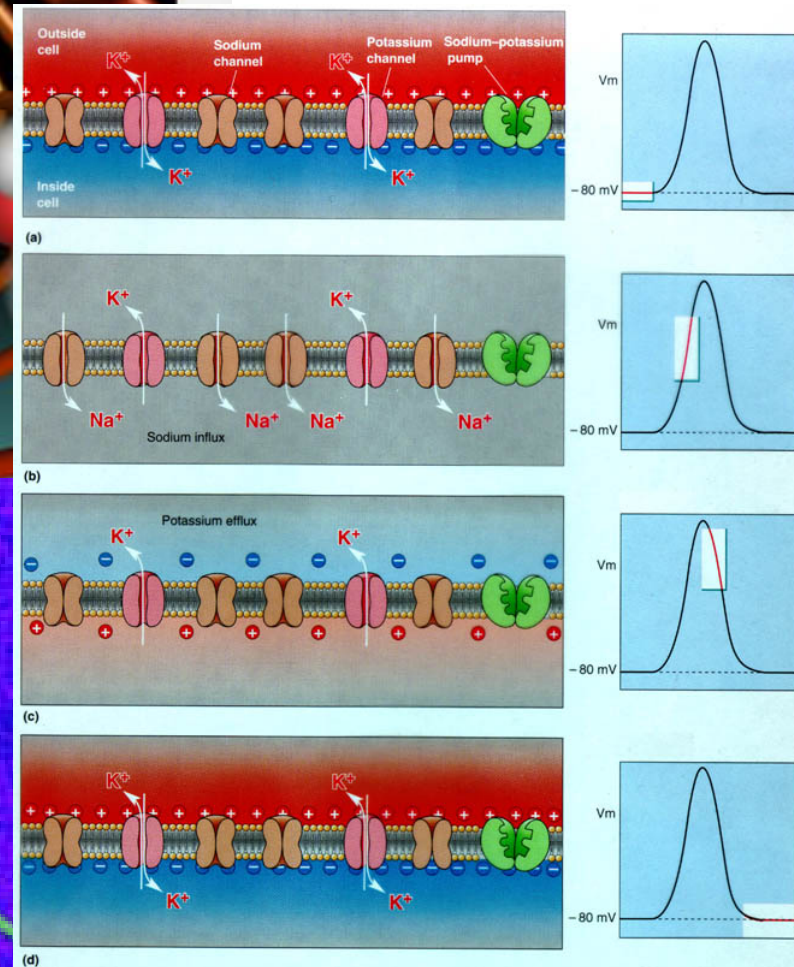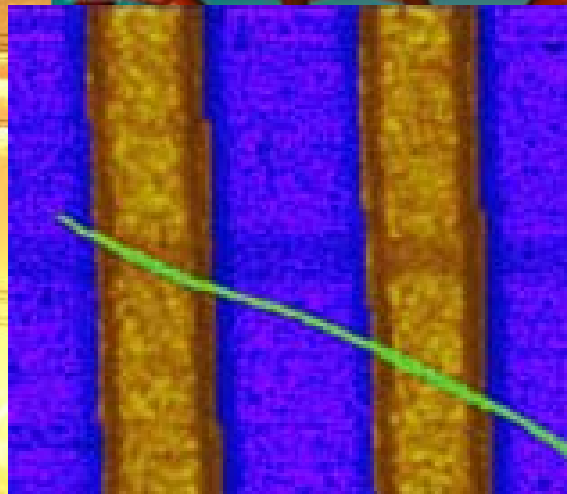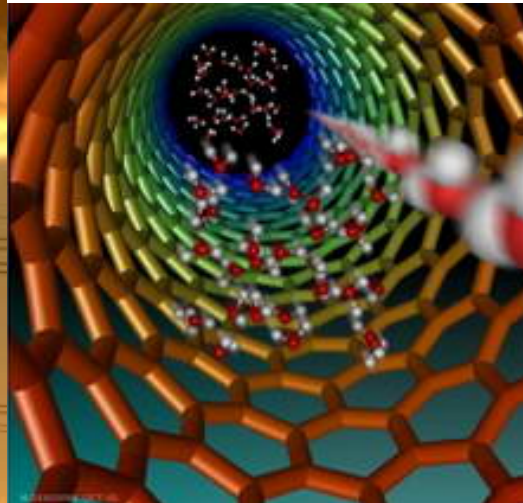
1.1 Simple Model

First we shall examine the propagation of an electromagnetic wave between two parallel plates located at a distance a one of the other as illustrated in the figure. The principal assumptions of this simple model are as follows:

1. No variation in the x direction i.e. $\partial_x = 0$.

2. Steady state e.g. $\exp(j\omega t)$.

3. The distance between the two plates (a) is very small so that even if there is any (field) variation in the y direction, it is negligible on the scale of the wavelength ($a \ll \lambda$)

$$\left|\frac{\partial}{\partial y}\right| \ll \left|\frac{\partial}{\partial z}\right| \Rightarrow \left|\frac{\partial}{\partial y}\right| \sim 0. \tag{1.1.1}$$

4. The constitutive relations of the vacuum:
   $\vec{D} = \varepsilon_0 \vec{E}$, $\vec{B} = \mu_0 \vec{H}$ where $\mu_0 = 4\pi \times 10^{-7}$ [Henry/meter] and
   $\varepsilon_0 = 8.85 \times 10^{-12}$ [Farad/Meter].

Based on the assumptions above, ME may be simplified.

2
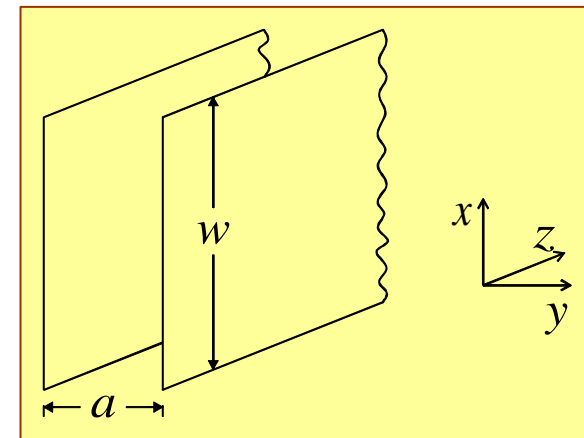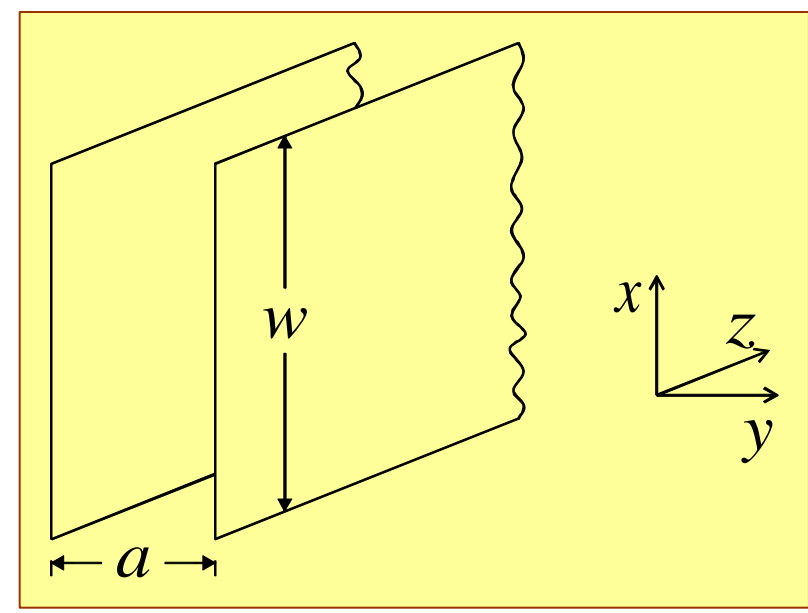
(a) Gauss' law $\vec{\nabla}\cdot\vec{E}=0 \quad \rightsquigarrow \quad \partial_z E_z = 0 \Rightarrow E_z = const.$ we conclude that E_z is uniform between the two plates. Imposing next the boundary conditions on the two plates

$$E_z(y=0)=0 \qquad E_z(y=a)=0 \tag{1.1.2}$$

which means that the longitudinal electric field vanishes $(E_z \equiv 0)$.

(b) In a similar way the magnetic induction satisfies $\vec{\nabla}\cdot\vec{B}=0$ and it may be shown that the longitudinal component of the magnetic induction vanishes $(B_z = 0)$.

(c) Faraday's equation reads $\nabla \times \vec{E} = -j\omega\vec{B}$ thus explicitly

$$\begin{vmatrix} 1_x & 1_y & 1_z \\ 0 & 0 & \partial_z \\ E_x & E_y & 0 \end{vmatrix} = -j\omega\vec{B} \Rightarrow \begin{matrix} 1_x & : & -\partial_z E_y & = & -j\omega B_x \\ 1_y & : & \partial_z E_x & = & -j\omega B_y \\ 1_z & : & 0 & = & 0 \end{matrix} \tag{1.1.3}$$

There is no variation in the y direction therefore since $E_x = 0$ for both $y = 0$ and $y = a$, as in the case of E_z, we have $E_x \equiv 0$ therefore $B_y = 0$ thus

$$\boxed{\frac{\partial}{\partial z}E_y = j\omega\mu_o H_x.} \tag{1.1.4}$$

(d) Ampere's law reads $\vec{\nabla} \times \vec{H} = j\omega \vec{D}$, or explicitly taking advantage of the vanishing components we get

$$\begin{vmatrix} \vec{1}_x & \vec{1}_y & \vec{1}_z \\ 0 & 0 & \partial_z \\ H_x & 0 & 0 \end{vmatrix} = j\omega\vec{D} \Rightarrow \begin{array}{lll} \vec{1}_x & : \ 0 & = \ 0 \\ \vec{1}_y & : \ \partial_z H_x & = \ j\omega D_y \\ \vec{1}_z & : \ 0 & = \ 0 \end{array} \quad (1.1.5)$$

hence

$$\boxed{\frac{\partial}{\partial z}H_x = j\omega\varepsilon_o E_y.} \tag{1.1.6}$$

From these two equations [(1.1.4) and (1.1.6)] it can be readily seen that we obtain the **wave-equation** for each one of the components:

$$\left. \begin{array}{l} \dfrac{\partial}{\partial z}H_x = j\omega\varepsilon_o E_y \\[2mm] \dfrac{\partial}{\partial z}E_y = j\omega\mu_o H_x \end{array} \right\} \quad \Rightarrow \quad \boxed{\left[\frac{\partial^2}{\partial z^2} + \frac{\omega^2}{c^2}\right]E_y = 0} \tag{1.1.7}$$

which has a solution of the form

$$E_y = A\exp\left(-j\frac{\omega}{c}z\right) + B\exp\left(j\frac{\omega}{c}z\right) \tag{1.1.8}$$
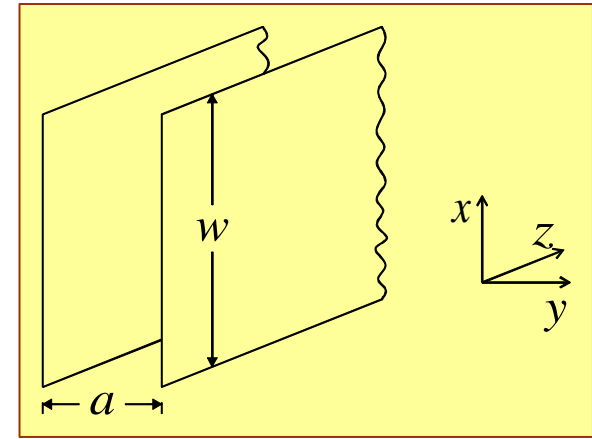
It is convenient at this point to introduce the notation in terms of voltage and current. The voltage can be defined since $\oint \vec{E} \cdot d\vec{\ell} = 0$; it reads

$$V(z) = -E_y(z)a. \qquad (1.1.9)$$

In order to define the current we recall that based on the boundary conditions we have $\vec{n} \times (\vec{H}_1 - \vec{H}_2) = \vec{K}$ where $\vec{K}$ is the surface current. Consequently, denoting by w the height of the metallic plates, the local current is $I = K_z w$ or

$$I(z) = H_x(z)w. \qquad (1.1.10)$$

Based on these two equations [(1.1.9)–(1.1.10)] it is possible to write

$$\frac{\partial}{\partial z}E_y = j\omega\mu_o H_x \Rightarrow \frac{\partial}{\partial z}\left[-\frac{V}{a}\right] = j\omega\mu_o \frac{I}{w} \Rightarrow \frac{\partial}{\partial z}V = -j\omega\left[\mu_o \frac{a}{w}\right]I$$

$$\frac{\partial}{\partial z}H_x = j\omega\varepsilon_o E_y \Rightarrow \frac{\partial}{\partial z}\left[\frac{I}{w}\right] = j\omega\varepsilon_o\left[-\frac{V}{a}\right] \Rightarrow \frac{\partial}{\partial z}I = -j\omega\left[\varepsilon_o \frac{w}{a}\right]V$$

$$(1.1.11)$$

The right hand side in both lines of (1.1.11) represent the so-called **transmission line equation** also known as **telegraph equations**.
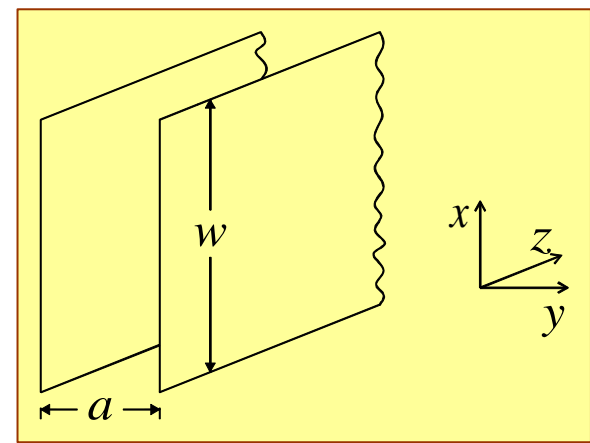
$$\boxed{\begin{aligned} \frac{d}{dz}V(z) &= -j\omega L\, I(z) \\ \frac{d}{dz}I(z) &= -j\omega C\, V(z) \end{aligned}}$$

(1.1.12)
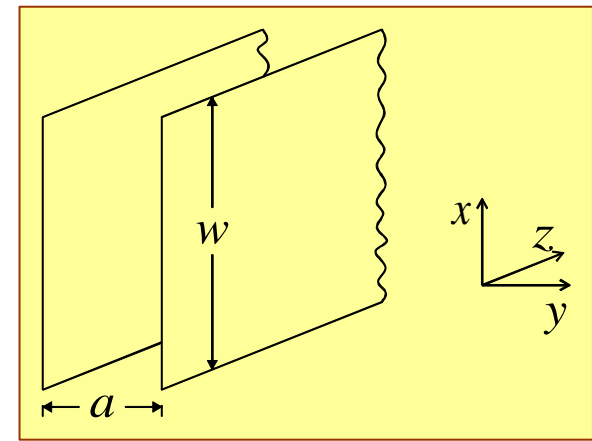
C being the **capacitance per unit length** whereas L is the **inductance per unit length**; $L = \mu_o \dfrac{a}{w}$ and $C = \varepsilon_o \dfrac{w}{a}$. As expected, these two equations lead also to the wave equation

$$\left. \begin{aligned} \frac{dV}{dz} &= -j\omega L\, I(z) \\ \frac{dI}{dz} &= -j\omega C\, V(z) \end{aligned} \right\} \qquad \left[\frac{d^2}{dz^2} + \beta^2\right]V(z) = 0$$

(1.1.13)

$$\boxed{\beta = \omega\sqrt{LC}}$$

The general solution is $V(z) = Ae^{-j\beta z} + Be^{j\beta z}$ and correspondingly, the expression for the current is given by

$$I(z) = \frac{-1}{j\omega L}\frac{dV}{dz} = \frac{\beta}{\omega L}\left[Ae^{-j\beta z} - Be^{j\beta z}\right]$$

(1.1.14)

defining the characteristic impedance $Z_c^{-1} = \dfrac{\beta}{\omega L} = \dfrac{\omega\sqrt{LC}}{\omega L}$ or $\boxed{Z_c \equiv \sqrt{\dfrac{L}{C}},}$ we get

6

$$I(z) = \frac{1}{Z_c}[Ae^{-j\beta z} - Be^{+j\beta z}].$$

(1.1.15)

In the *specific* case under consideration

$$Z_c = \sqrt{\frac{\mu_o \dfrac{a}{w}}{\varepsilon_o \dfrac{w}{a}}} = \eta_o \frac{a}{w} \quad , \quad \beta = \omega\sqrt{LC} = \frac{\omega}{c}.$$

(1.1.16)

1.2 Coaxial Transmission Line

As indicated in the previous case, two parameters are to be determined: the capacitance per unit length (C) and the inductance per unit length (L). According to (1.1.11) these two parameters can be determined in static conditions. We determine next the **capacitance per unit length** of a coaxial structure. For this purpose it is assumed that on the inner wire a voltage V_o is applied, whereas the outer cylinder is grounded.

$2R_{int}$

$2R_{ext}$
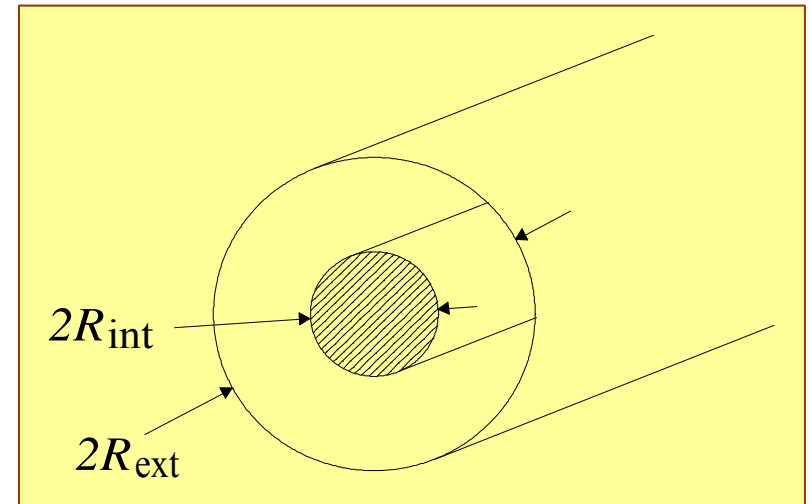
Consequently, the potential is given by

$$\varphi(r) = V_o \frac{\ln(r / R_{ext})}{\ln(R_{int} / R_{ext})}.$$ (1.2.1)

and the corresponding electric field associated with this potential is

$$E_r = -\frac{\partial \varphi}{\partial r} = -V_o \frac{1}{r} \frac{1}{\ln(R_{int} / R_{ext})}.$$ (1.2.2)

The charge per unit surface at $r = R_{ext}$ is calculated based on $\vec{n} \cdot (\vec{D}_1 - \vec{D}_2) = \rho_s$ and it is given by

$$\rho_s = \varepsilon_0 \frac{V_0}{R_{ext}} \frac{1}{\ln(R_{ext} / R_{int})}.$$ (1.2.3)

Based on this result, the charge per unit length (Δ_z) may be expressed as

$$\frac{Q}{\Delta_z} = \rho_s 2\pi R_{ext} = \varepsilon_0 \frac{V_o}{R_{ext}} \frac{1}{\ln\left(\dfrac{R_{ext}}{R_{int}}\right)} 2\pi R_{ext} = \frac{\varepsilon_o V_o 2\pi}{\ln(R_{ext}/R_{int})}.$$ (1.2.4)

Consequently, the capacitance per unit length is given by

8

$$C \equiv \frac{Q/\Delta_z}{V_o} = \frac{2\pi\varepsilon_o}{\ln(R_{ext}/R_{int})}. \qquad (1.2.5)$$

In a similar way, we shall calculate the **inductance per unit length**. Assuming that the inner wire carries a current I, based on Ampere law the azimuthal magnetic field is

$$H_\phi(r) = \frac{I_o}{2\pi r}. \qquad (1.2.6)$$

With this expression for the magnetic field, we can calculate the magnetic flux. It is given by

$$\Phi = \mu_o \Delta_z \int_{R_{int}}^{R_{ext}} dr H_\phi(r) = \mu_o \Delta_z \frac{I}{2\pi} \ln \frac{R_{ext}}{R_{int}}. \qquad (1.2.7)$$

The inductance per unit length Δ_z is

$$L \equiv \frac{\Phi/\Delta_z}{I} = \frac{\mu_o}{2\pi} \ln \left(\frac{R_{ext}}{R_{int}} \right). \qquad (1.2.8)$$

9
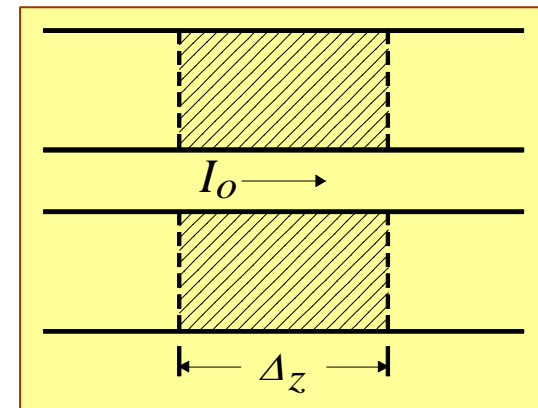
To summarize the parameters of a coaxial transmission line

$$\boxed{\begin{aligned} Z_c &= \sqrt{\frac{L}{C}} = \eta_o \frac{1}{2\pi} \ln\left(\frac{R_{ext}}{R_{int}}\right) \\ \beta &= \frac{\omega}{c} \end{aligned}}$$

(1.2.9)

Exercise 1.1: Determine Z_c and β for a coaxial line filled with a material (ε_r, μ_r)?

1.3 Low Loss System

Based on Ampere's law we obtained

$$\vec{\nabla} \times \vec{H} = j\omega\varepsilon_o\varepsilon\vec{E} \rightsquigarrow \frac{d}{dz}I(z) = -j\omega CV(z),$$
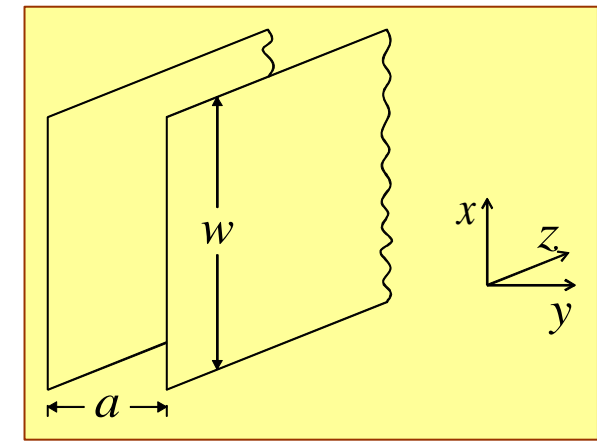
$$(1.3.1)$$

where we assumed a line without dielectric (ε_r) and Ohm (σ) loss. In the case of dielectric loss we have

$$\varepsilon_r = \varepsilon' - j\varepsilon'' \qquad (1.3.2)$$

or in our case

$$j\omega C \rightarrow j\omega C + G \equiv Y. \qquad (1.3.3)$$

In a similar way based on Faraday's law

$$\vec{\nabla} \times \vec{E} = -j\omega\mu_o\mu_r\vec{H} \Rightarrow \frac{d}{dz}V(z) = -j\omega LI(z) \qquad (1.3.4)$$

and the magnetic losses

$$\mu_r = \mu_r' - j\mu_r''$$

allows us to extend the definition according to

$$j\omega L \rightsquigarrow j\omega L + R \equiv Z \qquad (1.3.5)$$

hence the equations

$$\frac{d}{dz}I(z) = -YV(z)$$

$$\frac{d}{dz}V(z) = -ZI(z)$$

(1.3.6)
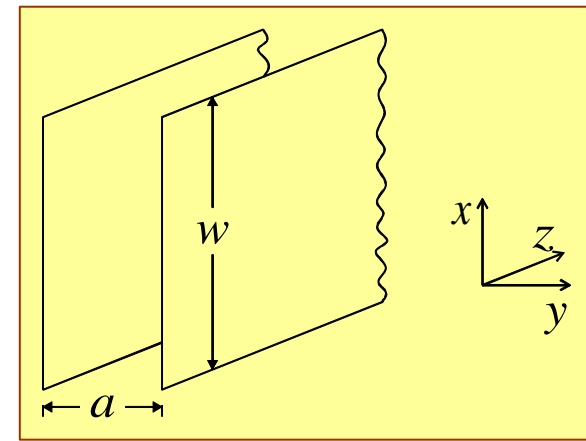
may be conceived as a generalization of the transmission line equations in the presence of loss. The characteristic impedance for small loss line is

$$Z_c = \sqrt{\frac{Z}{Y}} \simeq \sqrt{\frac{L}{C}}\left[1 + j\left(\frac{G}{2\omega C} - \frac{R}{2\omega L}\right)\right]$$

(1.3.7)

and the wave number

$$\gamma = \alpha + j\beta$$

$$\alpha \simeq \frac{R}{2Z_o} + \frac{GZ_o}{2}$$

(1.3.8)

$$\beta \simeq \omega\sqrt{LC}\left[1 - \frac{RG}{4\omega^2 LC} + \frac{G^2}{8\omega^2 C^2} + \frac{R^2}{8\omega^2 L^2}\right]$$

Exercise 1.2: Prove the relations in Eq. (1.3.8).

1.4 Generalization of the Transmission Line Equations
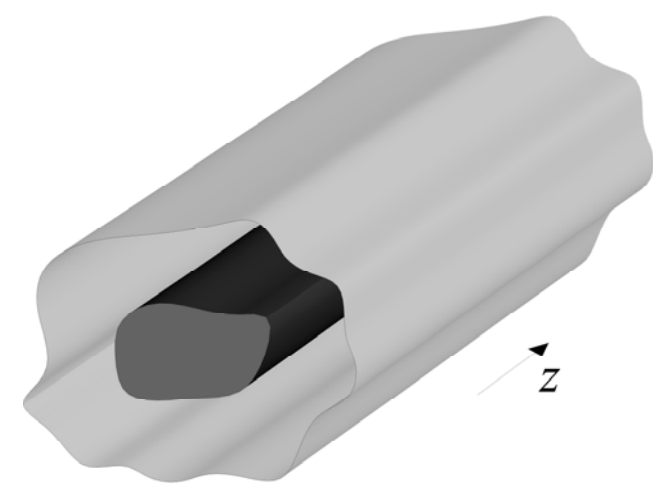
The fundamental assumptions of the analysis are:

(i) TEM, (ii) the wave propagates in the z direction, (iii) we distinguish between longitudinal (z) and transverse ($\perp$) components $\vec{\nabla} = \vec{\nabla}_\perp + \dfrac{\partial}{\partial z}\vec{1}_z$.

From Faraday law, $\vec{\nabla} \times \vec{E} = -j\omega\mu_o\mu_r\vec{H}$, we obtain

$$\begin{vmatrix} 1_x & 1_y & 1_z \\ \partial_x & \partial_y & \partial_z \\ E_x & E_y & 0 \end{vmatrix} = \begin{matrix} \vec{1}_x(-) & \partial_z E_y \\ \vec{1}_y & \partial_z E_x \\ \vec{1}_z & \partial_x E_y - \partial_y E_x \end{matrix}$$

(1.4.1)

thus

$$\left.\begin{array}{ll} 1_x: & -\partial_z E_y = -j\omega\mu_o\mu_r H_x \\ 1_y: & +\partial_z E_x = -j\omega\mu_o\mu_r H_y \\ 1_z: & \partial_x E_y - \partial_y E_x = 0 \end{array}\right\} \qquad \begin{array}{ll} \vec{1}_\perp: & \vec{1}_z \times \dfrac{\partial \vec{E}_\perp}{\partial z} = -j\omega\mu_o\mu_r\vec{H}_\perp \\ \\ \vec{1}_z: & \vec{\nabla}_\perp \times \vec{E}_\perp = 0. \end{array}$$

(1.4.2)
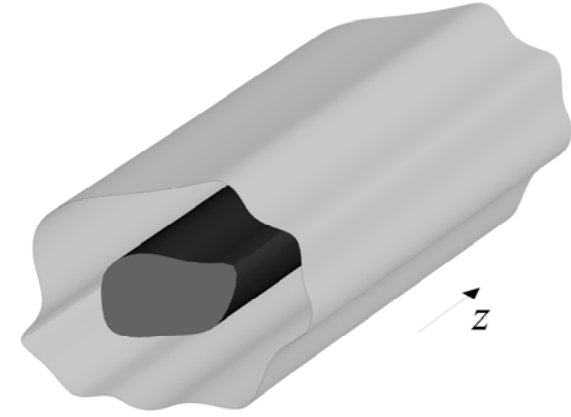
In a similar way, from Ampere's law we have

$$\vec{\nabla} \times \vec{H} = +j\omega\varepsilon_o\varepsilon_r\vec{E} \Rightarrow \begin{cases} \vec{1}_\perp : \vec{1}_z \times \dfrac{\partial \vec{H}_\perp}{\partial z} &=& j\omega\varepsilon_o\varepsilon_r\vec{E}_\perp \\[2mm] \vec{1}_z : \vec{\nabla}_\perp \times \vec{H}_\perp &=& 0. \end{cases} \qquad (1.4.3)$$

From the two curl equations

$$\begin{array}{lclclcl} \vec{\nabla}_\perp \times \vec{E}_\perp &=& 0 &\Rightarrow& \vec{E}_\perp = g(z)\nabla_\perp\varphi(x,y) &\Rightarrow& \nabla_\perp^2\varphi = 0 \\[2mm] \vec{\nabla}_\perp \times \vec{H}_\perp &=& 0 &\Rightarrow& \vec{H}_\perp = h(z)\nabla_\perp\psi(x,y) &\Rightarrow& \nabla_\perp^2\psi = 0, \end{array} \qquad (1.4.4)$$

we conclude that the *transverse variations* of the transverse field components are determined by **2D Laplace equation** justifying the use of DC quantities adopted above (capacitance and inductance per unit length). From the other two equations we get the wave equation

$$\frac{\partial}{\partial z}\left[\vec{1}_z \times \frac{\partial \vec{E}_\perp}{\partial z} \right] = -j\omega\mu_o\mu_r \frac{\partial \vec{H}_\perp}{\partial z}$$

$$\vec{1}_z \times \left[\vec{1}_z \times \frac{\partial^2 \vec{E}_\perp}{\partial z^2} \right] = -j\omega\mu_o\mu_r \left[\vec{1}_z \times \frac{\partial \vec{H}_\perp}{\partial z} \right] = -j\omega\mu_o\mu_r [j\omega\varepsilon_o\varepsilon_r\vec{E}_\perp],$$

$$(1.4.5)$$

or explicitly

$$\left[\frac{\partial^2}{\partial z^2}+\frac{\omega^2}{c^2}\mu_r\varepsilon_r\right]\vec{E}_\perp=0. \qquad (1.4.6)$$
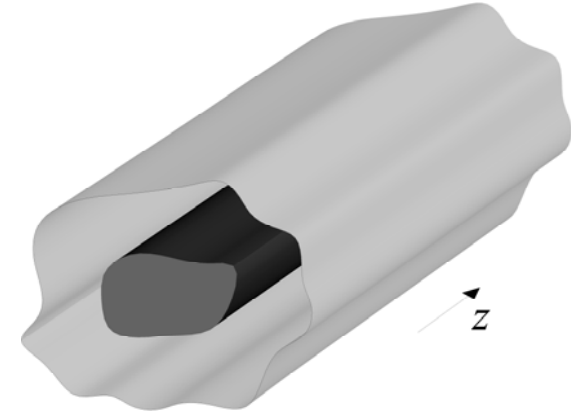
The last equation determines the dynamics of $g(z)$ [see (1.4.4)] and the solution has the form $g(z)=e^{-j\beta z}$ where $\beta=(\omega/c)\sqrt{\varepsilon_r\mu_r}$. Note that

$$\vec{1}_z\times\frac{\partial\vec{E}_\perp}{\partial z}=-j\omega\mu_o\mu_r\vec{H}_\perp \Rightarrow \vec{1}_z\times\vec{E}_\perp=\sqrt{\frac{\mu_o}{\varepsilon_o}\frac{\mu_r}{\varepsilon_r}}\vec{H}_\perp$$

$$\vec{1}_z\times\frac{\partial\vec{H}_\perp}{\partial z}=j\omega\varepsilon_o\varepsilon_r\vec{E}_\perp \Rightarrow \vec{1}_z\times\vec{H}_\perp=-\sqrt{\frac{\varepsilon_o}{\mu_o}\frac{\varepsilon_r}{\mu_r}}\vec{E}_\perp$$

$$(1.4.7)$$

As in the previous two cases we shall see next how the electric parameters can be calculated in the general case and for the sake of simplicity we shall assume that the medium has uniform transverse and longitudinal properties. The electric field in the entire space is given by $\vec{E}_\perp = -(\nabla_\perp \varphi)e^{-j\beta z}$ whereas the magnetic field is

$$\vec{H}_\perp = \sqrt{\frac{\varepsilon_o \, \varepsilon_r}{\mu_o \, \mu_r}}(-\vec{1}_z \times \nabla_\perp \varphi)e^{-j\beta z}. \qquad (1.4.8)$$

Note that associated to this electric field, one can define the voltage

$$V_o = -\int_{s_1}^{s_2} \vec{E}_\perp \cdot d\vec{\ell} = \int_{s_1}^{s_2} \nabla_\perp \varphi \cdot d\vec{\ell} = \int_{s_1}^{s_2} d\varphi \qquad (1.4.9)$$

such that $V(z) = V_o e^{-j\beta z}$. On the two (ideal) conductors the electric field generates a surface charge given by

$$\rho_s = \varepsilon_o \varepsilon_r \vec{n} \cdot \vec{E}_\perp, \qquad (1.4.10)$$

therefore the charge per unit length is

$$\frac{Q}{\Delta_z} = \oint dl \, \rho_s = \oint dl \, \varepsilon_o \varepsilon_r (\vec{n} \cdot \vec{E}_\perp). \qquad (1.4.11)$$

Since by virtue of linearity of Maxwell's equations

16
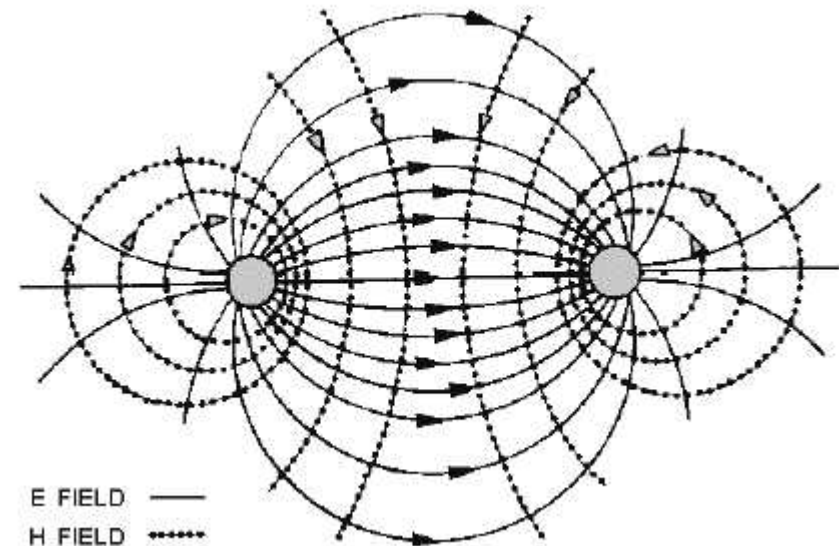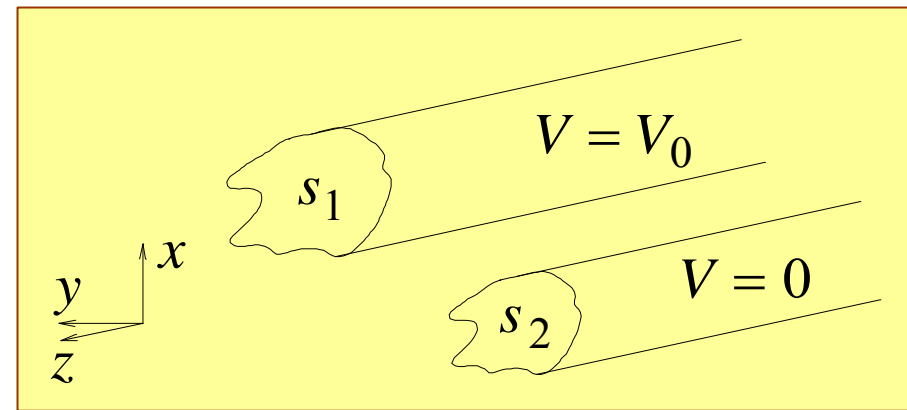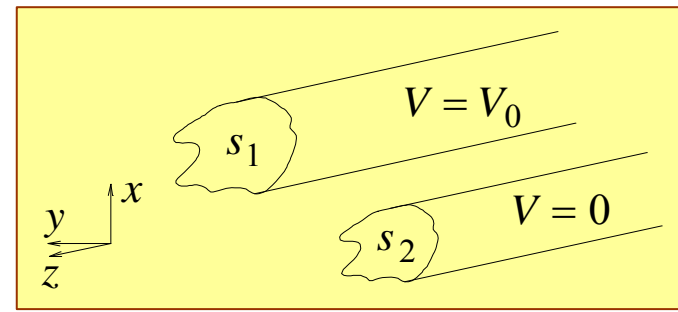
E FIELD ——
H FIELD ┄┄┄

the charge per unit length is proportional to the applied

voltage $\dfrac{Q}{\Delta_z} = CV_0$ we get

$$C = \varepsilon_o \varepsilon_r \frac{1}{V_0} \oint d\ell (\vec{n} \cdot \vec{E}_\perp). \tag{1.4.12}$$

In a similar way, the magnetic field generates on the metallic electrode (wire) a surface current given by

$$\vec{J}_s = \vec{n} \times \vec{H}_\perp. \tag{1.4.13}$$

Since it was shown that $\vec{H}_\perp = \sqrt{\dfrac{\varepsilon_o \varepsilon_r}{\mu_o \mu_r}} \, \vec{1}_z \times \vec{E}_\perp$ we conclude that

$$\vec{J}_s = \vec{n} \times \vec{H}_\perp = \vec{n} \times [\vec{1}_z \times \vec{E}_\perp] \sqrt{\frac{\varepsilon_o \varepsilon_r}{\mu_o \mu_r}} = \frac{\varepsilon_o \varepsilon_r}{\mu_o \mu_r} (\vec{n} \cdot \vec{E}_\perp) \vec{1}_z \tag{1.4.14}$$

hence the total current is

$$I_0 = \oint \vec{J}_s \cdot \vec{1}_z \, dl = \sqrt{\frac{\varepsilon_o \varepsilon_r}{\mu_o \mu_r}} \oint dl \left(\vec{n} \cdot \vec{E}_\perp \right) \tag{1.4.15}$$

At this point rather than calculating the inductance per unit length we combine the previous result for the charge per unit length and (1.4.15) the result being
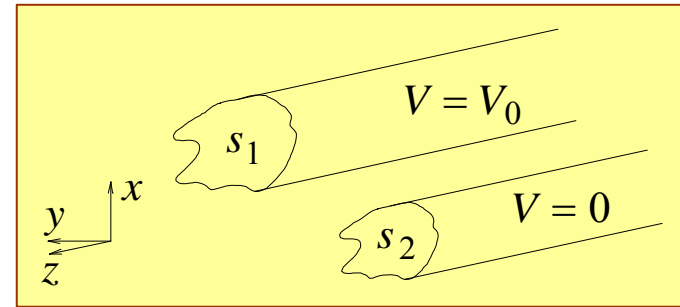
$$\frac{I_o}{Q/\Delta_z} = \frac{\sqrt{\dfrac{\varepsilon_o \varepsilon_r}{\mu_o \mu_r}} \oint dl\, \vec{n} \cdot \vec{E}_\perp}{\varepsilon_o \varepsilon_r \oint dl\, \vec{n} \cdot \vec{E}_\perp} = \frac{c}{\sqrt{\mu_r \varepsilon_r}}. \tag{1.4.16}$$

However, having established this relation between the current and the charge per unit length we may use again the linearity of Maxwell's equations and express $Q/\Delta_z = CV_0$. Substituting in Eq. (1.4.16) we get

$$\frac{I_0}{CV_o} = \frac{c}{\sqrt{\mu_r \varepsilon_r}} \tag{1.4.17}$$

but by definition

$$\frac{V_0}{I_0} = Z_c, \tag{1.4.18}$$

which finally implies that

$$\boxed{\frac{1}{CZ_c} = \frac{c}{\sqrt{\mu_r \varepsilon_r}}.}$$

This result leads to a very important conclusion namely, **in a transmission line of** *uniform* **electromagnetic properties it is sufficient to calculate the capacitance per unit length.** Bearing in mind that $Z_c = \sqrt{L/C}$ we find that once C is established,

$$L = \frac{\mu_r \varepsilon_r}{C c^2}. \qquad (1.4.19)$$
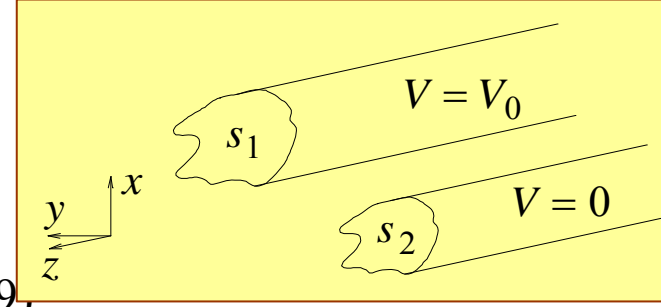
It is important to re-emphasize that this relation is valid only if the electromagnetic properties (ε_r, μ_r) are *uniform* over the cross-section.

Exercise 1.3: Calculate the capacitance per unit length of two wires of radius R which are at a distance $d > 2R$ apart.

Another quantity that warrants consideration is the **average power**

$$P = \frac{1}{2} \mathrm{Re} \left\{ \int dx dy \left(\vec{E}_\perp \times \vec{H}_\perp^* \right) \cdot \vec{1}_z \right\} = \frac{1}{2} \mathrm{Re} \left\{ \int dx dy \left[\vec{E}_\perp \times \left(\vec{1}_z \times \vec{E}_\perp^* \right) \right] \cdot \vec{1}_z \right\} \sqrt{\frac{\varepsilon_o \varepsilon_r}{\mu_o \mu_r}}$$

$$= \frac{1}{2} \mathrm{Re} \left\{ \int dx dy \, \vec{E}_\perp \cdot \vec{E}_\perp^* \right\} \sqrt{\frac{\varepsilon_o \varepsilon_r}{\mu_o \mu_r}} = \frac{2}{\varepsilon_o \varepsilon_r} \sqrt{\frac{\varepsilon_o \varepsilon_r}{\mu_o \mu_r}} \left[\frac{1}{4} \int dx dy \, \varepsilon_o \varepsilon_r \vec{E}_\perp \cdot \vec{E}_\perp^* \right] \qquad (1.4.20)$$

$$= \frac{2}{\sqrt{\varepsilon_o \mu_o \varepsilon_r \mu_r}} W_e = \frac{c}{\sqrt{\varepsilon_r \mu_r}} [W_e + W_m].$$

19

Exercise 1.4: In the last expression we used the fact that $W_e = W_m$ -- prove it.

Exercise 1.5: Show that the power can be expressed as $P = \dfrac{1}{2} Z_c \mid I_o \mid^2 = \dfrac{1}{2} V_o I_o^*$.

Finally, we may define the energy velocity as the average power propagating along the transmission line over the total average energy per unit length

$$V_{en} = \frac{P}{W_e + W_m} = \frac{c}{\sqrt{\mu_r \varepsilon_r}}.$$

Exercise 1.6: Show that the material is not frequency dependent, this quantity equals exactly the group velocity. What if not? Namely $\varepsilon_r(\omega)$.

1.5 Non-Homogeneous Transmission Line

There are cases when either the electromagnetic properties or the geometry vary along the structure. In these cases the impedance per unit length (Z) and admittance (Y) per unit length are z-dependent i.e.

$$\frac{dV(z)}{dz} = -Z(z)I(z)$$

$$\frac{dI(z)}{dz} = -Y(z)V(z).$$

(1.5.1)

As a result, the voltage or current satisfy an equation that to some extent differs from the regular wave equation

$$\frac{d^2V}{dz^2} = -\frac{dZ(z)}{dz}I(z) - Z(z)\frac{dI(z)}{dz}$$

$$= \left\{\frac{d}{dz}\ln\left[Z(z)\right]\right\}\frac{dV}{dz} + Z(z)Y(z)V(z)$$

A solution of a general character is possible only using numerical methods. However, an analytic solution is possible if we assume an ``exponential'' behavior of the
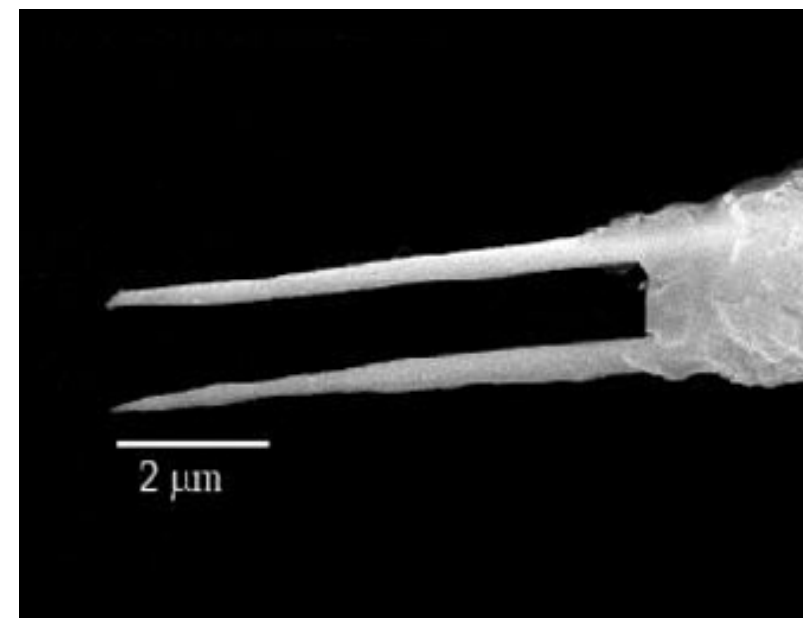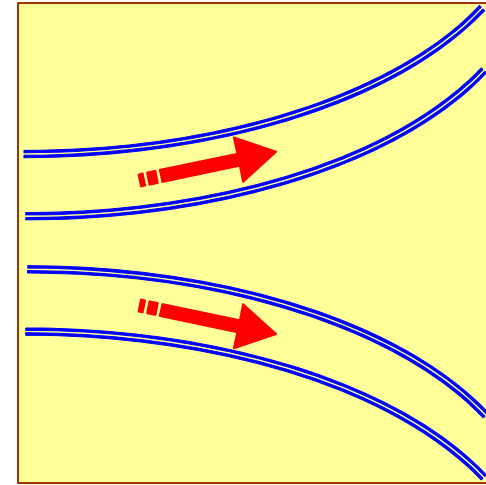
form

$$Z(z) = j\omega L_o \exp(qz)$$

$$Y(z) = j\omega C_o \exp(-qz)$$

(1.5.3)

Substituting these expressions in Eq. (1.5.2) we get

$$\frac{d^2 V(z)}{dz^2} - q\frac{dV}{dz} + \omega^2 L_o C_o V = 0$$

(1.5.4)

therefore assuming a solution of the form $V(z) = V_o e^{-\gamma_1 z}$ we conclude that

$$\gamma_1 = -\frac{1}{2}\left[q \pm \sqrt{q^2 - 4\omega^2 L_o C_o}\right].$$

(1.5.5)

In a similar way, the equation for the current is given by

$$\frac{d^2 I}{dz^2} - \frac{dI}{dz}\frac{d}{dz}\ln[Y(z)] - YZI(z) = 0.$$

(1.5.6)

Assuming a solution of the form $I = I_o e^{-\gamma_2 z}$ we obtain

$$\gamma_2 = \frac{1}{2}\left[q \pm \sqrt{q^2 - 4\omega^2 L_o C_o}\right].$$

(1.5.7)

It is convenient to define

$$\omega_c^2 \equiv \frac{q^2/4}{L_o^2 C_o^2},$$

(1.5.8)
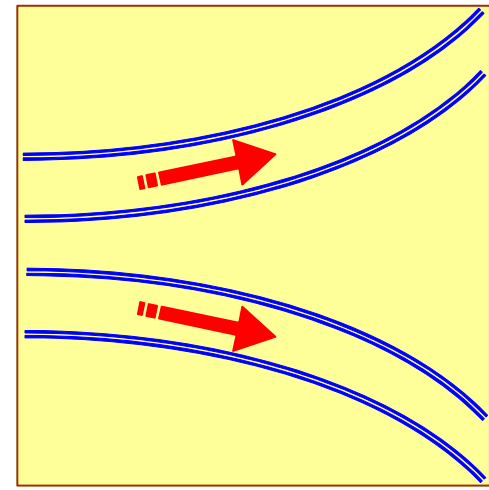
which sets a ``cut-off'' in the sense that for $\omega < \omega_c$ both γ_1 and γ_1 are real. The second important result is that the impedance along the transmission line

$$\frac{V(z)}{I(z)} = \frac{V_o e^{-\gamma_1 z}}{I_o e^{-\gamma_2 z}} = Z_c(0) e^{qz}$$

(1.5.9)

is *frequency independent.*

Exercise 1.7: Plot the average power along such a transmission line as well as the average electric and magnetic energies. What is the energy velocity?
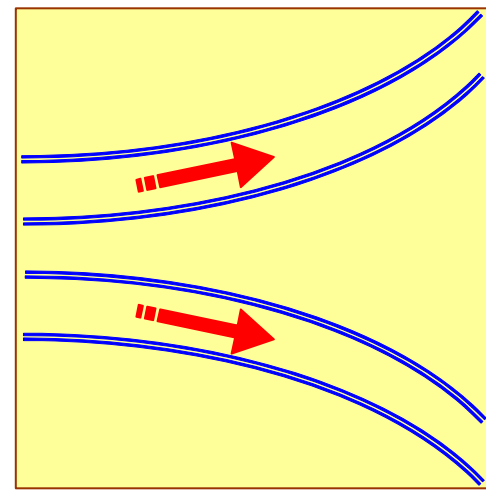
1.6 Coupled Transmission Lines

Microwave or high frequency circuits consist typically of many elements connected usually with wires that may be conceived as transmission lines. The proximity of one line to another may lead to **coupling phenomena**. Our purpose in this section is to formulate the telegraph equations in the presence of coupling. With this purpose in mind let us assume N transmission lines each one of which is denoted by an index $n(=1,2\cdots N)$ -- as illustrated in the figure above. Ignoring loss in the system we may conclude that the relation between the charge per unit length of each ``wire'' is related to the voltages by

$$\frac{Q_v}{\Delta_z} = \sum_{n=1}^{N} C_{vn} V_n \qquad (1.6.1)$$
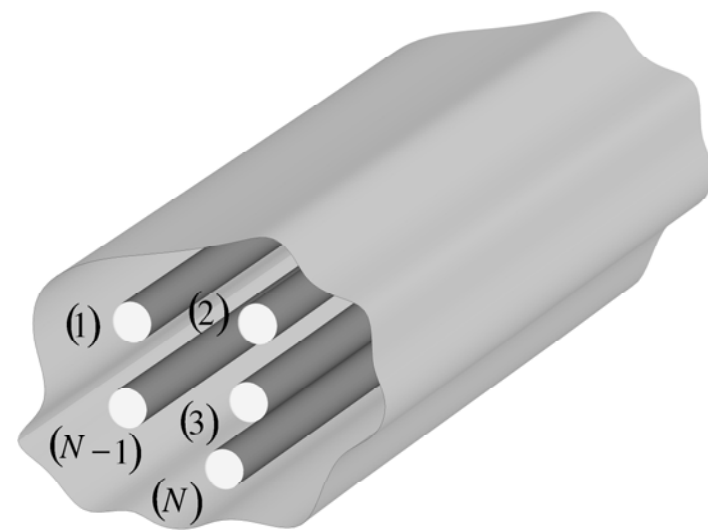
$C_{v,n}$ being the capacitance matrix per unit length. In a similar way, it is possible to establish the inductance matrix per unit length relating the voltage on wire v with all the currents

$$\frac{\Phi_v}{\Delta_z} = \sum_{n=1}^{N} L_{vn} I_n. \qquad (1.6.2)$$

Having these two equations [(1.6.1)–(1.6.2)] in mind, we may naturally extend the telegraph equations to read

$$\frac{d}{dz}V_v(z) = -j\omega \sum_{n=1}^{M} L_{vn} I_n(z) \qquad \frac{d}{dz}I_v(z) = -j\omega \sum_{n=1}^{M} C_{vn} V_n(z). \qquad (1.6.3)$$

Subsequently we shall discuss in more detail phenomena linked to this coupling process however, at this point we wish to emphasize that the number of wave-numbers (β^2) corresponds to the **number of ports**. This is evident since

$$\vec{V}(z) = \vec{V}_0 e^{-j\beta z} \qquad \vec{I}(z) = \vec{I}_0 e^{-j\beta z} \qquad (1.6.4)$$

enabling to simplify (1.6.3) to read

$$\beta \vec{V}_0 = \omega \underline{\underline{L}} \vec{I}_0 \qquad \beta \vec{I}_0 = \omega \underline{\underline{C}} \vec{V}_0 \qquad (1.6.5)$$

thus the wavenumber is the non-trivial solution of

$$[\omega^2 \underline{\underline{L}}\,\underline{\underline{C}} - \beta^2 \underline{\underline{\delta}}]\vec{V}_0 = 0 \quad \text{or} \quad [\omega^2 \underline{\underline{C}}\,\underline{\underline{L}} - \beta^2 \underline{\underline{\delta}}]\vec{I}_0 = 0. \qquad (1.6.6)$$

wherein $\underline{\underline{\delta}}$ is the unity matrix. Clearly the normalized wave number $\bar{\beta}^2 \equiv (\beta c / \omega)^2$ are the **eigen-values of the matrix** $\underline{\underline{L}}\,\underline{\underline{C}}$ ($= \underline{\underline{C}}\,\underline{\underline{L}}$ since both matrices are symmetric) and if the dimension of $\underline{\underline{C}}$ and $\underline{\underline{L}}$ is N then, the number of the eigen wavenumber is also N.

1.7 Microstrip

In this section we shall discuss in some detail some of the properties of a microstrip which is an essential component in any micro-electronic as well as microwave circuit. The microstrip consists of a thin and narrow metallic strip located on a thicker dielectric layer. On the other side of the latter, there is a ground metal; the side walls have been introduced in order to simplify the analysis and the width w is large enough such that it does not affect the physical processes in the vicinity of the strip. We shall examine a simplified model of this system and for this purpose we make the following **assumptions**:   (i) The width of the device is much larger than the height ($w \gg h$) and the width ($w \gg \Delta$) of the strip.
(ii) The charge on the strip is distributed uniformly.
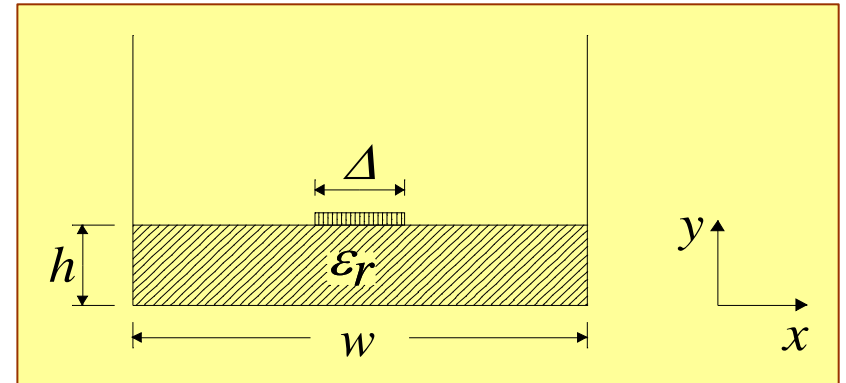
Our goal is to calculate the two parameters of the transmission line: **capacitance and inductance per unit length**. With this purpose in mind we shall start with evaluation of the capacitance therefore let us assume a general charge distribution on the
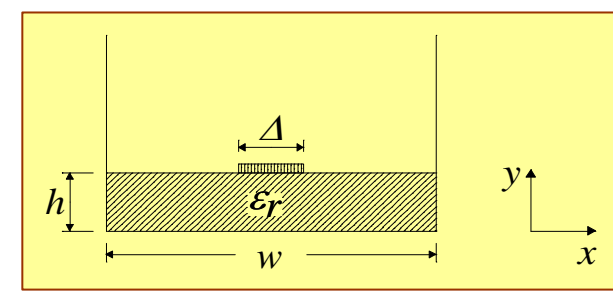
strip

$$\rho_s(x) = \begin{cases} \eta(x) & |x - \dfrac{w}{2}| < \dfrac{\Delta}{2} \\[2mm] 0 & |x - \dfrac{w}{2}| > \dfrac{\Delta}{2} \end{cases} \qquad (1.7.1)$$

With the exception of $y = h$ the potential is given by

$$\varphi(x, y) = \begin{cases} \displaystyle\sum_{n=0}^{\infty} A_n \sin\left(\dfrac{\pi n x}{w}\right) \sinh\left(\dfrac{\pi n y}{w}\right) & 0 \leq y \leq h \\[4mm] \displaystyle\sum_{n=0}^{\infty} B_n \sin\left(\dfrac{\pi n x}{w}\right) e^{-\dfrac{\pi n}{w}(y-h)} & y \geq h. \end{cases} \qquad (1.7.2)$$

The continuity of the potential at $y = h$ implies

$$\phi(x, y = h) = \sum_{n=0}^{\infty} A_n \sin\left(\pi n \dfrac{x}{w}\right) \sinh\left(\dfrac{\pi n h}{w}\right) = \sum_n B_n \sin\left(\dfrac{\pi n x}{w}\right)$$

$$(1.7.3)$$

$$\Rightarrow \quad \boxed{A_n \sinh\left(\dfrac{\pi n h}{w}\right) = B_n}.$$

27
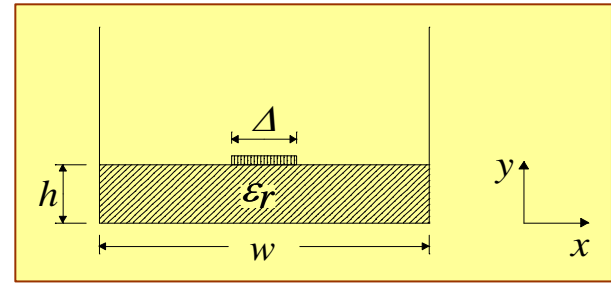
The electric induction D_y is discontinuous at this plane. In each one of the two regions the field is given by

$$D_y(x, 0 < h) = -\varepsilon_o \varepsilon_r \sum_n A_n \left(\frac{\pi n}{w} \right) \sin \left(\frac{\pi n x}{w} \right) \cosh \left(\frac{\pi n y}{w} \right)$$

$$D_y(x, y > h) = \varepsilon_o \sum_n B_n \left(\frac{\pi n}{w} \right) \sin \left(\frac{\pi n x}{w} \right) \exp \left[-\frac{\pi n}{w}(y - h) \right]. \tag{1.7.4}$$

With these expressions, we can write the boundary conditions i.e., $\vec{n} \cdot (\vec{D}_1 - \vec{D}_2) = \rho_s$ in the following form

$$\varepsilon_o \sum_n \left(\frac{\pi n}{w} \right) \sin \left(\frac{\pi n x}{w} \right) \left[B_n + \varepsilon_r A_n \cosh \left(\frac{\pi n h}{w} \right) \right] = \begin{cases} \eta(x) & |x - \frac{w}{2}| < \frac{\Delta}{2} \\ \\ 0 & |x - \frac{w}{2}| > \frac{\Delta}{2}. \end{cases} \tag{1.7.5}$$

Using the orthogonality of the sin function we obtain [for this reason the two side walls were introduced]

$$B_n + \varepsilon_r A_n \cosh \left(\frac{\pi n h}{w} \right) = \frac{1}{\varepsilon_o} \frac{2}{\pi n} \int_{\frac{w - \Delta}{2}}^{\frac{w + \Delta}{2}} dx \, \eta(x) \sin \left(\frac{\pi n x}{w} \right). \tag{1.7.6}$$

28
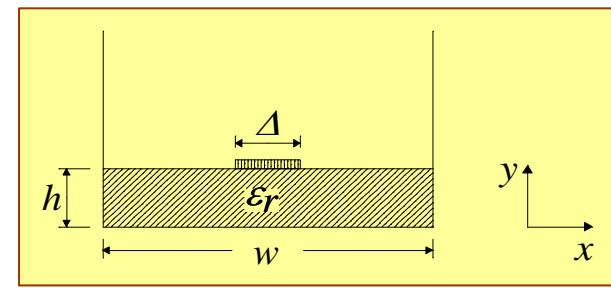
The next step is to substitute (1.7.3) into the last expression. The

result is

$$A_n \left[\sinh\left(\frac{\pi n h}{w}\right) + \varepsilon_r \cosh\left(\frac{\pi n h}{w}\right) \right] = \frac{1}{\varepsilon_o} \frac{2}{\pi n} \int_{\frac{w-\Delta}{2}}^{\frac{w+\Delta}{2}} dx \eta(x) \sin\left(\frac{\pi n x}{w}\right). \qquad (1.7.7)$$

Consequently, subject to the assumption that $\eta(x)$ is known, the potential is known in the entire space and specifically at $y = h$ is given by

$$\phi(x, y = h) = \sum_n \sin\left(\frac{\pi n x}{w}\right) \frac{1}{1 + \varepsilon_r \mathrm{ctanh}\left(\frac{\pi n h}{w}\right)} \frac{1}{\varepsilon_o} \frac{2}{\pi n} \int_{\frac{w-\Delta}{2}}^{\frac{w+\Delta}{2}} dx' \eta(x') \sin\left(\frac{\pi n x'}{w}\right). \quad (1.7.8)$$

In principle, this is an **integral equation** which can be solved numerically since the potential on the strip is constant and it equals V_0; many source solution.

At this point we shall employ our *second assumption* namely that the charge is *uniform* across the strip and determine an approximate solution. The first step is to average over the strip region, $|x - w/2| \le \Delta/2$. The left hand side is by definition constant thus
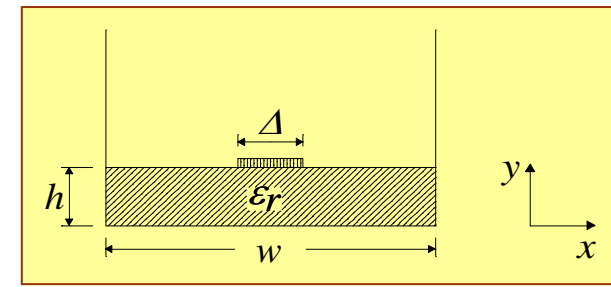
$$V_o = \frac{1}{\Delta}\int_{\frac{w-\Delta}{2}}^{\frac{w+\Delta}{2}} dx\, \phi(x, y = h)$$

$$= \sum_n \frac{(1/\varepsilon_o)(2/\pi n)}{1 + \varepsilon_r \mathrm{ctanh}\left(\frac{\pi n h}{w}\right)}\left[\frac{1}{\Delta}\int_{\frac{w-\Delta}{2}}^{\frac{w+\Delta}{2}} dx \sin\left(\frac{\pi n x}{w}\right)\right]\left[\int_{\frac{w-\Delta}{2}}^{\frac{w+\Delta}{2}} dx'\, \eta(x')\sin\left(\frac{\pi n x'}{w}\right)\right].$$

(1.7.9)

Explicitly our assumption that the charge is uniformly distributed, implies $\eta \simeq Q/\Delta_z\Delta$, therefore

$$V_o = \frac{Q}{\Delta_z}\frac{1}{\varepsilon_0}\sum_n \frac{2}{\pi n}\frac{1}{1 + \varepsilon_r \mathrm{ctanh}\left(\frac{\pi n h}{w}\right)}\left[\frac{1}{\Delta}\int_{\frac{w-\Delta}{2}}^{\frac{w+\Delta}{2}} dx \sin\left(\frac{\pi n x}{w}\right)\right]^2$$

and finally the capacitance per unit length is

Air

$\varepsilon_r = 4$

30
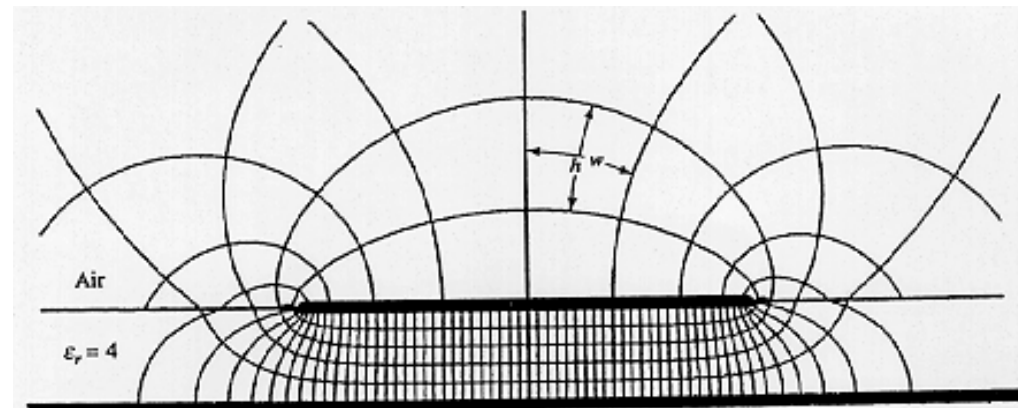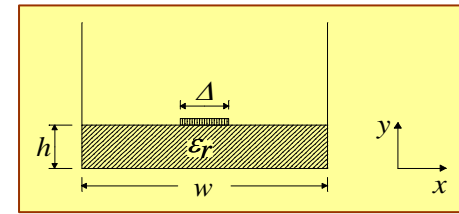
$$C = \frac{Q/\Delta_z}{V_o} \simeq \frac{\varepsilon_o \pi/2}{\displaystyle\sum_n \frac{1/n}{1 + \varepsilon_r \text{ctanh}\left(\dfrac{\pi n h}{w}\right)} \sin^2\left(\dfrac{\pi n}{2}\right) \text{sinc}^2\left(\dfrac{\pi n \Delta}{2w}\right)} \qquad (1.7.10)$$

With this expression we can, in principle calculate all the parameters of the microstrip. For evaluation of the **inductance per unit length** we use the fact that the dielectric material cannot have any impact on the DC inductance. Moreover, we know that in the absence of the dielectric ($\varepsilon_r = 1$), the propagation number is ω/c and the characteristic impedance satisfies

$$Z_c = \frac{1}{C(\varepsilon_r = 1)} \frac{1}{c} \sqrt{1} = \sqrt{\frac{L(\varepsilon_r = 1)}{C(\varepsilon_r = 1)}}. \qquad (1.7.11)$$

Since the DC the magnetic field is totally independent of the dielectric coefficient of the medium (electric property), we deduce from the expression of above that

$$\Rightarrow \quad L(\varepsilon_r = 1) = \frac{1}{c^2 C(\varepsilon_r = 1)}, \qquad (1.7.12)$$

or explicitly
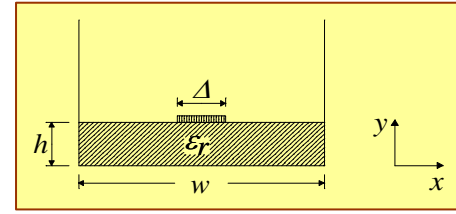
$$L = \mu_o \frac{2}{\pi} \sum_{v=0}^{\infty} \frac{1}{2v+1} \left\{ \exp\left[-\pi(2v+1)\frac{h}{w}\right] \sinh\left[\pi(2v+1)\frac{h}{w}\right] \right\} \mathrm{sinc}^2\left[\frac{\pi}{2}\frac{\Delta}{w}(2v+1)\right]. (1.7.13)$$

With the last expression and (1.7.10) we can calculate the characteristic impedance of the microstrip

$$Z_c = \sqrt{\frac{L}{C}} = \eta_o \frac{2}{\pi} \left[\sum_{v=0}^{\infty} \frac{e^{-h_v}\sinh(h_v)\mathrm{sinc}^2(\Delta_v)}{2v+1} \right]^{1/2} \left\{ \sum_{v=0}^{\infty} \frac{\mathrm{sinc}^2(\Delta_v)}{(2v+1)[1+\varepsilon_r \mathrm{ctanh}(h_v)]} \right\}^{1/2}, (1.7.14)$$

where $h_v \equiv \pi(2v+1)h/w$ and $\Delta_v \equiv \frac{\pi}{2}\frac{\Delta}{w}(2v+1)$. The next parameter that remains to be

determined is the phase velocity. Since L and C are known, we know that $\beta = \omega\sqrt{LC}$ implying that

$$V_{ph} = \frac{1}{\sqrt{LC}} = c \sqrt{\frac{\sum_{v=0}^{\infty} \frac{\mathrm{sinc}^2(\Delta_v)}{2v+1} \frac{1}{1+\varepsilon_r \mathrm{ctanh}(h_v)}}{\sum_{v=0}^{\infty} \frac{\mathrm{sinc}^2(\Delta_v)}{2v+1} \exp(-h_v)\sinh(h_v)}}. \qquad (1.7.15)$$
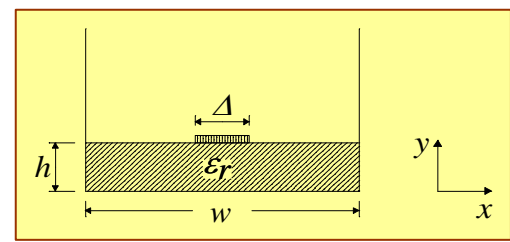
Contrary to cases encountered so far the dielectric material fills only **part** of the entire volume. As a result, only part of the electromagnetic field experiences the dielectric. It is therefore natural to determine the **effective dielectric coefficient** experienced by the field. This quantity may be defined in several ways. One possibility is to use the fact that when the dielectric fills the entire space we have the phase velocity in $V_{ph} = \dfrac{c}{\sqrt{\varepsilon_r}}$ it

becomes natural to define the effective dielectric coefficient as $\varepsilon_{eff} \equiv \dfrac{c^2}{V_{ph}^2}$ thus

$$\varepsilon_{eff} = \frac{\displaystyle\sum_{\nu=0}^{\infty} \frac{\mathrm{sinc}^2(\Delta_\nu)}{2\nu+1}\exp(-h_\nu)\sinh(h_\nu)}{\displaystyle\sum_{\nu=0}^{\infty} \frac{\mathrm{sinc}^2(\Delta_\nu)}{2\nu+1}\frac{1}{1+\varepsilon_r\mathrm{ctanh}(h_\nu)}}. \qquad (1.7.16)$$

The following figures illustrate the dependence of the various parameters on the geometric parameters.
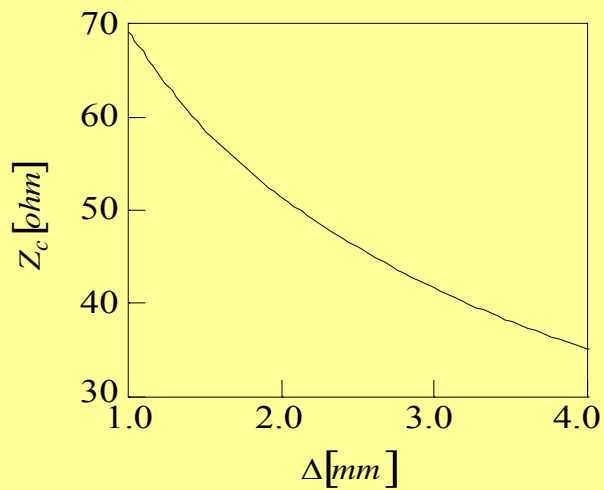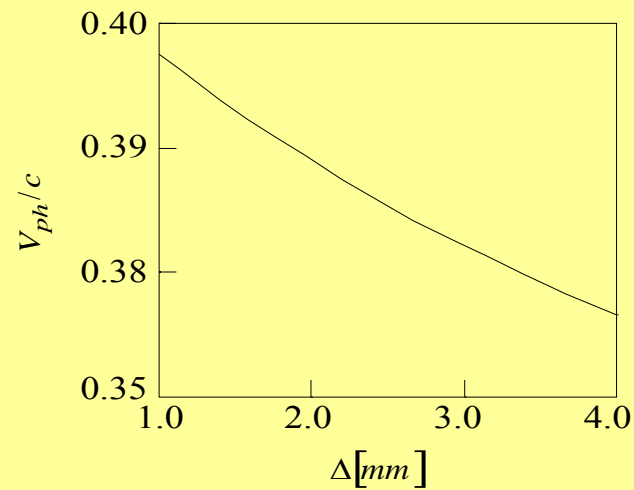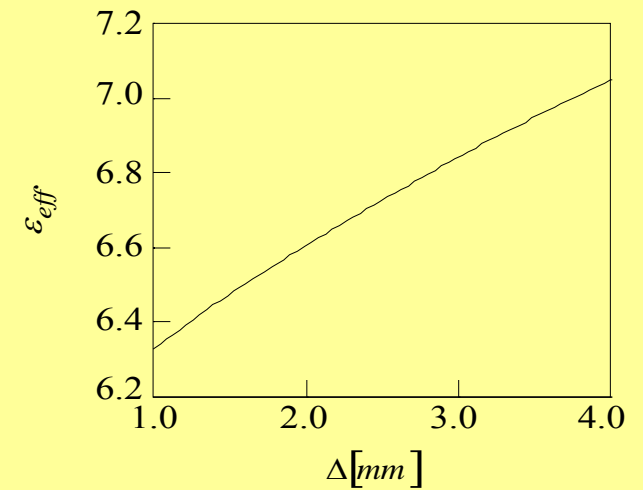
33

(a)   (b)   (c)

(a) Characteristic impedance vs. Δ; $h = 2\,\mathrm{mm}, w = 20\,\mathrm{mm}, \varepsilon_r = 10$ and $v < 100$.

(b) Phase velocity vs. Δ; $h = 2\,\mathrm{mm}$, $w = 20\,\mathrm{mm}$, $\varepsilon_r = 10$ and $v < 100$.

(c) Effective dielectric coefficient vs. Δ; $h = 2\,\mathrm{mm}$, $w = 20\,\mathrm{mm}$, $\varepsilon_r = 10$ and $v < 100$.

(a)   (b)   (c)
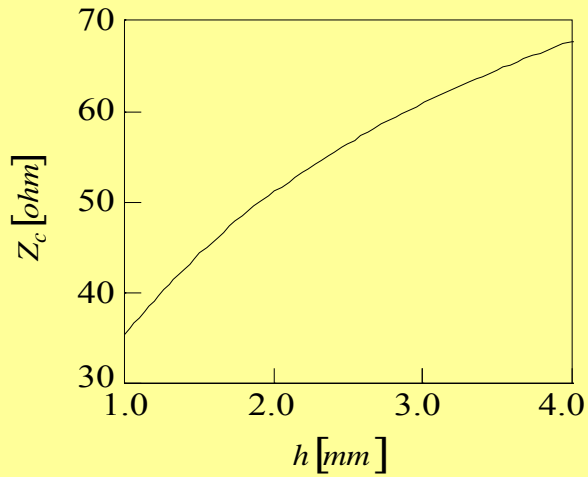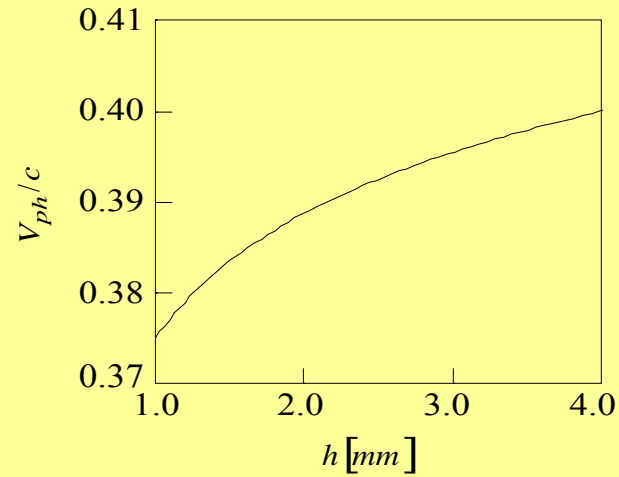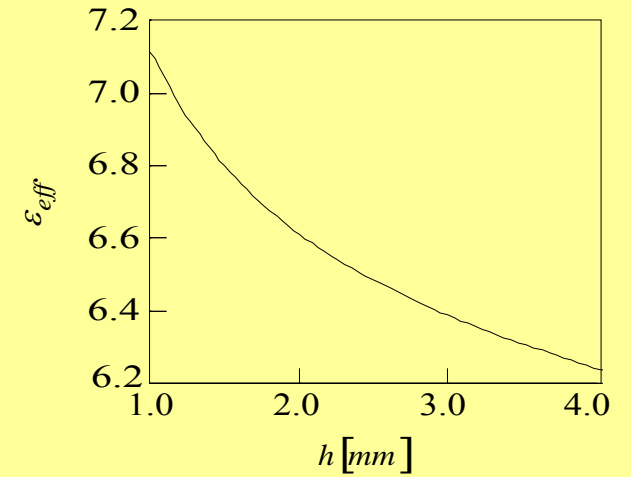
(a) Characteristic impedance vs. the height h; $\Delta = 2\,\text{mm}$, $w = 20\,\text{mm}$, $\varepsilon_r = 10$, $v < 100$.

(b) Phase velocity vs. the height h; $\Delta = 2\,\text{mm}$, $w = 20\,\text{mm}$, $\varepsilon_r = 10$, $v < 100$.

(c) Effective dielectric coefficient vs. the height h; $\Delta = 2\,\text{mm}$, $w = 20\,\text{mm}$, $\varepsilon_r = 10$, $v < 100$.

Finally the figure below shows several alternative configurations
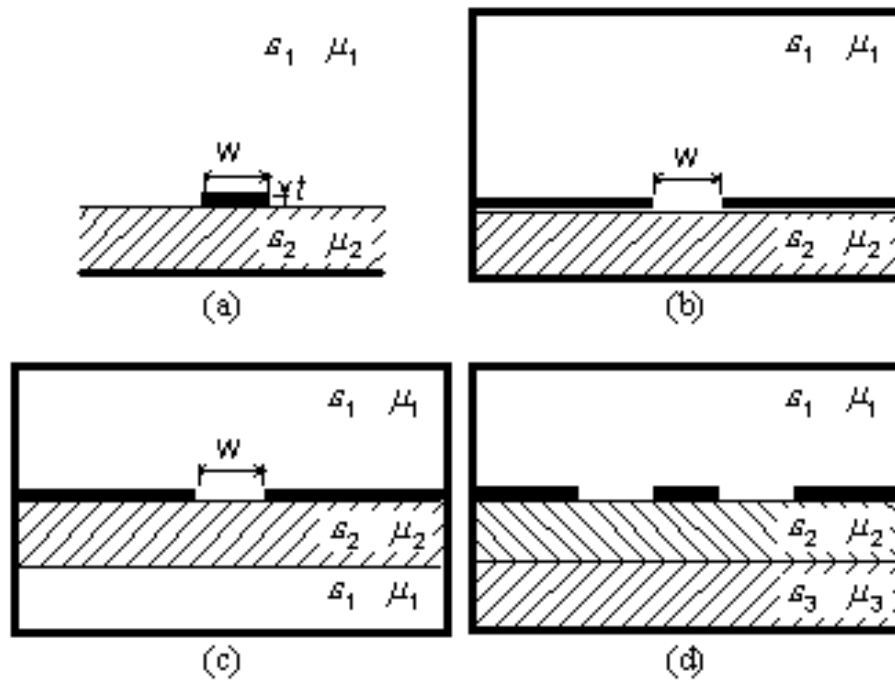
Exercise 1.8: Determine the effective dielectric coefficient relying on energy confinement.

Exercise 1.9: What fraction of the energy is confined in the dielectric and how the various parameters affect this fraction?

Exercise 1.10: Examine the effect of the dielectric coefficient on Z_c, ε_{eff} and V_{ph}. Compare with the case where the dielectric fills the entire space. (For solution see Appendix 11.1)

Exercise 1.11: Show that if $w \gg h, \Delta$ the various quantities are independent of w. Explain!! (For solution see Appendix 11.2)

Exercise 1.12: Analyze the effect of dielectric and permeability loss on a micro-strip.

Exercise 1.13: Calculate the ohmic loss. Analyze the effect of the strip and ground separately.

Exercise 1.14: Determine the effect of the edges on the electric parameters (L, C).

1.8 Stripline

Being open on the top side, the microstrip has limited ability to confine the electromagnetic field. For this reason we shall examine now the stripline which has a metallic surface on its top. The basic configuration of a stripline is illustrated below
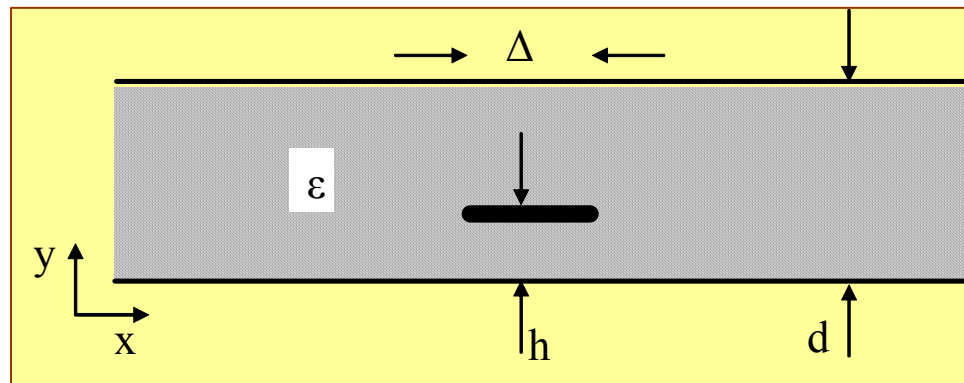
The model we shall utilize first replaces the central strip with a wire as illustrated below and as in Section 1.7 our goal is to calculate the parameters of the line.
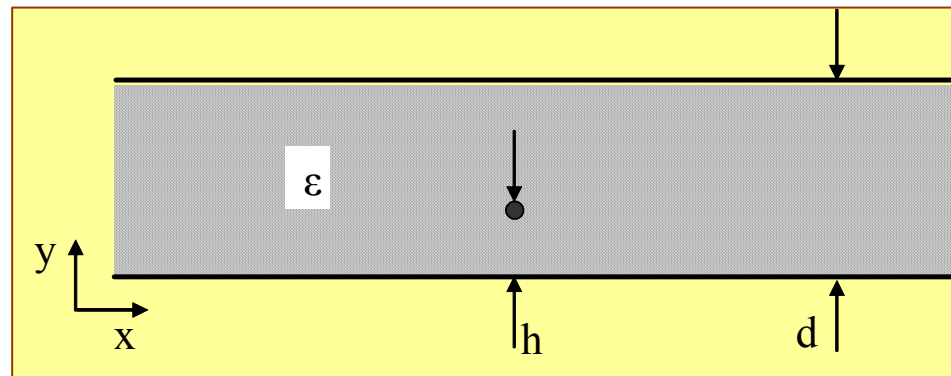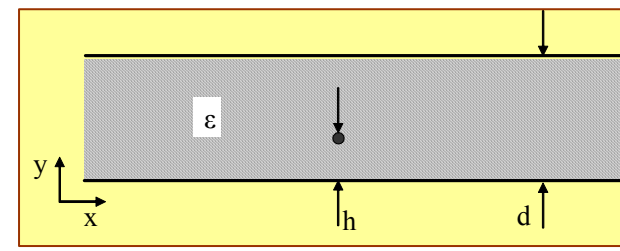
For evaluation of the capacitance per unit length it is first assumed that the charge density is given by

$$\rho(x,y) = \frac{Q}{\Delta_z}\delta(x)\delta(y-h), \tag{1.8.1}$$

and we need to solve the Poisson equation subject to trivial boundary conditions on the two electrodes. Thus

$$\left.\begin{array}{l} \nabla_t^2\phi = -\dfrac{\rho}{\varepsilon_o\varepsilon_r} \\[2mm] \phi(y=0)=0 \\[2mm] \phi(y=d)=0 \end{array}\right\} \Rightarrow \phi(x,y) = \sum_n \phi_n(x)\sin\left(\frac{\pi n y}{d}\right). \tag{1.8.2}$$

Substituting the expression in the right hand side in the Poisson equation we have

$$\sum_n \left[\frac{d^2}{dx^2}\phi_n(x) - \left(\frac{\pi n}{d}\right)^2 \phi_n(x)\right]\sin\left(\frac{\pi n y}{d}\right) = \frac{-Q}{\varepsilon_o\varepsilon_r\Delta_z}\delta(x)\delta(y-h) \tag{1.8.3}$$

and the orthogonality of the trigonometric function we obtain

39
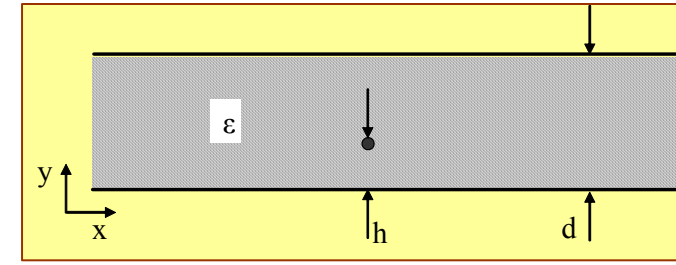
$$\left[\frac{d^2}{dx^2}-\left(\frac{\pi n}{d}\right)^2\right]\phi_n(x)=\frac{-Q}{\varepsilon_o\varepsilon_r\Delta_z}\delta(x)\frac{2}{d}\sin\left(\frac{\pi nh}{d}\right)=-Q_n\delta(x), \qquad (1.8.4)$$

where

$$Q_n\equiv\frac{2Q}{\varepsilon_o\varepsilon_r d\Delta_z}\sin\left(\frac{\pi nh}{d}\right).$$

The solution of (1.8.4) is given by

$$\phi_n(x)=\begin{cases}A_n\exp\left(-\pi n\frac{x}{d}\right) & x>0 \\[2mm] B_n\exp\left(\pi n\frac{x}{d}\right) & x<0\end{cases} \qquad (1.8.5)$$

and since the potential has to be continuous at $x=0$ then

$$A_n=B_n, \qquad (1.8.6)$$

integration of (1.8.4) determines the discontinuity:

$$\left.\frac{d\varphi_n}{dx}\right|_{x=0^+}-\left.\frac{d\varphi_n}{dx}\right|_{x=0^-}=-Q_n \quad\Rightarrow\quad -\left(\frac{\pi n}{d}\right)[A_n+B_n]=-Q_n. \qquad (1.8.7)$$

From (1.8.6) and (1.8.7) we find
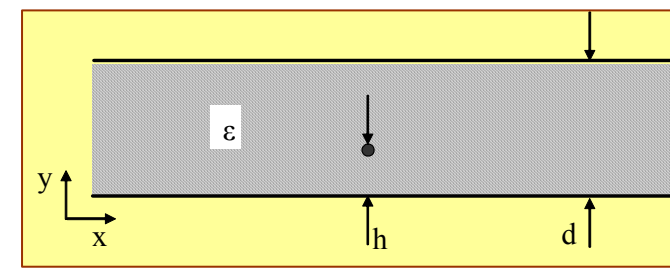
$$A_n = B_n = \frac{Q_n}{2\left(\dfrac{\pi n}{d}\right)} = \frac{Q}{\varepsilon_o \varepsilon_r \Delta_z} \frac{h}{d} \mathrm{sinc}\left(\pi n \frac{h}{d}\right).$$

(1.8.8)

This result permits us to write the solution of the potential in the entire space as

$$\phi(x, y) = \begin{cases} \dfrac{Q}{\varepsilon_o \varepsilon_r \Delta_z} \dfrac{h}{d} \displaystyle\sum_{n=1}^{\infty} \mathrm{sinc}\left(\dfrac{\pi n h}{d}\right) \sin\left(\dfrac{\pi n y}{d}\right) e^{-\frac{\pi n x}{d}} & x \geq 0 \\[4mm] \dfrac{Q}{\varepsilon_o \varepsilon_r \Delta_z} \dfrac{h}{d} \displaystyle\sum_{n=1}^{\infty} \mathrm{sinc}\left(\dfrac{\pi n h}{d}\right) \sin\left(\dfrac{\pi n y}{d}\right) e^{+\frac{\pi n x}{d}} & x \leq 0. \end{cases}$$

(1.8.9)

At this stage we can return to the initial configuration and assume that the central strip is a superposition of charges Q_i located at x_i and since the system is linear, we apply the superposition principle thus

$$\phi(x, y) = \frac{h/d}{\varepsilon_o \varepsilon_r \Delta_z} \sum_n \mathrm{sinc}\left(\frac{\pi n h}{d}\right) \sin\left(\frac{\pi n y}{d}\right) \sum_i Q_i \exp\left[-\pi n \frac{|x - x_i|}{d}\right].$$

(1.8.10)

In the case of a continuous distribution we should replace

41
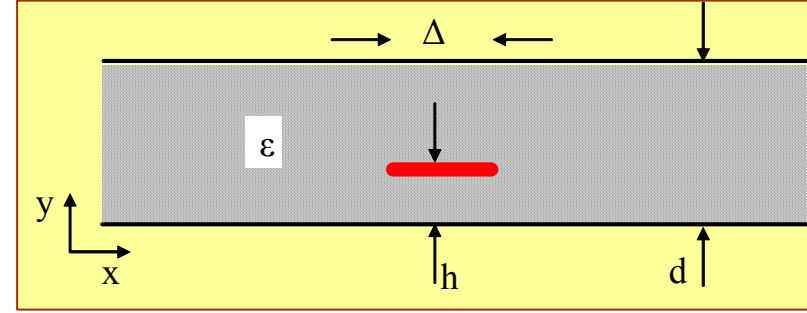
$$\sum_i Q_i e^{-\frac{\pi n}{d}|x-x_i|} = \frac{1}{\Delta}\int dx' Q(x') e^{-\frac{\pi n}{d}|x-x'|} \qquad (1.8.11)$$

and consequently

$$\phi(x,y) = \frac{h/d}{\varepsilon_o \varepsilon_r \Delta_z}\sum_n \mathrm{sinc}\left(\frac{\pi n h}{d}\right)\sin\left(\frac{\pi n y}{d}\right)\frac{1}{\Delta}\int dx' Q(x')\exp\left(-\frac{\pi n}{d}|x-x'|\right), \quad (1.8.12)$$

which again leads us to an integral equation; note that the surface changes density as $\rho_s(x) = Q(x)/\Delta\Delta_z$. As in the microstrip case, we shall assume *uniform* distribution therefore

$$\phi(x,y) = \frac{h/d}{\varepsilon_o \varepsilon_r \Delta_z}\sum_n \mathrm{sinc}\left(\frac{\pi n h}{d}\right)\sin\left(\frac{\pi n y}{d}\right)\frac{Q_o}{\Delta}\int_{-\Delta/2}^{\Delta/2} dx'\exp\left(-\frac{\pi n}{d}|x-x'|\right). \quad (1.8.13)$$

The potential is constant on the strip
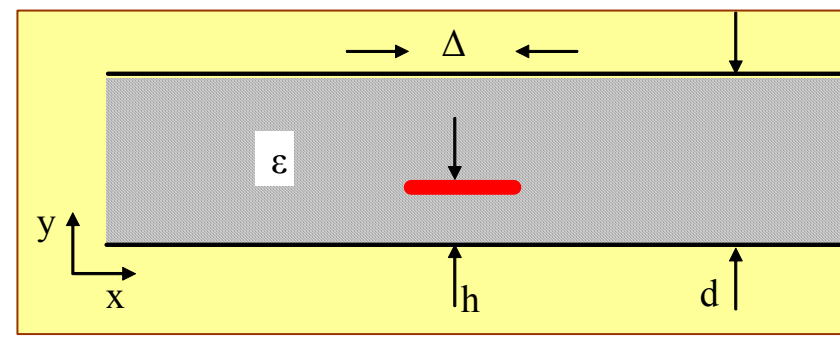
$$V_o = \frac{1}{\Delta} \int_{-\Delta/2}^{\Delta/2} dx\, \phi(x, y = h)$$

$$= \frac{(h/d)Q_o}{\varepsilon_o \varepsilon_r \Delta_z} \sum_{n=1}^{\infty} \left(\frac{\pi n h}{d} \right)^{-1} \sin^2\left(\frac{\pi n h}{d} \right) \frac{1}{\Delta} \int_{-\Delta/2}^{\Delta/2} dx \frac{1}{\Delta} \int_{-\Delta/2}^{\Delta/2} dx' \exp\left(-\frac{\pi n}{d} |x - x'| \right) \tag{1.8.14}$$

and the two integrals may be simplified to read

$$\frac{1}{\Delta} \int_{-\Delta/2}^{\Delta/2} dx \frac{1}{\Delta} \int_{-\Delta/2}^{\Delta/2} dx' \exp\left(-\frac{\pi n}{d} |x - x'| \right) = \left(\frac{\pi n}{2} \frac{\Delta}{d} \right)^{-1} \left[1 - \exp\left(-\frac{\pi n}{2} \frac{\Delta}{d} \right) \text{sinhc}\left(\frac{\pi n \Delta}{2d} \right) \right] \tag{1.8.15}$$

such that

$$V_o = \frac{(h/d)Q_o \left(\dfrac{2h}{\Delta} \right)}{\varepsilon_o \varepsilon_r \Delta_z} \sum_{n=1}^{\infty} \text{sinc}^2\left(\frac{\pi n h}{d} \right) \left[1 - \exp\left(-\frac{\pi n \Delta}{2d} \right) \text{sinhc}\left(\frac{\pi n \Delta}{2d} \right) \right]. \tag{1.8.16}$$

The last result enables us to write the following expression for the capacitance per unit length

$$C = \frac{Q_o/\Delta_z}{V_o} = \varepsilon_o \varepsilon_r \frac{1}{2} \left(\frac{\Delta d}{h^2} \right) \left\{ \sum_n \text{sinc}^2\left(\frac{\pi n h}{d} \right) \left[1 - \exp(-\xi_n) \text{sinhc}(\xi_n) \right] \right\}^{-1} \tag{1.8.17}$$

43

whereas $\xi_n = \pi n \Delta / 2d$, thus with it the characteristic impedance reads

$$Z_c = \frac{1}{CV_{ph}} = \eta_o \frac{2}{\sqrt{\varepsilon_r}} \frac{h^2}{\Delta d} \sum_n \mathrm{sinc}^2\left(\frac{\pi n h}{d}\right)\left[1 - \exp\left(-\xi_n\right)\mathrm{sinhc}(\xi_n)\right]. \qquad (1.8.18)$$

The two frames show the impedance dependence on the width and height of the strip
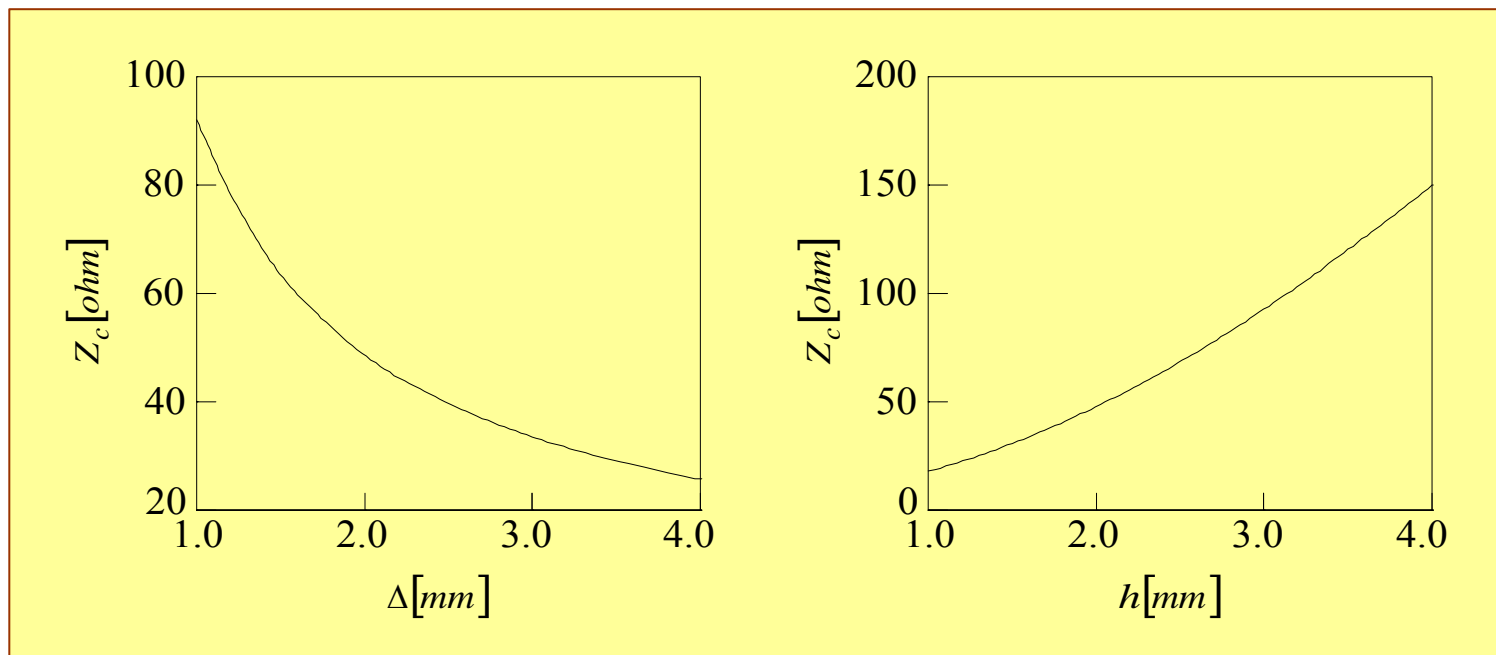
Left: Characteristic impedance vs. the width Δ [$h = 2\,\mathrm{mm}$, $\varepsilon_r = 10$ and $n = 0,1,...200$]
Right: Characteristic impedance vs. the height h [$\Delta = 2\,\mathrm{mm}$, $\varepsilon_r = 10$ and $n = 0,1,...200$]

Exercise 1.15: Determine the inductivity per unit length and analyse the dependence of the various characteristics on the geometric parameters. (For solution see Appendix 11.3)

Exercise 1.16: Compare the dependence of the various characteristics of the stripline and microstrip as a function of the geometric parameters.

Exercise 1.17: Compare micro-strip and strip-line from the perspective of sensitivity to the dielectric coefficient. (For solution see Appendix 11.4)

Exercise 1.18: Determine the error associated with the assumption that the charge is *uniform* across the strip.

Exercise 1.19: Analyze the effect of a strip of finite thickness. Remember that throughout this calculation the strip was assumed to have a negligible thickness.

1.9 Resonator Based on Transmission Line

1.9.1 Short Recapitulation

Resonant circuits are of great importance for oscillator circuits, tuned amplifiers, frequency filter networks, wavemeters for measuring frequency. Electric resonant circuits have many features in common, and it will be worthwhile to review some of these by using a conventional lumped-parameter RLC parallel network as an example Figure 8 illustrates a typical low-frequency resonant circuit. The resistance R is usually only an equivalent resistance that accounts for the power loss in the inductor L and capacitor C as well as the power extracted from the resonant system by some external load coupled to the resonant circuit. One possible definition of resonance relies on the fact that at resonance the input impedance is pure real and equal to R implying

$$Z_{in} = \frac{P_l + 2j\omega(W_m - W_e)}{II^*/2}.$$

Although this equation is valid for a one-port circuit, resonance always occurs when $W_m = W_e$, if we define resonance to be that condition which corresponds to a pure resistive input impedance or explicitly $\omega_0 = 1/\sqrt{LC}$; note that these are the lumped capacitance (C) and inductance (L).
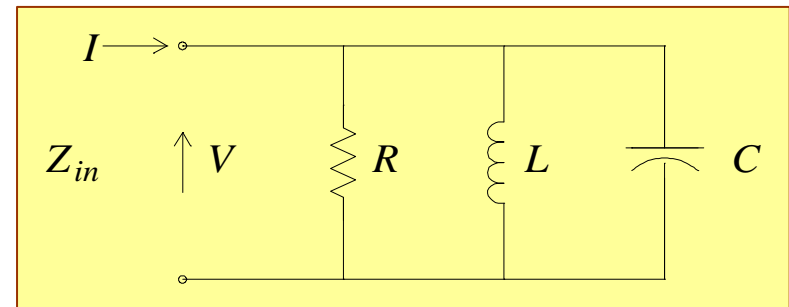
An important parameter specifying the frequency selectivity, and performance in general, of a resonant circuit is the quality factor, or Q. A very general definition of Q that is applicable to all resonant ($W_e = W_m$) systems is

$$Q = \frac{\omega_0 (\text{time} - \text{average energy stored in the system})}{\text{energy loss per second in the system.}} \qquad (1.9.2)$$

hence,

$$Q = \omega_0 RC = R / \omega_0 L. \qquad (1.9.3)$$

In the vicinity of resonance, say $\omega = \omega_0 + \Delta\omega$, the input impedance can be expressed in a relatively simple form. We have

$$Z_{in} = \frac{\omega_0^2 RL}{\omega_0^2 L + j2R\Delta\omega} = \frac{R}{1 + j2Q(\Delta\omega / \omega_0)}. \qquad (1.9.4)$$

A plot of Z_{in} as a function of $\Delta\omega / \omega_0$ is given below. When $|Z_{in}|$ has fallen to $1/\sqrt{2}$ (half the power) of its maximum value, its phase is $45°$ if $\omega < \omega_0$ and $-45°$ if $\omega > \omega_0$ thus

$$2Q\frac{\Delta\omega}{\omega_0} = 1 \Rightarrow \boxed{\Delta\omega = \frac{\omega_0}{2Q}} \qquad (1.9.5)$$
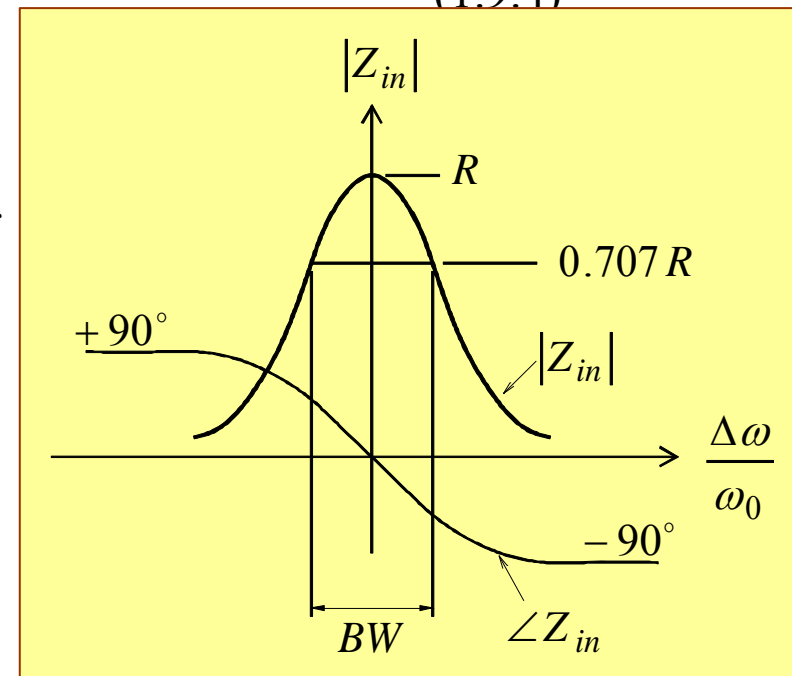
The fractional bandwidth BW between the $0.707R$ points is twice this value, hence

$$Q = \frac{\omega_0}{2\Delta\omega} = \frac{1}{BW}. \tag{1.9.6}$$

If the resistor R in Fig. 8 represents the loss in the resonant circuit only, the Q give by (1.9.3) is called the **unloaded** Q. If the resonant circuit is coupled to an external load that absorbs a certain amount of power, this loading effect can be represented by an additional resistor R_L in parallel with R. The total resistance is now less, and consequently the new Q is also smaller. The Q, called the loaded Q and denoted Q_L, is

$$Q_L = \frac{RR_L/(R+R_L)}{\omega_0 L}. \tag{1.9.7}$$

The external Q, denoted Q_e, is defined to be the Q that would result if the *resonant circuit were loss-free* and only the loading by the external load was present. Thus

$$Q_e = \frac{R_L}{\omega_0 L} \tag{1.9.8}$$

leading to

$$\frac{1}{Q_L} = \frac{1}{Q_e} + \frac{1}{Q}. \tag{1.9.9}$$

Another parameter of importance in connection with a resonant circuit is the decay factor τ. This parameter measures the rate at which the oscillations would decay if the driving

source were removed. Significantly, with losses present, the energy stored in the resonant circuit will decay at a rate proportional to the average energy present at any time (since $P_l \propto VV^*$ and $W \propto VV^*$, we have $P_l \propto W$), so that

$$\frac{dW}{dt} = -\frac{2}{\tau}W \quad \Rightarrow \quad W = W_0 \exp\left(-2\frac{t}{\tau}\right) \tag{1.9.10}$$

where W_0 is the average energy present at $t = 0$. But the rate of decrease of W must equal the power loss, so that

$$-\frac{dW}{dt} = \frac{2}{\tau}W = P_l$$

and consequently,

$$\frac{1}{\tau} = \frac{P_l}{2W} = \frac{\omega_0}{2}\frac{P_l}{\omega_0 W} = \frac{\omega_0}{2Q}. \tag{1.9.11}$$

Thus, the decay factor is proportional to the Q. In place of (1.9.10) we now have

$$W = W_0 \exp\left(-\frac{\omega_0}{Q}t\right). \tag{1.9.12}$$
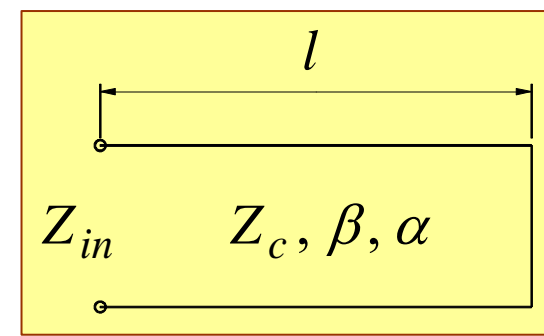
1.9.2 Short-Circuited Line

By analogy to the previous section, consider a short-circuited line of length l, parameters R, L, C per unit length, as in Fig. 10. Let $l = \lambda_0 / 2$ at $f = f_0$, that is, at $\omega = \omega_0$. For f near f_0, say $f = f_0 + \Delta f$, $\beta l = 2\pi f l / c = \pi \omega / \omega_0 = \pi + \pi \Delta \omega / \omega_0$, since at ω_0, $\beta l = \pi$. The input impedance is given by

$$Z_{in} = Z_c \tanh(j\beta l + \alpha l) = Z_c \frac{\tanh \alpha l + j \tan \beta l}{1 + j \tan \beta l \tanh \alpha l}. \qquad (1.9.13)$$

But $\tanh \alpha l \simeq \alpha l$ since we are assuming small losses, so that $\alpha l \ll 1$. Also $\tan \beta l = \tan(\pi + \pi \Delta \omega / \omega_0) = \tan \pi \Delta \omega / \omega_0 \simeq \pi \Delta \omega / \omega_0$ since $\Delta \omega / \omega_0$ is small. Hence

$$Z_{in} = Z_c \frac{\alpha l + j\pi \Delta \omega / \omega_0}{1 + j\alpha l \pi \Delta \omega / \omega_0} \approx Z_c \left(\alpha l + j\pi \frac{\Delta \omega}{\omega_0} \right) \qquad (1.9.14)$$

since the second term in the denominator is very small. Now $Z_c = \sqrt{L / C}$, $\alpha = \frac{1}{2} R Y_c = (R/2)\sqrt{C / L}$, and $\beta l = \omega_0 \sqrt{LC} l = \pi$; so $\pi / \omega_0 = l\sqrt{LC}$, and the expression for Z_{in} becomes

50
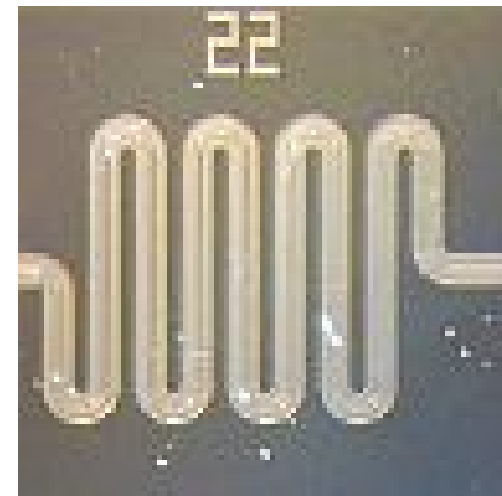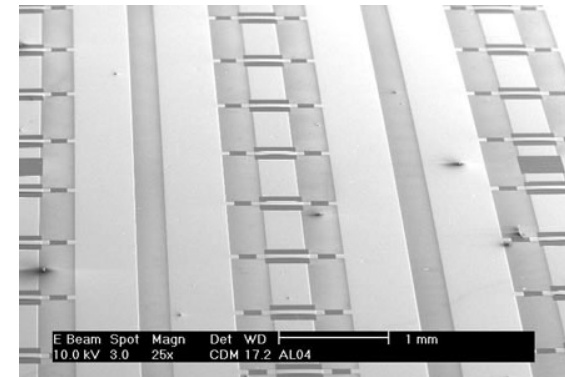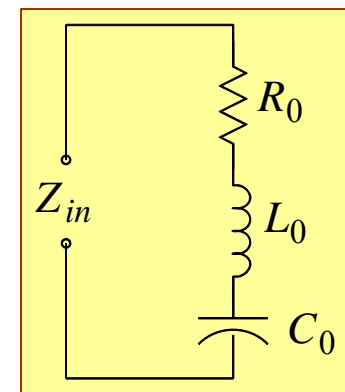
$$Z_{in} = \sqrt{\frac{L}{C}} \left(\frac{l}{2} R \sqrt{\frac{C}{L}} + j\Delta\omega l \sqrt{LC} \right) = \frac{1}{2} Rl + jlL\Delta\omega.$$

(1.9.15)

It is of interest to compare (1.9.15) with a series $R_0 L_0 C_0$ circuit illustrated above. For this circuit

$$Z_{in} = R_0 + j\omega L_0 \left(1 - 1/\omega^2 L_0 C_0 \right).$$

If we let $\omega_0^2 = 1/L_0 C_0$, then $Z_{in} = R_0 + j\omega L_0 \left(\omega^2 - \omega_0^2 \right)/\omega^2$. Now if $\omega - \omega_0 = \Delta\omega$ is small then

$$Z_{in} \simeq R_0 + 2 j L_0 \Delta\omega.$$

(1.9.16)

By comparison with (1.9.15), we see that in the vicinity of the frequency for which $l = \lambda_0/2$, the short-circuited line behaves as a series resonant circuit with resistance $R_0 = Rl/2$ and inductance $L_0 = Ll/2$. We note that Rl, Ll are the total resistance and inductance of the line; so we might wonder why the factors $1/2$ arise: recall that the current on the short-circuited line is half sinusoid, and hence the effective circuit parameters R_0, L_0 are only one-half of the total line quantities. The Q of the short-circuited line may be defined as for the circuit

$$Q = \frac{\omega_0 L_0}{R_0} = \frac{\omega_0 L}{R} = \frac{\beta}{2\alpha}.$$

(1.9.17)
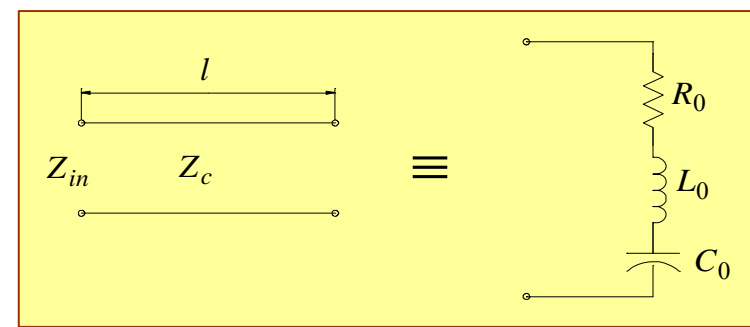
1.9.3 Open-Circuited Line

By means of an analysis similar to that used earlier, it is readily verified that an open-circuited transmission line is equivalent to a series resonant circuit in the vicinity of the frequency for which it is an odd multiple of a quarter wavelength long. The equivalent relations are

$$Z_{in} \simeq \left[\alpha l + j(\pi/2)(\Delta\omega/\omega_0)\right] Z_c = Rl/2 + j\Delta\omega Ll$$

$$(1.9.18)$$

$$l = \lambda_0/4, \ R_0 = Rl/2, \ L_0 = Ll/2, \ \omega_0^2 = 1/L_0 C_0$$

Comment: Note that formally from (1.9.13) in the lossless case i.e., $Z_{in} = jZ_c \tan\beta l$ we conclude that there are many (infinite) resonances since $\tan(\beta l)$ vanishes for $\beta l = \pi$ but also for $\beta l = \pi n$, $n = 1,2,3\ldots$ corresponding to all the ``series'' resonances. In case of ``parallel'' resonances the condition $\tan\beta l \simeq \pm\infty$ is satisfied for $\beta l = \dfrac{\pi}{2} + \pi n$, $n = 1,2,\ldots$. In practice, only the first resonance is used since beyond that the validity of the approximations leading to the equations are questionable.
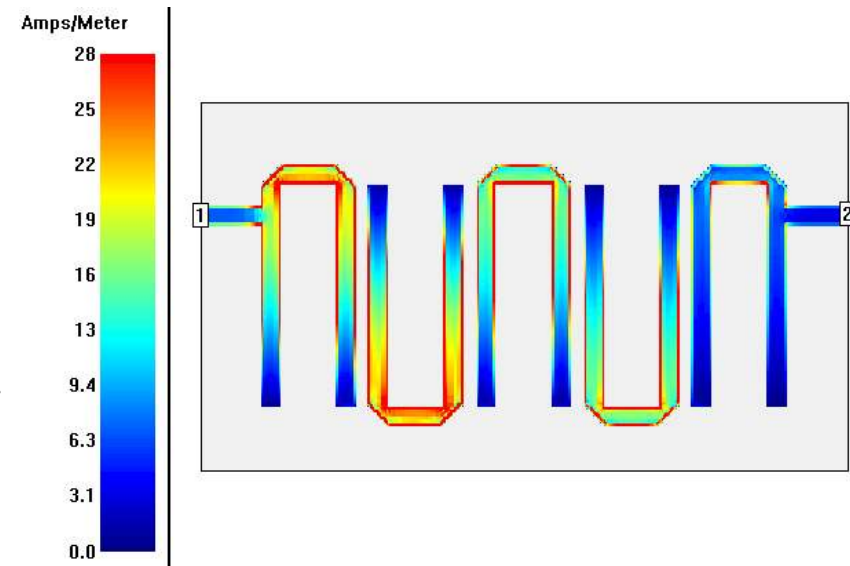
1.10 Pulse Propagation

1.10.1 Semi-Infinite Structure

So far the discussion has focused on solution of problems in the frequency domain. In this section we shall discuss some **time-domain** features. Let us assume that at the input of a semi-infinite and lossless transmission line we know the voltage pulse $V(z=0,t)=V_0(t)$. In general in the absence of reflections

$$V(z,t) = \int d\omega \overline{V}(\omega) e^{j\omega t - j\beta(\omega)z}$$

(1.10.1)

and specifically

$$V(z=0,t) = \int d\omega \overline{V}(\omega) e^{j\omega t}$$

(1.10.2)

or explicitly, **the voltage spectrum $\overline{V}(\omega)$ is the Fourier transform of the input voltage**

$$\overline{V}(\omega) = \frac{1}{2\pi}\int_{-\infty}^{\infty} dt V(z=0,t) e^{-j\omega t} = \frac{1}{2\pi}\int_{-\infty}^{\infty} dt V_0(t) e^{-j\omega t}.$$

(1.10.3)

Consequently, substituting in Eq.(1.10.1) we get

$$V(z,t) = \int_{-\infty}^{\infty} d\omega e^{j\omega t - j\beta(\omega)z} \frac{1}{2\pi}\int_{-\infty}^{\infty} dt' V(z=0,t') e^{-j\omega t'}$$

$$= \int_{-\infty}^{\infty} dt' V(z=0,t') \frac{1}{2\pi}\int_{-\infty}^{\infty} d\omega e^{j\omega(t-t') - j\beta(\omega)z}$$

(1.10.4)

and in the case of a **dispersionless line** we have $\beta(\omega) = \dfrac{\omega}{c}\sqrt{\varepsilon_r}$ which leads to

$$V(z,t) = \int_{-\infty}^{\infty} dt' V(z=0,t')\delta\left(t'-t+\frac{z}{c}\sqrt{\varepsilon_r}\right) = V\left(z=0,t'=t-\frac{z}{c}\sqrt{\varepsilon_r}\right) \quad (1.10.5)$$

implying that the **pulse shape is preserved** as it propagates in the z-direction. If the phase velocity is frequency-dependent, then different frequencies propagate at *different velocities* and the shape of the pulse is not preserved. As a simple example let us assume that the transmission line is filled with gas

$$\varepsilon(\omega) = 1 - \frac{\omega_p^2}{\omega^2}. \quad (1.10.6)$$

Since

$$V(z,t) = \int_{-\infty}^{\infty} dt' V\left(z=0,t'\right)\frac{1}{2\pi}\int d\omega \exp\left[j\omega(t-t') - \frac{z}{c}\sqrt{\omega_p^2 - \omega^2}\right] \quad (1.10.7)$$

it is evident that sufficiently far away from the input, the low frequencies ($\omega < \omega_p$) have no contribution and the system acts as a high-pass filter.

The dispersion process may be used to determine the frequency content of a signal. In order to envision the process let us assume that the spectrum of the signal at the *input* is given by

$$\overline{V}(\omega) = \sum_{v=1}^{M} a_v \exp\left[-\left(\frac{\omega - \omega_v}{\Delta\omega_v}\right)^2\right] \tag{1.10.8}$$

where all the parameters are known and that $\Delta\omega_v/\omega_v \ll 1$; note that at the limit that $\Delta\omega_v/\omega_v \to 0$ the Gaussian function behaves very similar to Dirac delta function. In such a case it is convenient to expand

$$\sqrt{\varepsilon(\omega)} \simeq \sqrt{\varepsilon(\omega_v)} + \left[\frac{1}{2\sqrt{\varepsilon(\omega)}} \frac{\partial\varepsilon(\omega)}{\partial\omega}\right]_{\omega=\omega_v} (\omega - \omega_v) \tag{1.10.9}$$

and also to use the fact that

$$\frac{1}{V_{gr}} = \frac{\partial\beta}{\partial\omega} = \frac{\partial}{\partial\omega}\left[\frac{\omega}{c}\sqrt{\varepsilon(\omega)}\right] = \frac{\sqrt{\varepsilon(\omega)}}{c} + \frac{\omega}{c}\frac{1}{2\sqrt{\varepsilon(\omega)}}\frac{\partial\varepsilon(\omega)}{\partial\omega}$$

$$= \frac{1}{V_{ph}} + \frac{\omega}{c}\frac{1}{2}\frac{1}{\sqrt{\varepsilon(\omega)}}\frac{\partial\varepsilon(\omega)}{\partial\omega}. \tag{1.10.10}$$

With these two observations, we now aim to develop an analytic expression for the voltage at any location z and at any time t. Specifically, to demonstrate that the peak of the Gaussian pulses depends on $t = z/V_{gr}(\omega_r)$ and reveal the way this signal varies in space.

The voltage variation in time is given by

$$V(z,t) = \int_{-\infty}^{\infty} d\omega \overline{V}(\omega) e^{j\omega t - j\beta(\omega)z}$$

$$= \sum_v a_v \int_{-\infty}^{\infty} d\omega e^{j\omega t - j\beta(\omega)z} \exp\left[-\left(\frac{\omega - \omega_v}{\Delta\omega_v}\right)^2\right]$$

(1.10.11)

wherein the wave number is $\beta(\omega) = \dfrac{\omega}{c}\sqrt{\varepsilon(\omega)}$ therefore,

$$V(z,t) = \sum_v a_v \int_{-\infty}^{\infty} d\omega \exp\left[-\left(\frac{\omega - \omega_v}{\Delta\omega_v}\right)^2\right]$$

$$\times \exp\left\{ j\omega t - j\frac{\omega}{c} z \left\{ \sqrt{\varepsilon(\omega_v)} + (\omega - \omega_v)\left[\frac{1}{2\sqrt{\varepsilon(\omega)}}\frac{\partial\varepsilon}{\partial\omega}\right]_{\omega=\omega_v} \right\} \right\}$$

(1.10.12)

Rearranging the terms we have

$$V(z,t) = \sum_{v} a_v \exp\left\{ j\omega_v \left[t - \frac{z}{c}\sqrt{\varepsilon(\omega_v)} \right] \right\}$$

$$\times \int d\omega \exp\left\{ j(\omega - \omega_v)\left[t - \frac{z}{c}\sqrt{\varepsilon(\omega_v)} - \frac{z}{c}\frac{\omega_v}{2\sqrt{\varepsilon(\omega_v)}}\left(\frac{d\varepsilon}{d\omega} \right]_{\omega_v} \right] \right\} \qquad (1.10.13)$$

$$\times \exp\left\{ -(\omega - \omega_v)^2 \left[\frac{1}{\Delta\omega_v^2} + j\frac{z}{c}\frac{1}{2\sqrt{\varepsilon(\omega_v)}}\left(\frac{d\varepsilon}{d\omega} \right]_{\omega_v} \right] \right\}.$$

The first term in the integrand can be written as

$$\exp\left[j(\omega - \omega_v)\left(t - \frac{z}{V_{gr}} \right) \right] \qquad (1.10.14)$$

whereas for the second term it is convenient to write

$$\frac{1}{c}\frac{1}{2\sqrt{\varepsilon(\omega_v)}}\left(\frac{d\varepsilon}{d\omega} \right]_{\omega = \omega_v} = \frac{1}{\omega_v}\left(\frac{1}{V_{gr}} - \frac{1}{V_{ph}} \right) \qquad (1.10.15)$$

and define

$$\frac{1}{\Delta\Omega_v^2(z)} \equiv \frac{1}{\Delta\omega_v^2} + j\frac{1}{\omega_v^2}\left(\frac{\omega_v}{c}z \right)\left(\frac{c}{V_{gr,v}} - \frac{c}{V_{ph,v}} \right). \qquad (1.10.16)$$

Consequently,

$$V(z,t) = \sum_v a_v \exp\left[j\omega_v \left[t - \frac{z}{c}\sqrt{\varepsilon(\omega_v)} \right] \right] \int_{-\infty}^{\infty} d\omega \exp\left[j(\omega - \omega_v)\left(t - \frac{z}{V_{gr}} \right) - \left(\frac{\omega - \omega_v}{\Delta\Omega_v} \right)^2 \right]$$

$$= \sum_v a_v \exp\left\{ j\omega_v \left[t - \frac{z}{V_{ph}(\omega_v)} \right] \right\} \Delta\Omega_v \int_{-\infty}^{\infty} d\xi \exp\left(-\xi^2 + j\xi\Delta\Omega_v\left(t - \frac{z}{V_{gr}} \right) \right).$$

$$(1.10.17)$$

The integral may be evaluated analytically since $\int_{-\infty}^{\infty} d\alpha\, e^{-\alpha^2} = \sqrt{\pi}$ such that finally we get

$$V(z,t) = \sum_{v=1}^{M} a_v \Delta\Omega_v(z)\sqrt{\pi} \exp\left[j\omega_v\left(t - \frac{z}{V_{gr,v}} \right) \right] \exp\left\{ -\left[\frac{\Delta\Omega_v(z)}{2}\left(t - \frac{z}{V_{gr,v}} \right) \right]^2 \right\}. (1.10.18)$$

According to (1.10.16) the **width of the pulse varies with the distance** from the input.

Comment: Discuss possibilities of spectrum measurement by its decomposition in space.

1.10.2 Propagation and Reflection

Other phenomena which may significantly affect the propagation of a pulse along a transmission line are **discontinuities**. For a glimpse into those phenomena let us consider three transmission lines connected in series.
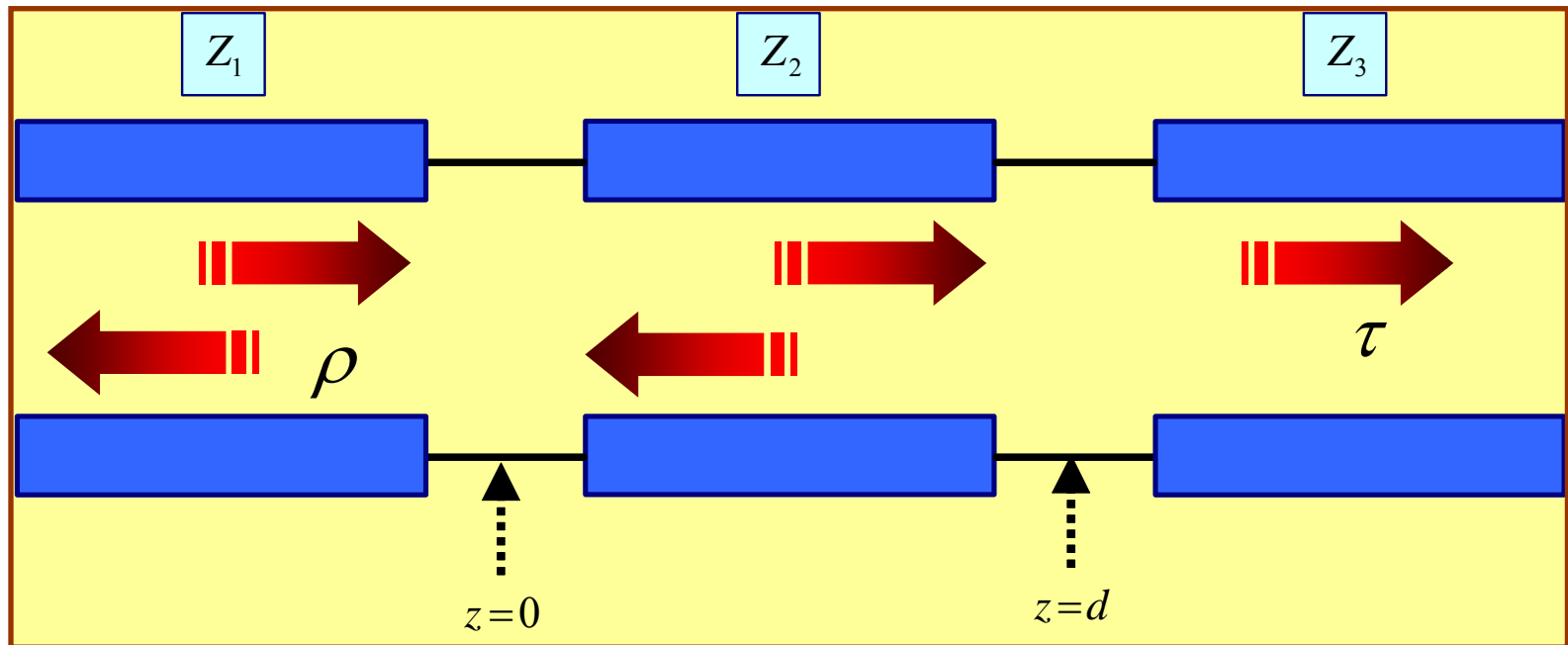
The reflection and transmission coefficients in the frequency-domain are

$$\rho = \frac{\cos\psi(Z_1 - Z_3)Z_2 + j\sin\psi(Z_1 Z_3 - Z_2^2)}{\cos\psi(Z_1 + Z_3)Z_2 + j\sin\psi(Z_1 Z_3 + Z_2^2)}$$

$$\tau = \frac{2Z_1 Z_2}{\cos\psi(Z_1 + Z_3)Z_2 + j\sin\psi(Z_1 Z_3 + Z_2^2)} \qquad (1.10.19)$$

$$\psi = \beta_2 d.$$

With these coefficients we aim to determine the transmitted signal in the time domain. Assuming that the incoming voltage is

$$V^{(in)}(z,t) = \int_{-\infty}^{\infty} d\omega \overline{V}(\omega) \exp\left[j\omega t - j\beta_1(\omega)z \right] \qquad (1.10.20)$$

wherein

$$\overline{V}(\omega) = \frac{1}{2\pi} \int_{-\infty}^{\infty} dt\, V^{(in)}(z=0,t) e^{-j\omega t}. \qquad (1.10.21)$$

Based on this expression, the transmitted signal is

$$V^{(tr)}(z,t) = \int_{-\infty}^{\infty} d\omega \overline{V}(\omega) \exp\left[j\omega t - j\beta_3(\omega)(z-d) \right] \tau(\omega) \qquad (1.10.22)$$

which assuming dispersionless transmission lines entails

$$V^{(tr)}(t,z) = \int_{-\infty}^{\infty} d\omega \left[\frac{1}{2\pi} \int_{-\infty}^{\infty} dt' V^{(in)}(z=0,t') e^{-j\omega t'} \right]$$

$$\times \frac{4 Z_1 Z_2 \exp(-j\psi) \exp\left[j\omega \left(t - \dfrac{z-d}{V_3} \right) \right]}{(1+e^{-2j\psi})(Z_1+Z_3)Z_2 + (1-e^{-2j\psi})(Z_1 Z_3 + Z_2^2)}.$$ (1.10.23)

We now define

$$\xi = \frac{4 Z_1 Z_2}{Z_2(Z_1+Z_3) + Z_1 Z_3 + Z_2^2}, \quad \chi = \frac{-(Z_1+Z_3)Z_2 + Z_1 Z_3 + Z_2^2}{(Z_1+Z_3)Z_2 + Z_1 Z_3 + Z_2^2}$$

enabling us to write

$$V^{(tr)}(z,t) = \xi \int_{-\infty}^{\infty} dt' V^{(in)}(z=0,t') \frac{1}{2\pi} \int_{-\infty}^{\infty} d\omega \frac{\exp\left\{ j\omega \left[t - t' - \dfrac{z-d}{V_3} - \dfrac{d}{V_2} \right] \right\}}{1 - \chi \exp\left(-2j\dfrac{\omega}{V_2} d \right)}.$$ (1.10.24)

Since $\chi < 1$ we may expand

$$\frac{1}{1-u} = \sum_{v=0}^{\infty} u^v \tag{1.10.25}$$

and further simplify

$$V^{(tr)}(z,t) = \xi \int_{-\infty}^{\infty} dt' V^{(in)}(z=0,t') \frac{1}{2\pi} \int_{-\infty}^{\infty} d\omega \exp\left\{ j\omega\left[t - t' - \frac{z-d}{V_3} - \frac{d}{V_2} \right] \right\}$$
$$\times \sum_{v=0}^{\infty} \chi^v \exp\left(-2jv\frac{\omega}{V_2}d \right). \tag{1.10.26}$$

The integration over ω is straight forward resulting in a Dirac delta function therefore

$$V^{(tr)}(z,t) = \xi \sum_{v=0}^{\infty} \chi^v V^{(in)} \left[z=0, t - \frac{z-d}{V_3}(2v+1) \right]. \tag{1.10.27}$$

A delay in the occurrence of the pulse reflects in the third term. The term $v=0$ represents the first pulse which reaches the output end. After a full round-trip, the second contribution occurs. Effects of round-trip time and pulse duration as well as the sign of χ are revealed by the following frames.

Top-left plot:

$Z_1 = 200$
$\beta_2 = 0.75$
$\chi = -0.143$
$Z_2 = 100$
$\beta_3 = 0.9$
$Z_3 = 0.4$
$d = 1.0$
$T_p = 2.0$

y-axis: $V\left(z/d, 9T_p\right)$
x-axis: z/d

Top-right plot:

$Z_1 = 200$
$\beta_2 = 0.75$
$\chi = 0.286$
$Z_2 = 40$
$\beta_3 = 0.9$
$Z_3 = 100$
$d = 1.0$
$T_p = 2.0$

y-axis: $V\left(z/d, 9T_p\right)$
x-axis: z/d

Bottom-left plot:

$Z_1 = 200$
$\beta_3 = 0.85$
$\chi = -0.143$
$Z_2 = 100$
$\beta_3 = 0.9$
$Z_3 = 0.4$
$d = 0.5$
$T_p = 2.0$

y-axis: $V\left(z/d, 4T_p\right)$
x-axis: z/d

Bottom-right plot:

$Z_1 = 200$
$\beta_2 = 0.85$
$\chi = 0.286$
$Z_2 = 40$
$\beta_3 = 0.9$
$Z_3 = 100$
$d = 0.5$
$T_p = 2.0$

y-axis: $V\left(z/d, 4T_p\right)$
x-axis: z/d

63
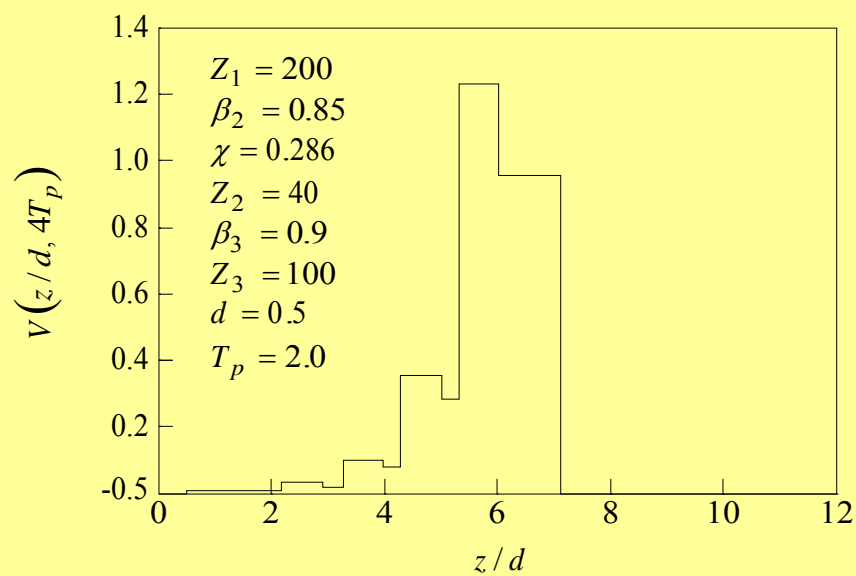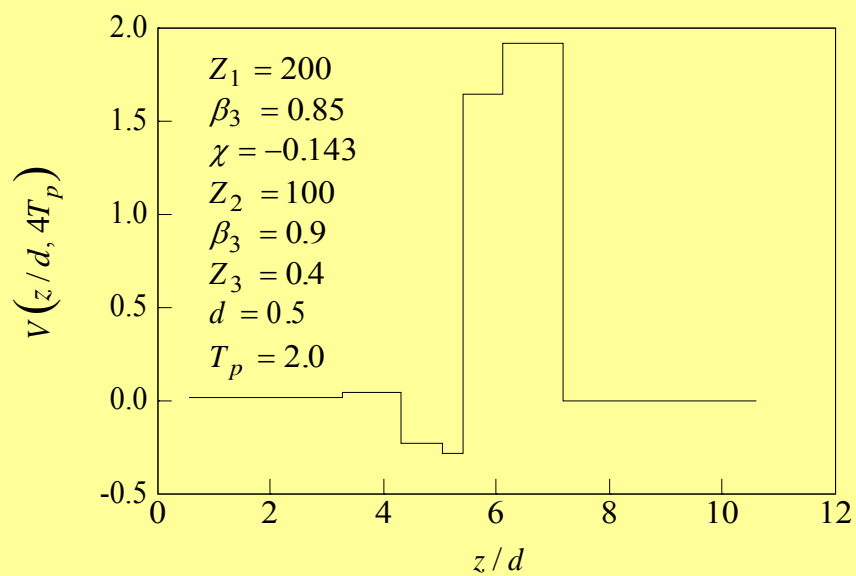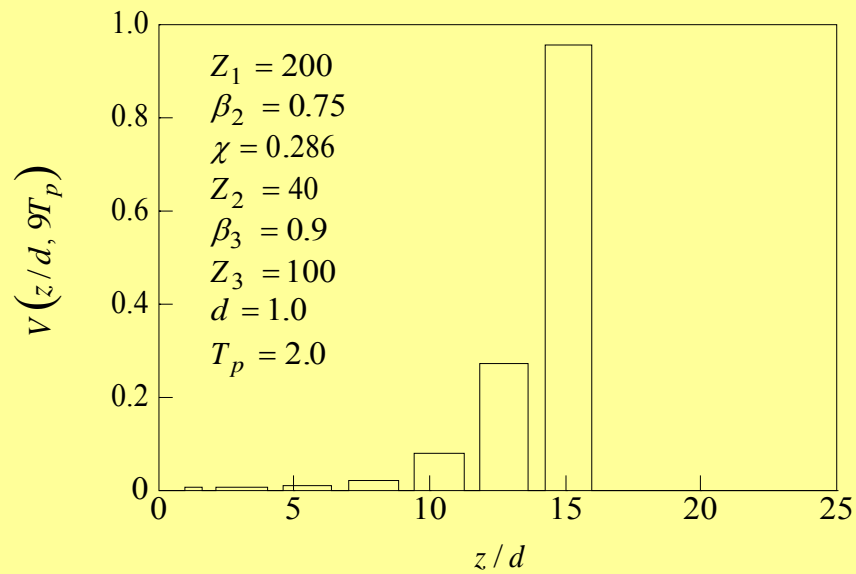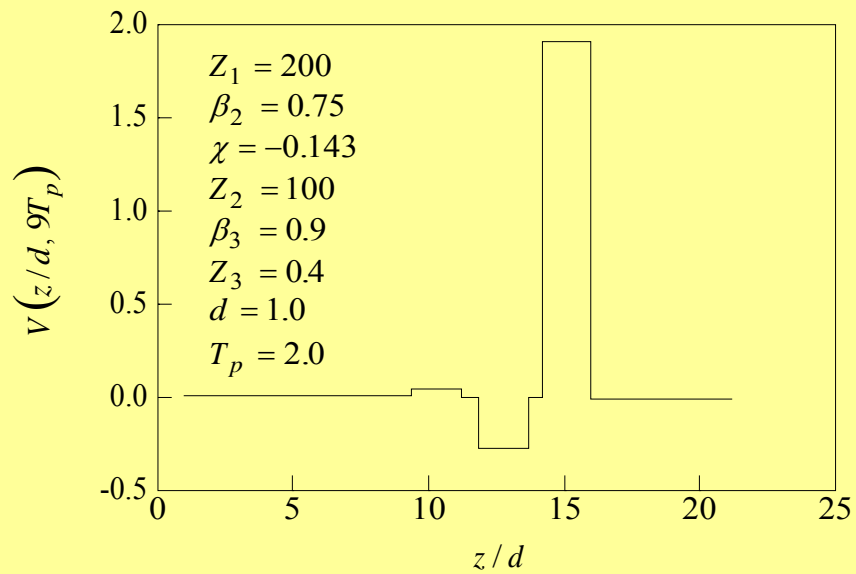
1.11 Appendix
1.11.1 Solution to Exercise 1.10

Microstrip: dependence of various parameters on the geometric parameters and the dielectric coefficient. For all the graphs the paramters are (when they are not the variable): $\Delta = 2$ mm, $w = 20$ mm, $h = 2$ mm, $\varepsilon_r = 10$ and $\nu = 0,1\cdots100$.
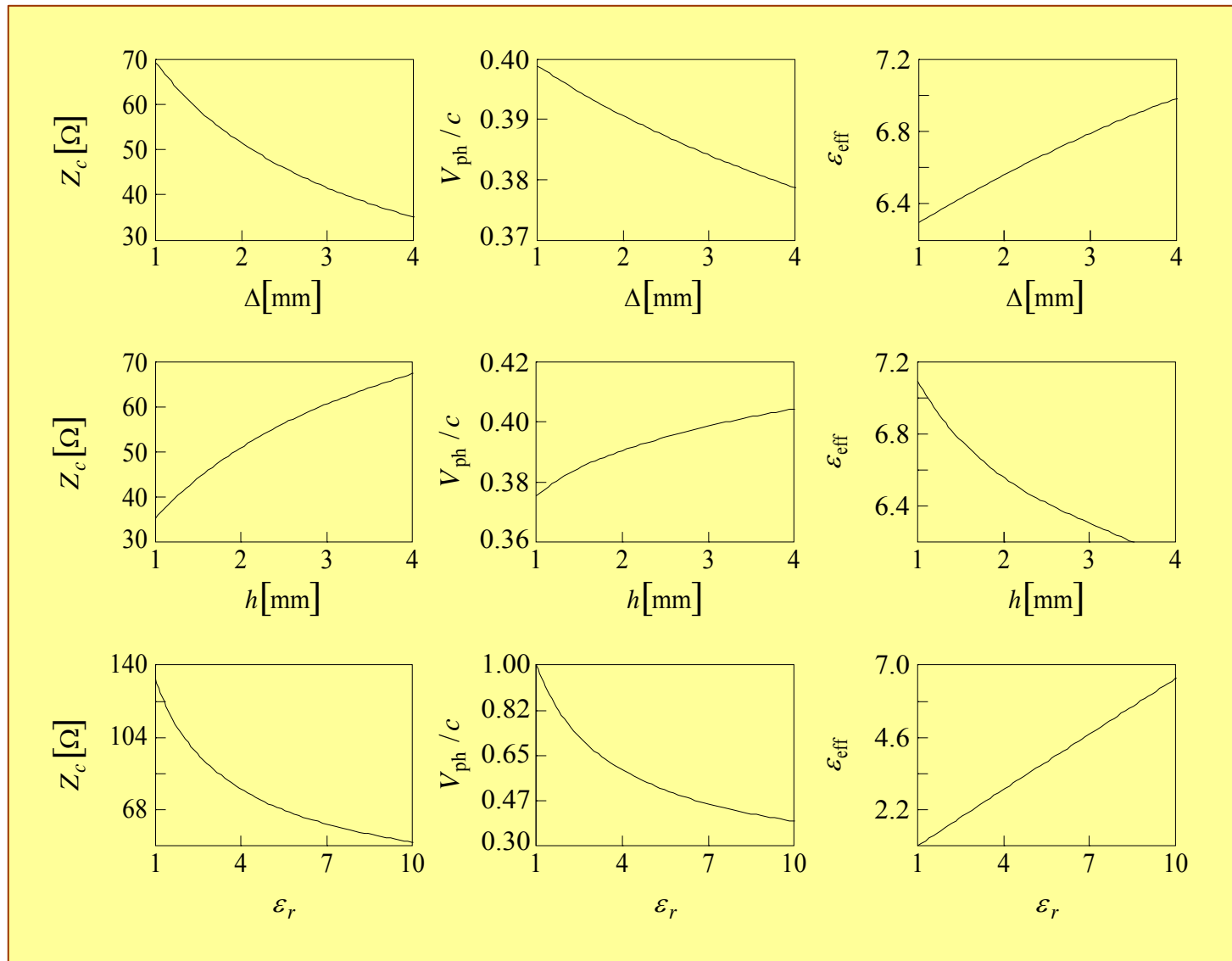
1.11.2 Solution to Exercise 1.11

Show that if $w \gg h, \Delta$ the various quantities are independent of w.

Dependence of various parameters in w. $[\Delta = 2$ mm, $\varepsilon_r = 10$, $h = 2$ mm and $v = 0, 1 \cdots 100]$.
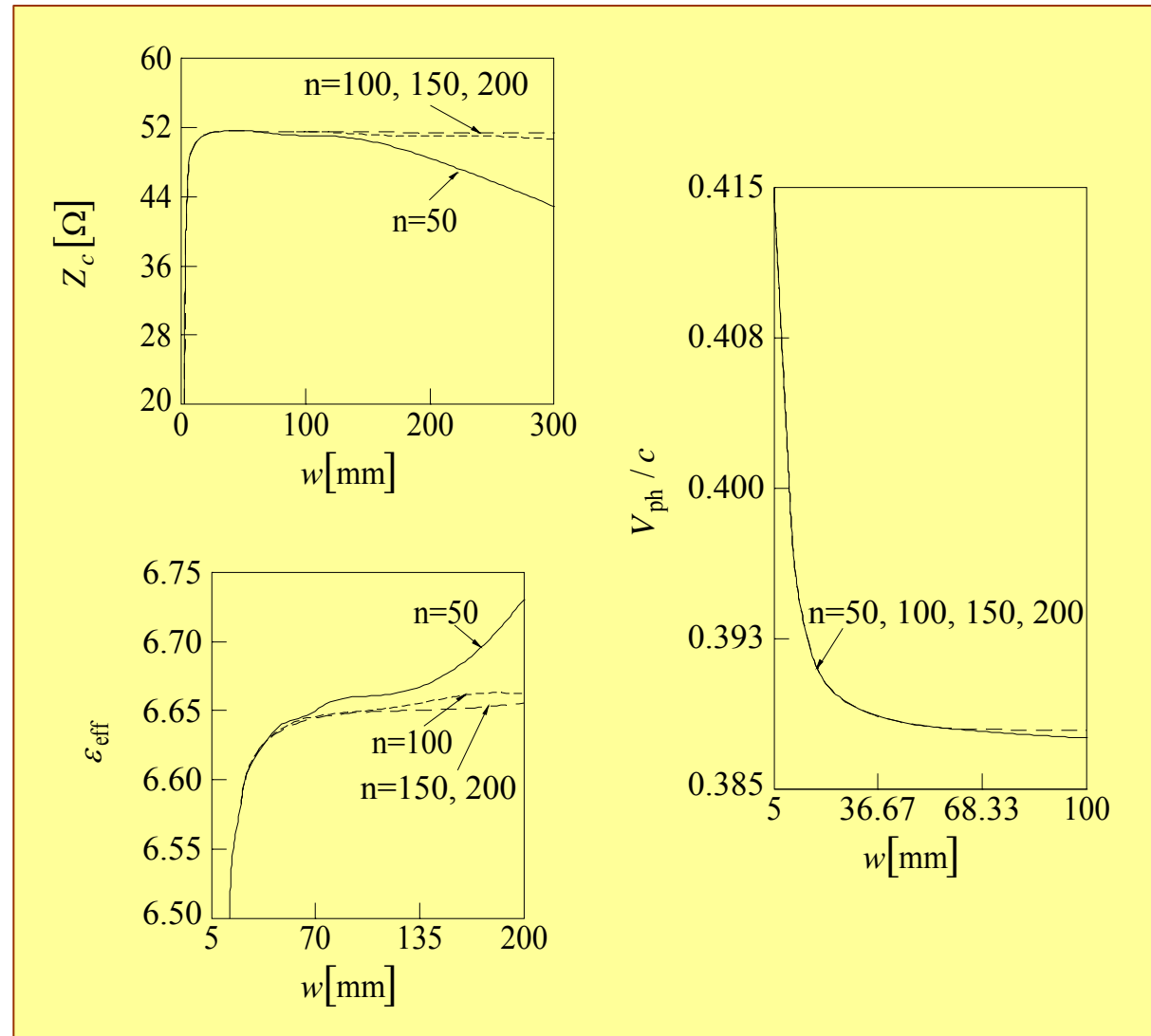
1.11.3 Solution to Exercise 1.15

Determine the inductivity per unit length and determine its dependence on the various parameters.

The inductivity per unit length of the stripline can be determined according to Eq. (1.7.12) $L = 1/c^2 C(\varepsilon_r = 1)$ substituting the expression for the capacitance per unit length given by Eq. (1.8.17) $L = 2\mu_0 \dfrac{h^2}{\Delta d} \sum\limits_{n=1}^{\infty} \mathrm{sinc}^2\left(\pi n \dfrac{h}{d}\right)\left[1 - \exp(-\xi_n)\dfrac{\sinh(\xi_n)}{\xi_n}\right]$

where $\xi_n = \dfrac{1}{2}\pi n \dfrac{\Delta}{d}$.

The figure shows the inductance per unit length of a stripline as a function of h. Clearly it is symmetrical around the maxima point $h = 2$ mm, corresponding to the symmetrical stripline configuration. [$d = 4$ mm, $\Delta = 2$ mm, $n = 1, 2, \cdots 200$].
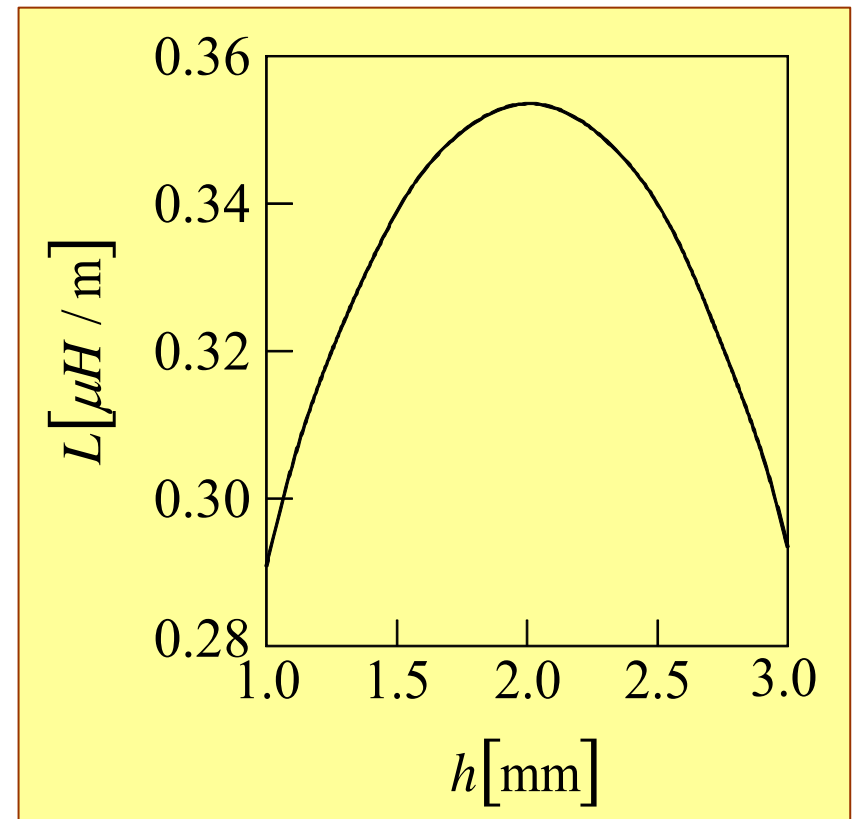
The figure shows the dependence of L on Δ, the strip width. The inductance per unit length of the stripline decreases as the strip width increases, and saturates as Δ becomes very large compared to h. From this result one can conclude that the inductance per unit length of a metallic wire is larger than that of a strip [$h = 2$ mm, $d = 4$ mm $n = 1,2,\cdots 200$].
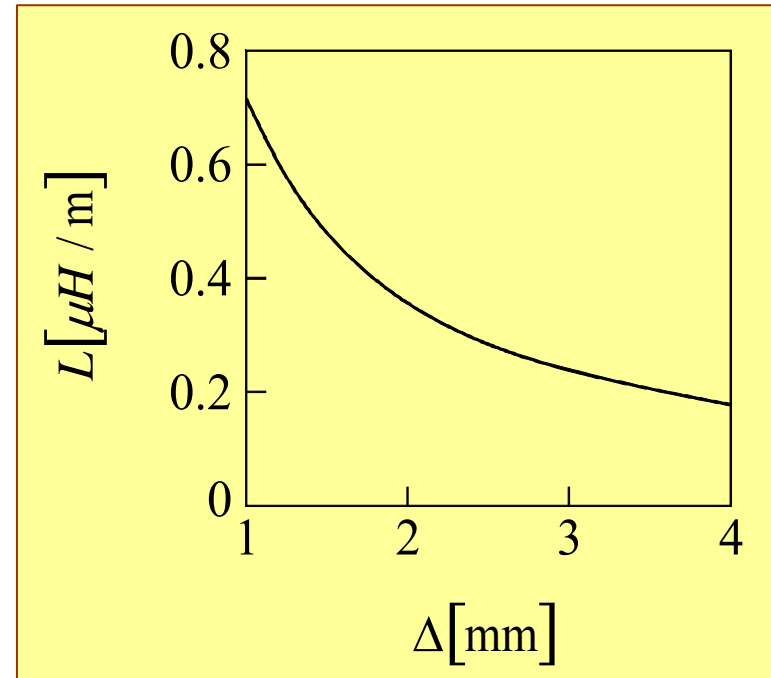
The characteristic impedance of a stripline as a function of d (Eq. (1.8.18)). The impedance decreases as d decreases, due to increase in the capacitance per unit length of the stripline as shown in Figure 20. The symmetrical case where $d = 2h$, is obtained at the knee of the graph corresponding to $d = 4$ mm. An asymptotic behavior is observed as d becomes large compared to h,Δ. [$h = \Delta = 2$ mm, $\varepsilon_r = 10$, $n = 1,2,\cdots 200$].
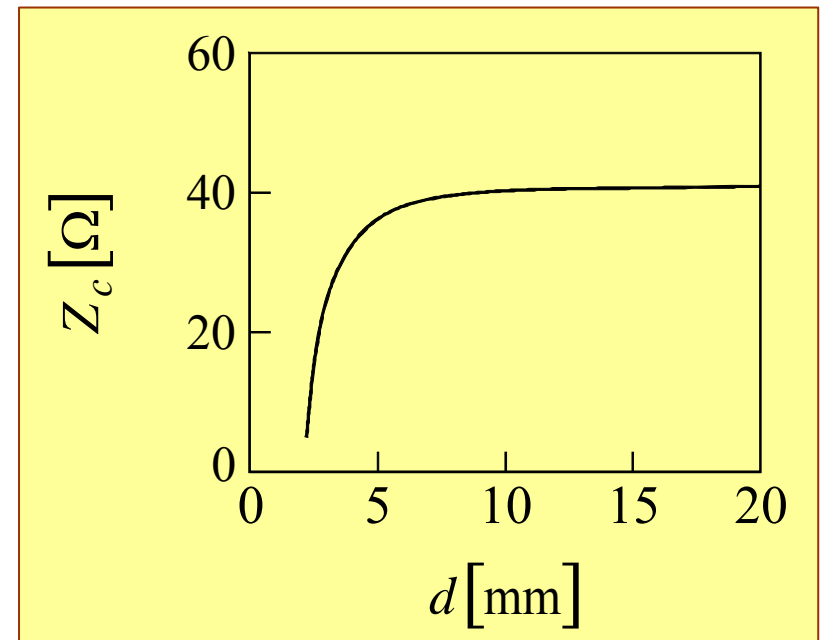
1.11.4 Solution to Exercise 1.17

Compare micro-strip and strip-line from the perspective of sensitivity to the dielectric coefficient.

The characteristic impedance of a microstrip (the red solid line) and a stripline (the blue dotted line) as a function of ε_r. The characteristic impedances of both the microstrip and the stripline decrease as ε_r increases. This result can be explained by noting that increasing the dielectric constant increases the capacitance per unit length of the line (C) and thus decreases the characteristic impedance, which is inverse proportional to the capacitance according to $Z_c = 1/CV_{ph}$, where V_{ph} is the phase velocity, in turn ε_r decreases V_{ph} but in lower rate than the increase of C. [$h = \Delta = 2$ mm, $d = 4$ mm (stripline), $\omega = 20$ mm, $n = 1, 2, \cdots 200$, and $v = 0,1,\ldots 200$].
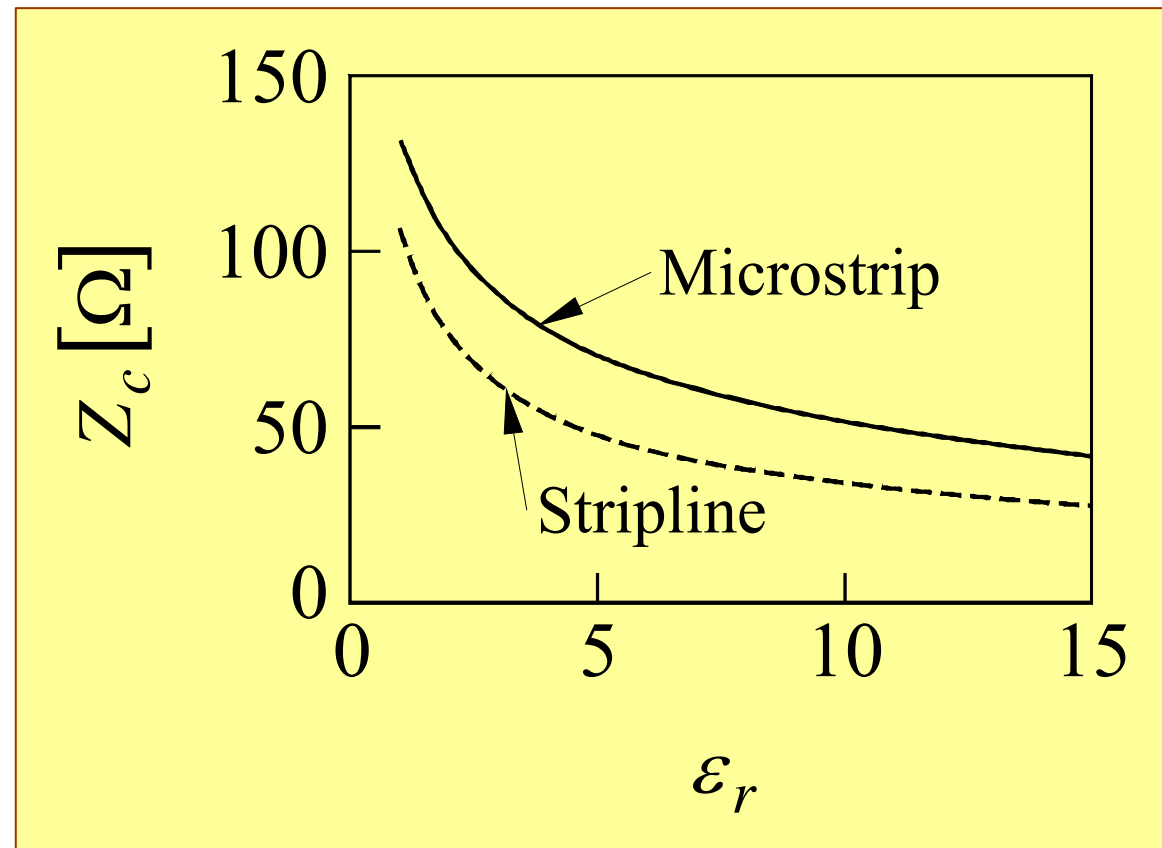
The derivative of the characteristic impedance of a microstrip (solid line) and a stripline (dotted line) as a function of ε_r. At low values of ε_r, the absolute value of the $dZ_c / d\varepsilon_r$ is larger in stripline (dotted line) than in microstrip (solid line), implying a higher sensitivity to variations in ε_r in the stripline geometry at that low range of ε_r. As ε_r is increased, the sensitivity of the microstrip characteristic impedance (Z_c) becomes slightly larger than that of the stripline. At high values of ε_r, the sensitivity of both configurations approach zero asymptotically as expected. [$h = \Delta = 2$ mm, $d = 4$ mm, $\omega = 20$ mm, $n = 1,2,\cdots 200$, and $v = 0,1,\ldots 200$].
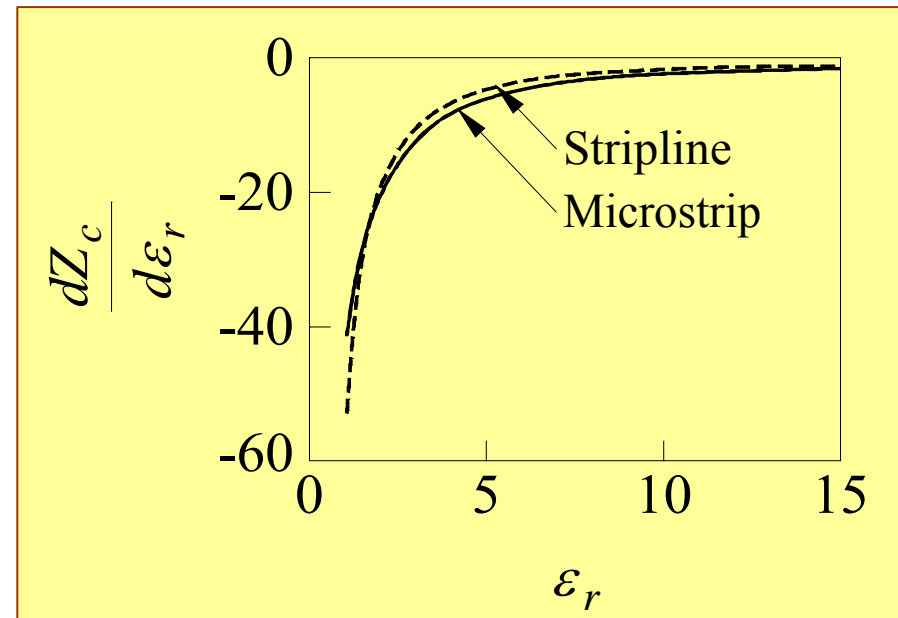
Sensitivity to dielectric coefficient of a microstrip (solid line) and a stripline (dotted line) as a function of ε_r. The figure shows clearly that the stripline geometry is more sensitive with respect to ε_r than the microstrip configuration [$h = \Delta = 2$ mm, $d = 4$ mm (stripline), $\omega = 20$ mm, $n = 1,2,\cdots 200$, and
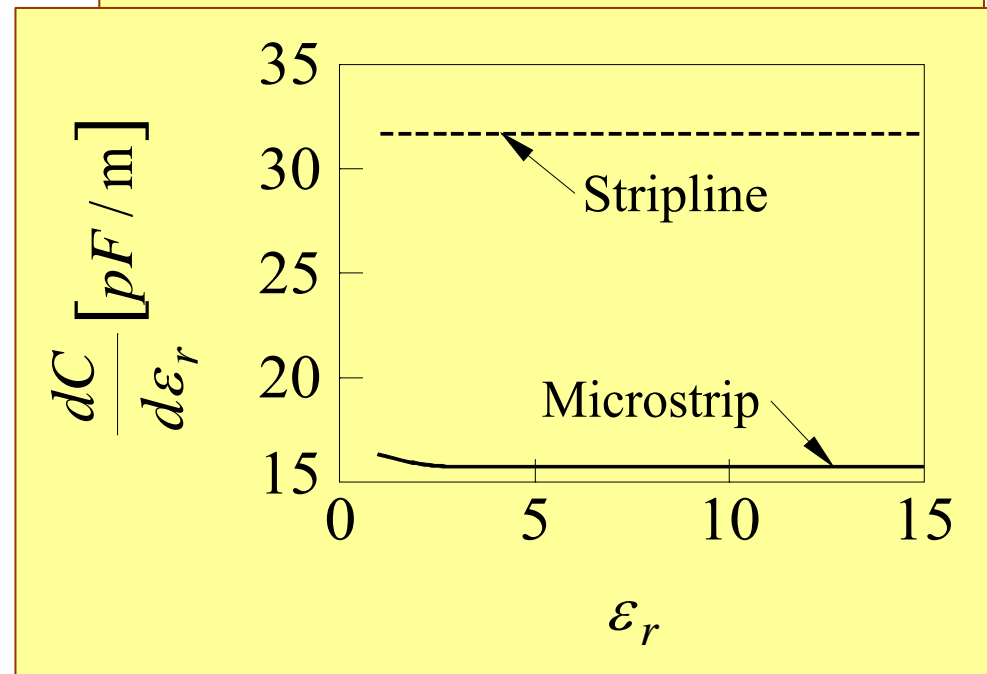
$v = 0, 1, \ldots 200$].

      The normalized phase velocity of a microstrip (solid line) and a stripline (dotted line) as a function of ε_r, V_{ph} of stripline is simply $c / \sqrt{\varepsilon_r}$ (for a TEM mode), V_{ph} of microstrip (for the quasi-TEM mode) is $c / \sqrt{\varepsilon_{eff}}$, where ε_{eff} is given by Eq. (7.17). As ε_r is increased, V_{ph} / c decreases as expected, according to $1 / \sqrt{\varepsilon_r}$ and $1 / \sqrt{\varepsilon_{eff}}$ relations, for stripline and microstrip cases respectively, where the following inequality holds $1 < \varepsilon_{eff} < \varepsilon_r$. In the special case $\varepsilon_r = 1$ where only vacuum is experienced by the electromagnetic field, V_{ph} is simply c for both geometries [$h = \Delta = 2$ mm, $d = 4$ mm (stripline), $\omega = 20$ mm, $n = 1, 2, \cdots 200$, and $v = 0, 1, \ldots 200$].
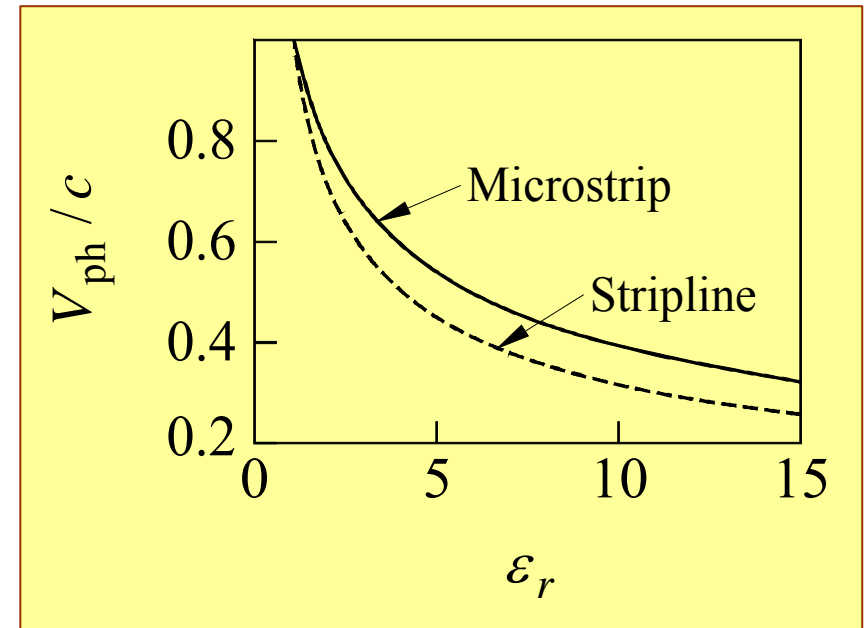
      The derivative of the normalized phase velocity of a microstrip (solid line) and a stripline (dotted line) as a function of ε_r. The absolute value of the derivative is higher for the stripline case compared to the microstrip case, implying higher sensitivity in the stripline with respect to changes in ε_r. For relatively high values of ε_r the sensitivity of both configurations approaches zero asymptotically [$h = \Delta = 2$ mm, $d = 4$ mm (stripline),

70
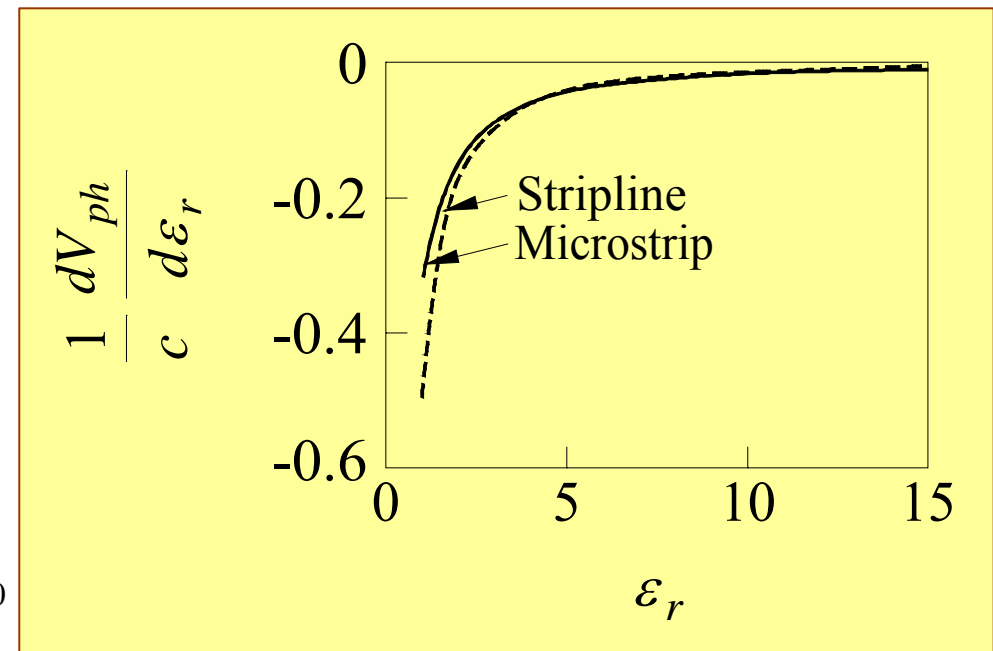
Chapter 2: Waveguides – Fundamentals

2.1 General Formulation

So far we have examined the propagation of electromagnetic waves in a structure consisting of two or more metallic surfaces. This type of structure supports a transverse electromagnetic (TEM) mode. However, if the electromagnetic characteristics of the structure are not uniform across the structure, the mode is not a pure TEM mode but it has a longitudinal field component.

In this chapter we consider the propagation of an electromagnetic wave in a closed metallic structure which is infinite in one direction (z) and it has a rectangular (or cylindrical) cross-section as illustrated in Fig. 1. While the use of this type of waveguide is relatively sparse these days, we shall adopt it since it provides a very convenient mathematical foundation in the form of a set of trigonometric functions. This is an orthogonal set of functions which may be easily manipulated. The approach is valid whenever the transverse dimensions of the structure are comparable with the wavelength.
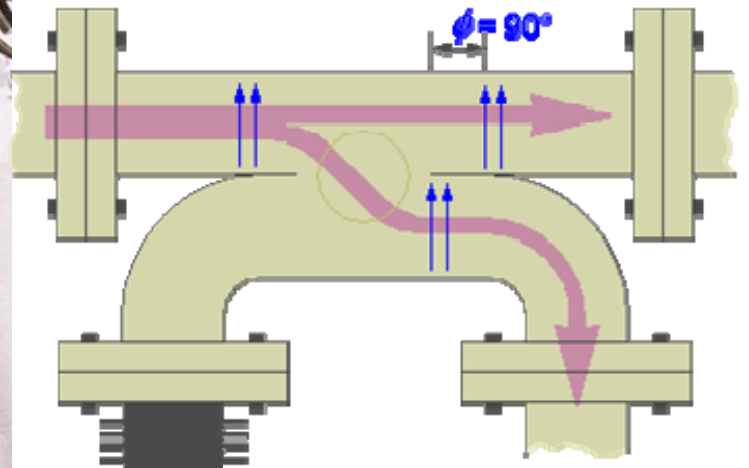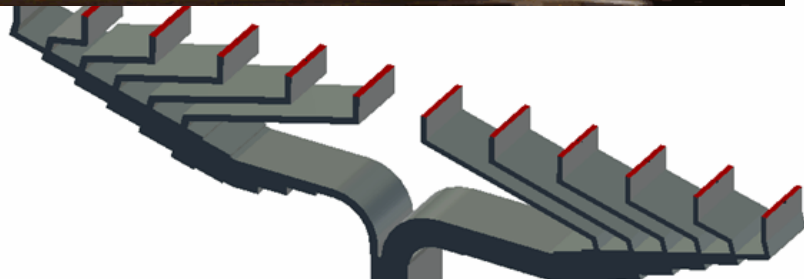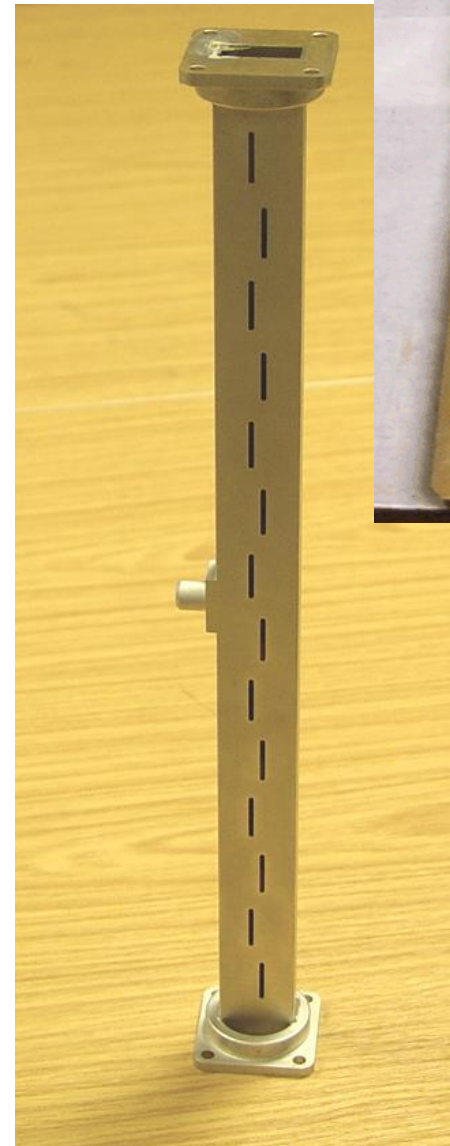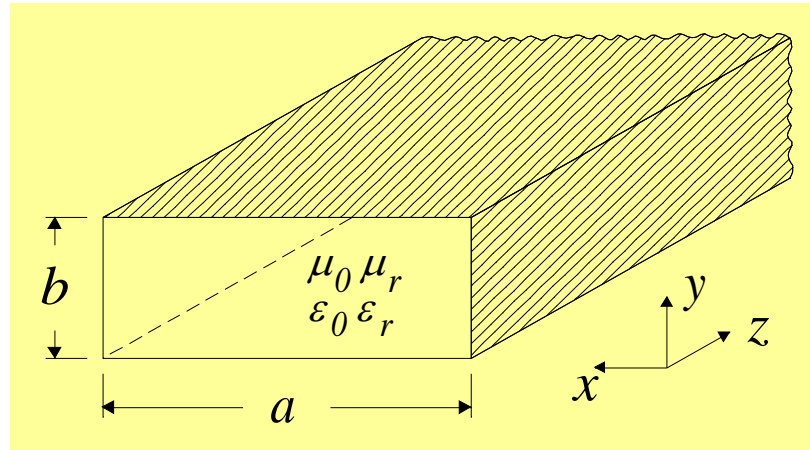
Rectangular waveguide; a and b are the dimensions of the rectangular cross section. a corresponding to the x coordinate, b to the y coordinate.

The first step in our analysis is to establish the basic ***assumptions*** of our approach:

a) The electromagnetic characteristics of the medium: $\mu = \mu_0 \mu_r$ and $\varepsilon = \varepsilon_0 \varepsilon_r$.

b) Steady state operation of the type $\exp(j\omega t)$.

c) No sources in the pipe.

d) Propagation in the z direction -- $\exp(-jk_z z)$; k_z can be either real or imaginary or complex number.

e) The conductivity (σ) of the metal is assumed to be arbitrary large $(\sigma \to \infty)$.
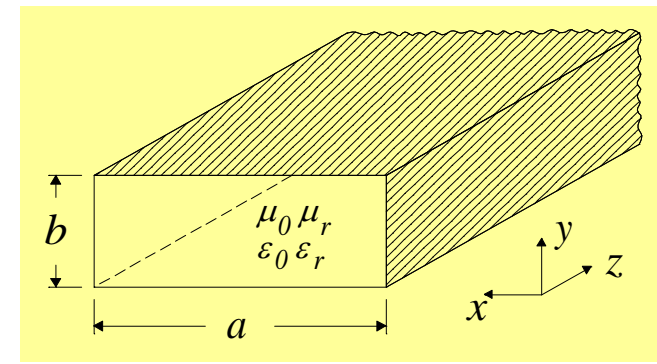
Subject to these assumptions Maxwell's Equations may be written in the following form

$$\nabla \times \vec{E} = -j\omega\mu\vec{H} \qquad \vec{\nabla} \times \vec{H} = j\omega\varepsilon\vec{E} \qquad (2.1.1)$$

Substituting one equation into the other we obtain the wave equation

$$\vec{\nabla} \times (\vec{\nabla} \times \vec{E}) = -j\omega\mu(\vec{\nabla} \times \vec{H}) \qquad \vec{\nabla} \times (\vec{\nabla} \times \vec{H}) = j\omega\varepsilon(\vec{\nabla} \times \vec{E})$$

$$\nabla(\vec{\nabla} \cdot \vec{E}) - \nabla^2\vec{E} = -j\omega\mu(j\omega\varepsilon\vec{E}) \qquad \nabla(\vec{\nabla} \cdot \vec{H}) - \nabla^2\vec{H} = j\omega\varepsilon(-j\omega\mu\vec{H})$$

$$\nabla(\vec{\nabla} \cdot \vec{E}) - \nabla^2\vec{E} = \left(\frac{\omega}{v}\right)^2\vec{E} \qquad \nabla(\vec{\nabla} \cdot \vec{H}) - \nabla^2\vec{H} = \left(\frac{\omega}{v}\right)^2\vec{H}$$

$$\vec{\nabla} \cdot \varepsilon\vec{E} = 0 \qquad \vec{\nabla} \cdot \mu\vec{H} = 0 \qquad (2.1.2)$$

$$\boxed{\left[\nabla^2 + \left(\frac{\omega}{v}\right)^2\right]\vec{E} = 0} \qquad \boxed{\left[\nabla^2 + \left(\frac{\omega}{v}\right)^2\right]\vec{H} = 0}$$

where $v = 1/\sqrt{\mu\varepsilon}$ is the phase-velocity of a plane wave in the medium. Specifically, we conclude that the z components of the electromagnetic field satisfies

$$\left[\nabla^2 + \frac{\omega^2}{v^2}\right]E_z = 0, \qquad \left[\nabla^2 + \frac{\omega^2}{v^2}\right]H_z = 0 \qquad (2.1.3)$$

74
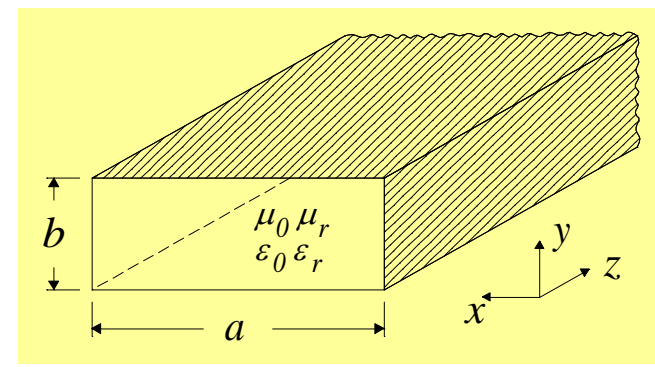
and subject to assumption (d) we have

$$\left(\nabla_\perp^2 - k_z^2 + \frac{\omega^2}{v^2}\right)E_z = 0 \qquad \left(\nabla_\perp^2 - k_z^2 + \frac{\omega^2}{v^2}\right)H_z = 0.$$

As a second step, it will be shown that assuming the longitudinal components of the electromagentic field are known, the transverse components are readily established. For this purpose we observe that Faraday's Law reads

$$\nabla \times \vec{E} = -j\omega\mu\vec{H} \Rightarrow \begin{vmatrix} 1_x & 1_y & 1_z \\ \partial_x & \partial_y & -jk_z \\ E_x & E_y & E_z \end{vmatrix} = -j\omega\mu\vec{H}. \qquad (2.1.4)$$

(i) 1_x: $\quad \partial_y E_z + jk_z E_y \quad = - \quad j\omega\mu H_x \quad \rightsquigarrow \quad jk_z E_y + j\omega\mu H_x \quad = - \quad \partial_y E_z$

(ii) 1_y: $-\ (\partial_x E_z + jk_z E_x) \quad = - \quad j\omega\mu H_y \quad \rightsquigarrow \quad -jk_z E_x + j\omega\mu H_y \quad = \quad \partial_x E_z$

(iii) 1_z: $\quad \partial_x E_y - \partial_y E_x \quad = - \quad j\omega\mu H_z \quad \rightsquigarrow \quad \partial_x E_y - \partial_y E_x \quad = - \quad j\omega\mu H_z.$

In a similar way, Ampere's law reads

$$\vec{\nabla} \times \vec{H} = j\omega\varepsilon\vec{E} \Rightarrow \begin{vmatrix} 1_x & 1_y & 1_z \\ \partial_x & \partial_y & -jk_z \\ H_x & H_y & H_z \end{vmatrix} = j\omega\varepsilon\vec{E}, \qquad (2.1.5)$$

75
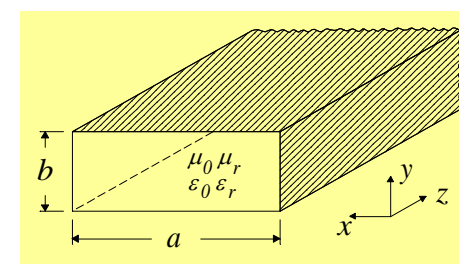
or explicitly

(iv) 1_x: $\quad \partial_y H_z + jk_z H_y \quad = \quad j\omega\varepsilon E_x \quad \rightsquigarrow \quad j\omega\varepsilon E_x - jk_z H_y \quad = \quad \partial_y H_z$

(v) 1_y: $-\ (\partial_x H_z + jk_z H_x) \quad = \quad j\omega\varepsilon E_y \quad \rightsquigarrow \quad j\omega\varepsilon E_y + jk_z H_x \quad = - \quad \partial_x H_z$

(vi) 1_z: $\quad \partial_x H_y - \partial_y H_x \quad = \quad j\omega\varepsilon E_z \quad \rightsquigarrow \quad \partial_x H_y - \partial_y H_x \quad = \quad j\omega\varepsilon E_z.$

From equations **(ii)** and **(iv)** we obtain

$$
\left.
\begin{aligned}
-jk_z E_x + j\omega\mu H_y &= \partial_x E_z \\
j\omega\varepsilon E_x - jk_z H_y &= \partial_y H_z
\end{aligned}
\right\}
\rightarrow
\quad
\begin{aligned}
H_y &= \frac{jk_z\omega\varepsilon}{k_z^2 - (\omega/v)^2}\left[\frac{1}{k_z}\partial_x E_z + \frac{1}{\omega\varepsilon}\partial_y H_z\right] \\[2mm]
E_x &= \frac{j}{k_z^2 - (\omega/v)^2}\left[k_z\partial_x E_z + \omega\mu\partial_y H_z\right]
\end{aligned}
\tag{2.1.6}
$$

It is convenient at this point to define the **transverse wavenumber**

$$
k_\perp^2 \equiv \frac{\omega^2}{v^2} - k_z^2
\tag{2.1.7}
$$

That as we shall shortly see, has a special physical meaning.
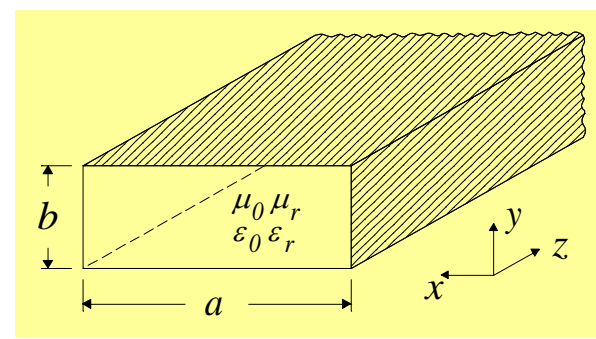
This allows us to write the last two expressions in the following form

$$E_x = \frac{-jk_z}{k_\perp^2} \partial_x E_z - \frac{j\omega\mu}{k_\perp^2} \partial_y H_z, \tag{2.1.8}$$

$$H_y = \frac{-j\omega\varepsilon}{k_\perp^2} \partial_x E_z - \frac{jk_z}{k_\perp^2} \partial_y H_z. \tag{2.1.9}$$

In a similar way, we use equations **(i)** and **(v)** and obtain

$$E_y = \frac{-jk_z}{k_\perp^2} \partial_y E_z + \frac{j\omega\mu}{k_\perp^2} \partial_x H_z \tag{2.1.10}$$

$$H_x = \frac{j\omega\varepsilon}{k_\perp^2} \partial_y E_z - \frac{jk_z}{k_\perp^2} \partial_x H_z. \tag{2.1.11}$$

Equations (2.1.8),(2.1.10) and (2.1.9),(2.1.11) can be written in a vector form

$$\boxed{\vec{E}_\perp = -\frac{jk_z}{k_\perp^2} \nabla_\perp E_z + \frac{j\omega\mu}{k_\perp^2} \vec{1}_z \times \nabla_\perp H_z} \tag{2.1.12}$$

$$\boxed{\vec{H}_\perp = -\frac{jk_z}{k_\perp^2} \nabla_\perp H_z - \frac{j\omega\varepsilon}{k_\perp^2} \vec{1}_z \times \nabla_\perp E_z}. \tag{2.1.13}$$

Comments:

1. The wave equations for E_z and H_z with the corresponding boundary conditions and the relations in ((2.1.12)--(2.1.13)) determine the electromagnetic field in the entire space (at any time).

2. Note that the only assumption made so far was that in the z direction the propagation is according to $\exp(-jk_z z)$. No boundary conditions have been imposed so far.

3. Therefore it is important to note within the framework of the present notation that ***TEM mode*** ($H_z = 0, E_z = 0$) is possible provided that $k_\perp \equiv 0$ or substituting in the wave equations
$$\nabla_\perp^2 \vec{E}_\perp = 0; \qquad \nabla_\perp^2 \vec{H}_\perp = 0. \tag{2.1.14}$$

4. By the superposition principle and the structure of ((2.1.12)--(2.1.13)), the ransverse field components may be derived from the longitudinal ones.

$$\text{Complete Solution} = \underbrace{(E_z = 0) \text{ and}(H_z \neq 0)}_{\text{Transverse Electric(TE)}} + \underbrace{(E_z \neq 0) \text{ and } (H_z = 0)}_{\text{Transverse Magnetic(TM)}}.$$

2.2 Transverse Magnetic (TM) Mode [$H_z = 0$]
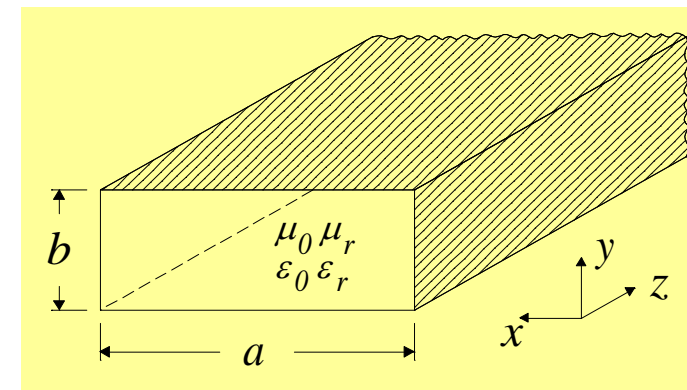
In this section our attention will be focused on a specific case where $H_z = 0$. This step is justified by the fact that equations ((2.1.12)--(2.1.13)) are linear, therefore by virtue of the superposition principle (e.g. circuit theory) and regarding H_z and E_z as sources of the transverse field, we may turn off one and solve for the other and vice versa. As indicated in the last comment of the previous section, the overall solution is, obviously the superposition of the two. The boundary conditions impose that the longitudinal electric field E_z vanishes on the metallic wall therefore

$$E_z = \sum_{n,m} A_{nm} \sin\left(\frac{\pi m x}{a}\right) \sin\left(\frac{\pi n y}{b}\right) e^{-jk_{zn,m}z}. \tag{2.2.1}$$

This further implies that the transverse wave vector, $k_\perp$, is entirely determined by the geometry of the waveguide (substitute in (2.1.3))

$$k_\perp^2 = \left(\frac{\pi m}{a}\right)^2 + \left(\frac{\pi n}{b}\right)^2 = \frac{\omega^2}{v^2} - k_z^2. \tag{2.2.2}$$

From these two equations we obtain

$$k_{z,n,m}^2 = \frac{\omega^2}{v^2} - k_\perp^2 = \frac{\omega^2}{v^2} - \left(\frac{\pi m}{a}\right)^2 - \left(\frac{\pi n}{b}\right)^2$$

$$k_z = \pm \sqrt{\frac{\omega^2}{v^2} - \left(\frac{\pi m}{a}\right)^2 - \left(\frac{\pi n}{b}\right)^2}. \qquad (2.2.3)$$
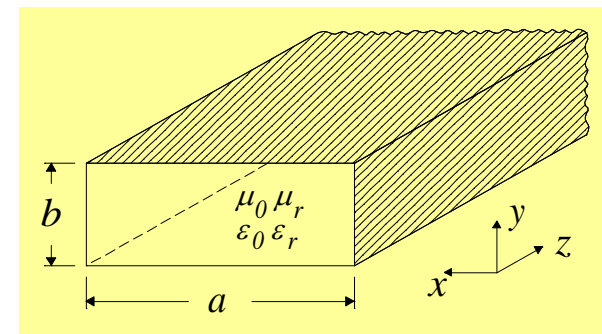
This expression represents the *dispersion equation* of the electromagnetic wave in the waveguide.

Exercise 2.1: Analyze the effect of the material characteristics on the cut-off frequency.

Exercise 2.2: What is the impact of the geometry?

Exercise 2.3: Can two different modes have the same cut-off frequency?!
What is the general condition for such a degeneracy to occur?
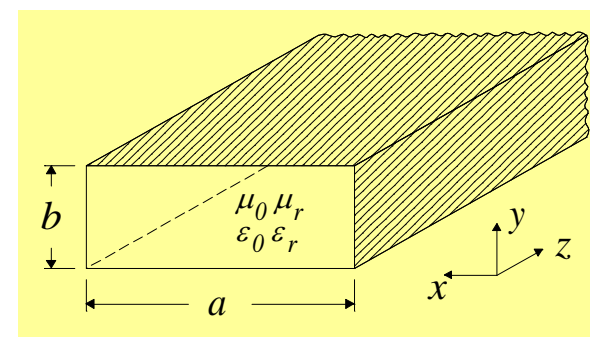
Comments:

a) Asymptotically ($\omega \gg k_\perp v$) this dispersion relation behaves as if no walls were present i.e. $\omega \simeq k_z v$.

b) There is an angular frequency $\omega_{c,n,m}$ for which the wavenumber k_z **vanishes**. This is called the **cutoff frequency**.

$$\left(\omega_c\right)_{m,n} \equiv v k_\perp = v \sqrt{\left(\frac{\pi m}{a}\right)^2 + \left(\frac{\pi n}{b}\right)^2} \Rightarrow \left(f_c\right)_{m,n} = \frac{1}{2} v \sqrt{\left(\frac{m}{a}\right)^2 + \left(\frac{n}{b}\right)^2}, \qquad (2.2.4)$$

where $v = c/\sqrt{\varepsilon_r \mu_r}$.

c) Below this frequency the wavenumber k_z is imaginary and the wave **decays** or **grows exponentially** in space.

d) The indices n and m define the mode $TM_{m,n}$; m represents the wide transverse dimension (x) whereas n represents the narrow transverse dimension (y).

81
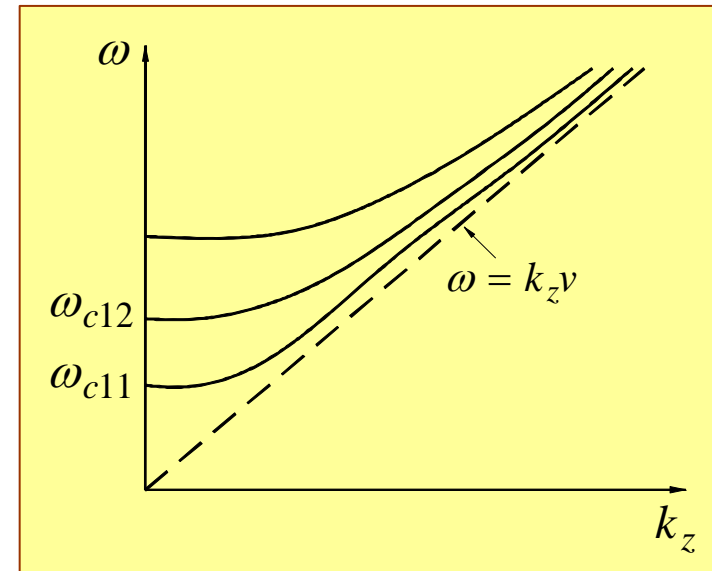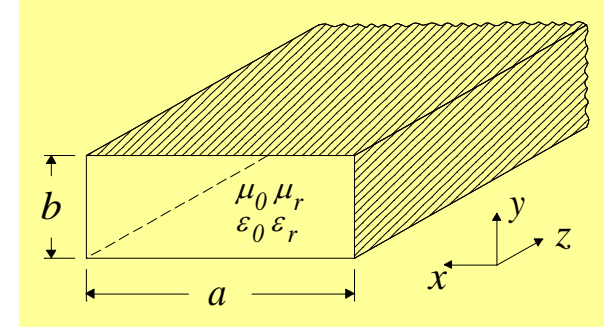
2.3 Transverse Electric (TE) Mode [$E_z = 0$]

The second possible solution according to (2.1.12)--(2.1.13) is when $E_z = 0$ and since the derivative of the longitudinal magnetic field H_z vanishes on the walls (see (2.1.12)) we conclude that

$$H_z = \sum_{m,n} A_{m,n} \cos\left(\frac{\pi m x}{a}\right) \cos\left(\frac{\pi n y}{b}\right) e^{-jk_{zm,n}z}. \tag{2.3.1}$$

The expression for the transverse wavenumber $k_\perp$ is identical to the TM case and so is the dispersion relation. However, note that contrary to the TM mode where if n or m were zero the field component vanishes, in this case we may allow $n = 0$ or $m = 0$ without forcing a trivial solution.
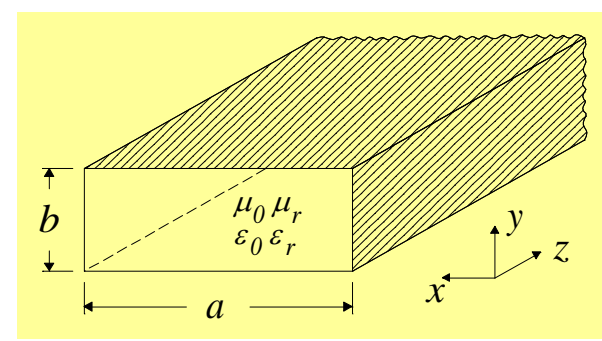
For convenience, we present next a comparison table of the various field components of the two modes.

TM mode	TE mode
$E_z = \sum_{mn} A_{mn} \sin\left(\dfrac{\pi m x}{a}\right) \sin\left(\dfrac{\pi n y}{b}\right) e^{-jk_{zmn}z}$	$H_z = \sum_{mn} B_{mn} \cos\left(\dfrac{\pi m x}{a}\right) \cos\left(\dfrac{\pi n y}{b}\right) e^{-jk_{mn}z}$
$H_x = \sum_{mn} A_{mn} \dfrac{j\omega\varepsilon}{k_{\perp n,m}^2}\left(\dfrac{\pi n}{b}\right)\sin\left(\dfrac{\pi m x}{a}\right)\cos\left(\dfrac{\pi n y}{b}\right)\ldots$	$E_x = \sum_{mn} B_{mn} \dfrac{j\omega\mu}{k_\perp^2}\left(\dfrac{\pi n}{b}\right)\cos\left(\dfrac{\pi m x}{a}\right)\sin\left(\dfrac{\pi n y}{b}\right)\ldots$
$H_y = \sum_{mn} A_n \dfrac{-j\omega\varepsilon}{k_\perp^2}\left(\dfrac{\pi m}{a}\right)\cos\left(\dfrac{\pi m x}{a}\right)\sin\left(\dfrac{\pi n y}{b}\right)\ldots$	$E_y = \sum_{mn} B_{mn} \dfrac{j\omega\mu}{k_\perp^2}\left(-\dfrac{\pi m}{a}\right)\sin\left(\dfrac{\pi m x}{a}\right)\cos\left(\dfrac{\pi m y}{b}\right)\ldots$
$H_z = 0$	$E_z = 0$
$E_x = \sum_{mn} A_{mn} \dfrac{-jk_z}{k_\perp^2}\left(\dfrac{\pi m}{a}\right)\cos\left(\dfrac{\pi m x}{a}\right)\sin\left(\dfrac{\pi n y}{b}\right)\ldots$	$H_x = \sum_{mn} B_{mn} \dfrac{+jk_z}{k_\perp^2}\left(\dfrac{\pi m}{a}\right)\sin\left(\dfrac{\pi m x}{a}\right)\cos\left(\dfrac{\pi m y}{b}\right)\ldots$
$E_y = \sum_{mn} A_{mn} \dfrac{-jk_z}{k_\perp^2}\left(\dfrac{\pi n}{b}\right)\sin\left(\dfrac{\pi m x}{a}\right)\cos\left(\dfrac{\pi n y}{b}\right)\ldots$	$H_y = \sum_{mn} B_{mn} \dfrac{+jk_z}{k_\perp^2}\left(\dfrac{\pi n}{b}\right)\cos\left(\dfrac{\pi m x}{a}\right)\sin\left(\dfrac{\pi m y}{b}\right)\ldots$
$E_{x,mn} = Z_{mn}^{(TM)} H_{y,mn} \;;\; Z_{mn}^{(TM)} = \sqrt{\dfrac{\mu}{\varepsilon}}\left[1-\left(\dfrac{f_{c,m,n}}{f}\right)^2\right]^{1/2}$	$H_{x,mn} = -\dfrac{E_{y,mn}}{Z_{mn}^{(TE)}} \;;\; Z_{mn}^{(TE)} = \sqrt{\dfrac{\mu}{\varepsilon}}\left[1-\left(\dfrac{f_{c,m,n}}{f}\right)^2\right]^{-1/2}$
$E_{y,mn} = -Z_{mn}^{(TM)} H_{x,mn}$	$H_{y,mn} = \dfrac{E_{x,mn}}{Z_{mn}^{(TE)}}$

Exercise 2.4: Check all the expressions presented in the table above.
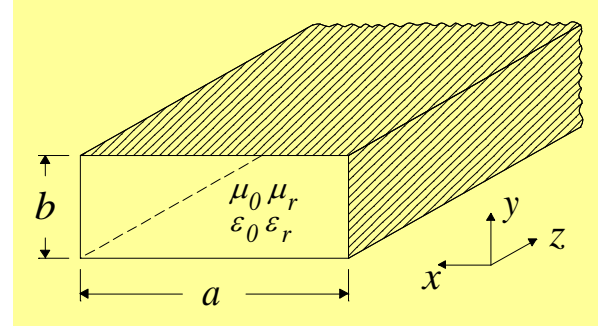
Comments:

1. The **phase velocity** of the wave is the velocity an imaginary observer has to move in order to measure a constant phase i.e. $\omega t - k_z z = \text{const.}$. This implies,

$$ v_{ph} \equiv \frac{\omega}{k_z} = v \left[1 - \frac{f_c^2}{f^2} \right]^{-1/2} . \tag{2.3.2} $$

2. The phase velocity is always **faster** than v!! Specifically, in vacuum the phase velocity of a wave is larger than c. In fact close to cutoff this velocity becomes ``infinite"!!

3. The **group velocity** is defined from the requirement that an observer sees a constant envelope in the case of a relatively narrow wave packet. At the continuous limit this is determined by

$$ v_{gr} = \frac{\partial \omega}{\partial k_z} = v \left[1 - \frac{f_c^2}{f^2} \right]^{1/2} . \tag{2.3.3} $$

4. The group velocity is alway **smaller** than v. Specifically, in vacuum it is always smaller than c. It is the group velocity is responsible to information transfer.

5. When the waveguide is uniform

$$ v_{ph} v_{gr} = v^2 . \tag{2.3.4} $$
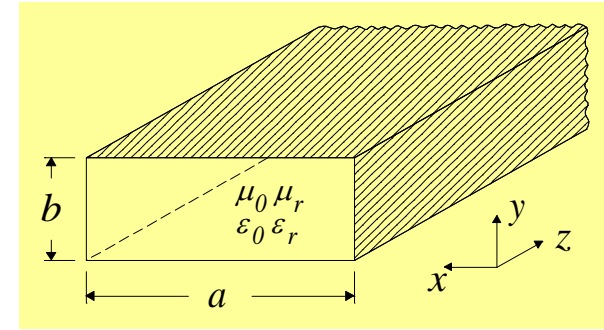
2.4 Power Considerations

2.4.1 Power Flow

Let us now consider the power associated with a specific TM mode; say

$$E_z = A_{mn} \sin\left(\frac{\pi m x}{a}\right)\sin\left(\frac{\pi n y}{b}\right)e^{-jk_{z,mn}z}.$$

At this stage, for simplicity sake, we assume that this is the **only** mode in the waveguide. Based on Poynting's theorem, the power carried by this mode is given by

$$P_{mn} = Re\left\{\int_0^a dx \int_0^b dy\, S_{z,mn}\right\}. \tag{2.4.1}$$

Explicitly the longitudinal component of the Poynting vector is

$$S_{z,mn} = \frac{1}{2}(\vec{E}\times\vec{H}^*)\cdot\vec{1}_z = \frac{1}{2}[E_x H_y^* - E_y H_x^*]$$

$$= \frac{1}{2}\left[Z^{(TM)}\left|H_y\right|^2 + Z^{(TM)}\left|H_x\right|^2\right] = \frac{1}{2}Z^{(TM)}\left[\left|H_y\right|^2 + \left|H_x\right|^2\right]. \tag{2.4.2}$$

Above cutoff the characteristic impedance is a real number therefore the next step is to substitute the explicit expressions for the magnetic field components and perform the spatial integration:
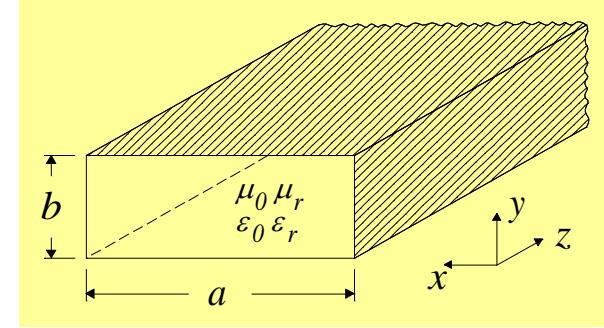
$$P_{mn} = \frac{1}{2} Z^{(TM)} \int_0^a dx \int_0^b dy \left[|H_y|^2 + |H_x|^2 \right]$$

$$= \frac{1}{2} Z^{(TM)} |A_{mn}|^2 \frac{\omega^2 \varepsilon^2}{k_\perp^4} \frac{a}{2} \cdot \frac{b}{2} \left[\underbrace{\left(\frac{\pi m}{a}\right)^2 + \left(\frac{\pi n}{b}\right)^2}_{k_\perp^2} \right]$$

$$P_{mn} = \frac{1}{2} Z^{(TM)} |A_{mn}|^2 \frac{\omega^2 \varepsilon^2}{k_\perp^2} \frac{ab}{4}. \qquad (2.4.3)$$

The last expression represents the **average power** carried by the specific mode.

Exercise 2.5: What is the power at any particular point in time?

Exercise 2.6: Since the two sets $\sin(\pi mx / a)$ and $\sin(\pi ny / b)$ are two orthogonal sets of functions, the total average power carried by the wave in the forward direction is a superposition of the average power carried by each individual mode separately. In other words show that $P = \sum_{n,m} P_{mn}$.

Exercise 2.7: Show that below cutoff, the power is **identically zero** although the field is **not zero**.
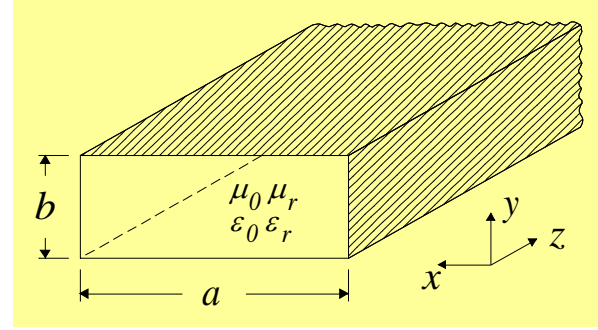
Exercise 2.8: Note that the average power is proportional to the average magnetic energy per unit length. Calculate this quantity. Compare it with the average electric energy per unit length.

Exercise 2.9: Calculate the energy velocity of a specific mode $v_{EM} = \langle P \rangle / W_{EM}$. Compare to the group velocity. What happens if the frequency is below cutoff?

Exercise 2.10: Repeat the last exercise for a **superposition** of modes $A_{n,m}$.
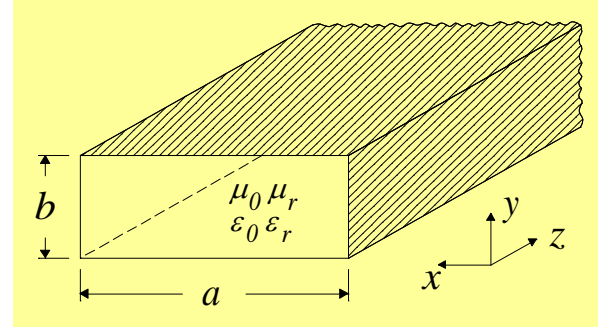
2.4.2 Ohm Loss

So far it was assumed that the walls are made of an **ideal metal** ($\sigma \to \infty$). If this is not the case (σ) a finite amount of power is absorbed by the wall. In order to calculate this absorbed power we firstly realize that the magnetic field is ``discontinuous'' which is compensated by a surface current

$$\vec{J}_s = \vec{n} \times \vec{H}. \tag{2.4.4}$$

This current flows in a very thin layer which is assumed to be on the scale of the **skin-depth** [$J = J_s / \delta$] therefore, the dissipated average power per unit length is given by

$$P_D = \frac{1}{2}\frac{1}{\sigma}\int_\delta dxdy \left|\vec{J}_s\right|^2, \tag{2.4.5}$$

or explicitly

$$P_D = \frac{1}{2\sigma}\oint dl\delta \left|\frac{\vec{J}_s}{\delta}\right|^2 = \frac{1}{2\delta\sigma}\oint dl\left|\vec{J}_s\right|^2 = \frac{R_s}{2}\oint dl\left|\vec{J}_s\right|^2, \tag{2.4.6}$$

where $\delta \equiv \sqrt{2/\omega\mu_o\sigma}$, $R_s \equiv \sqrt{\omega\mu_o/2\sigma}$ and the integration is over the **circumference** of the waveguide

88

$$P_D = \frac{1}{2} R_s \oint dl \, |\vec{J}_s|^2. \qquad (2.4.7)$$
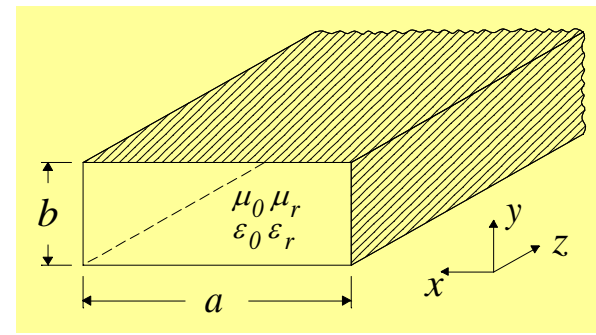
This is the **average electromagnetic power** per unit length which is converted into **heat** (dissipation) due to Ohm loss. Based on Poynting's theorem we may deduce that the spatial change in the electromagnetic power is given by

$$\frac{d}{dz} P = -P_D \qquad (2.4.8)$$

and since in case of a single mode both P and P_D are proportional to $|A|^2$,

$$P \propto |A|^2 \qquad \text{and} \qquad P_D \propto |A|^2 \qquad (2.4.9)$$

we conclude that the change in the amplitude of the mode is given by

$$\frac{d|A|^2}{dz} = -2\alpha |A|^2 \quad \Rightarrow \quad |A(z)|^2 = |A(z=0)|^2 \, e^{-2\alpha z}. \qquad (2.4.10)$$

The coefficient α represents the **exponential decay** of the amplitude and based on the arguments of above is given by

$$\alpha \equiv \frac{P_D}{2P}. \qquad (2.4.11)$$

Let us denote by $k_z^{(0)}$ the wavenumber in a lossless waveguide. Subject to the

89
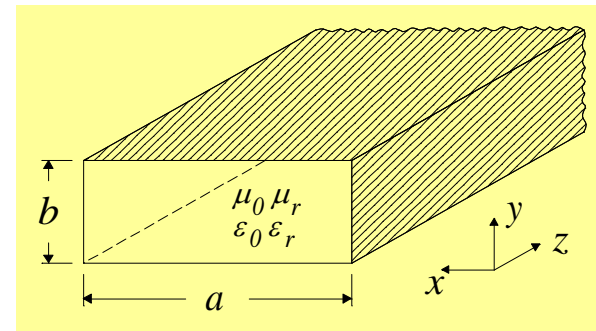
assumption of small losses $(k_z^{(0)} \gg \alpha)$ we can generalize the solution in a waveguide with lossy walls by $k_z = k_z^{(0)} - j\alpha$.

Exercise 2.11: Based on the previous calculation of the power show that this parameter is given by

$$\boxed{\alpha_{m,n}^{(TM)} = \frac{2R_s}{\eta\sqrt{1-(f_c/f)^2}} \frac{1}{b} \frac{m^2 b^3 + n^2 a^3}{m^2 b^2 a + n^2 a^3}} \qquad (2.4.12)$$

R_s is the surface resistance. Note that α is ***very large close to cutoff***.   Explain the difficulty/contradiction.

2.4.3 Dielectric Loss

If the dielectric coefficient of the material is not ideal, in other words, it has an imaginary component $\varepsilon_r = \varepsilon' - j\varepsilon''$, then the wavenumber is given by

$$k_z \simeq k_z^{(0)} - j\varepsilon'' \frac{1}{2} \frac{\omega}{c} \frac{\omega}{ck_z^{(0)}}, \qquad (2.4.13)$$

where we assumed that (i) the dielectric loss is small and (ii) the system operates remote from cutoff conditions [i.e. $k_z^{(0)} \gg \sqrt{\varepsilon''}\omega/c$].

We can now repeat the entire procedure described in the previous subsection for a TE mode. Here are the main steps and results
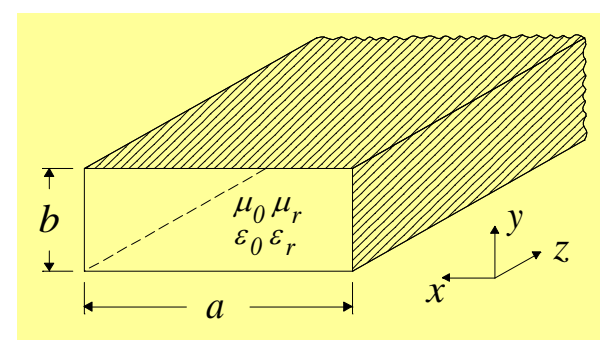
$$H_z = A_{mn} \cos\left(\frac{\pi m x}{a}\right) \cos\left(\frac{\pi n y}{b}\right) e^{-jk_{z,mn}z}, \quad P_{mn} = \mathrm{Re}\left\{\int_0^a dx \int_0^b dy S_{z,mn}\right\},$$

$$S_{z,mn} = \frac{1}{2}\left(E_x H_y^* - E_y H_x^*\right)_{mn} = \frac{1}{2Z_{mn}^{(TE)}}\left[|E_x|^2 + |E_y|^2\right]_{mn}. \tag{2.4.14}$$

$$
\begin{aligned}
P_{mn} &= \frac{1}{2}\frac{1}{Z_{mn}^{(TE)}}|A_{mn}|^2\left[\frac{\omega^2\mu^2}{k_\perp^4}\left(\frac{\pi n}{b}\right)^2\frac{1}{2}a\frac{1}{2}b + \frac{\omega^2\mu^2}{k_\perp^4}\left(\frac{\pi m}{a}\right)^2\frac{1}{2}a\frac{1}{2}b\right] \\
&= \frac{1}{8}\frac{ab}{Z_{mn}^{(TE)}}|A_{mn}|^2\frac{\omega^2\mu^2}{k_\perp^2}
\end{aligned}
\tag{2.4.15}
$$

$$\boxed{\alpha_{mn}^{(TE)} = \frac{2R_s}{\eta\left[1-(f_c/f)^2\right]^{1/2}}\frac{1}{b}\frac{m^2(b/a)^3 + n^2}{m^2(b/a)^2 + n^2}.} \tag{2.4.16}$$

Exercise 2.12: Check equation (2.4.16). In particular check the cases $n = 0$ or $m = 0$. Repeat all the exercises from the above (TM mode) for the TE mode. Make a comparison table where relevant.

Exercise 2.13: Note that both $\alpha^{(TE)}$ and $\alpha^{(TM)}$ are large close to cutoff and increase as $\sqrt{\omega}$ for large frequencies. In between there is a **minimum loss for an optimal frequency**. Calculate it.

Exercise 2.14: Calculate the loss **very close to cutoff**.

2.5 Mode Comparison

CHARACTERISTICS OF COMMON WAVEGUIDES

TE_{12}

TE_{10} TE_{20} TE_{21}
TE_{01} TM_{11} TE_{02} TM_{12}
TE_{11} TM_{21}

$b/a = 1$

1 2 3

$fel(f_c)_{TE_{10}}$

TE_{01}
TE_{10} TE_{20} TE_{11}
TM_{11}

$b/a = 1/2$

1 2 3

$fel(f_c)_{TE_{10}}$

0.20

$TE_{10} \dfrac{b}{a} = \dfrac{1}{10}$

0.16

Attenuation, decibels/meter

0.12

b

$\leftarrow a = 2" \rightarrow$

$TM_{11} \dfrac{b}{a} = \dfrac{1}{2}$

0.08

$TE_{10} \dfrac{b}{a} = \dfrac{1}{2}$

0.04

$TM_{11} \dfrac{b}{a} = 1$

$TE_{10} \dfrac{b}{a} = 1$

0

0   5,000   10,000   15,000   20,000   25,000   30,000

Frequency, megacycles/sec.
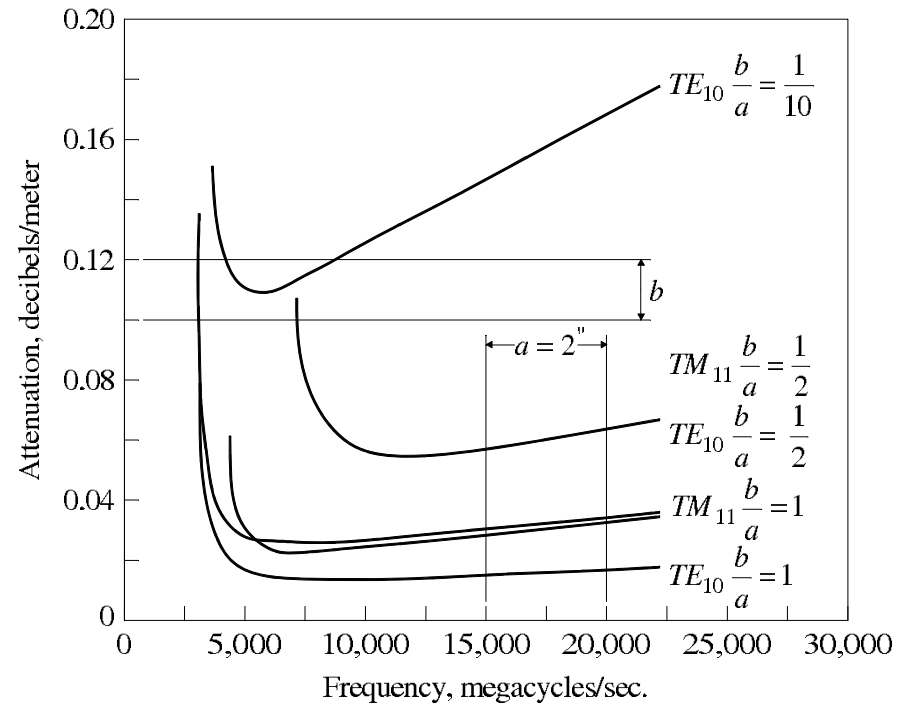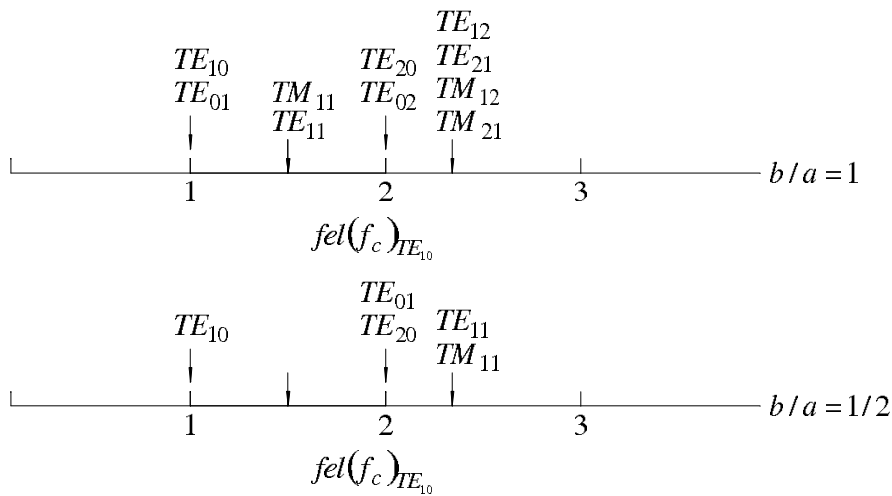
Attenuation due to copper losses in rectangular
waveguides of fixed width.

Mode comparison for a rectangular waveguide.

94
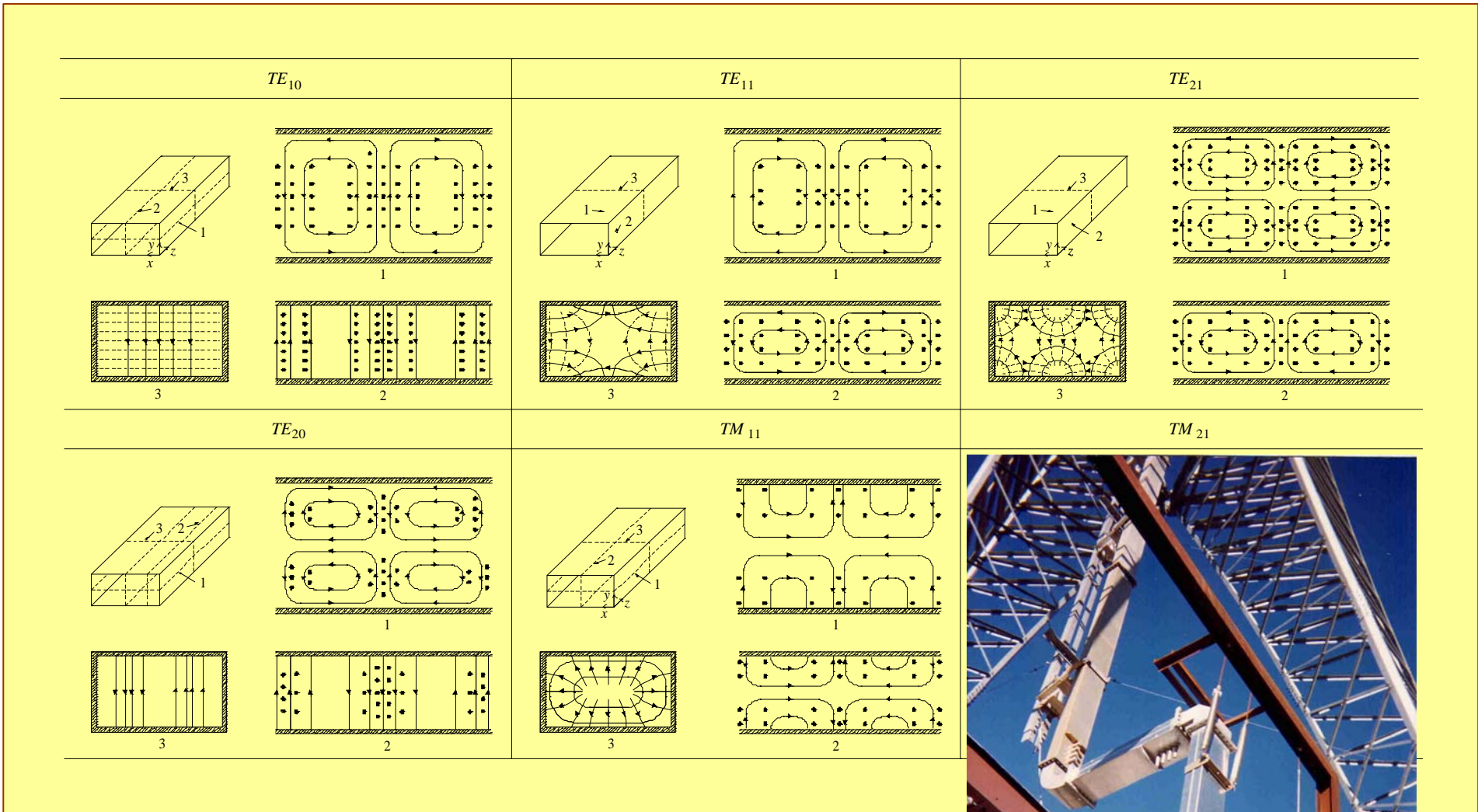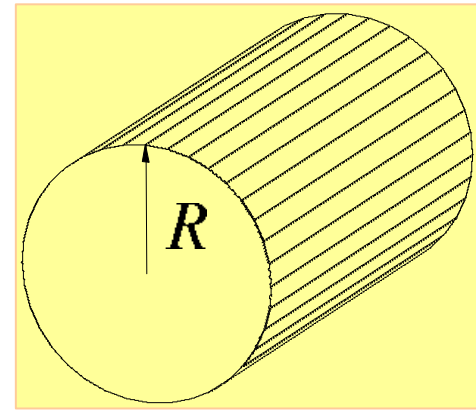
2.6 Cylindrical Waveguide

2.6.1 Transverse Magnetic (TM) Mode $[H_z = 0]$

In this section we shall investigate the propagation of a wave in a cylindrical waveguide. The longitudinal component of the electric field satisfies

$$[\nabla_\perp^2 + k_\perp^2] E_z = 0, \tag{2.6.1}$$

where $k_\perp^2 = \dfrac{\omega^2}{v^2} - k_z^2$ or explicitly

$$\left[\frac{\partial^2}{\partial r^2} + \frac{1}{r}\frac{\partial}{\partial r} + \frac{1}{r^2}\frac{\partial^2}{\partial \varphi^2} + k_\perp^2 \right] E_z = 0. \tag{2.6.2}$$

The solution of this equation subject to the **boundary conditions** $E_z(r = R) = 0$ reads

$$E_z = \sum_{n,s} J_n\left(p_{s,n} \frac{r}{R} \right) e^{-jk_{zs,n}z} \left[A_{ns} \cos(n\varphi) + B_{ns}\sin(n\varphi) \right], \tag{2.6.3}$$

where $J_n(u)$ if the n'th **order Bessel function of the first kind**. This function behaves similar to a trigonometric function ($\sin$ or $\cos$). It has zeros, denoted by $p_{s,n}$ i.e.,

$$p_{s,n}: \quad J_n(p_{s,n}) \equiv 0.$$
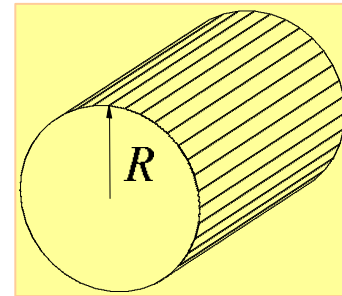
The first few **zeros** of the **Bessel function** are tabulated next.

	s=1	s=2	s=3
n= 0	2.405	5.52	8.654
n=1	3.832	7.016	10.174
n=2	5.135	8.417	11.62

Substituting (2.6.3) in (2.6.2) we obtain

$$\left[\frac{\partial^2}{\partial r^2} + \frac{1}{r}\frac{\partial}{\partial r} + \frac{1}{r^2}\frac{\partial^2}{\partial \varphi^2} + \left(\frac{p_{s,n}}{R} \right)^2 \right] E_z = 0 \tag{2.6.4}$$

thus

$$k_\perp^2 \equiv \frac{\omega^2}{v^2} - k_z^2 = \left(\frac{p_{s,n}}{R} \right)^2 \quad \Rightarrow \quad \boxed{k_{zs,n}^2 = \frac{\omega^2}{v^2} - \frac{p_{s,n}^2}{R^2}}. \tag{2.6.5}$$

Based on this expression the characteristic impedance of the TM mode is given by

$$\boxed{Z_{s,n}^{(TM)} = \eta \frac{k_{z,s,n} v}{\omega}}. \tag{2.6.6}$$
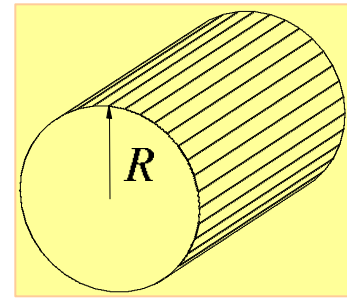
2.6.2 Transverse Electric (TE) Mode $[E_z = 0]$

In this case the wave equation reads

$$[\nabla_\perp^2 + k_\perp^2] H_z = 0 \tag{2.6.7}$$

and its solution has the form

$$H_z = \sum_{s,n} J_n\left(p'_{s,n} \frac{r}{R} \right) e^{-jk_{zs,n}z} \left[A_{s,n} \cos(n\varphi) + B_{s,n} \sin(n\varphi) \right], \tag{2.6.8}$$

where

$$\left. \frac{\partial H_z}{\partial r} \right|_{r=R} = 0 \quad \Rightarrow \quad p'_{s,n} : \; J'_n(p'_{s,n}) = 0. \tag{2.6.9}$$

The first few zeros of the **derivatives** of the Bessel function are

	s=1	s=2	s=3
N=0	3.832	7.016	10.174
N=1	1.841	5.331	8.536
N=2	3.054	6.706	9.970

thus

$$Z_{s,n}^{(TE)} = \eta \frac{\omega}{\mathrm{v} k_{z,s,n}}, \quad k_{z,s,n} = \sqrt{\left(\frac{\omega}{\mathrm{v}} \right)^2 - \left(\frac{p'_{s,n}}{R} \right)^2} \tag{2.6.10}$$
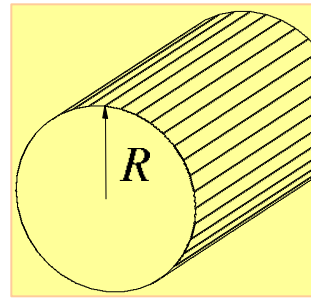
Summary

	TE modes	TM modes
$H_z =$	$J_n\!\left(p'_{sn}\dfrac{r}{R}\right)e^{-jk_{sn}z}\begin{cases}\cos n\varphi\\ \sin n\varphi\end{cases}$	0
$E_z =$	0	$J_n\!\left(p_{sn}\dfrac{r}{R}\right)e^{-jk_{sn}z}\begin{cases}\cos n\varphi\\ \sin n\varphi\end{cases}$
$H_r =$	$-\dfrac{jk_{sn}p'_{sn}}{Rk^2_{\perp,sn}}J_{n'}\!\left(p'_{sn}\dfrac{r}{R}\right)e^{-jk_{sn}z}\begin{cases}\cos n\varphi\\ \sin n\varphi\end{cases}$	$-E_\varphi/Z^{(TM)}_{sn}$
$H_\varphi =$	$-\dfrac{jnk_{sn}}{rk^2_{\perp,sn}}J_n\!\left(p'_{sn}\dfrac{r}{R}\right)e^{-jk_{sn}z}\begin{cases}-\sin n\varphi\\ \cos n\varphi\end{cases}$	$E_r/Z^{(TM)}_{sn}$
$E_r =$	$Z^{(TE)}_{sn}H_\varphi$	$-\dfrac{jk_{sn}p_{sn}}{Rk^2_{\perp,sn}}J_{n'}\!\left(p_{sn}\dfrac{r}{R}\right)e^{-jk_{sn}z}\begin{cases}\cos n\varphi\\ \sin n\varphi\end{cases}$
$E_\varphi =$	$-Z^{(TE)}_{sn}H_r$	$-\dfrac{jnk_{sn}}{rk^2_{\perp,sn}}J_n\!\left(p_{sn}\dfrac{r}{R}\right)e^{-jk_{sn}z}\begin{cases}-\sin n\varphi\\ \cos n\varphi\end{cases}$
$k_{sn} =$	$\left[\dfrac{\omega^2}{v^2}-\left(\dfrac{p'_{sn}}{R}\right)^2\right]^{1/2}$	$\left[\dfrac{\omega^2}{v^2}-\left(\dfrac{p_{sn}}{R}\right)^2\right]^{1/2}$
$Z^{(TE)}_{sn} =$	$\dfrac{\omega}{vk_{sn}}\eta$	$Z^{(TM)}_{sn}=\dfrac{vk_{sn}}{\omega}\eta$
$k_{\perp,sn} =$	p'_{sn}/R	p_{sn}/R

98

	TE modes	TM modes
Power=	$\dfrac{\eta k_0 k_{sn}\pi}{2k_{\perp,sn}^4 g_{0,n}}(p_{sn}'^2 - n^2)J_n^2(p_{sn}')$	$\dfrac{\eta k_0 k_{sn}\pi}{2k_{\perp,sn}^4 g_{0,n}} p_{sn}^2 [J_n'(k_{\perp,sn}R)]^2$
$\alpha =$	$\dfrac{R_s}{R\eta}\left(1-\dfrac{k_{\perp,sn}^2 \mathrm{v}^2}{\omega^2}\right)^{-1/2}\left[\dfrac{k_{\perp,sn}^2 c^2}{\omega^2}+\dfrac{n^2}{p_{sn}'^2-n^2}\right]$	$\dfrac{R_s}{R\eta}\left(1-\dfrac{k_{\perp,sn}^2 \mathrm{v}^2}{\omega^2}\right)^{-1/2}$

$$\mathrm{v}=\frac{1}{\sqrt{\mu_0\mu_r\varepsilon_0\varepsilon_r}}, \quad \eta=\sqrt{\frac{\mu_0\mu_r}{\varepsilon_0\varepsilon_r}} \quad g_{0,n}=\begin{cases}1 & n=0\\[2mm] 2 & n\neq 0\end{cases}$$
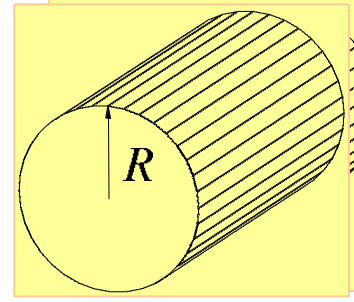
2.6.3 Power Considerations

According to Maxwell's Equations for a **single mode** we have

$$\vec{E}_\perp = -\frac{jk_z}{k_\perp^2}\nabla_\perp E_z, \qquad H_\varphi = \frac{E_r}{Z_{TM}}, \qquad H_r = -E_\varphi / Z_{TM}.$$

Consequently, the average Poynting vector is

$$S_z = \frac{1}{2}\left(\vec{E}_\perp \times \vec{H}_\perp^*\right)\cdot\vec{1}_z$$

and the average power flowing in the waveguide

$$P = \text{Re}\left\{\frac{1}{2}\int_{c.s.} da\left[\vec{E}_\perp \times \vec{H}_\perp^*\right]_z\right\} = \frac{1}{2}\text{Re}\left\{\int_{c.s.} da\left[E_r H_\varphi^* - E_\varphi H_r^*\right]\right\}$$

$$= \frac{1}{2}\text{Re}\left\{\int_{c.s.} da\left[\frac{|E_r|^2}{Z_{TM}} + \frac{|E_\varphi|^2}{Z_{TM}}\right]\right\} = \frac{1}{2Z_{TM}}\text{Re}\left\{\int_{c.s.} da\left[|E_r|^2 + |E_\varphi|^2\right]\right\}$$

$$= \frac{1}{2Z_{TM}}\text{Re}\left\{\int_{c.s.} da\left(\frac{k_z}{k_\perp^2}\right)^2 |\nabla_\perp E_z|^2\right\} = \frac{1}{2Z_{TM}}\frac{k_z^2}{k_\perp^4}\text{Re}\left\{\int_{c.s.} da|\nabla_\perp E_z|^2\right\}. \qquad (2.6.11)$$

In order to further simplify the last expression let us examine the wave equation:

$$\left(\nabla_\perp^2 + k_\perp^2\right)E_z = 0 \qquad (2.6.12)$$
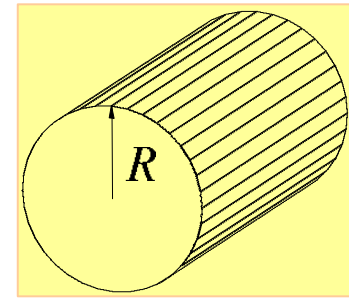
we multiply by the complex conjugate of E_z

$$E_z^* \left(\nabla_\perp^2 + k_\perp^2 \right) E_z = 0 \qquad (2.6.13)$$

and integrate over the entire cross section

$$\Delta_z \int da \left[E_z^* \nabla_\perp^2 E_z + k_\perp^2 \left| E_z \right|^2 \right] = 0$$

$$\Delta_z \int da \left[\nabla_\perp \left(E_z^* \nabla_\perp E_z \right) - \left| \nabla_\perp E_z \right|^2 + k_\perp^2 \left| E_z \right|^2 \right] = 0. \qquad (2.6.14)$$

The first term in the integrand is zero since

$$\int da \nabla_\perp \left[E_z^* \nabla_\perp E_z \right] = \int d\vec{\ell}_\perp \cdot \left[E_z^* \nabla_\perp E_z \right] = 0$$

hence

$$\int da \left| \nabla_\perp E_z \right|^2 = k_\perp^2 \int da \left| E_z \right|^2. \qquad (2.6.15)$$

Now back to the propagating power for a **superposition of modes** starting from the expression for a single mode we get

101
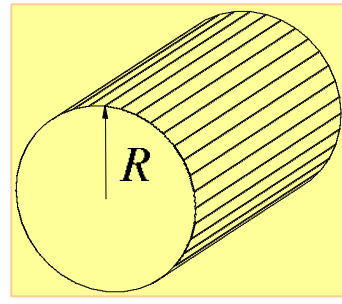
$$P_{s,n} = \frac{1}{2Z_{s,n}^{(TM)}} \frac{k^2}{k_\perp^4} \operatorname{Re}\left\{ \int da \left| \nabla_\perp E_z \right|^2 \right\} = \frac{1}{2Z^{(TM)}} \frac{k_z^2}{k_\perp^2} \int da \left| E_z \right|^2$$

$$P = \frac{1}{2\eta} \int_0^{2\pi} d\phi \int_0^R dr\, r \left[\begin{array}{c} \displaystyle\sum_{s,n} \frac{k_z}{k_\perp} A_{s,n} J_n\left(p_{s,n} \frac{r}{R} \right)\cos(n\varphi) \\[2mm] \displaystyle\left[\sum_{s',n'} \frac{\omega/\mathrm{v}}{k_\perp} A_{s',n'} J_{n'}\left(p_{s',n'} \frac{r}{R} \right)\cos(n'\varphi) \right] \end{array} \right]$$

The integration over the angle it is sraight forward

$$\int_0^{2\pi} d\phi \cos(n\varphi)\cos(n'\varphi) = 2\pi g_n \delta_{n,n'} \ , \quad g_n = \begin{cases} 1 & n = 0 \\ \dfrac{1}{2} & n \neq 0 \end{cases}$$

and after integration over r we get

$$P = 2\pi \sum_{n,s,s'} g_n \frac{1}{2Z_{s,n}^{(TM)}} \frac{k_{z,s,n}^2}{k_{\perp,s,n}^2} A_{s,n}^2 \frac{R^2}{2} \left[J_n'(p_{s,n}) \right]^2 \delta_{ss'}$$

where we used

$$\int_0^R dr\, r\, J_n\left(p_{n,s} \frac{r}{R} \right) J_n\left(p_{n,s'} \frac{r}{R} \right) = \frac{R^2}{2} \left[J_n'(p_{n,s}) \right]^2 \delta_{s,s'} \tag{2.6.16}$$
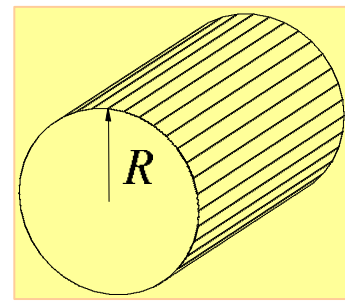
In the case of a single mode we have

$$P_{s,n} = \left(\frac{1}{2\eta} \left| R A_{s,n} \right|^2 \right) \left(\frac{\omega}{v} R \right) \text{Re} \left(R \sqrt{ \frac{\omega^2}{v^2} - \frac{p_{s,n}^2}{R^2} } \right) \pi g_n \left[\frac{J_n'(p_{s,n})}{p_{s,n}} \right]^2 . \qquad (2.6.17)$$

Note that there is power flow only if the wave is **above cutoff** and as in the rectangular case, the the total power is the superposition of the power in each mode separately

Exercise 2.15: Calculate the average **energy per unit length** stored in the electromagnetic field.
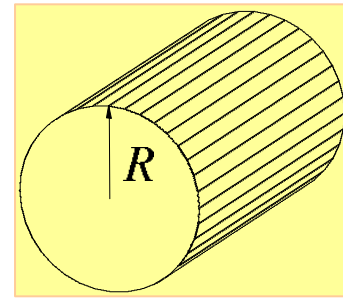
2.6.4 Ohm Loss

Now to the general expression for the losses. Starting from the dissipated power

$$P_{D,sn} = \frac{R_{su}}{2}\oint_{bound}\left|J_{z_1}^{(su)}\right|^2 d\ell = \frac{1}{2}R_s\oint\left|H_\phi\right|^2 d\ell = \frac{1}{2}R_s\oint\left|\frac{E_{r,sn}}{Z_{sn}^{(TM)}}\right|^2 d\ell$$

$$= \frac{1}{2}\frac{R_s}{\left|RZ_{sn}^{(TM)}\right|^2}k^2R^2\left[\frac{J_n'(p_{ns})}{p_{ns}}\right]^2 2\pi g_n\left|A_{sn}R\right|^2$$

$$= \frac{1}{2}\frac{R_s}{\left|\eta R\right|^2}\left(\frac{\omega}{v}R\right)^2\left[\frac{J_n'(p_{ns})}{p_{ns}}\right]^2 2\pi g_n\left|A_{sn}R\right|^2 \qquad (2.6.18)$$

which finally entails for a **single mode**

$$\alpha_{ns}^{(TM)} = \frac{1}{R}\frac{R_s}{\eta}\left(\frac{v_{ph,sn}}{v}\right). \qquad (2.6.19)$$

Exercise 2.16: Check Eq. (2.6.19).

Exercise 2.17: Calculate $\alpha_{ns}^{(TE)}$.

Exercise 2.18: Calculate the exponential decay due to dielectric loss.

Attenuation due to copper losses in circular waveguides at 3000 Mc/sec.
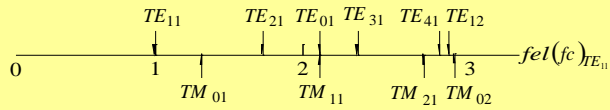
Relative cutoff frequencies of waves in a circular guide.

Frequency, megacycles/second

Attenuation due to co...
waveguides; d...

Mode comparison for cylindrical waveguide.

105

Wave Type	TM_{01}	TM_{02}	TM_{11}	TE_{01}	TE_{11}
Field distribution in cross-sectional plane, at plane of maximum transverse fields					
Field distribution along guide					
Field components present	E_z, E_r, H_φ	E_z, E_r, H_φ	$E_z, E_r, E_\varphi, H_r, H_\varphi$	H_z, H_r, E_φ	$H_z, H_r, H_\varphi, E_r, E_\varphi$
p or p'	2.405	5.52	3.83	3.83	1.84
(k_c)	$\dfrac{2.405}{\alpha}$	$\dfrac{5.52}{\alpha}$	$\dfrac{3.83}{\alpha}$	$\dfrac{3.83}{\alpha}$	$\dfrac{1.84}{\alpha}$
(λ_c)	2.61α	1.14α	1.64α	1.64α	3.41α
(f_c)	$\dfrac{0.383}{\alpha\sqrt{\mu\varepsilon}}$	$\dfrac{0.877}{\alpha\sqrt{\mu\varepsilon}}$	$\dfrac{0.609}{\alpha\sqrt{\mu\varepsilon}}$	$\dfrac{0.609}{\alpha\sqrt{\mu\varepsilon}}$	$\dfrac{0.293}{\alpha\sqrt{\mu\varepsilon}}$
Attenuation due to imperfect conductors	$\dfrac{R_s}{\alpha_n}\dfrac{1}{\sqrt{1-(f_c/f)^2}}$	$\dfrac{R_s}{\alpha_n}\dfrac{1}{\sqrt{1-(f_c/f)^2}}$	$\dfrac{R_s}{\alpha_n}\dfrac{1}{\sqrt{1-(f_c/f)^2}}$	$\dfrac{R_s}{\alpha_n}\dfrac{(f_c/f)^2}{\sqrt{1-(f_c/f)^2}}$	$\dfrac{R_s}{\alpha_n}\dfrac{1}{\sqrt{1-(f_c/f)^2}}$
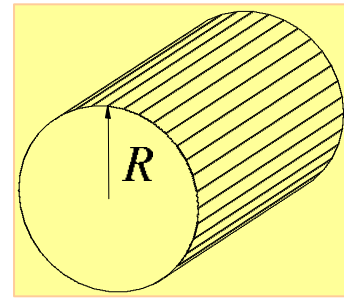
2.7 Pulse Propagation

Let us consider an **azimuthally symmetric** TM mode described by

$$E_z(r,z,t) = \sum_{s=1}^{\infty} J_0(p_s \frac{r}{R}) \int_{-\infty}^{\infty} d\omega \exp\left[j\omega t - \Gamma_s z \right] \mathcal{E}_s(\omega) \qquad (2.7.1)$$

wherein $\Gamma_s^2 = p_s^2 / R^2 - \omega^2 / c^2$ and $\mathcal{E}_s(\omega)$ is the Fourier transform of this field component at $z = 0$

$$\mathcal{E}_s(\omega) = \frac{1}{\frac{R^2}{2} J_1^2(p_s)} \int_0^R dr' r' J_0\left(p_s \frac{r}{R} \right) \frac{1}{2\pi} \int_{-\infty}^{\infty} dt' \exp\left(- j\omega t'\right) E_z(r', z = 0, t'). \qquad (2.7.2)$$

Let us now calculate the **energy associated with the radiation field** as it propagates in an empty waveguide. The transverse field components are

$$E_r(r,z,t) = \sum_{s=1}^{\infty} J_1\left(p_s \frac{r}{R} \right) \frac{p_s}{R} \int_{-\infty}^{\infty} d\omega \exp\left(j\omega t - \Gamma_s z \right) \frac{\mathcal{E}_s \Gamma_s}{\Gamma_s^2 + \dfrac{\omega^2}{c^2}}$$

$$H_\varphi(r,z,t) = \sum_{s=1}^{\infty} J_1\left(p_s \frac{r}{R} \right) \frac{p_s}{R} \int_{-\infty}^{\infty} d\omega \exp\left(j\omega t - \Gamma_s z \right) \frac{1}{\mu_0} \frac{j\omega}{c^2} \frac{\mathcal{E}_s}{\Gamma_s^2 + \dfrac{\omega^2}{c^2}} \qquad (2.7.3)$$

therefore, the z-component of the Poynting vector is
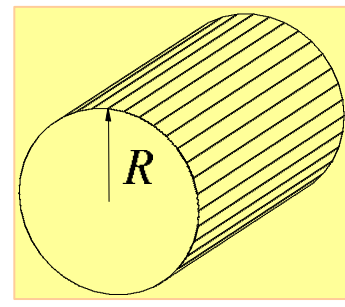
$$S_z(r,z,t) = \left\{ \sum_{s=1}^{\infty} J_1\left(p_s \frac{r}{R} \right) \int_{-\infty}^{\infty} d\omega \exp\left(j\omega t - \Gamma_s z \right) \mathcal{E}_s(\omega)\left(\Gamma_s \frac{R}{p_s} \right) \right\}$$

$$\times \left\{ \sum_{\sigma=1}^{\infty} J_1\left(p_\sigma \frac{r}{R} \right) \int_{-\infty}^{\infty} d\Omega \exp\left(j\Omega t - \Gamma_\sigma(\Omega) z \right) \mathcal{E}_\sigma(\Omega) \frac{1}{\eta_0}\left(j\Omega \frac{R}{c p_\sigma} \right) \right\}. \quad (2.7.4)$$

Using the orthogonality of Bessel functions

$$\int_0^R dr\, r J_1\left(p_s \frac{r}{R} \right) J_1\left(p_\sigma \frac{r}{R} \right) = \frac{R^2}{2} J_1^2(p_s)\delta_{s\sigma} \quad (2.7.5)$$

the power propagating is

$$P(z,t) = 2\pi \sum_{s=1}^{\infty} \frac{R^2}{2} J_1^2(p_s)\left\{ \int_{-\infty}^{\infty} d\omega \exp\left(j\omega t - \Gamma_s z \right) \mathcal{E}_s(\omega)\left(\Gamma_s \frac{R}{p_s} \right) \right\}$$

$$\times \left\{ \int_{-\infty}^{\infty} d\Omega \exp\left(j\Omega t - \Gamma_s z \right) \mathcal{E}_s(\Omega) \frac{1}{\eta_0}\left(j\Omega \frac{R}{c p_s} \right) \right\} \quad (2.7.6)$$

and the energy associated with this power

108
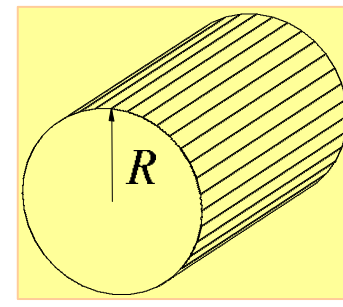
$$W_R(z) = \int_{-\infty}^{\infty} dt P(z,t)$$

$$= (2\pi)\sum_{s=1}^{\infty} \frac{R^2}{2} J_1^2(p_s) \int d\omega \mathcal{E}_s(\omega) \exp\left[-\Gamma_s(\omega)z\right] \int d\Omega \mathcal{E}_s(\Omega) \exp\left[-\Gamma_s(\Omega)z\right]$$

$$\times \left(\Gamma_s(\omega)\frac{R}{p_s}\right)\frac{1}{\eta_0}\left(j\frac{\Omega}{c}R\frac{1}{p_s}\right)\int_{-\infty}^{\infty} dt \exp\left[j(\omega+\Omega)t\right].$$

(2.7.7)

With the definition of the Dirac delta function $\delta(\Omega+\omega) \equiv \dfrac{1}{2\pi}\int dt\, e^{j(\omega+\Omega)t}$ we have

$$W_R(z) = (2\pi)^2 \sum_{s=1}^{\infty} \frac{R^2}{2} J_1^2(p_s) \int_{-\infty}^{\infty} d\omega\, \mathcal{E}_s(\omega)\mathcal{E}_s(-\omega)\exp\left\{-z\left[\Gamma_s(\omega)+\Gamma_s(-\omega)\right]\right\}$$

$$\times \left(\frac{\Gamma_s(\omega)R}{p_s}\right)\frac{1}{\eta_o}\left(-j\frac{\omega}{c}R\frac{1}{p_s}\right).$$

(2.7.8)

For proceeding it is important to emphasize two features: since the field components are *real* functions, it is evident that the integrand ought to satisfy $\mathcal{F}_s(-\omega) = \mathcal{F}_s^*(\omega)$. Consequently

$$\mathcal{E}_s(-\omega) = \mathcal{E}_s^*(\omega)$$

(2.7.9)

and

$$\Gamma_s(-\omega) = \Gamma_s^*(\omega).$$

(2.7.10)
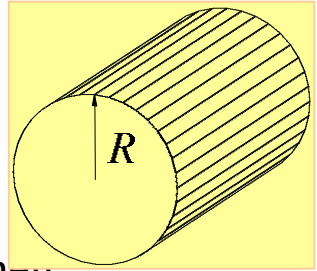
This last conclusion implies that if the frequency is below cut-off ($|\omega| < p_s c / R$) then

$$\Gamma_s(-\omega) = |\Gamma_s(\omega)| \tag{2.7.11}$$

whereas if $|\omega| > cp_s / R$

$$\Gamma_s(-\omega) = -j|\Gamma_s(\omega)|. \tag{2.7.12}$$

With these observations we conclude that

$$W_R(z) = \frac{(2\pi)^2}{\eta_0} \sum_{s=1}^{\infty} \frac{R^2}{2} J_1^2(p_s) 2\text{Re}\left\{ \int_0^{cp_s/R} d\omega \,|\mathcal{E}_s(\omega)|^2\, e^{-2|\Gamma_s(\omega)|z} \right.$$

$$\times \left[\frac{-j\omega R}{cp_s}\frac{|\Gamma_s(\omega)|R}{p_s} \right] + \int_{cp_s/R}^{\infty} d\omega \,|\mathcal{E}_s(\omega)|^2 \left[\frac{\omega R}{cp_s}\frac{|\Gamma_s(\omega)|R}{p_s} \right] \right\}. \tag{2.7.13}$$

Clearly the **first integrand is pure imaginary** therefore, its contribution is identically zero and as a result, in the lossless case considered here, the energy associated with the propagating signal does not change as a function of the location

$$W = \frac{(2\pi)^2}{\eta_0} \sum_{s=1}^{\infty} \frac{R^2}{2} J_1^2(p_s)\, 2\int_{cp_s/R}^{\infty} d\omega \,|\mathcal{E}_s(\omega)|^2 \left[\frac{\omega R}{cp_s}\frac{|\Gamma_s(\omega)|R}{p_s} \right]. \tag{2.7.14}$$
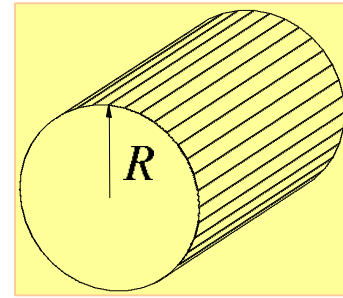
Comments:

1. Only the propagating components contribute to the radiated energy.
2. The non-propagating components are **confined** to the close vicinity of the **input** (where initial conditions were defined).
3. If all the spectrum is confined to the region $0 < \omega < p_1 c / R$, no energy will propagate.
4. Since the waveguide is lossless, the propagating energy does not change as a function of z.

Exercise 2.19: Calculate the electromagnetic energy per unit length. Compare with (2.7.14).

Let us now simplify the discussion and focus on a source which excites only the **first mode** ($s = 1$) i.e., $E_z(r, z = 0, t) = J_0(p_1 r/R)E_0(t)$ therefore according to Eq.(2.7.2) we get

$$
\begin{aligned}
\mathcal{E}_s(\omega) &= \frac{1}{\frac{R^2}{2}J_1^2(p_s)}\left[\int_0^R dr' r' J_0\left(p_s \frac{r}{R}\right)J_0\left(p_1 \frac{r}{R}\right)\right]\frac{1}{2\pi}\int_{-\infty}^{\infty} dt' e^{-j\omega t'} E_0(t') \\
&= \frac{\delta_{s,1}}{2\pi}\int_{-\infty}^{\infty} dt' e^{-j\omega t'} E_0(t')
\end{aligned}
\tag{2.7.15}
$$
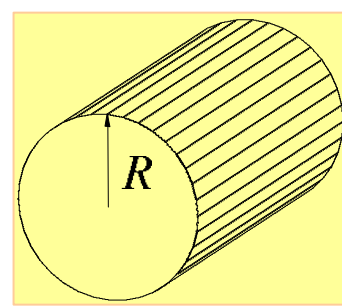
As an example, consider a signal starting from t=0 ramping up and oscillating and decaying

$$E_0(t') = E_0 \sin(\Omega t) \exp\left(-\frac{t}{T}\right) h(t) \Rightarrow \mathcal{E}_s(\omega) = \frac{\delta_{s,1}}{2\pi} E_0 \frac{\Omega T^2}{1 + 2j\omega T + T^2(\Omega^2 - \omega^2)} \quad (2.7.16)$$

Substituting in Eq.(2.7.14)

$$W = \frac{1}{\eta_0 c^2} E_0^2 R^4 \left[\frac{J_1(p_1)}{p_1}\right]^2 \int_{\omega_1 = cp_1/R}^{\infty} d\omega \frac{(\Omega^2 T^4)\left(\omega\sqrt{\omega^2 - \omega_1^2}\right)}{\left[1 + T^2(\Omega^2 - \omega^2)\right]^2 + (2\omega T)^2} \quad (2.7.17)$$

Normalizing to the cutoff frequency, $u = \omega/\omega_1$ as well as $\bar{\Omega} = \Omega/\omega_1$, $\bar{T} = T\omega_1$ the last integral simplifies to read

$$W = \varepsilon_0 E_0^2 R^3 \frac{J_1^2(p_1)}{p_1} \bar{\Omega}^2 \int_1^{\infty} du \frac{u\sqrt{u^2 - 1}}{\left[\bar{T}^{-2} + \bar{\Omega}^2 - u^2\right]^2 + 4u^2 \bar{T}^{-2}} \quad (2.7.18)$$

Its numerical analysis reveals that

$$W \sim \varepsilon_0 E_0^2 R^3 \frac{J_1^2(p_1)}{p_1} \frac{\pi}{4} \bar{\Omega}^2 \begin{cases} 1 & \bar{\Omega} < 1 \\ \bar{T} & \bar{\Omega} > 1 \end{cases} \quad (2.7.19)$$

Exercise 2.20: Compare with the dependence of the propagating energy in the frequency Ω when the signal prescribed by Eq.(2.7.16) propagates in **free space**.

112

2.8 Waveguide Modes in Coaxial Line

Chapter 3: Waveguides – Advanced Topics

After paving the foundations of electromagnetic phenomena in waveguides, in this chapter we shall consider some advanced phenomena including:
1. Hybrid modes, whereby the TM and TE are coupled
2. Dielectric loaded waveguide
3. Mode coupling due to geometric discontinuity
4. Reactive elements
5. Excitation of Waveguides
6. Coupling between two waveguides
7. Surface waveguides
8. Transients
9. Cavities
10. Wedge in a Waveguide

3.1 Hybrid Modes

In Section 2.1 it was demonstrated that if the waveguide's electromagnetic characteristics are **uniform** on the cross-section, the transverse components may be derived from the two longitudinal components that in turn are **independent**. For example in a rectangular waveguide we had

$$E_z(x, y, z; \omega) = \sum_{n_x, n_y} A_{n_x, n_y} \sin\left(\pi n_x \frac{x}{a_x} \right) \sin\left(\pi n_y \frac{y}{a_y} \right) e^{-\gamma_{n_x, n_y} z}$$

$$H_z(x, y, z; \omega) = \sum_{m_x, m_y} B_{m_x, m_y} \cos\left(\pi m_x \frac{x}{a_x} \right) \cos\left(\pi m_y \frac{y}{a_y} \right) e^{-\gamma_{m_x, m_y} z} \quad (3.1.1)$$

wherein $\gamma^2 = k_\perp^2 - \varepsilon_r \mu_r (\omega/c)^2$ and $k_\perp^2 = (\pi n_x / a_x)^2 + (\pi n_y / a_y)^2$ for the transverse magnetic (TM) mode or $k_\perp^2 = (\pi m_x / a_x)^2 + (\pi m_y / a_y)^2$ for the transverse electric (TE) mode. The transverse components being given by

$$\vec{E}_\perp = -\frac{\gamma}{k_\perp^2} \nabla_\perp E_z + \frac{j\omega\mu}{k_\perp^2} \vec{1}_z \times \nabla_\perp H_z, \quad \vec{H}_\perp = -\frac{\gamma}{k_\perp^2} \nabla_\perp H_z - \frac{j\omega\varepsilon}{k_\perp^2} \vec{1}_z \times \nabla_\perp E_z \quad (3.1.2)$$

Let us now assume that the relative **dielectric coefficient** (ε_r) **depends on the transverse coordinates** (e.g. x and y in a rectangular geometry) and so is the relative permeability coefficient (μ_r), the goal being to determine the character of the modes supported by the structure. Our starting point again is Maxwell's equations

$$\nabla \times \vec{E} = -j\omega\mu_0\mu_r\vec{H} \qquad\qquad \vec{\nabla}\cdot(\mu_0\mu_r\vec{H}) = 0$$

$$\nabla \times \vec{H} = j\omega\varepsilon_o\varepsilon_r\vec{E} \qquad\qquad \vec{\nabla}\cdot(\varepsilon_0\varepsilon_r\vec{E}) = 0 \qquad\qquad (3.1.3)$$

which lead to the following wave equations

$$\vec{\nabla}\times(\vec{\nabla}\times\vec{E}) = -j\omega\mu_0\nabla\times(\mu_r\vec{H}) = -j\omega\mu_0[\nabla\mu_r\times\vec{H} + \mu_r\vec{\nabla}\times\vec{H}]$$

$$-\nabla^2\vec{E} + \nabla(\vec{\nabla}\cdot\vec{E}) = -j\omega\mu_0[\nabla\mu_r\times\vec{H} + \mu_r(j\omega\varepsilon_0\varepsilon_r\vec{E})]$$

$$\left[\nabla^2 + \frac{\omega^2}{c^2}\varepsilon_r\mu_r\right]E_z = \left[\nabla(\vec{\nabla}\cdot\vec{E}) + j\omega\mu_0\nabla\mu_r\times\vec{H}\right]\vec{1}_z \qquad\qquad (3.1.4)$$

Bearing in mind Gauss' law $\vec{\nabla}\cdot(\varepsilon_r\vec{E}) = 0 \Rightarrow \vec{\nabla}\cdot\vec{E} = -\vec{E}\cdot\nabla\ln\varepsilon_r$ we get

$$\left[\nabla_\perp^2 + \gamma^2 + \varepsilon_r\mu_r\frac{\omega^2}{c^2}\right]E_z = \gamma(\vec{E}_\perp\cdot\nabla_\perp\ln\varepsilon_r) + j\omega\mu_0\mu_r(\nabla_\perp\ln\mu_r\times\vec{H}_\perp)\cdot\vec{1}_z \qquad\qquad (3.1.5)$$

and in a similar way

$$\left[\nabla_{\perp}^2 + \gamma^2 + \varepsilon_r \mu_r \frac{\omega^2}{c^2}\right] H_z = -\gamma(\vec{H}_{\perp} \cdot \nabla_{\perp} \ln \mu_r) - j\omega\varepsilon_0 \varepsilon_r (\nabla_{\perp} \ln \varepsilon_r \times \vec{E}_{\perp}) \cdot \vec{1}_z \qquad (3.1.6)$$

It is evident from these two equations (3.1.5)--(3.1.6) that E_z and H_z are no longer independent if transverse variations in the cross-section occur. Modes which are **linear combinations of TE and TM modes are called hybrid modes** and they frequently occur in microwave components.

In order to illustrate the coupling of TE and TM modes let us consider a dielectric loaded waveguide as illustrated in the figure. A fraction of the waveguide $(0 < x \leq d)$ is filled with dielectric material (ε_r) whereas the remainder $(d < x \leq a)$ has the same characteristics as the vacuum. In each region the material is uniform which means that the wave equation is
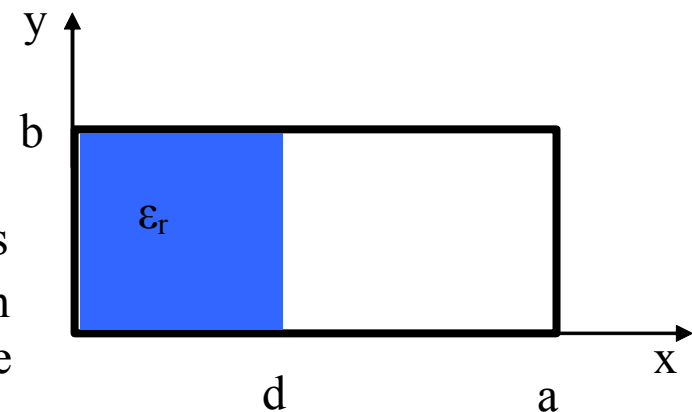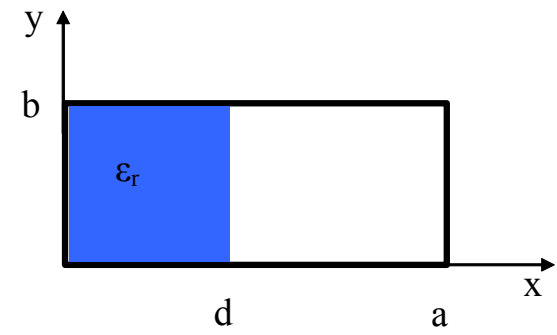
$$\left[\nabla_{\perp}^2 + \begin{pmatrix} \varepsilon_r \\ 1 \end{pmatrix} \frac{\omega^2}{c^2} + \gamma^2 \right] E_z = 0 \qquad (3.1.7)$$

and its solution is

$$E_z = e^{-\gamma z} \sin\left(\pi m \frac{y}{b}\right) \begin{cases} A \sinh\left[x \sqrt{\left(\frac{\pi m}{b}\right)^2 - \gamma^2 - \varepsilon_r \frac{\omega^2}{c^2}} \right] & 0 \le x \le d \\ \\ B \sinh\left[(x-a)\sqrt{\left(\frac{\pi m}{b}\right)^2 - \gamma^2 - \frac{\omega^2}{c^2}} \right] & d \le x \le a \end{cases} \qquad (3.1.8)$$

wherein we impose the boundary condition at $x = 0$ and $x = a$.

Similarly, for H_z we have

$$\left[\nabla_{\perp}^2 + \begin{pmatrix} \varepsilon_r \\ 1 \end{pmatrix} \frac{\omega^2}{c^2} + \gamma^2 \right] H_z = 0 \qquad (3.1.9)$$

and

$$H_z = e^{-\gamma z} \cos\left(\frac{\pi m}{b} y\right) \begin{cases} C\cosh\left[x\sqrt{\left(\frac{\pi m}{b}\right)^2 - \gamma^2 - \varepsilon_r \frac{\omega^2}{c^2}} \right] & 0 \le x \le d \\[4mm] D\cosh\left[(x-a)\sqrt{\left(\frac{\pi m}{b}\right)^2 - \gamma^2 - \frac{\omega^2}{c^2}} \right] & d \le x \le a \end{cases}$$

$\triangleright$ (3.1.10)
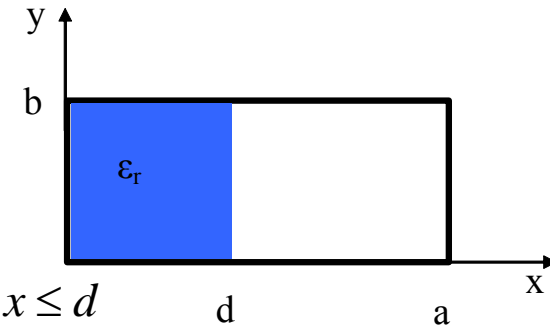
 Imposing the boundary condition at $x=d$ leads us to the **dispersion relation**. In order to emphasize the coupling between TE and TM modes we shall develop the dispersion relation in two steps.

Step I: we impose the continuity of E_z and H_z facilitating to redefine the amplitudes thus $\overline{A}$ and $\overline{D}$ according to

$$E_z = \overline{A}e^{-\gamma z}\sin\left(\pi m \frac{y}{b}\right) \begin{cases} \dfrac{\sinh(\Lambda_\varepsilon x)}{\sinh(\Lambda_\varepsilon d)} & 0 \le x \le d \\[4mm] \dfrac{\sinh\left[\Lambda_v (a-x)\right]}{\sinh\left[\Lambda_v (a-d)\right]} & d \le x \le a \end{cases}$$

(3.1.11)

 and
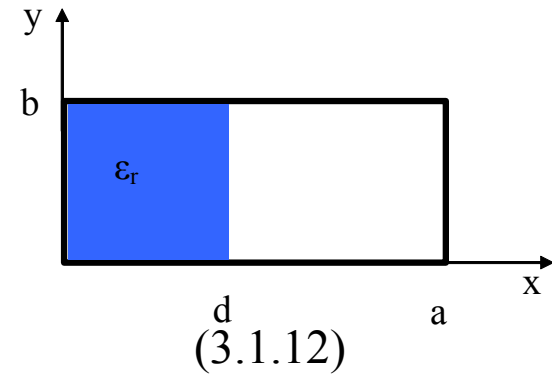
$$H_z = \overline{D} e^{-\gamma z} \cos\left(\pi m \frac{y}{b}\right) \begin{cases} \dfrac{\cosh(\Lambda_\varepsilon x)}{\cosh(\Lambda_\varepsilon d)} & 0 \le x \le d \\[3mm] \dfrac{\cosh\left[\Lambda_v (a-x)\right]}{\cosh\left[\Lambda_v (a-d)\right]} & d \le x \le a \end{cases}$$

$$(3.1.12)$$

wherein $\Lambda_\varepsilon^2 \equiv (\pi m/b)^2 - \gamma^2 - \varepsilon(\omega/c)^2$ is the horizonthal wave number in the dielectric (subscript ε) and $\Lambda_v^2 \equiv (\pi m/b)^2 - \gamma^2 - (\omega/c)^2$ represents the horizonthal wave number in the vacuum (subscript v). It is evident that if $d = 0$ or $d = a$ (i.e. the waveguide is filled uniformly), the regular solutions may be readily retrieved $\Lambda_v a = j\pi n$ or $\Lambda_\varepsilon a = j\pi n$.

Step II: In our second step if $0 < d < a$ we need to impose continuity of E_y and H_y at $x = d$. According to (3.1.2) the transverse components are

$$E_y = -\frac{\gamma}{\gamma^2 + \varepsilon_r \dfrac{\omega^2}{c^2}} \partial_y E_z + \frac{j\omega\mu_0}{\gamma^2 + \varepsilon_r \dfrac{\omega^2}{c^2}} \partial_x H_z$$

$$H_y = -\frac{\gamma}{\gamma^2 + \varepsilon_r \dfrac{\omega^2}{c^2}} \partial_y H_z - \frac{j\omega\varepsilon_0 \varepsilon_r}{\gamma^2 + \varepsilon_r \dfrac{\omega^2}{c^2}} \partial_x E_z \qquad (3.1.13)$$
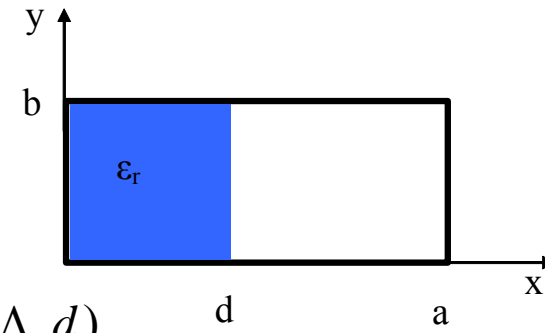
Based on (3.1.13) and (3.1.11)-(3.1.12) we get

$$E_y(x = d - 0) = \frac{\gamma}{\gamma^2 + \varepsilon_r \dfrac{\omega^2}{c^2}} \overline{A}\left(\frac{\pi m}{b}\right) + \frac{j\omega\mu_0}{\gamma^2 + \varepsilon_r \dfrac{\omega^2}{c^2}} \overline{D}\,\Lambda_\varepsilon \tanh(\Lambda_\varepsilon d)$$

$$E_y(x = d + 0) = \frac{\gamma}{\gamma^2 + \dfrac{\omega^2}{c^2}} \overline{A}\,\frac{\pi m}{b} - \frac{j\omega\mu_0}{\gamma^2 + \dfrac{\omega^2}{c^2}} \overline{D}\,\Lambda_v \tanh[\Lambda_v(a - d)] \qquad (3.1.14)$$

thus their continuity implies

$$\overline{A}\left(\frac{\dfrac{\pi m}{b}\gamma}{\gamma^2 + \varepsilon_r \dfrac{\omega^2}{c^2}} - \frac{\dfrac{\pi m}{b}\gamma}{\gamma^2 + \dfrac{\omega^2}{c^2}}\right) = -j\omega\mu_0 \overline{D}\left[\frac{\Lambda_v \tanh\left[\Lambda_v(a - d)\right]}{\gamma^2 + \dfrac{\omega^2}{c^2}} + \frac{\Lambda_\varepsilon \tanh(\Lambda_\varepsilon d)}{\gamma^2 + \varepsilon_r \dfrac{\omega^2}{c^2}}\right] (3.1.15)$$
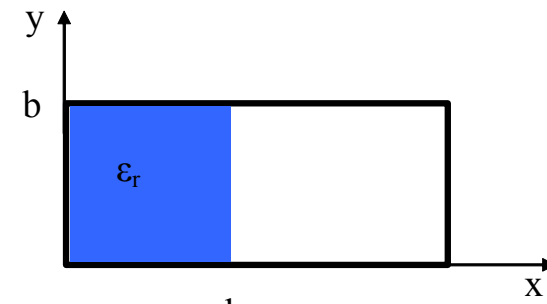
Similarly

$$H_y(x = d - 0) = \frac{-\gamma}{\gamma^2 + \varepsilon_r \dfrac{\omega^2}{c^2}} \overline{D}\left(-\frac{\pi m}{b}\right) - \frac{j\omega\varepsilon_0 \varepsilon_r}{\gamma^2 + \varepsilon_r \dfrac{\omega^2}{c^2}} \overline{A}\,\Lambda_\varepsilon \coth(\Lambda_\varepsilon d) \qquad (3.1.16)$$

$$H_y(x = d + 0) = \frac{-\gamma}{\gamma^2 + \dfrac{\omega^2}{c^2}} \overline{D}\left(-\frac{\pi m}{b}\right) - \frac{j\omega\varepsilon_0}{\gamma^2 + \dfrac{\omega^2}{c^2}} \overline{A}(-\Lambda_v)\coth[\Lambda_v(a - d)] \quad (3.1.17)$$

thus

$$\overline{A}\left\{\frac{j\omega\varepsilon_0}{\gamma^2 + \dfrac{\omega^2}{c^2}}\Lambda_v \coth[\Lambda_v(a-d)] + \frac{j\omega\varepsilon_0\varepsilon_r}{\gamma^2 + \varepsilon_r\dfrac{\omega^2}{c^2}}\Lambda_\varepsilon \coth(\Lambda\varepsilon d)\right\} + \overline{D}\left(\frac{-\dfrac{\pi m}{b}\gamma}{\gamma^2 + \varepsilon_r\dfrac{\omega^2}{c^2}} + \frac{\dfrac{\pi m}{b}\gamma}{\gamma^2 + \dfrac{\omega^2}{c^2}}\right) = 0.$$

$$(3.1.18)$$

The dispersion relation, in a matrix form, may by now be expressed using (3.1.15) and (3.1.18)
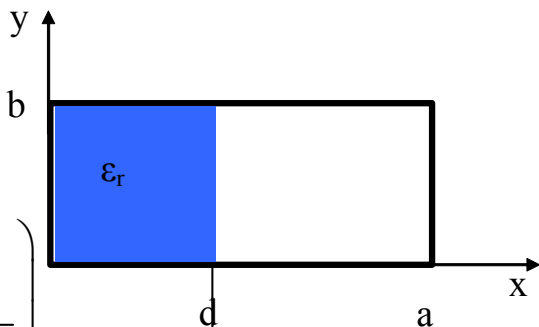
$$
\left[
\begin{array}{c}
\underbrace{\dfrac{\Lambda_{\varepsilon}\tanh(\Lambda_{\varepsilon}d)}{\left(\gamma^2+\varepsilon_r\dfrac{\omega^2}{c^2}\right)\dfrac{1}{j\omega\mu_0}}+\dfrac{\Lambda_v\tanh[\Lambda_v(a-d)]}{\left(\gamma^2+\dfrac{\omega^2}{c^2}\right)\dfrac{1}{j\omega\mu_0}}}_{\textbf{TE}} \qquad \dfrac{\pi m}{b}\gamma\left(\dfrac{1}{\gamma^2+\varepsilon_r\dfrac{\omega^2}{c^2}}-\dfrac{1}{\gamma^2+\dfrac{\omega^2}{c^2}}\right)\\[4ex]
\dfrac{\pi m}{b}\gamma\left(\dfrac{-1}{\gamma^2+\varepsilon_r\dfrac{\omega^2}{c^2}}+\dfrac{1}{\gamma^2+\dfrac{\omega^2}{c^2}}\right) \qquad \underbrace{\dfrac{j\omega\varepsilon_0\Lambda_v}{\gamma^2+\dfrac{\omega^2}{c^2}}\coth[\Lambda_v(a-d)]+\dfrac{j\omega\varepsilon_0\varepsilon_r\Lambda_{\varepsilon}}{\gamma^2+\varepsilon_r\dfrac{\omega^2}{c^2}}\coth(\Lambda_{\varepsilon}d)}_{\textbf{TM}}
\end{array}
\right]\left(\begin{array}{c}\overline{D}\\[1ex]\overline{A}\end{array}\right)=0
$$

(3.1.19)

 or formally

$$
\begin{pmatrix}\mathcal{D}_{11} & \mathcal{D}_{12}\\[2ex]\mathcal{D}_{21} & \mathcal{D}_{22}\end{pmatrix}\begin{pmatrix}\overline{D}\\[2ex]\overline{A}\end{pmatrix}=0
$$

(3.1.20)

implying that for a non trivial solution the determinant of the matrix must be zero

$$
\det\begin{pmatrix}\mathcal{D}_{11} & \mathcal{D}_{12}\\[2ex]\mathcal{D}_{21} & \mathcal{D}_{22}\end{pmatrix}=0 \Rightarrow \boxed{\mathcal{D}_{11}\mathcal{D}_{22}+\left(\mathcal{D}_{12}\right)^2=0.}
$$

(3.1.21)
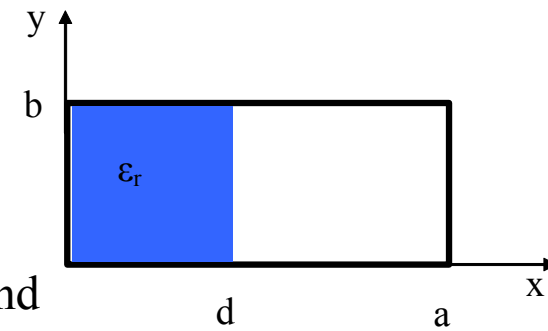
Comments:

    1. The **diagonal** terms represent the dispersion relation of TE and TM modes.

    2. If there are **no variations in one transverse dimension** (e.g. $m = 0$), the TE and TM modes are **decoupled**. Such an example will be considered in the next section.

Exercise 3.1: Analyze the solution of the dispersion relation as a function of d. Specifically, compare to the case $d = 0$ and $d = a$.

Exercise 3.2: Calculate the group velocity and the energy velocity.

Exercise 3.3: For a given propagating power, determine the ratio of electric and magnetic energy (per unit length) as a function of d.

3.2 Dielectric Loading – TM$_{01}$

In the previous section it was concluded that partial loading in one direction and the field variations in the other direction leads to hybrid modes. Moreover, we claimed that if there are no field variations in the second transverse direction the modes are not coupled. We shall examine this kind of configuration next, namely, a partially filled with dielectric ε_r configuration as illustrated in Figure 2. The radius of the waveguide is R and the inner radius of the dielectric is denoted with R_d. We shall assume a solution of the form $E_z(r,z) = E(r)\exp(-jkz)$ in which case the amplitude $E(r)$ satisfies
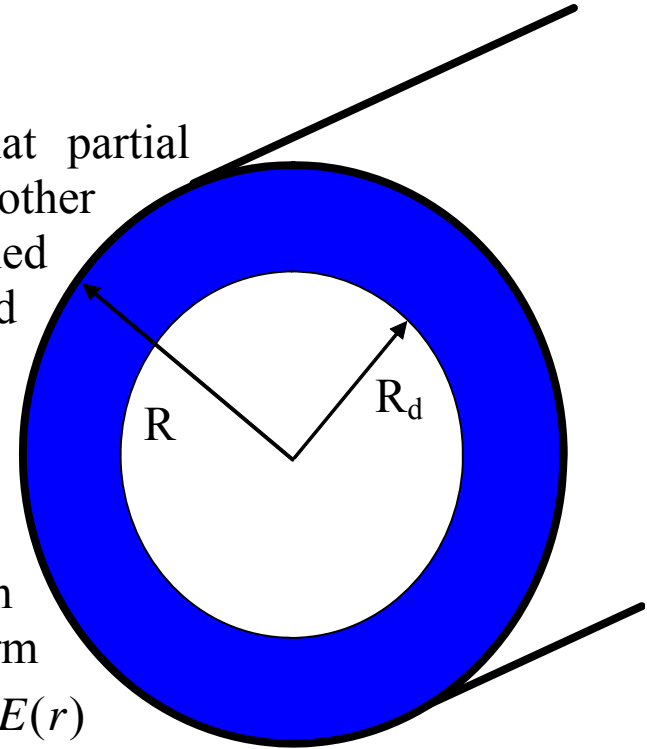
$$\left[\frac{1}{r}\frac{d}{dr}r\frac{d}{dr} + \frac{\omega^2}{c^2}\varepsilon_r(r) - k^2\right]E(r) = 0 \qquad (3.2.1)$$
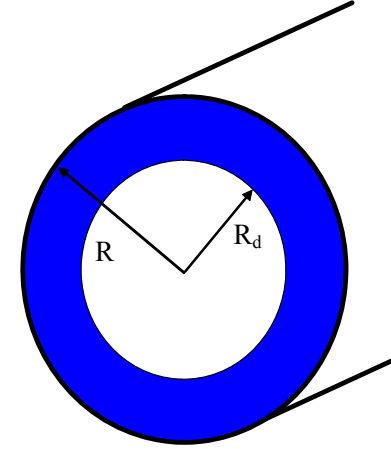
in the **dielectric** region or explicitly for $R_d < r < R$:

$$\left[\frac{1}{r}\frac{d}{dr}r\frac{d}{dr} + \underbrace{\frac{\omega^2}{c^2}\varepsilon - k^2}_{\kappa_\varepsilon^2}\right]E_1(r) = 0 \qquad (3.2.2)$$

whereas in the **vacuum** $0 < r < R_d$:

$$\left[\frac{1}{r}\frac{d}{dr}r\frac{d}{dr} + \underbrace{\frac{\omega^2}{c^2} - k^2}_{\kappa_v^2}\right]E_2(r) = 0. \qquad (3.2.3)$$

It is therefore convenient to define the radial wave number $\kappa_v^2 \equiv (\omega/c)^2 - k^2$ in vacuum (subscript v) whereas the corresponding quantity in the dielectric is defined as $\kappa_\varepsilon^2 \equiv \varepsilon(\omega/c)^2 - k^2$ based on which the solution reads

$$E_z(r) = \begin{cases} AS_0(r) & 0 < r < R_d \\ BT_0(r) & R_d < r < R \end{cases}$$

$$T_0(r) \equiv \begin{cases} J_0(\kappa_\varepsilon r)Y_o(\kappa_\varepsilon R) - Y_o(\kappa_\varepsilon r)J_0(\kappa_\varepsilon R) & \kappa_\varepsilon^2 > 0 \\ I_0(|\kappa_\varepsilon| r)K_0(|\kappa_\varepsilon| R) - K_0(|\kappa_\varepsilon| r)I_0(|\kappa_\varepsilon| R) & \kappa_\varepsilon^2 < 0 \end{cases}$$

(3.2.4)

$$S_0(r) = \begin{cases} J_0(\kappa_v r) & \kappa_v^2 > 0 \\ I_0(|\kappa_v| r) & \kappa_v^2 < 0 \end{cases}$$
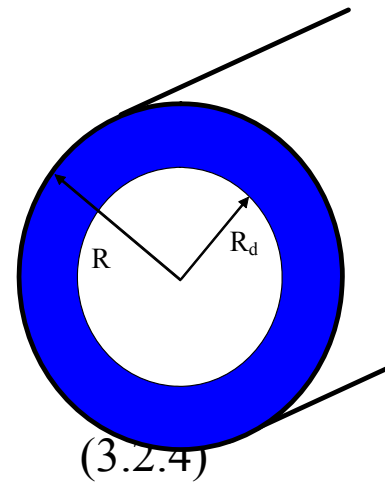
As in the previous section the dispersion relation will be now determined by imposing the boundary conditions at the interface between the two regions. Firstly, we impose the continuity of E_z at $r = R_d$:

$$E_z \Rightarrow \boxed{AS_0(R_d) = BT_0(R_d)} \qquad (3.2.5)$$

and secondly, the continuity of H_φ at $r = R_d$

$$H_\varphi = \frac{j\omega\varepsilon_0\varepsilon_r}{k^2 - \varepsilon_r(\omega/c)^2}\frac{\partial E_z}{\partial r} \Rightarrow \boxed{\frac{|\kappa_\varepsilon|}{\kappa_\varepsilon^2}\varepsilon_r B\overset{\circ}{T}_0(R_d) = \frac{|\kappa_v|}{\kappa_v^2}A\overset{\circ}{S}_0(R_d)} \qquad (3.2.6)$$

wherein

$$\overset{\circ}{T}_0(r) \equiv \begin{cases} -J_1(\kappa_\varepsilon r)Y_o(\kappa_\varepsilon R) + Y_1(\kappa_\varepsilon r)J_0(\kappa_\varepsilon R) & \kappa_\varepsilon^2 > 0 \\ I_1(|\kappa_\varepsilon|r)K_0(|\kappa_\varepsilon|R) + K_1(|\kappa_\varepsilon|r)I_0(|\kappa_\varepsilon|R) & \kappa_\varepsilon^2 < 0 \end{cases}$$

$$\overset{\circ}{S}_0(r) = \begin{cases} -J_1(\kappa_v r) & \kappa_v^2 > 0 \\ I_1(|\kappa_v|r) & \kappa_v^2 < 0 \end{cases}$$

(3.2.7)
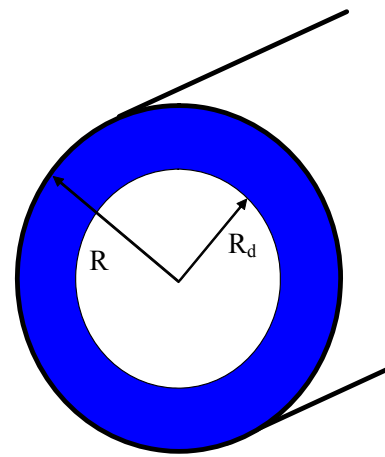
From the previous two equations[(3.2.5), (3.2.6)] we obtain the dispersion equation

$$\boxed{\frac{|\kappa_\varepsilon|}{\kappa_\varepsilon^2}\varepsilon_r S_0 \overset{\circ}{T}_0 = \frac{|\kappa_v|}{\kappa_v^2}\overset{\circ}{S}_0 T_0}$$

(3.2.8)

which can be solved numerically as illustrated below.

According to the frequency, the mode varies from the characteristics of empty space (close to cut-off) of dielectric filled case.
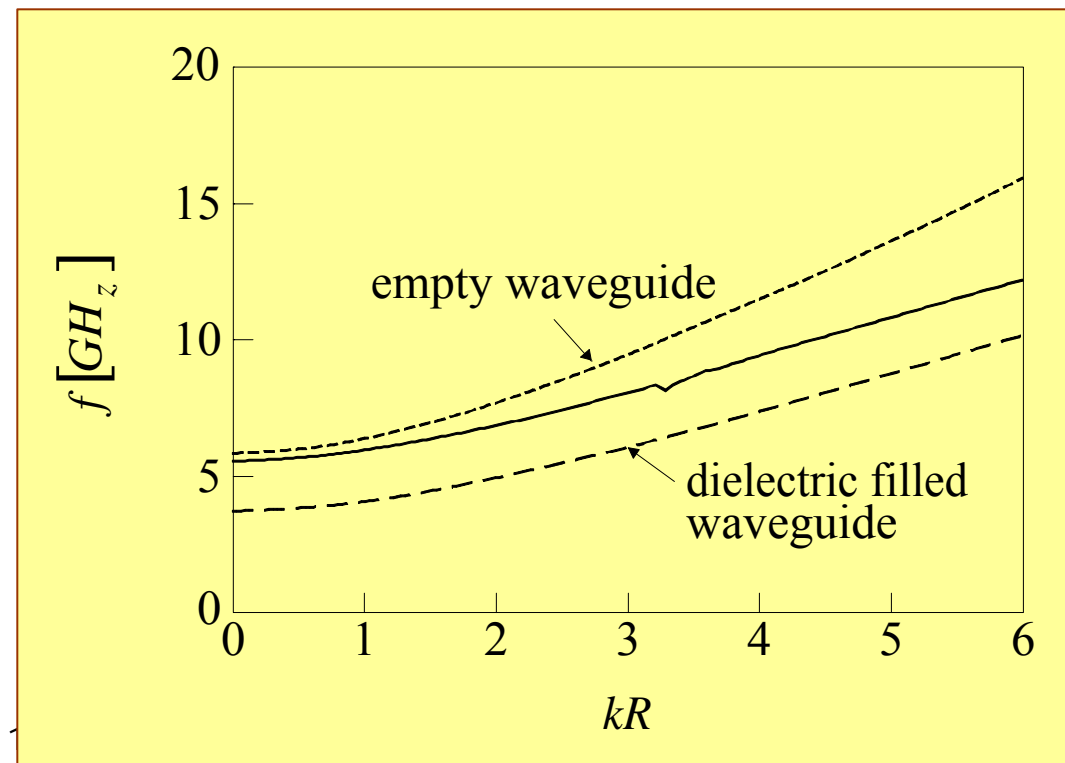
Exercise 3.4: Analyse the effect of R_d on the phase velocity, group velocity and ohm loss of the metal. What about dielectric loss?

Exercise 3.5: Analyze the ratio of the electric energy stored per unit length vs. magnetic energy per unit length.

Exercise 3.6: Compare the energy stored in the dielectric with that in air.

Exercise 3.7: Determine the higher modes of a coaxial line illustrated below. The radii are R_{in}, R_d, R_{ext}.
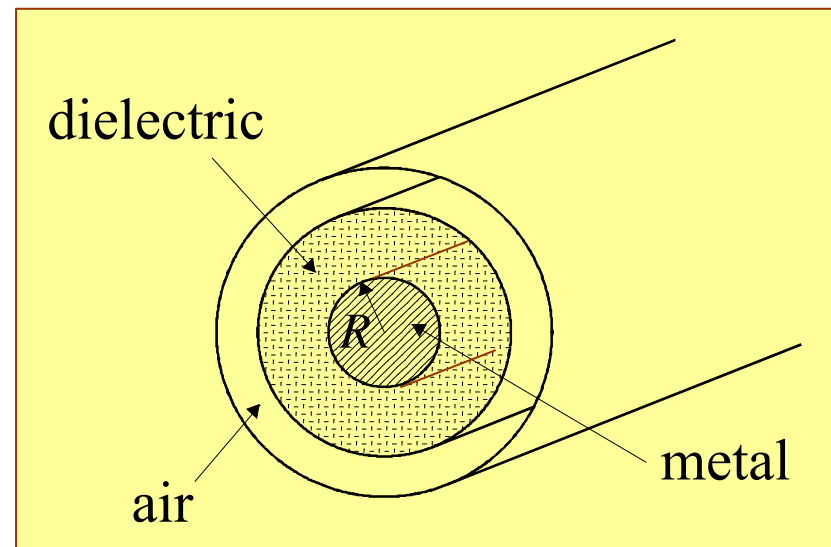
3.3 Mode Coupling

3.3.1 Step Transition – TE mode

A longitudinal change in the cross-section of the waveguide leads to a coupling process between virtually all possible modes. **Excitation of modes** is an inherent process associated with the necessity to **satisfy the boundary conditions**. Whether these modes propagate or not, it is only a question of what is the frequency (or frequencies) of the incoming signal. In general, the coupling occurs between TE and TM or between various hybrid modes however, in what follows we shall consider a configuration whereby the coupling is between the various eigen-modes of a TE mode.
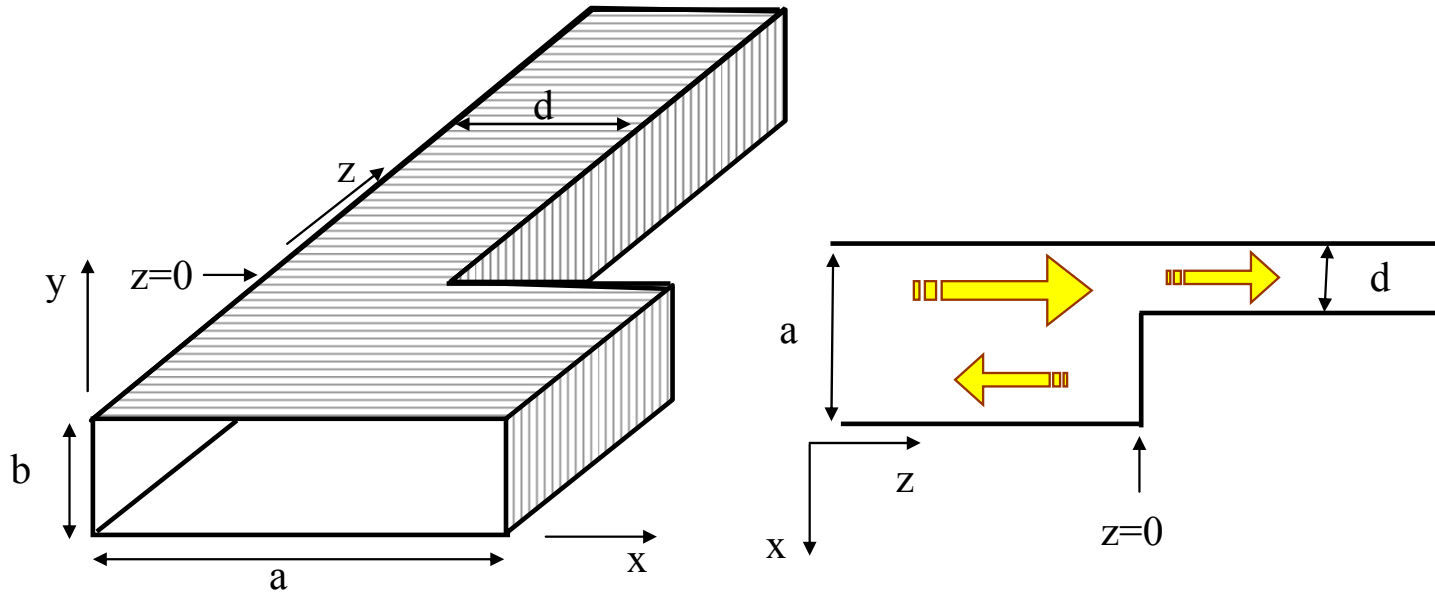
A TE$_{01}$ wave propagates from $z \to -\infty$ towards the discontinuity at $z = 0$

$$H_z^{(\text{inc})} = H_0 \cos\left(\pi \frac{x}{a} \right) \exp\left(j k_z z \right) \qquad (3.3.1)$$

in a waveguide of width a and height b; note that $k_z^2 = (\omega/c)^2 - (\pi/a)^2$. At the discontinuity the width of the waveguide varies abruptly from a to $d < a$. A direct result of the discontinuity is a reflected field described by

$$H_z^{(\text{ref})} = H_0 \sum_{n=0}^{\infty} \rho_n \cos\left(\frac{\pi n x}{a} \right) \exp\left(\Gamma_n z \right); \quad \Gamma_m = \sqrt{(\pi m/a)^2 - (\omega/c)^2} \qquad (3.3.2)$$

131
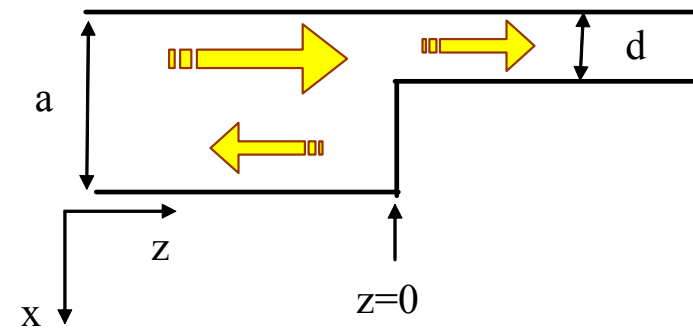
ρ_m are the **reflection coefficients** of the various modes.

Similarly, the transmitted field is given by

$$H_z^{(tr)} = H_0 \sum_{m=0}^{\infty} \tau_m \cos\left(\frac{\pi m x}{d}\right) \exp\left(-\Lambda_m z\right); \ \ \Lambda_m = \sqrt{\left(\pi m / d\right)^2 - \left(\omega / c\right)^2} \qquad (3.3.3)$$

τ_m representing the **transmitted coefficient** of each mode. Three observations at this stage:

1. The amplitude of both reflected (ρ_m) and transmitted (τ_m) will be determined by the **boundary conditions** to be imposed shortly.
2. The character of the mode (propagating or evanescent) is determined by the angular frequency (ω) of the incident wave.
3. The choice of TE_{01} is dictated by the need for a simple analysis. If a higher mode is launched (e.g. TE_{11}) there will be **coupling** to TM modes.

132

Step 1: Continuity of the y-component of the **electric field** in the range $0 < x < a$ implies

$$(E_y^{(inc)} + E_y^{(sc)})|_{z=0} = \begin{cases} E_y^{(tr)}|_{z=0} & 0 < x < d \\ 0 & d < x < a. \end{cases} \qquad (3.3.4)$$

Faraday's law, in our case $\partial_x E_y = -j\omega\mu_0 H_z$, thus

$$E_y^{(inc)}|_{z=0} = -j\omega\mu_0 H_o \left(\frac{a}{\pi}\right)\sin\left(\frac{\pi x}{a}\right)$$

$$E_y^{(sc)}|_{z=0} = -j\omega\mu_0 H_o \sum_m \rho_m \left(\frac{a}{\pi m}\right)\sin\left(\frac{\pi m x}{a}\right)$$

$$E_y^{(tr)}|_{z=0} = -j\omega\mu_0 H_o \sum_{m'} \tau_{m'} \left(\frac{d}{\pi m'}\right)\sin\left(\frac{\pi m' x}{d}\right). \qquad (3.3.5)$$

Substituting in (3.3.4) we get

$$\sum_m \frac{a}{\pi m}[\delta_{m,1} + \rho_m]\sin\left(\frac{\pi m x}{a}\right) = \begin{cases} \sum_{m'} \frac{d}{\pi m'}\tau_{m'}\sin\left(\frac{\pi m' x}{d}\right) & 0 < x < d \\ 0 & d < x < a. \end{cases} \qquad (3.3.6)$$

Using the orthogonality of the trigonometric function we obtain

133
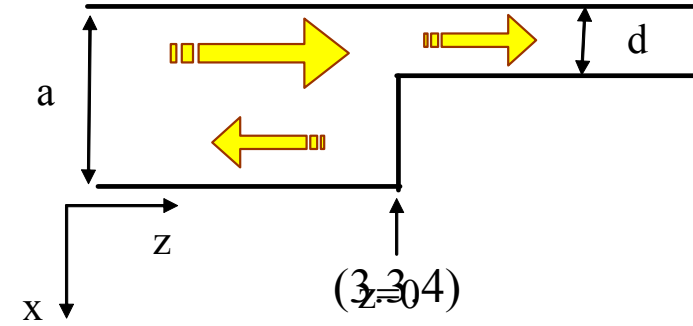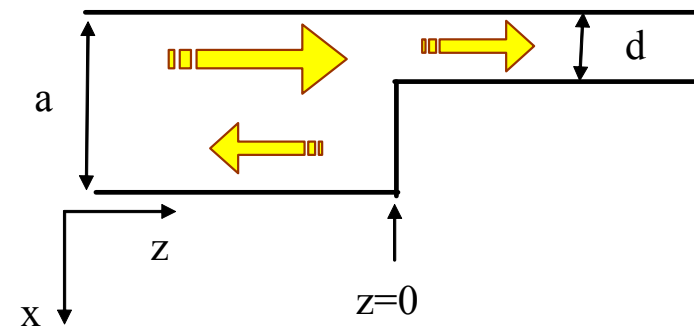
$$\frac{a}{\pi m}[\delta_{m,1} + \rho_m]\frac{1}{2} = \sum_{m'} \frac{d}{\pi m'} \tau_{m'} \frac{1}{a} \int_0^d dx \sin\left(\frac{\pi m'x}{d}\right) \sin\left(\frac{\pi mx}{a}\right),$$

(3.3.7)

or

$$\boxed{\delta_{m,1} + \rho_m = \sum_{m'} A_{mm'} \tau_{m'},}$$

(3.3.8)

wherein the matrix $A_{mm'}$ is proportional to the **overlap integral** of the modes from both sides of the discontinuity

$$A_{mm'} \equiv 2\left(\frac{d}{a}\right)^2 \left(\frac{m}{m'}\right) \frac{1}{d} \int_0^d dx \sin\left(\frac{\pi m'}{d}x\right) \sin\left(\frac{\pi m}{a}x\right).$$

(3.3.9)

Step 2: Continuity of the x-component of the **magnetic field** in the region $0 < x < d$ implies

$$H_x^{(inc)} + H_x^{(sc)} \big|_{z=0} = H_x^{(tr)} \big|_{z=0}$$

(3.3.10)

and since $\vec{\nabla} \cdot \vec{H} = 0$ or explicitly $\partial_z H_z + \partial_x H_x = 0$ we get at $z = 0$
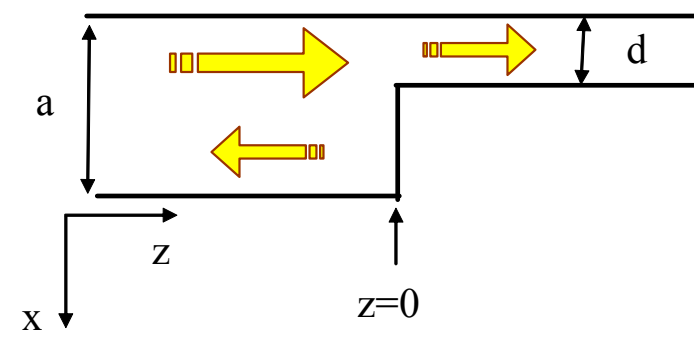
$$H_x^{(\text{inc})} = -H_0 \frac{a}{\pi} \sin\left(\frac{\pi x}{a}\right)(-jk_{z01})$$

$$H_x^{(\text{sc})} = -H_0 \sum_m \rho_m \frac{a}{\pi m} \sin\left(\frac{\pi m x}{a}\right)\Gamma_m$$

$$H_x^{(\text{tr})} = -H_0 \sum_{m'} \tau_{m'} \frac{d}{\pi m'} \sin\left(\frac{\pi m' x}{d}\right)(-\Lambda_m). \tag{3.3.11}$$

Thus, in the region $z = 0$ and $0 < x < d$

$$\sum \frac{a}{\pi m}\Gamma_{0m}[-\delta_{m,1} + \rho_m]\sin\left(\frac{\pi m x}{a}\right) = -\sum_{m'} \frac{d}{\pi m'}\Lambda_{0m'}\tau_{m'}\sin\left(\frac{\pi m' x}{d}\right); \tag{3.3.12}$$

this time we use the orthogonality of $\sin(\pi m' x / d)$ in the range $0 \le x \le d$ we get

$$\frac{1}{2}\tau_{m'}\left[\frac{d}{\pi m'}\Lambda_{m'}\right] = \sum_m \left[\frac{a}{\pi m}\Gamma_m\right]\left[\delta_{m,1} - \rho_m\right]\frac{1}{d}\int_0^d dx \sin\left(\frac{\pi m'}{d}x\right)\sin\left(\frac{\pi m}{a}x\right), \tag{3.3.13}$$

or

$$\boxed{\tau_{m'} = \sum_m B_{m'm}[\delta_{m,1} - \rho_m],} \tag{3.3.14}$$

where the matrix $B_{m'm}$ is also proportional to the overlap integral
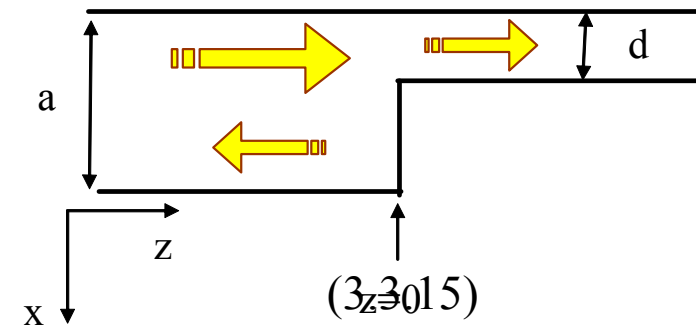
$$B_{m'm} \equiv 2 \frac{a}{d} \frac{m'}{m} \frac{\Gamma_m}{\Lambda_{m'}} \frac{1}{d} \int_0^d dx \sin\left(\frac{\pi m'}{d}x\right) \sin\left(\frac{\pi m}{a}x\right).$$

We can now write (3.3.8) and (3.3.14) in a vector form

$$\vec{\delta} + \vec{\rho} = \underline{A}\vec{\tau} \quad \text{and} \quad \vec{\tau} = \underline{B}(\vec{\delta} - \vec{\rho}) \tag{3.3.16}$$

respectively. Substituting the expression for τ we obtain $\vec{\delta} + \vec{\rho} = \underline{AB}(\vec{\delta} - \vec{\rho})$, or $[\underline{I} + \underline{AB}]\vec{\rho} = [\underline{AB} - \underline{I}]\vec{\delta}$. Finally the amplitudes of the reflected and transmitted amplitudes are given by

$$\vec{\rho} = [\underline{I} + \underline{AB}]^{-1}[\underline{AB} - \underline{I}]\vec{\delta}$$
$$\vec{\tau} = 2[\underline{I} + \underline{BA}]^{-1}\vec{\delta}. \tag{3.3.17}$$

For evaluation of the matrices A and B we need to evaluate the integral

$$\frac{1}{d}\int_0^d dx \sin\left(\frac{\pi m'x}{d}\right) \sin\left(\frac{\pi mx}{a}\right) = \mathrm{sinc}\left[\pi\left(m' - m\frac{d}{a}\right)\right] - \mathrm{sinc}\left[\pi\left(m' + m\frac{d}{a}\right)\right]. \tag{3.3.18}$$
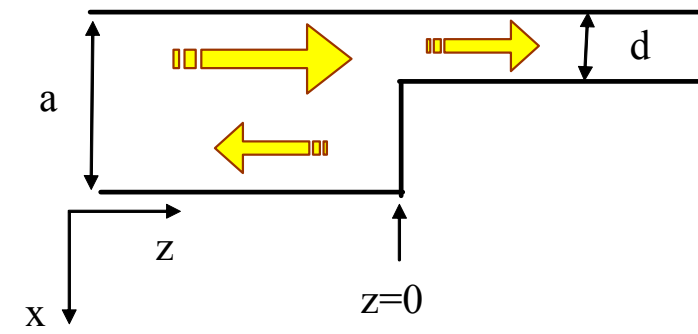
With the amplitudes established we may proceed and evaluate the power in the system:

$$P_{inc} = \frac{1}{2} H_0^2 b \frac{a}{2} \sum_{m=1}^{\infty} |\delta_{m,1}|^2 \left(\frac{a}{\pi m}\right)^2 \mathrm{Re}(-j\omega\mu_0\Gamma_m)$$

$$P_{ref} = \frac{1}{2} H_0^2 b \frac{a}{2} \sum_{m=1}^{\infty} |\rho_m|^2 \left(\frac{a}{\pi m}\right)^2 \mathrm{Re}(j\omega\mu_0\Gamma_m)$$

$$P_{tr} = \frac{1}{2} H_0^2 b \frac{d}{2} \sum_{m=1}^{\infty} |\tau_{m'}|^2 \left(\frac{d}{\pi m'}\right)^2 \mathrm{Re}(-j\omega\mu_0\Lambda_m) \qquad (3.3.19)$$

Assuming that at the operating frequency there is only **a single propagating mode** in each region, then the average power may be written **as in a transmission line**

$$P_{inc} = \frac{1}{2} |I_1|^2 Z_1 \Rightarrow Z_1 = \eta_0 \frac{\omega}{ck_1}, \quad I_1 = H_0 \frac{k_1 a}{\pi}\sqrt{\frac{ab}{2}}$$

$$P_{ref} = \frac{1}{2} |I_1|^2 |\rho_1|^2 Z_1$$

$$P_{tr} = \frac{1}{2} |I_2|^2 |\tau_1|^2 Z_2 \Rightarrow Z_2 = \eta_0 \frac{\omega}{ck_2}, \quad I_2 = H_0 \frac{k_2 d}{\pi}\sqrt{\frac{db}{2}} \qquad (3.3.20)$$

wherein $k_1 = \sqrt{(\omega/c)^2 - (\pi/a)^2}$ and $k_2 = \sqrt{(\omega/c)^2 - (\pi/d)^2}$.

Let us examine closely the **normalized reflected power** $\left[P_1^{(\text{ref})} / P_1^{(\text{inc})} \right]$ in the **first mode** as a function of the frequency:

$f\,[GH_z]$

1. The power can be injected at frequencies above 6GHz (a=2.5cm).
2. To the point whereby the first mode in the second part is above cutoff
    $$f_c \simeq 8.485\,\text{GHz} \ (d = a/\sqrt{2})$$
    the reflection coefficient of the first mode is **unity**.
3. Above 8.485GHz power can be transferred to the second part therefore the reflected power drops yet $P_1^{(\text{inc})} = P_1^{(\text{ref})} + P_1^{(\text{tr})}$.
4. Above 12 GHz for which the second mode in the left-hand side may carry power, the power reflected in the first mode decreases further yet beyond this point $P_1^{(\text{inc})} \neq P_1^{(\text{ref})} + P_1^{(\text{tr})}$ but rather $P_1^{(\text{inc})} = P_1^{(\text{ref})} + P_2^{(\text{ref})} + P_1^{(\text{tr})}$.
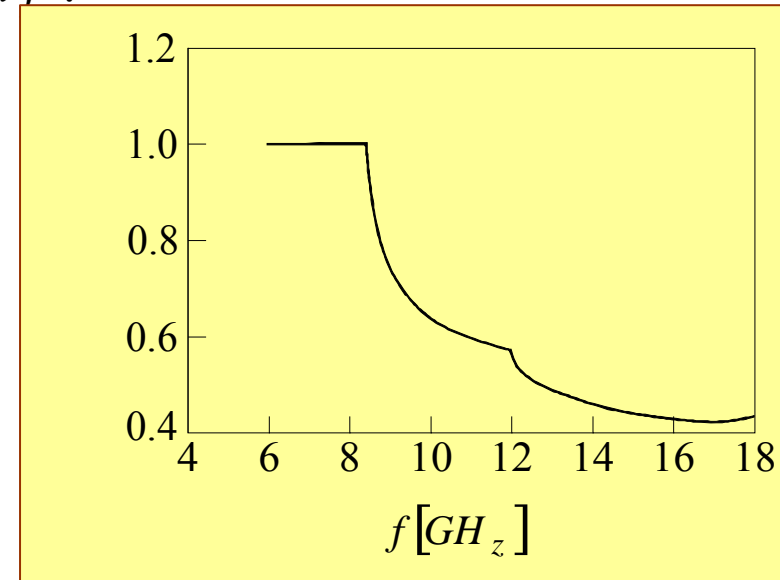
3.3.2 Step Transition – TM$_{0n}$ Mode in Cylindrical Waveguide

An additional example illustrating mode-coupling due to discontinuity in the transverse geometry is brought next. In fact, in this case there are **two discontinuities**, and the first and last sections have the same cross section. It will be reiterated that even if the incident wave is composed of a single (lowest) mode, the coupling causes other modes that in turn may carry part of the electromagnetic energy.

In the left hand side ($z < 0$) of a cylindrical waveguide of radius R_{ext}, there is an incident and a reflected **TM** wave

$$E_z^{(inc)}(r, z) = E_0 J_0\left(p_1 \frac{r}{R_{ext}} \right) \exp\left(-\Gamma_1 z\right)$$

$$E_z^{(ref)}(r, z) = E_0 \sum_{s=1}^{\infty} \rho_s J_0\left(p_s \frac{r}{R_{ext}} \right) \exp\left(\Gamma_1 z\right), \tag{3.3.21}$$

where $\Gamma_s \equiv \sqrt{(p_s/R_{ext})^2 - (\omega/c)^2}$ and ρ_s represents the normalized amplitudes of the
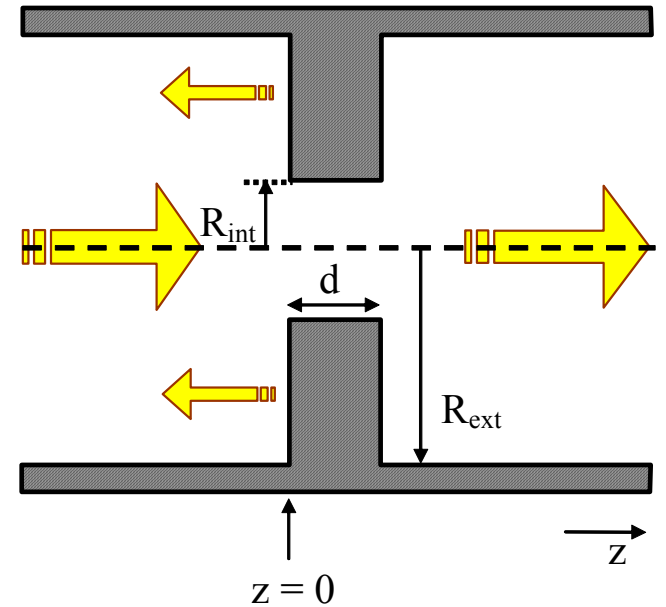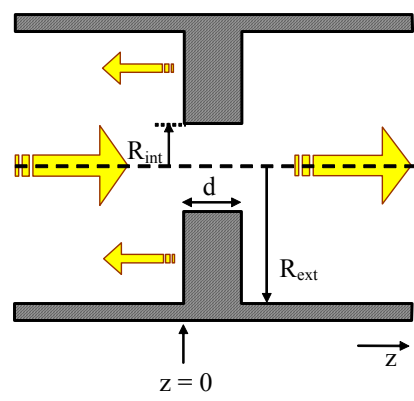
reflected modes. In the region $0 \le z \le d$ the radius of the waveguide is smaller $R_{int} < R_{ext}$ however for $z \ge d$ the radius returns to its initial value. Consequently, in the other regions we have

$$E_z^{(d)}(r, z < d) = E_0 \sum_{n=1}^{\infty} J_0 \left(p_n \frac{r}{R_{int}} \right) \left[A_n \exp(-\Lambda_n z) + B_n \exp(\Lambda_n z) \right]$$

(3.3.22)

$$E_z^{(tr)}(r, z > d) = E_0 \sum_{s=1}^{\infty} \tau_s J_0 \left(p_s \frac{r}{R_{ext}} \right) \exp \left[-\Gamma_s (z - d \right]$$

where $\Lambda_n = \sqrt{(p_n / R_{int})^2 - (\omega / c)^2}$. As previously, the goal is to determine the amplitudes of the transmitted and reflected waves ($\bar{\tau}_s$ and $\bar{\rho}_s$). For this purpose let us concentrate on the field components at $z = 0$.

$$\begin{pmatrix} H_\varphi^{(\text{left})} \\ E_r^{(\text{left})} \end{pmatrix} = E_0 \sum_s \frac{R_{ext}}{p_1} \begin{pmatrix} j\omega\varepsilon_0 \\ \Gamma_s \end{pmatrix} J_1 \left(p_s \frac{r}{R_{ext}} \right) \begin{pmatrix} \delta_{s,1} \exp(-\Gamma_1 z) + \rho_s \exp(\Gamma_s z) \\ \delta_{s,1} \exp(-\Gamma_1 z) - \rho_s \exp(\Gamma_s z) \end{pmatrix}$$

$$\begin{pmatrix} H_\varphi^{(d)} \\ E_r^{(d)} \end{pmatrix} = E_0 \sum_n \frac{R_{int}}{p_n} \begin{pmatrix} j\omega\varepsilon_0 \\ \Lambda_n \end{pmatrix} J_1 \left(p_n \frac{r}{R_{int}} \right) \begin{pmatrix} A_n \exp(-\Lambda_n z) + B_n \exp(\Lambda_n z) \\ A_n \exp(-\Lambda_n z) - B_n \exp(\Lambda_n z) \end{pmatrix}$$

(3.3.23)

With these field components we impose the boundary conditions at $z = 0$. Continuity of

the **radial electric field** implies

$$E_r(r, z = 0^-) = \begin{cases} E_r(r, z = 0^+) & 0 < r < R_{int} \\ 0 & R_{int} < r < R_{ext} \end{cases} \quad (3.3.24)$$
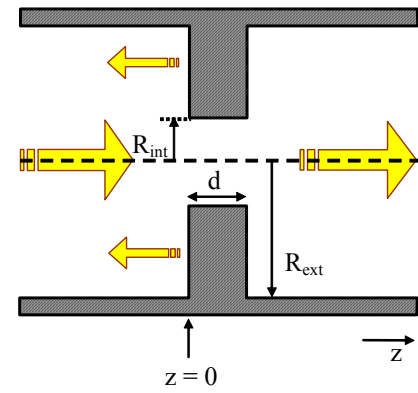
Using the orthogonality of the Bessel functions

$$\int_0^{R_{ext}} dr\, r J_1\left(p_s \frac{r}{R_{ext}}\right) J_1\left(p_{s'} \frac{r}{R_{ext}}\right) = \frac{R_{ext}^2}{2} J_1^2(p_s) \delta_{ss'} \quad (3.3.25)$$

we obtain from (3.3.24)

$$\delta_{s,1} - \rho_s = \frac{1}{\dfrac{\Gamma_s R_{ext}}{p_s} \dfrac{R_{ext}^2}{2} J_1^2(p_s)} \sum_{n=1}^{\infty} \frac{R_{int}}{p_n} \Lambda_n [A_n - B_n] \int_0^{R_{int}} dr\, r J_1\left(p_s \frac{r}{R_{ext}}\right) J_1\left(p_n \frac{r}{R_{int}}\right) (3.3.26)$$

or

$$\boxed{\delta_{s,1} - \rho_s = \sum_{n=1}^{\infty} \mathcal{L}_{sn}[A_n - B_n],} \quad (3.3.27)$$

where the matrix $\mathcal{L}_{sn}$ is proportional to the overlap integral

$$\mathcal{L}_{sn} \equiv \frac{p_s}{p_n} \frac{\Lambda_n}{\Gamma_s} \frac{1}{J_1^2(p_s)} \frac{R_{int}^3}{R_{ext}^3} U_{s,n}, \quad U_{s,n} \equiv \frac{2}{R_{int}^2} \int_0^{R_{int}} dr\, r J_1\left(p_s \frac{r}{R_{ext}}\right) J_1\left(p_n \frac{r}{R_{int}}\right) \quad (3.3.28)$$
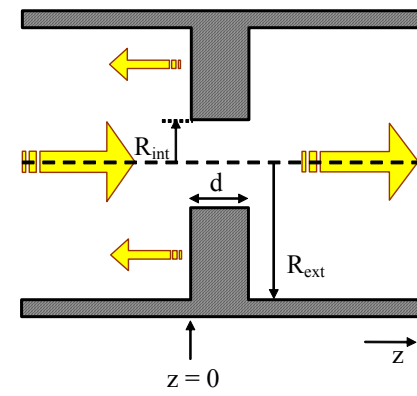
The continuity of the **azimuthal magnetic field** in the region $0 < r < R_{int}$ is $H_\phi^{(d)}(r, z = 0^-) = H_\phi^{(d)}(r, z = 0^+)$. Again we use the orthogonality of the Bessel functions in the inner region

$$\frac{R_{int}}{p_n}[A_n + B_n]\frac{R_{int}^2}{2}J_1^2(p_n) = \sum_{s=1}^{\infty}[\delta_{s,1} + \rho_s]\frac{R_{ext}}{p_s}\int_0^{R_{int}} drrJ_1\left(p_s\frac{r}{R_{ext}}\right)J_1\left(p_n\frac{r}{R_{int}}\right) \quad (3.3.29)$$

hence

$$A_n + B_n = \sum_s \mathcal{M}_{ns}(\delta_{s,1} + \rho_s), \quad (3.3.30)$$

where using the definition (3.3.28) we have further defined

$$\mathcal{M}_{sn} \equiv \frac{R_{ext}}{R_{int}}\frac{p_n}{p_s}\frac{1}{J_1^2(p_n)}U_{s,n}. \quad (3.3.31)$$

From these expressions we can easily deduce the two equations representing the boundary conditions at $z = d$:

$$A_n\exp(-\Lambda_n d) + B_n\exp(\Lambda_n d) = \sum_{s=1}^{\infty}\mathcal{M}_{ns}\tau_s \quad (3.3.32)$$

$$\boxed{\tau_s = \sum_{n=1}^{\infty} \mathcal{L}_{s,n}[A_n \exp(-\Lambda_n d) - B_n \exp(\Lambda_n d)].}$$ (3.3.33)
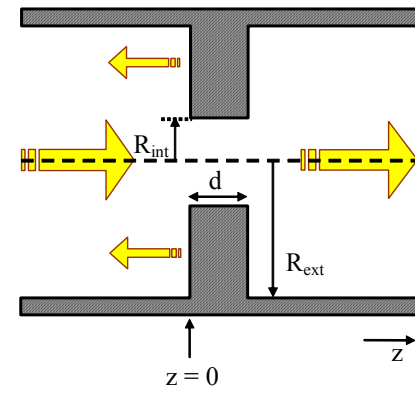
All four equations (3.3.27), (3.3.30), (3.3.32), (3.3.33) can be formulated in a vector (matrix) notation

$$
\begin{aligned}
(3.3.27) &\rightarrow & \delta - \rho = \mathcal{L}(A - B) \\
(3.3.30) &\rightarrow & A + B = \mathcal{M}(\delta + \rho)
\end{aligned}
\left. \right\}
\Rightarrow
\begin{pmatrix} A \\ B \end{pmatrix} =
\begin{pmatrix} I & -I \\ I & I \end{pmatrix}^{-1}
\begin{pmatrix} \mathcal{L}^{-1} & -\mathcal{L}^{-1} \\ \mathcal{M} & \mathcal{M} \end{pmatrix}
\begin{pmatrix} \delta \\ \rho \end{pmatrix}
$$

$$
\begin{aligned}
(3.3.32) &\rightarrow & A e^{-\Lambda d} + B e^{\Lambda d} = \mathcal{M}\tau \\
(3.3.33) &\rightarrow & \mathcal{L}\left(A e^{-\Lambda d} - B e^{\Lambda d}\right) = \tau
\end{aligned}
\left. \right\}
\Rightarrow
\begin{pmatrix} A \\ B \end{pmatrix} =
\begin{pmatrix} e^{-\Lambda d} & 0 \\ 0 & e^{\Lambda d} \end{pmatrix}^{-1}
\begin{pmatrix} I & -I \\ I & I \end{pmatrix}^{-1}
\begin{pmatrix} \mathcal{L}^{-1} & -\mathcal{L}^{-1} \\ \mathcal{M} & \mathcal{M} \end{pmatrix}
\begin{pmatrix} \tau \\ 0 \end{pmatrix}
$$

(3.3.34)

Substituing we get
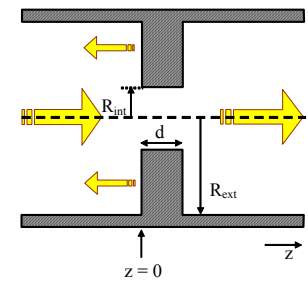
$$\begin{pmatrix} \delta \\ \rho \end{pmatrix} = \begin{pmatrix} \mathcal{L}^{-1} & -\mathcal{L}^{-1} \\ \mathcal{M} & \mathcal{M} \end{pmatrix}^{-1} \begin{pmatrix} I & -I \\ I & I \end{pmatrix} \begin{pmatrix} e^{-\Lambda d} & 0 \\ 0 & e^{\Lambda d} \end{pmatrix}^{-1} \begin{pmatrix} I & -I \\ I & I \end{pmatrix}^{-1} \begin{pmatrix} \mathcal{L}^{-1} & -\mathcal{L}^{-1} \\ \mathcal{M} & \mathcal{M} \end{pmatrix} \begin{pmatrix} \tau \\ 0 \end{pmatrix}$$

or (3.3.35)

$$\begin{pmatrix} \tau \\ 0 \end{pmatrix} = \begin{pmatrix} \mathcal{L}^{-1} & -\mathcal{L}^{-1} \\ \mathcal{M} & \mathcal{M} \end{pmatrix}^{-1} \begin{pmatrix} I & -I \\ I & I \end{pmatrix} \begin{pmatrix} e^{-\Lambda d} & 0 \\ 0 & e^{\Lambda d} \end{pmatrix} \begin{pmatrix} I & -I \\ I & I \end{pmatrix}^{-1} \begin{pmatrix} \mathcal{L}^{-1} & -\mathcal{L}^{-1} \\ \mathcal{M} & \mathcal{M} \end{pmatrix} \begin{pmatrix} \delta \\ \rho \end{pmatrix}$$

or using a short notation

$$\begin{pmatrix} Q_{11} & Q_{12} \\ Q_{21} & Q_{22} \end{pmatrix} \begin{pmatrix} \delta \\ \rho \end{pmatrix} = \begin{pmatrix} \tau \\ 0 \end{pmatrix}$$

(3.3.36)

thus $Q_{11}\delta + Q_{12}\rho = \tau$ and $Q_{21}\delta + Q_{22}\rho = 0$. Consequently,

$$\rho = -Q_{22}^{-1}Q_{21}\delta, \quad \tau = [Q_{11} - Q_{12}Q_{22}^{-1}Q_{21}]\delta.$$

(3.3.37)

The Figure below illustrates the reflection coefficient and power conservation as a function of the frequency. We observe that below the cut-off of the second mode all the propagating power is in the first mode. As the frequencies exceed the cut-off of the second mode, part of the power leaves the system through the second mode.
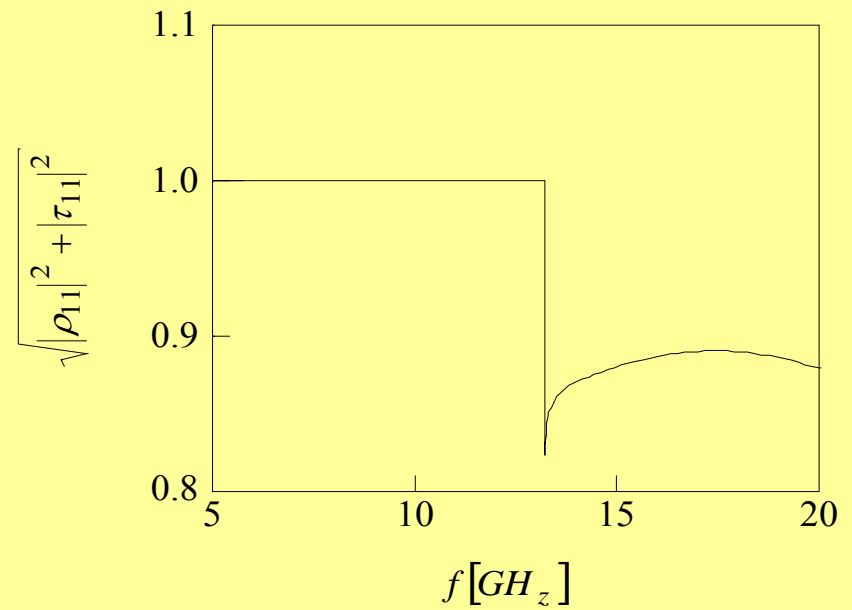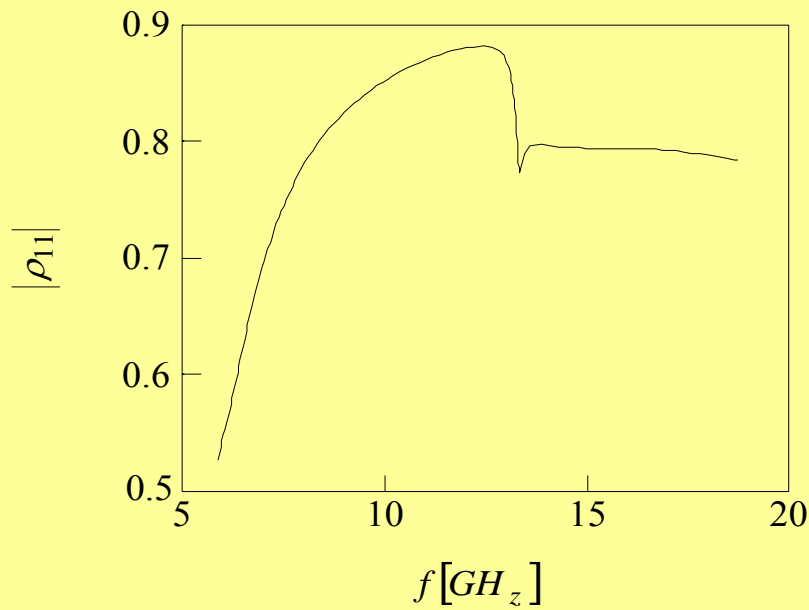
The reflection coefficient as a function of the frequency and energy conservation of the first mode. Note that as long as the higher mode is below cutoff, $\sqrt{|\overline{\rho}_{1,1}|^2 + |\overline{\tau}_{1,1}|^2} = 1$ while above cutoff, energy is transferred from the first mode to the second and therefore $\sqrt{|\overline{\rho}_{1,1}|^2 + |\overline{\tau}_{1,1}|^2} \neq 1$.

3.4 Reactive Elements

Obstacles in waveguides or transmission lines may cause reflections which in turn may be detrimental. Power reflected implies obviously reduction in the transmitted power but it entails that some energy is stored in the evanescent waves which develop in the vicinity of the obstacle.

3.4.1 Inductive Post

As an example we shall examine a cylindrical post and an incident TE_{01} mode determined by

$$E_y^{(p)}(x,z) = E_0 \sin\left(\pi\frac{x}{a}\right)\exp(-\Gamma_1 z); \ \Gamma_1 = \sqrt{(\pi/a)^2 - (\omega/c)^2} = j\beta \qquad (3.4.1)$$

In zero order this **primary field** excites in the metallic cylinder a current density

$$J_y(x,z) = I\delta(z)\delta(x-d) \qquad (3.4.2)$$

which may be interpreted as surface current density
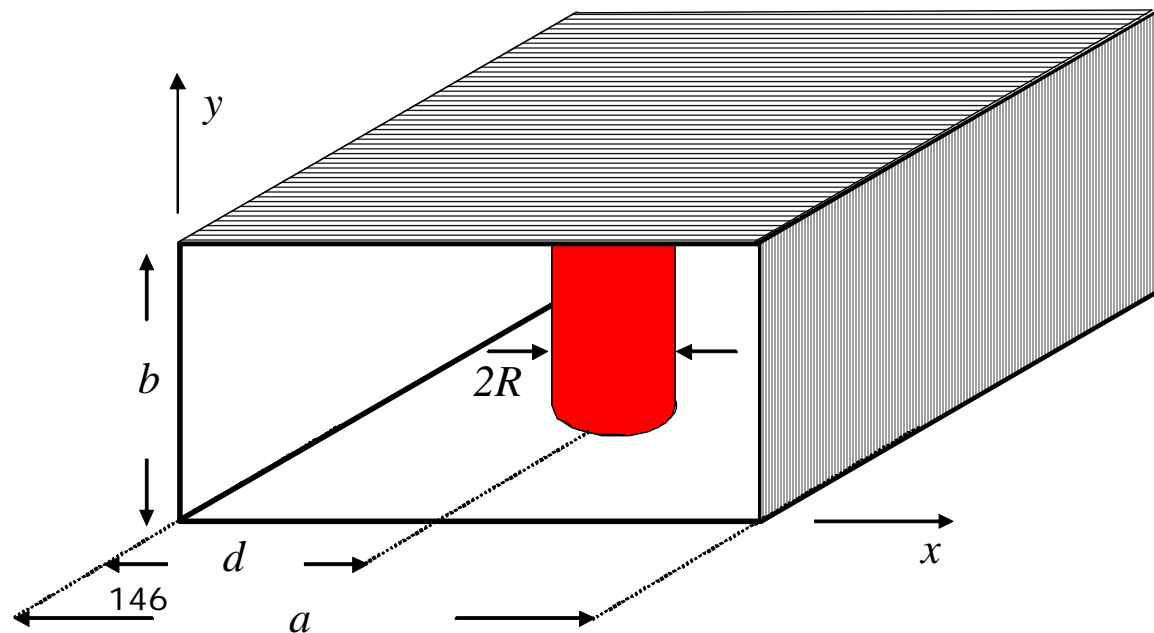
$$J_{y,s}(x) = I\delta(x-d) = \sum_{m=1}^{\infty} U_m \sin\left(\pi m \frac{x}{a}\right) \qquad (3.4.3)$$

hence

$$U_m = \frac{2}{a} I \sin\left(\pi m \frac{d}{a}\right). \qquad (3.4.4)$$

This current generates a **secondary field**

$$E_y^{(\text{sec})}(x,z) = \sum_{m=1}^{\infty} \mathcal{E}_m \sin\left(\pi m \frac{x}{a}\right) \exp\left(-\Gamma_m |z|\right) \qquad (3.4.5)$$

where $\Gamma_m^2 = (\pi m / a)^2 - \omega^2 / c^2$. In order to establish the relation between the current's ``harmonics'' and the secondary field we observe that based on Maxwell's equations the magnetic field

$$H_x^{(\text{sec})}(x,z) = \frac{-1}{j\omega\mu_0} \sum_{m=1}^{\infty} \Gamma_m \mathcal{E}_m \sin\left(\pi m \frac{x}{a}\right) \exp\left(-\Gamma_m |z|\right) \text{sgn}(z) \qquad (3.4.6)$$

enables via its discontinuity condition

$$H_x(x, z = 0^+) - H_x(x, z = 0^-) = J_{y,s} \qquad (3.4.7)$$

to determine the amplitudes of the modes describing the secondary field in terms of the current on the filament

$$\mathcal{E}_m = -\frac{I}{a}\sin\left(\pi m\frac{d}{a}\right)\frac{j\omega\mu_0}{\Gamma_m}. \qquad (3.4.8)$$
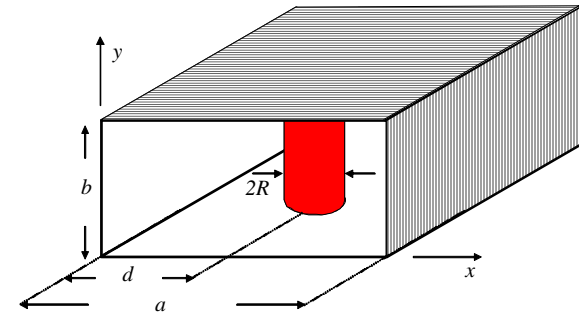
We have yet to determine the relation between the current (I) in the filament and the amplitude of the incident wave. This is done by relaxing the condition of our infinitely small filament and imposing that the **tangential electric field** vanishes on the wall of the post. Specifically, **averaging** the electric field over the azimuthal coordinate at $r = R$ we must get zero total field, namely

$$\int_0^{2\pi} d\phi [E_y^{(inc)} + E_y^{(sec)}]_{\substack{x=d+R\cos\phi \\ z=R\sin\phi}} = 0. \qquad (3.4.9)$$

explicitly

$$\sum_{m=1}^{\infty}\int_0^{2\pi} d\phi\left[E_0\delta_{m,1}\exp(-\Gamma_m R\sin\phi) + \mathcal{E}_m\exp(-\Gamma_m R|\sin\phi|)\right]\sin\left[\frac{\pi m}{a}(d + R\cos\phi)\right] \qquad (3.4.10)$$

which formally may be rewritten by defining

$$\mathcal{L}_m^{(1)} \equiv \frac{1}{2\pi}\int_0^{2\pi} d\phi\, \exp(-\Gamma_m R\sin\phi)\sin\left[\frac{\pi m}{a}(d + R\cos\phi)\right] \qquad (3.4.11)$$

and

$$\mathcal{L}_m^{(2)} \equiv \frac{1}{2\pi}\int_0^{2\pi} d\phi\, \exp(-\Gamma_m R|\sin\phi|)\sin\left[\frac{\pi m}{a}(d + R\cos\phi)\right] \qquad (3.4.12)$$
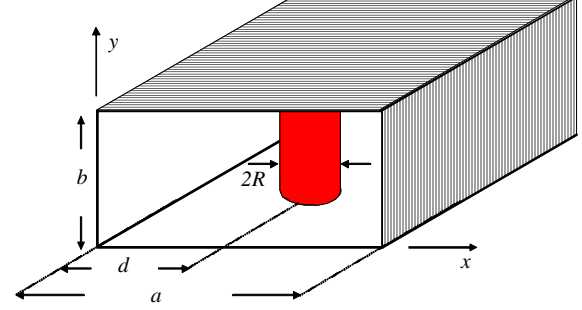
hence

$$E_0 \mathcal{L}_1^{(1)} - I \sum_{m=1}^{\infty} \frac{1}{a} \sin\left(\pi m \frac{d}{a}\right) \frac{j\omega\mu_0}{\Gamma_m} \mathcal{L}_m^{(2)} = 0 \Rightarrow I = \frac{\mathcal{L}_1^{(1)}}{\sum_{m=1}^{\infty} \mathcal{L}_m^{(2)} \left(j\omega / c\Gamma_m\right) \sin\left(\pi m d / a\right)} \frac{E_0 a}{\eta_0}.$$

(3.4.13)

At this stage we may define the reflection coefficient

$$\rho_m \equiv \frac{\mathcal{E}_m}{E_0} = \frac{-\mathcal{L}_1^{(1)} \left(j\omega / c\Gamma_m\right) \sin\left(\pi m d / a\right)}{\sum_{n=1}^{\infty} \mathcal{L}_n^{(2)} \left(j\omega / c\Gamma_n\right) \sin\left(\pi n d / a\right)}$$

(3.4.14)

or for the fundamental

$$\rho_1 = \frac{-\mathcal{L}_1^{(1)} \left(\omega / c\beta\right) \sin\left(\pi d / a\right)}{\mathcal{L}_1^{(2)} \left(\omega / c\beta\right) \sin\left(\pi d / a\right) + \sum_{n=2}^{\infty} \mathcal{L}_n^{(2)} \left(j\omega / c\Gamma_n\right) \sin\left(\pi n d / a\right)}.$$

(3.4.15)

At this point it can be shown that since $m = 1$ is a propagating mode $\mathcal{L}_1^{(1)} = \mathrm{Re}(\mathcal{L}_1^{(2)})$ and the second term in the denominator is pure imaginary

$$\rho_1 = \frac{-1}{1 + j \frac{\mathrm{Im}(\mathcal{L}_1^{(2)})}{\mathcal{L}_1^{(1)}} + j \sum_{n=2}^{\infty} \frac{\mathcal{L}_n^{(2)}}{\mathcal{L}_1^{(1)}} \left(\frac{\beta}{\Gamma_n}\right) \frac{\sin\left(\pi n d / a\right)}{\sin\left(\pi d / a\right)}}.$$

(3.4.16)

149
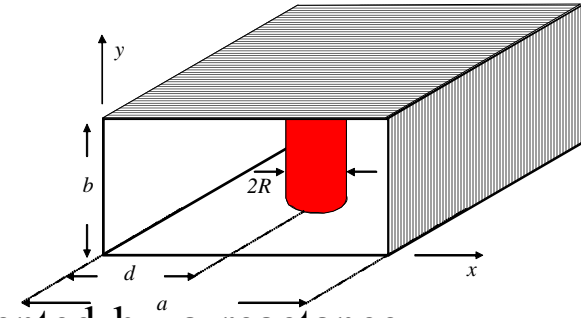
Based on this last result, we conclude that the post may be represented by a reactance since according to the equivalent scheme below

$$\rho_1 = \frac{-1}{1+2\overline{Z}_L} = \frac{-1}{1+2j\overline{X}_L}$$

and

$$\overline{X}_L = \frac{1}{2}\frac{\mathrm{Im}[\mathcal{L}_1^{(2)}]}{\mathcal{L}_1^{(1)}} + \sum_{n=2}^{\infty}\frac{\mathcal{L}_n^{(2)}}{\mathcal{L}_1^{(1)}}\frac{\beta}{\Gamma_n}\frac{\sin(\pi n d/a)}{\sin(\pi d/a)}.$$
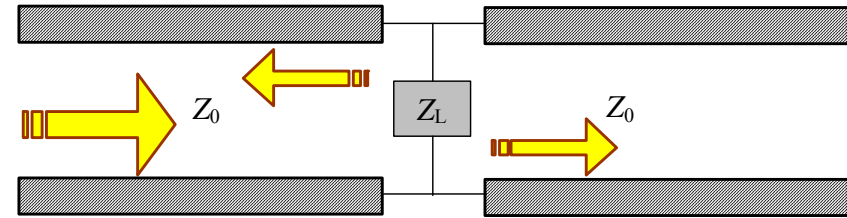
Further simplification, is achieved assuming that $R \ll d$ we get

$$\mathcal{L}_m^{(1)} \simeq \sin\left(\pi m \frac{d}{a}\right)\frac{1}{2\pi}\int_{-\pi}^{\pi}d\phi\,\exp(-\Gamma_m R\sin\phi) \simeq \sin\left(\pi m \frac{d}{a}\right)I_0(\Gamma_m R) \qquad (3.4.17)$$

$$\mathcal{L}_m^{(2)} \simeq \sin\left(\pi m \frac{d}{a}\right)\frac{2}{2\pi}\int_{0}^{\pi}d\phi\,\exp(-\Gamma_m R\sin\phi)$$

$$\simeq \sin\left(\pi m \frac{d}{a}\right)\left[I_0(\Gamma_m R)+2\sum_{k=1}^{\infty}(-1)^k\,\mathrm{sinc}\left(\frac{1}{2}\pi k\right)I_k(\Gamma_m R)\right]$$

(3.4.18)

thus

$$\overline{X}_L = \frac{\sum_{n=2}^{\infty}\left[\dfrac{I_0\left(\Gamma_n R\right)}{\Gamma_n R} - \dfrac{4}{\pi}\sum_{k=0}^{\infty}\dfrac{\left(-1\right)^k}{2k+1}\dfrac{I_{2k+1}\left(\Gamma_n R\right)}{\Gamma_n R}\right]\sin^2\left(\pi n\dfrac{d}{a}\right)}{\dfrac{J_0\left(\beta R\right)}{\beta R}\sin^2\left(\pi\dfrac{d}{a}\right)} \qquad (3.4.19)$$

At the limit $R \to 0$ or more precisely assuming $\beta R \ll 1$ and $\Gamma_n R \ll 1$ thus $I_\nu\left(x \ll 1\right) \simeq \left(x/2\right)^\nu / \nu!$ we get

$$\overline{X}_L = \frac{\sum_{n=2}^{\operatorname{Int}\left(\frac{a}{R}\frac{1}{\pi}\right)}\left[\dfrac{1}{\Gamma_n R} - \dfrac{4}{\pi}\sum_{k=0}^{\infty}\dfrac{\left(-1\right)^k}{2k+1}\dfrac{\left(\Gamma_n R\right)^{2k}}{\left(2k+1\right)!}\left(\dfrac{1}{2}\right)^{2k+1}\right]\sin^2\left(\pi n\dfrac{d}{a}\right)}{\dfrac{1}{\beta R}\sin^2\left(\pi\dfrac{d}{a}\right)} \qquad (3.4.20)$$

151

Exercise 3.8: Analyze (numerically) the dependence of the normalized reactance on three parameters; the angular frequency (ω), its location (d) and its radius (R). It is possible to simplify the two quantities defined in (3.4.11) and (3.4.12) by using

$$\exp\left[\frac{z}{2}\left(t-\frac{1}{t}\right)\right] = \sum_{k=-\infty}^{\infty} t^k J_k(z) \; ; \;\; J_{-k}(z) = (-1)^k J_k(z).$$

(For solution see Appendix 10.1)

Exercise 3.9: Calculate the energy stored in the vicinity of the post and compare it with energy per unit length carried by the incident wave.

Exercise 3.10: Analyze the ratio of electric to magnetic energy stored around the post.

3.4.2 Diaphragm

Another element (obstacle) that may deflect radiation but not absorb it is the diaphragm. This is a thin metallic layer occupying part of the cross-section. Consider a diaphragm occupying the region $d < x < a$ its thickness being negligible compared to the wavelength and the skin depth. The electric field is given by
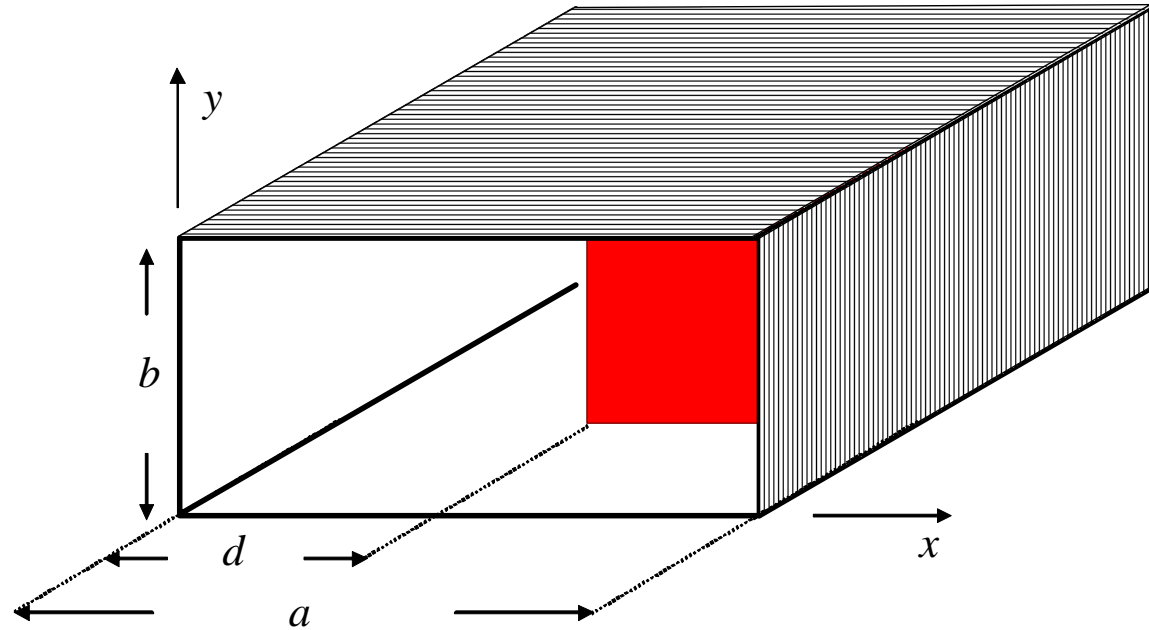
$$E_y = E_0 \begin{cases} \left[\exp(-j\beta z) + \rho_1 \exp(j\beta z)\right]\sin\left(\pi\frac{x}{a}\right) + \sum_{m=2}^{\infty}\rho_m \exp(\Gamma_m z)\sin\left(\pi m\frac{x}{a}\right) & z < 0 \\ \\ \tau_1 e^{-j\beta z}\sin\left(\pi\frac{x}{a}\right) + \sum_{m=2}^{\infty}\tau_m \exp(-\Gamma_m z)\sin\left(\pi m\frac{x}{a}\right) & z > 0. \end{cases}$$

(3.4.21)

Let us denote by $E_y\left(x, z = 0\right) = E_0\mathcal{E}(x)$ the transverse electric field in the **aperture**, thus
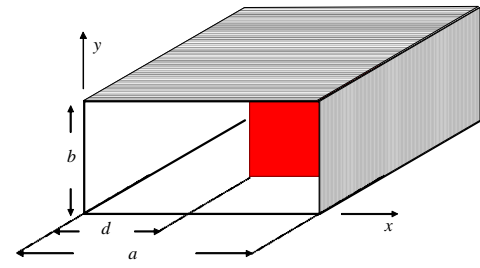
$$m = 1: \qquad 1 + \rho_1 = \tau_1 = \frac{2}{a} \int_0^d dx \, \mathcal{E}(x) \sin\left(\pi \frac{x}{a} \right) \qquad\qquad (3.4.22)$$

$$m \geq 2: \qquad \rho_m = \tau_m = \frac{2}{a} \int_0^d dx \, \mathcal{E}(x) \sin\left(\pi m \frac{x}{a} \right). \qquad\qquad (3.4.23)$$

$\mathcal{E}(x)$ represents the horizontal variation of the vertical electric field $\left(E_y \right)$. Continuity of H_x in the aperture $(0 < x < d)$ implies

$$-j\beta(1 - \rho_1) \sin\left(\pi \frac{x}{a} \right) + \sum_{m=2}^{\infty} \rho_m \Gamma_m \sin\left(\pi m \frac{x}{a} \right) = -j\beta \tau_1 \sin\left(\pi \frac{x}{a} \right) - \sum_{m=2}^{\infty} \tau_m \Gamma_m \sin\left(\pi m \frac{x}{a} \right).$$

$$\qquad\qquad (3.4.24)$$

Substituting (3.4.23) we get

$$-2\rho_1 \sin\left(\pi \frac{x}{a} \right) = -\sum_{m=2}^{\infty} \left(\frac{\Gamma_m}{-j\beta} \right) \sin\left(\pi m \frac{x}{a} \right) \frac{4}{a} \int_0^d dx' \mathcal{E}(x') \sin\left(\pi m \frac{x'}{a} \right) \qquad (3.4.25)$$

and further multiplying and deviding by $1 + \rho_1$ and using (3.4.22) we finally obtain

$$\frac{2\rho_1}{1 + \rho_1} \sin\left(\pi \frac{x}{a} \right) \int_0^d dx' \mathcal{E}(x') \sin\left(\pi \frac{x'}{a} \right) = 2j \sum_{m=2}^{\infty} \left(\frac{\Gamma_m}{\beta} \right) \sin\left(\pi m \frac{x}{a} \right) \int_0^d dx' \mathcal{E}(x') \sin\left(\pi m \frac{x'}{a} \right).$$

$$\qquad\qquad (3.4.26)$$
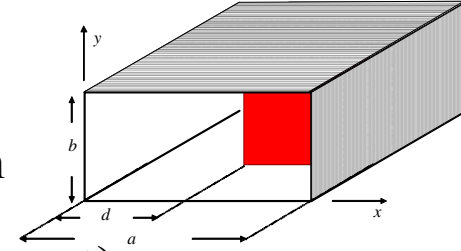
Since the admittance is $\bar{Y}_L = -\dfrac{2\rho_1}{1+\rho_1}$ in the left hand side may be rewritten

$$\bar{Y}_L \sin\left(\pi\frac{x}{a}\right)\int_0^d dx'\mathcal{E}(x')\sin\left(\pi\frac{x'}{a}\right) = -2j\sum_{m=2}^{\infty}\left(\frac{\Gamma_m}{\beta}\right)\sin\left(\pi m\frac{x}{a}\right)\int_0^d dx'\mathcal{E}(x')\sin\left(\pi m\frac{x'}{a}\right).\ (3.4.27)$$

So far the formulation is **exact** (of course subject to the specified assumptions). At this stage we multiply both sides by $\mathcal{E}(x)$ and integrate over the cross section of the aperture and get

$$\bar{Y}_L = -2j\sum_{m=2}^{\infty}\left(\frac{\Gamma_m}{\beta}\right)\frac{\left[\int_0^d dx'\mathcal{E}(x')\sin\left(\pi m\frac{x'}{a}\right)\right]^2}{\left[\int_0^d dx'\mathcal{E}(x')\sin\left(\pi\frac{x'}{a}\right)\right]^2}.\ \ (3.4.28)$$

which evidently entails that the **distribution of the electric field in the aperture determines the admittance of the diaphragm** as experienced by the wave. For a rough **approximation** we may consider the simplest form of $\mathcal{E}(x)$ that satisfies the boundary conditions at $x=0$ and $x=d$ but it ignores edge effect namely, $\mathcal{E}(x)\propto x(d-x)$. An estimate of the edge effect may be considered by $\mathcal{E}(x)\propto x(d-x)^{\nu}$ with $0<\nu\leq 1$.

Exercise 3.11: Compare the admittace using the approximation $\mathcal{E}(x) = x(d - x)$ with that evaluated by Lewin (Theory of Waveguides)

$$\overline{Y}_L = j\frac{2\pi}{\beta a}\left[1 - \sin^{-4}\left(\frac{\pi}{2}\frac{d}{a}\right)\right].$$

Exercise 3.12: What is the effect of the *edge* of the diaphragm?

3.5 Excitation of Waveguides – Probe Antenna

   Coupling of fields from one guide to another may be accomplished by means of small antennas by means of small radiating apertures located at appropriate positions in the common wall separating the two guides. A completely rigorous solution of the antenna boundary-value problem in a waveguide is beyond the scope of this course. Nevertheless, by making suitable approximations, solutions which shed considerable light on the behavior of antennas in waveguides, as well as providing useful engineering results, can be obtained for many practical cases. In this section attention will be confined to the small coaxial-line probe.

Input impedance. The type of coaxial-line probe antenna to be analyzed is illustrated next. It consists of a small coaxial line, terminated in the center of the broad face of a rectangular guide, with its inner conductor extending a distance d into the guide.
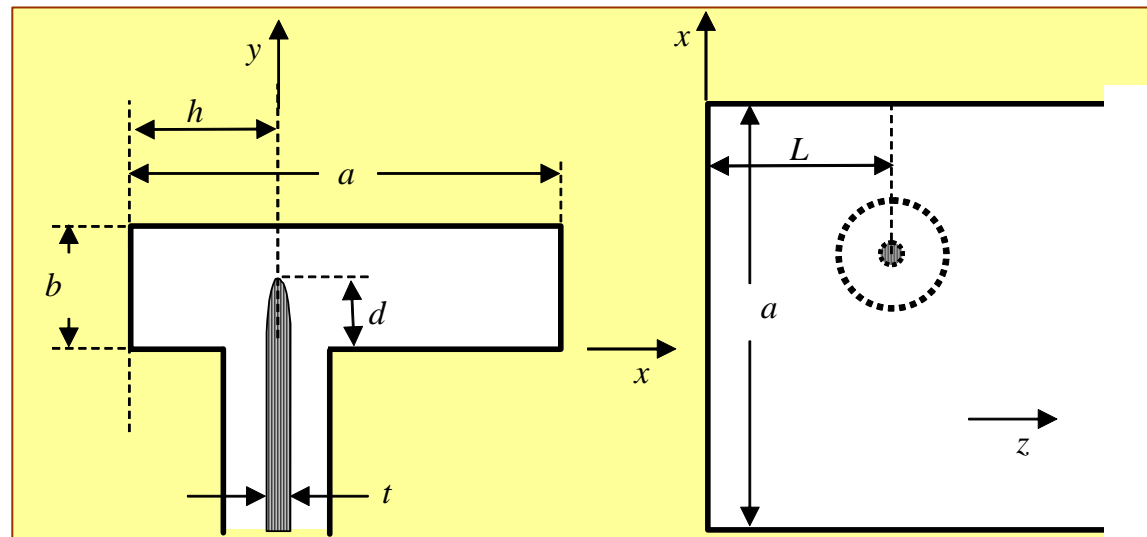
In order to have the antenna radiate in one direction only, a short-circuiting plunger is placed at a distance L to the left of the probe. The basic concept is to **generate a current** (I) at a location where the **parallel electric field is maximum** -- quarter wavelength from a short circuiting plane.
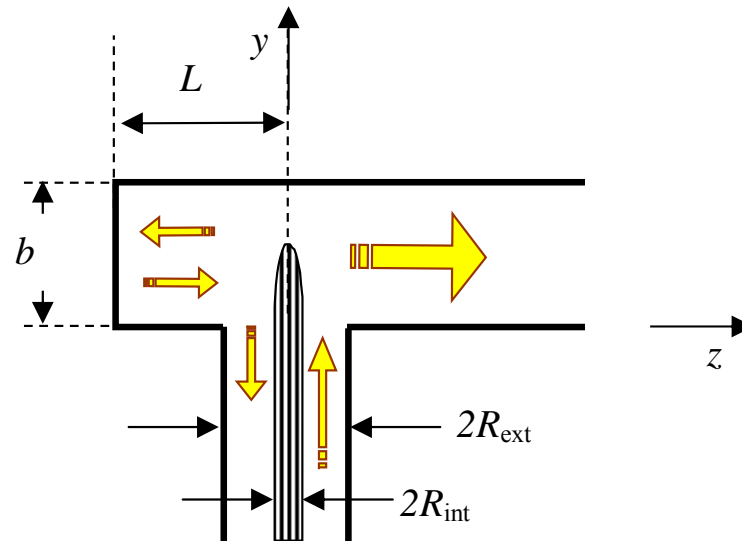
The total field in the waveguide could be found if E_a and H_a, the **total tangential fields in the aperture** were known. Unfortunately, these aperture fields are unknown, but, if the **coaxial-line opening is *small***, we may, to a first approximation, assume that the higher-order coaxial-line modes which being excited, are negligible. The field in the aperture will then be that associated with the ***incident and reflected* TEM modes** in the coaxial line.
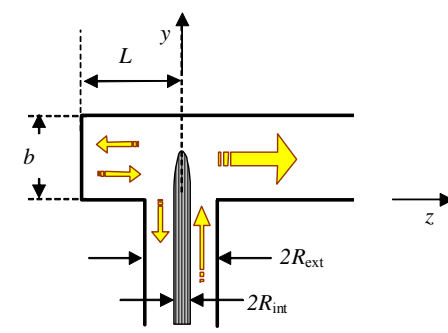
Relying on Poynting's complex theorem we find by denoting by P the power flow far away from the probe that

$$-\frac{1}{2}\int dV J_y^* E_y = P + 2j\omega[\langle W_M \rangle - \langle W_E \rangle] \qquad (3.5.1)$$

where the current density may be approximated, assuming a *thin* probe, by

$$J_y(x,y,z) = \frac{I(y)}{\pi R_{int}^2} u\left[R_{int} - \sqrt{(x-h)^2 + (z-L)^2} \right]. \qquad (3.5.2)$$

This current density excites a TE_{nm} mode satisfying

$$\left(\nabla^2 + \frac{\omega^2}{c^2} \right) E_y = j\omega\mu_0 J_y - \frac{1}{j\omega\varepsilon_0}\frac{\partial^2}{\partial y^2} J_y \qquad (3.5.3)$$

which in terms of Green's function reads

$$E_y(x,y,z) = -j\omega\mu_0 \int dx' dy' dz' G_y(x,y,z \mid x',y',z')\left[J_y(x',y',z') + \frac{c^2}{\omega^2}\frac{\partial^2}{\partial y'^2} J_y(x',y',z') \right]. \qquad (3.5.4)$$

In turn Green's function for our configuration is given by

159
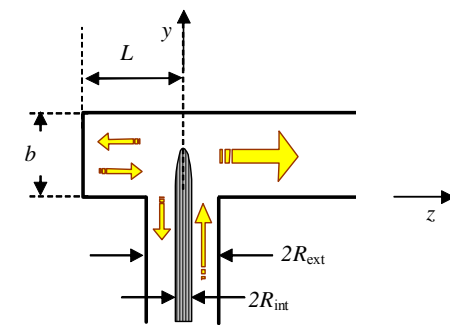
$$G_y(\vec{r}\,|\,\vec{r}\,') = \sum_{n=1,m=0}^{\infty} \frac{1}{(2\Gamma_{nm})ab}(1+\delta_{m,0})\sin\left(\pi n\frac{x}{a}\right)\sin\left(\pi n\frac{x'}{a}\right)$$

$$\times\cos\left(\pi m\frac{y}{b}\right)\cos\left(\pi m\frac{y'}{b}\right)\left\{\exp\left[-\Gamma_{n,m}|z-z'|\right]-\exp\left[-\Gamma_{n,m}(z+z')\right]\right\}$$

$$(3.5.5)$$

Exercise 3.13: Prove that this is the solution of

$$\left(\nabla^2 +\frac{\omega^2}{c^2}\right)G_y = -\delta(x-x')\delta(y-y')\delta(z-z')$$

$$G_y(x=0,a) = 0, \quad \left.\frac{\partial G_y}{\partial y}\right|_{y=0,b} = 0, \quad G_y(x,y,z=0) = 0.$$

Substituting (3.5.4) and (3.5.2) in (3.5.1) as well as taking advantage of the probe being thin we have

$$\frac{j\omega\mu_0}{2}\int dy I^*(y)\int dy' g(y\,|\,y')\left[I(y')+\frac{c^2}{\omega^2}\frac{\partial^2}{\partial y^2}I(y')\right] = P+2j\omega[\langle W_M\rangle-\langle W_E\rangle] \quad (3.5.6)$$

wherein
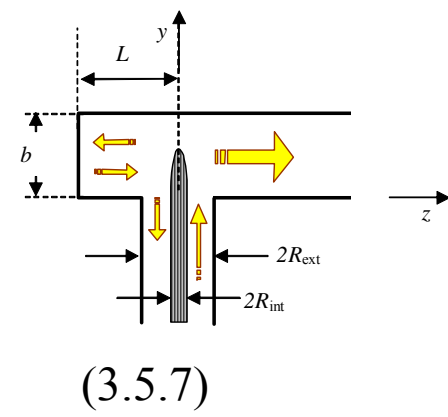
$$g(y \mid y') \equiv G\left(x = h, y, z = L \mid x' = h, y', z' = L\right) = \sum_{\substack{n=1 \\ m=0}} \frac{1}{(2\Gamma_{n,m})ab}(1+\delta_{m,0})$$

(3.5.7)

$$\times \sin^2\left(\pi n \frac{h}{a}\right)\left[1 - \exp\left(-2\Gamma_{n,m}L\right)\right]\cos\left(\pi m \frac{y}{b}\right)\cos\left(\pi m \frac{y'}{b}\right)$$

In terms of the current at the *aperture* of the coax (interface coax-waveguide) the current is $I(0)$ therefore, we may define the input impedance

$$Z_{in} \equiv \frac{P + 2j\omega[\langle W_M \rangle - \langle W_E \rangle]}{\frac{1}{2}|I(0)|^2}$$

(3.5.8)

hence

$$Z_{in} \simeq j\omega\mu_0 \int_0^d dy \, \overline{I}^*(y)\int_0^d dy' \, g(y \mid y')\left[\overline{I}(y') + \frac{c^2}{\omega^2}\frac{\partial^2}{\partial y^2}\overline{I}(y')\right].$$

(3.5.9)

At the end of the probe the current is zero, therefore, for simplicity sake we assume

$$\overline{I}(y) = \frac{I(y)}{\overline{I}(0)} = \left(\frac{y - d}{d}\right)^2$$

(3.5.10)

or

$$Z_{in} = j\omega\mu_0 \int_0^d dy \left(\frac{y-d}{d}\right)^2 \int_0^d dy' g(y|y') \left[\left(\frac{y'-d}{d}\right)^2 + \frac{2c^2}{\omega^2 d^2}\right] \qquad (3.5.11)$$

Let us assume now that **except the first mode, all the modes are evanescent**. Clearly their contribution to the impedance is pure imaginary (inductive). Only the propagating mode has both imaginary and real contribution to the impedance

$$Z_{in} = \frac{\eta_0}{18} \frac{d^2}{ab} \frac{\omega}{c\beta} \sin^2\left(\pi\frac{h}{a}\right) \sin(\beta L)\left[\sin(\beta L) + j\cos(\beta L)\right]\left[1 + 6\left(\frac{\omega}{c}d\right)^{-2}\right] \qquad (3.5.12)$$

Comment: The required values of L and d to make $X = 0$ and $R = Z_c$, so that **all the incident power is coupled into the guide**, may be found graphically from a plot of the $X = 0$ and $R =$ constant contours in the $k_0 d - \beta L$ plane. Such a plot is given in the figure above for a guide of dimensions 2.3×1 cm and a probe diameter equal to 0.23 cm at a wavelength of 3.14 cm. The
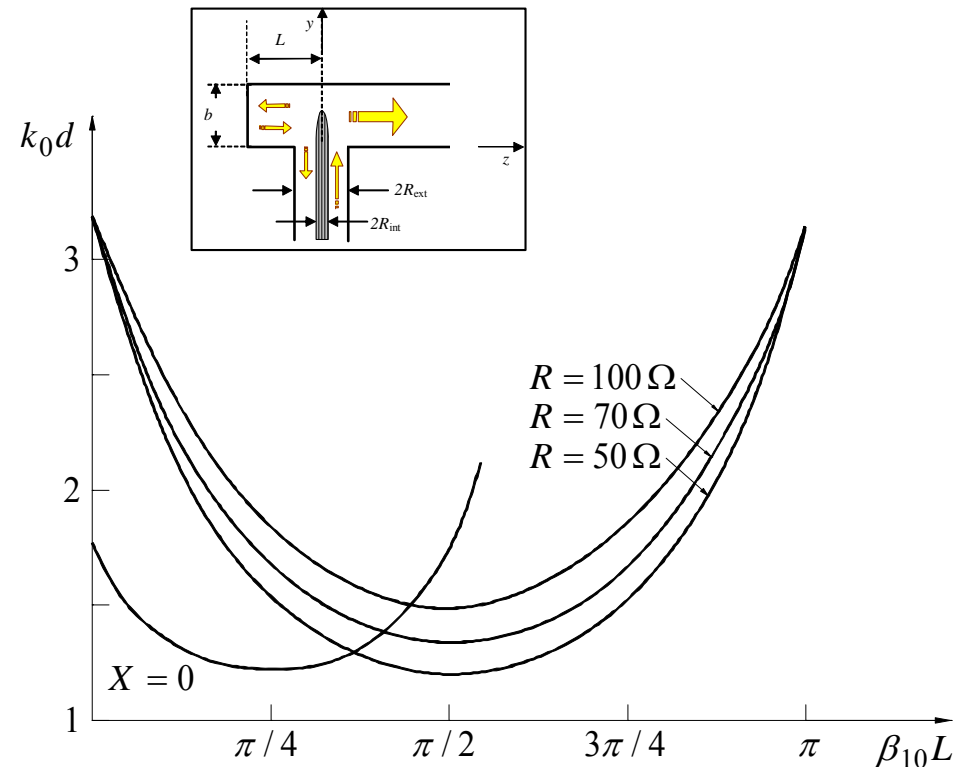
intersection of the two curves determines the required parameters. From the figure it is seen that the self-resonant length of the antenna, corresponding to $\beta L = 0$ or $\pi/2$, is $0.28\lambda_0$. Also it is seen that, for $k_0 d$ less than 1.22 ($d < 0.61$ centimeter), a value of βL which will make $X = 0$ does not exist. The reason is that the TE_{10} mode standing wave between the antenna and the short-circuiting plunger cannot provide enough inductive reactance to counterbalance the high capacitive reactance of a short probe.

3.6 Coupling between Waveguides by Small Apertures

Electromagnetic energy may be coupled from one waveguide into another guide or into a cavity resonator by a small aperture located at a suitable position in the common wall. For apertures whose linear dimensions are small compared with the wavelength, an approximate theory is available which states that the aperture is equivalent to a combination of radiating electric and magnetic dipoles, whose dipole moments are respectively proportional to the normal electric field and tangential magnetic field of the incident wave. This theory was originally developed by H.A. Bethe in ``Theory of Diffraction by Small Holes'', Physical Review, vol. 66, pp. 163--182, 1944.

3.7 Surface Waveguides

In addition to the *closed* cylindrical conducting tube and the conventional TEM wave-transmission line, there exists a class of *open* boundary structures which are capable of guiding an electromagnetic wave. The field is characterized by an exponential decay away from the surface and having the usual propagation function $\exp(-j\beta z)$ along the axis of the structure. Moreover it has a discrete spectrum of eigenmodes. This type of wave is called a **surface wave**, and the structure which guides this wave may be appropriately referred to as a surface waveguide. Some typical structures that are capable of supporting a surface wave are illustrated in Figure 10. These consist of dielectric-slabs, fibers, dielectric-coated planes and wires and corrugated planes and wires.
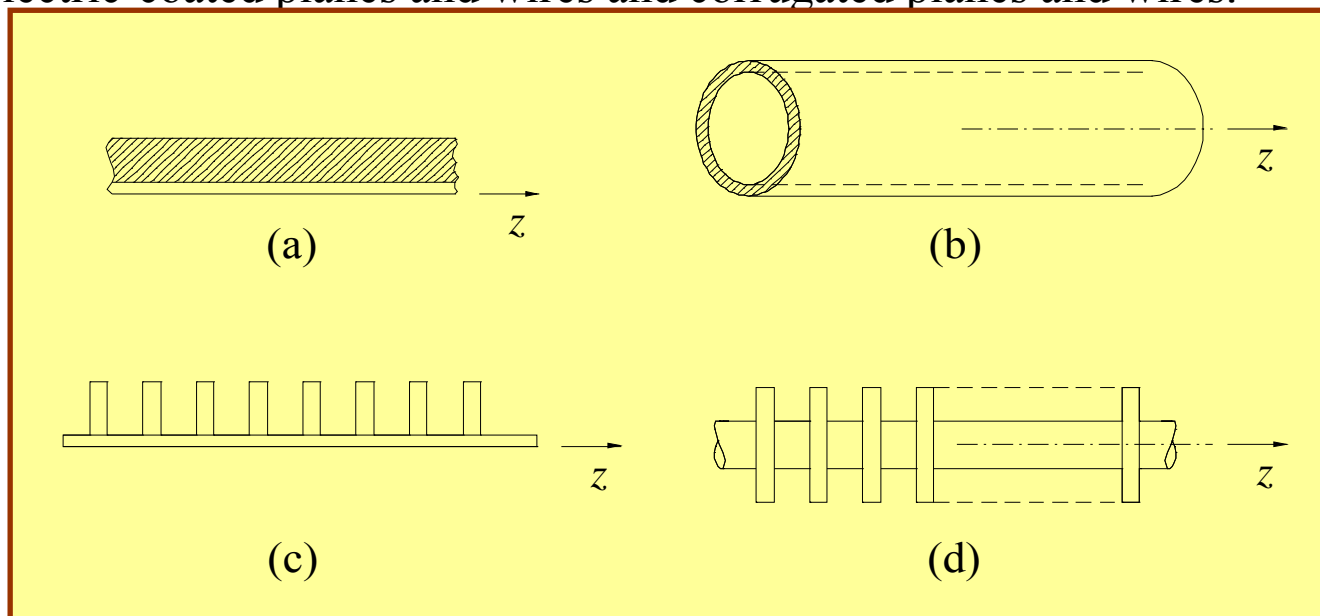
Although surface waveguides have several features which are similar to those of the cylindrical conducting-tube guide, they have many characteristics which are quite different. Some of the outstanding differences are:

1. Propagation with no low-frequency cutoff.
2. Finite number of discrete modes of propagation at a given frequency.
3. Phase velocity smaller than that of plane wave in vacuum.

3.7.1 Dielectric Layer above a Metallic Surface

Consider a TM mode and for the sake of simplicity, yet without significant loss of generality, we shall examine the case when $\partial_y = 0$, or more specifically TM_{01}. This mode may be derived from the longitudinal electric field
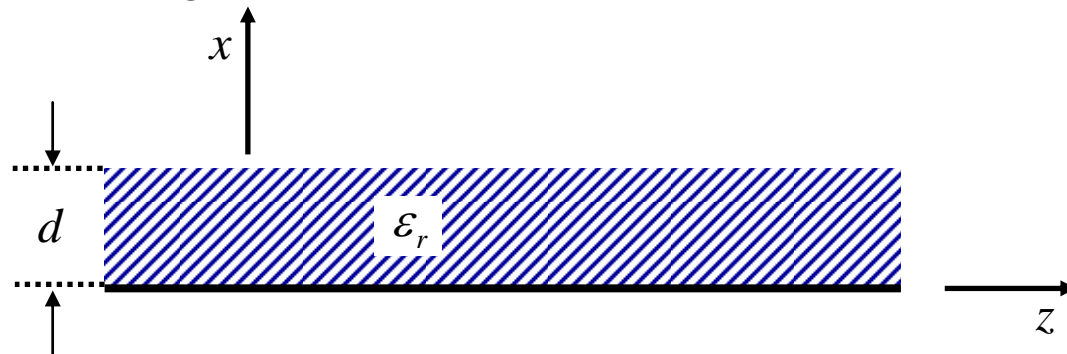
Basic configuration of the open dielectric waveguide.
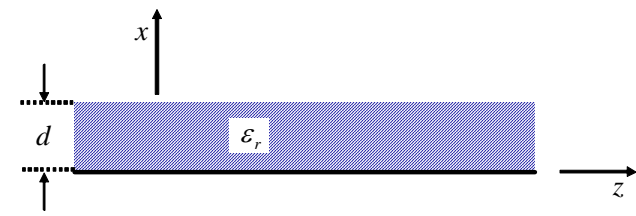
$$E_z(x,z) = \exp(-jkz)\begin{cases} A\sin\left(x\sqrt{\dfrac{\omega^2}{c^2}\varepsilon_{\mathrm r}-k^2}\right) & 0 < x < d \\[3em] B\exp\left[-(x-d)\sqrt{k^2-\dfrac{\omega^2}{c^2}}\right] & x > d \end{cases} \qquad (3.7.1)$$

The x-component of the electric field may be derived using Gauss' law ($\vec{\nabla}\cdot\vec{E}=0$)

$$E_x(x,z) = \exp(-jkz)\begin{cases} \dfrac{-jkA}{\sqrt{\dfrac{\omega^2}{c^2}\varepsilon_{\mathrm r}-k^2}}\cos\left(x\sqrt{\dfrac{\omega^2}{c^2}\varepsilon_{\mathrm r}-k^2}\right) & 0 < x < d \\[3em] \dfrac{-jkB}{\sqrt{k^2-\dfrac{\omega^2}{c^2}}}\exp\left[-(x-d)\sqrt{k^2-\dfrac{\omega^2}{c^2}}\right] & x > d \end{cases} \qquad (3.7.2)$$

for establishing the magnetic field we use Ampere's law ($\vec{\nabla}\times\vec{H} = j\omega\varepsilon_0\varepsilon_{\mathrm r}\vec{E}$)
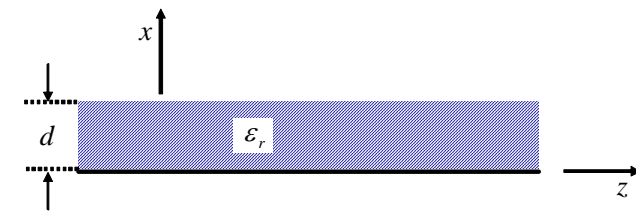
$$H_y(x,z) = \exp(-jkz) \begin{cases} \dfrac{-j\omega\varepsilon_0\varepsilon_r A}{\sqrt{\varepsilon_r\dfrac{\omega^2}{c^2}-k^2}} \cos\left[x\sqrt{\varepsilon_r\dfrac{\omega^2}{c^2}-k^2}\right] & 0 < x < d \\[3em] \dfrac{-j\omega\varepsilon_0 B}{\sqrt{k^2-\dfrac{\omega^2}{c^2}}} \exp\left[-(x-d)\sqrt{k^2-\dfrac{\omega^2}{c^2}}\right] & d < x < \infty. \end{cases}$$

<div align="center">(3.7.3)</div>

Continuity of the tangential electric field implies

$$E_z: \quad A\sin\left[d\sqrt{\varepsilon_r\frac{\omega^2}{c^2}-k^2}\right] = B \qquad\qquad\qquad (3.7.4)$$

whereas the continuity of the tangential magnetic field

$$H_y: \quad \frac{\varepsilon_r}{\sqrt{\varepsilon_r\dfrac{\omega^2}{c^2}-k^2}} A\cos\left[d\sqrt{\varepsilon_r\frac{\omega^2}{c^2}-k^2}\right] = \frac{1}{\sqrt{k^2-\dfrac{\omega^2}{c^2}}} B. \qquad (3.7.5)$$

These two equations lead to the following dispersion relation
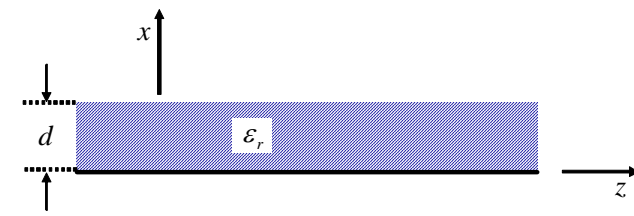
$$\xi \tan(\xi) = \varepsilon_r d \sqrt{k^2 - \frac{\omega^2}{c^2}} \,, \tag{3.7.6}$$

where $\xi \equiv d\sqrt{\varepsilon_r \dfrac{\omega^2}{c} - k^2}$. It is also convenient to define $\xi_0 = \dfrac{\omega}{c}d\sqrt{\varepsilon_r - 1}$ therefore, we may write

$$\xi^2 = d^2 \left[(\varepsilon_r - 1)\frac{\omega^2}{c^2} + \frac{\omega^2}{c^2} - k^2 \right] \Rightarrow d\sqrt{k^2 - \frac{\omega^2}{c^2}} = \sqrt{\xi_0^2 - \xi^2} \tag{3.7.7}$$

Consequently, the dispersion relation reads

$$\boxed{\xi \tan(\xi) = \varepsilon_r \sqrt{\xi_0^2 - \xi^2}.}$$

(3.7.8)

The two sides of the equation are plotted in the figure below
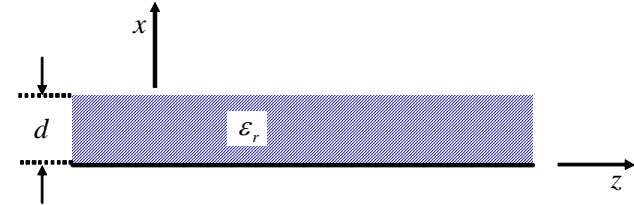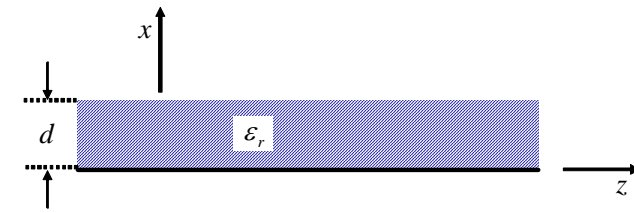
Clearly for a single mode operation, we require that $\xi_0 < \pi \Rightarrow \dfrac{\omega}{c} < \dfrac{\pi}{d}\dfrac{1}{\sqrt{\varepsilon_r - 1}}$.

We shall examine what happens at low frequencies i.e. $\xi \to 0, \xi_0 \to 0$. At this limit the dispersion relation reads

$$\xi^2 = \varepsilon_r \sqrt{\xi_0^2 - \xi^2}$$

The solution of the fourth order polynomial which corresponds to a low-frquency propagating wave is

$$\xi^2 = \frac{1}{2}\left[-\varepsilon_r^2 + \varepsilon_r^2 \sqrt{1 + 4\frac{\xi_0^2}{\varepsilon_r^2}} \right]$$

and now substituting the definitions of ξ and ξ_0 we get

$$k^2 = \varepsilon_{\text{eff}}\left(\frac{\omega}{c}\right)^2 \tag{3.7.11}$$

which is only weakly dependent on the thickness (provided $d \ll \lambda$) but is dependent on
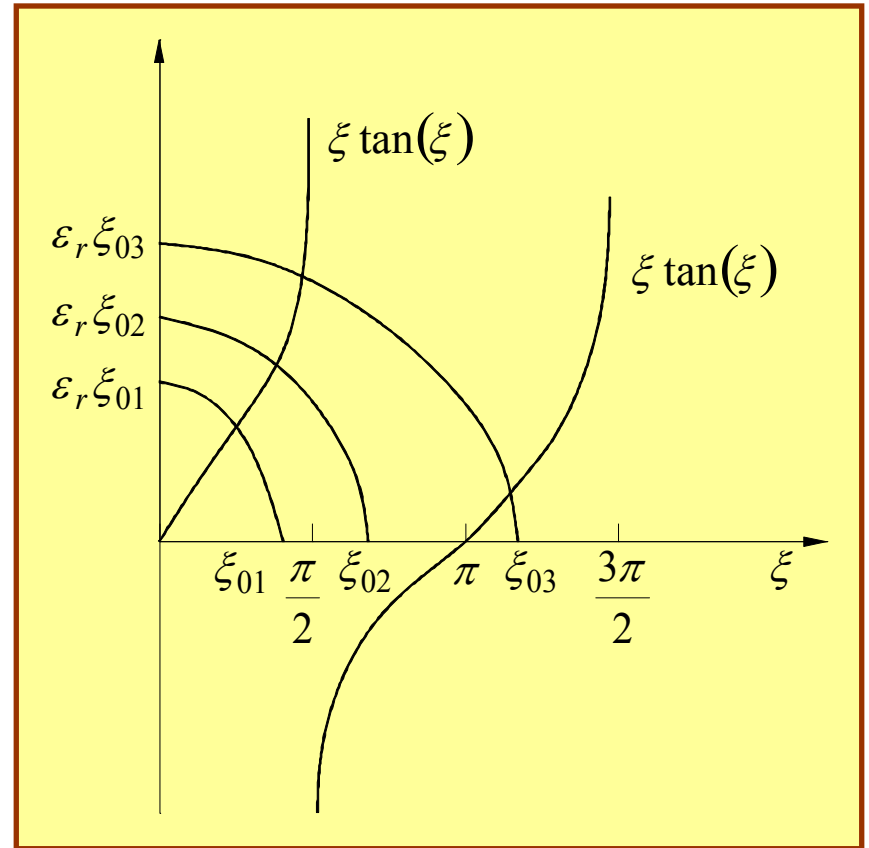
the dielectric coefficient (but $\varepsilon_r > 1$). To be more accurate

$$\varepsilon_r \frac{\omega^2}{c^2} - k^2 = \frac{\varepsilon_r^2}{2d^2}\left[-1 + \sqrt{1 + \frac{4}{\varepsilon_r^2}\left(\frac{\omega}{c}d\right)^2(\varepsilon_r - 1)}\right]$$

(3.7.12)

$$k^2 = \frac{\omega^2}{c^2}$$

where the effective dielectric coefficient is unity.
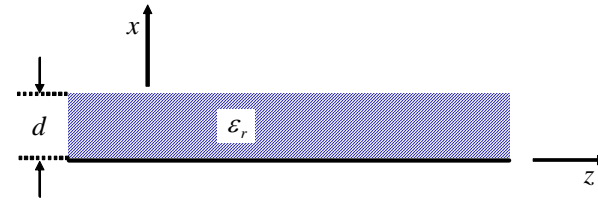
The figure below illustrates the dispersion relation of the system.
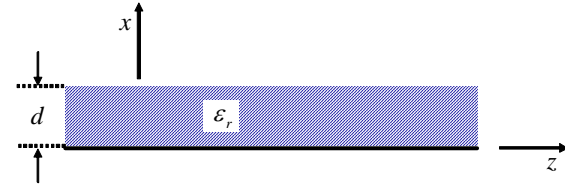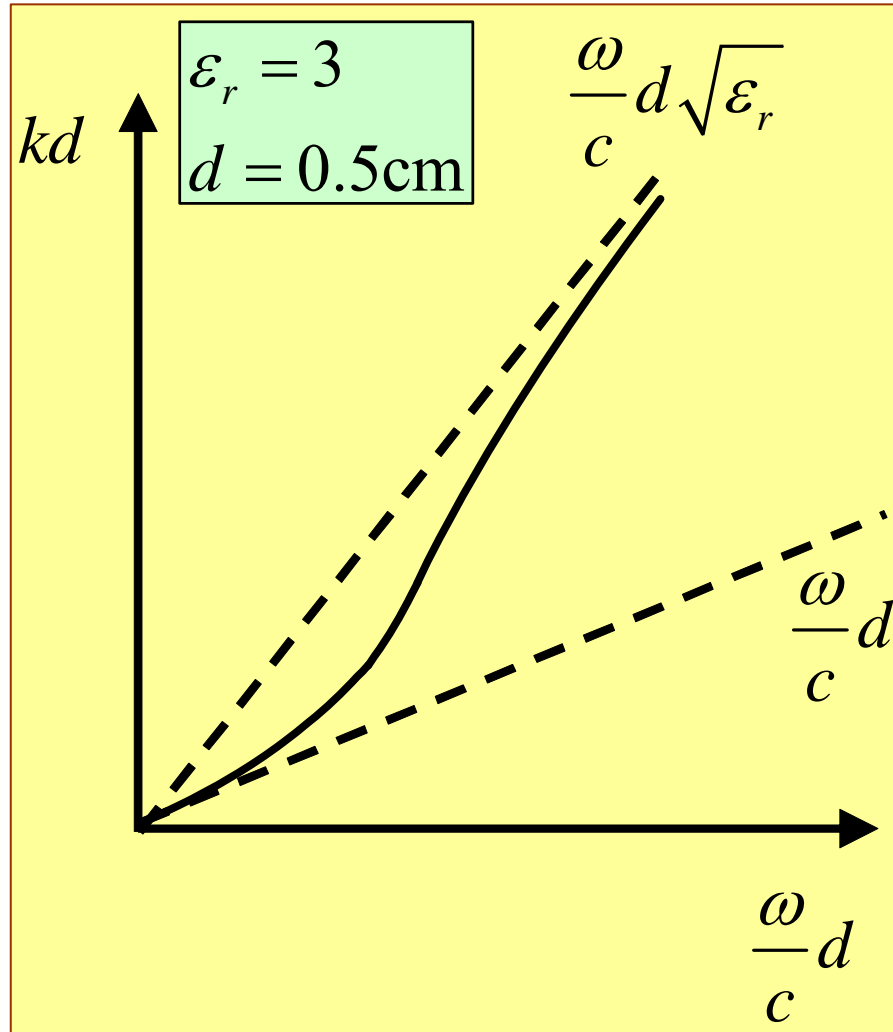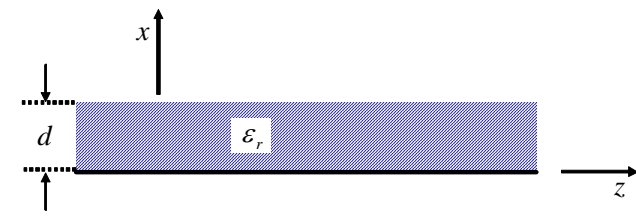
Our next step is to examine the *energy* distribution in the system. Denoting $\xi \equiv d\sqrt{\varepsilon_r (\omega/c)^2 - k^2}$ and $\chi \equiv d\sqrt{k^2 - (\omega/c)^2}$ we calculate the average electric energy per unit surface $(\Delta_y \Delta_z)$ in the dielectric and the air

$$
\begin{aligned}
W_E^{(d)} &= \frac{\varepsilon_0 \varepsilon_r}{4} \int_0^d dx \left[A^2 \sin^2\left(\frac{x}{d}\xi\right) + A^2 \frac{(kd)^2}{\xi^2} \cos^2\left(\frac{x}{d}\xi\right) \right] \\
&= \varepsilon_0 \varepsilon_r \frac{A^2}{8} d \left\{ 1 - \frac{\sin(2\xi)}{2\xi} + \left(\frac{kd}{\xi}\right)^2 \left[1 + \frac{\sin(2\xi)}{2\xi} \right] \right\}
\end{aligned}
\tag{3.7.13}
$$

$$
\begin{aligned}
W_E^{(air)} &= A^2 \frac{\varepsilon_0}{4} \sin^2(\xi) \int_d^\infty dx \left[1 + \frac{k^2 d^2}{\chi^2} \right] \exp\left(-2\frac{x-d}{d}\chi \right) \\
&= A^2 \frac{\varepsilon_0}{4} \sin^2(\xi) \left[1 + \frac{k^2 d^2}{\chi^2} \right] \frac{d}{2\chi}.
\end{aligned}
\tag{3.7.14}
$$

Similarly the average magnetic energy

$$W_M^{(d)} = \frac{\mu_0}{4} \int_0^d dx \frac{\omega^2 \varepsilon_0^2 \varepsilon_r^2 d^2}{\xi^2} A^2 \cos^2\left(\frac{x}{d}\xi\right) = \frac{1}{4}\mu_0 A^2 \frac{\omega^2 \varepsilon_0^2 \varepsilon_r^2 d^2}{\xi^2} \frac{1}{2} d\left[1 + \frac{\sin(2\xi)}{2\xi}\right]$$

$$W_M^{(a)} = \frac{1}{4}\mu_0 A^2 \sin^2\xi \frac{\omega^2 \varepsilon_0^2 d^2}{\chi^2} \frac{d}{2\chi}$$

<div align="right">(3.7.15)</div>

The ratio of energy stored in the dielectric relative to the total energy is illustrated below as a function of the frequency
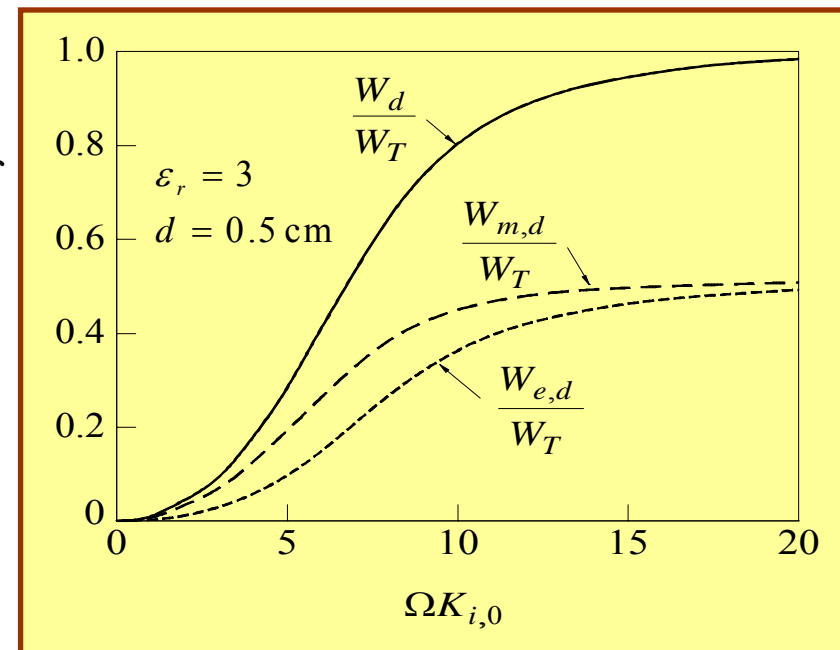
Exercise 3.14: Show that for a dielectric layer (ε_r) of thickness $2d$ there are *even* TE modes that satisfy

$$\xi \tan \xi = \sqrt{\xi_0^2 - \xi^2} \qquad\qquad (3.7.16)$$

and *odd* TE modes satisfying

$$\xi \, \text{ctan} \, \xi = -\sqrt{\xi_0^2 - \xi^2}. \qquad\qquad (3.7.17)$$

What happens at low frequencies in each case? Calculate the energy ratio in each case.

Exercise 3.15: A metallic ``wire'' of radius R_{int} is coated with a dielectric layer (ε_r) the external radius being R_{ext}. Show that the TM$_{on}$ mode is described by

$$E_z = \begin{cases} A K_0(\Gamma r) & r > R_{int} \\ B[J_0(\Lambda r)Y_0(\Lambda R_{int}) - Y_0(\Lambda r)J_0(\Lambda R_{int}) & R_{int} < r < R_{ext} \end{cases}$$

wherein $\Gamma = \sqrt{k^2 - \omega^2/c^2}$ and $\Lambda = \sqrt{\varepsilon\omega^2/c^2 - k^2}$. Demonstrate that the dispersion relation is

$$\frac{K_1(\Gamma R_{ext})}{\Gamma K_0(\Gamma R_{ext})} = -\frac{\varepsilon}{\Lambda} \frac{J_1(\Lambda R_{ext})Y_0(\Lambda R_{int}) - Y_1(\Lambda R_{ext})J_0(\Lambda R_{int})}{J_0(\Lambda R_{ext})Y_0(\Lambda R_{int}) - Y_0(\Lambda R_{ext})J_0(\Lambda R_{int})}.$$

Analyze the mode.

3.7.2 Surface Waves along a Dielectric Fiber
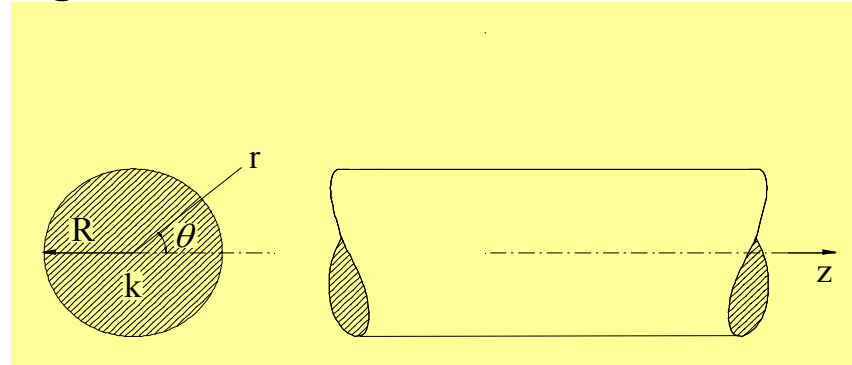
As a second example of a structure capable of supporting a surface wave, we consider a dielectric rod of radius a, as in the figure above. Dielectric rods are similar in behavior to dielectric sheets in that a number of surface-wave modes exist. Pure TM or TE modes are possible only if the field is independent of the azimuthal coordinate ϕ. As the radius of the rod increases, the number of TM and TE modes also increases. These modes do, however, have a cutoff point such that, below some minimum value of R/λ_0, the mode cannot exist any longer. All modes with angular dependence are a combination of a TM and a TE mode, and are classified as hybrid EH or HE modes, depending on whether the TM or TE mode predominates, respectively. All these modes, with the exception of the HE_{11} mode, exhibit cutoff phenomena similar to that of the axially symmetric modes. Since the HE_{11} mode has no low-frequency cutoff, it is the dominant mode. For small-diameter rods, the field extends for a considerable distance beyond the

surface, and the axial propagation constant β is only slightly larger than k_0. As the radius increases, the field is confined closer and closer to the rod, and β approaches $\beta = k_0\sqrt{\varepsilon_r}$ in the limit of infinite radius. Since $\beta > k_0$, the phase velocity is less than that of plane waves in free space. In all of the above respects, the dielectric rod does not differ from the plane-dielectric sheet. Omitting the term $\exp(-jn\phi - j\beta z)$, the field expansion components are

$r < R$	$r > R$
$E_z = A_n J_n(\Lambda r)$	$E_z = C_n K_n(\Gamma r)$
$E_r = -\dfrac{j\beta}{\Lambda} A_n J_n'(\Lambda r) - \dfrac{n\omega\mu_0}{\Lambda^2 r} B_n J_n(\Lambda r)$	$E_r = \dfrac{j\beta}{\Gamma} C_n K_n'(\Gamma r) + \dfrac{n\omega\mu_0}{\Gamma^2 r} D_n K_n(\Gamma r)$
$E_\phi = -\dfrac{n\beta}{\Lambda^2 r} A_n J_n(\Lambda r) + \dfrac{j\omega\mu_0}{\Lambda} B_n J_n'(\Lambda r)$	$E_\phi = \dfrac{n\beta}{\Gamma^2 r} C_n K_n(\Gamma r) - \dfrac{j\omega\mu_0}{\Gamma} D_n K_n'(\Gamma r)$
$H_z = B_n J_n(\Lambda r)$	$H_z = D_n K_n(\Gamma r)$
$H_r = \dfrac{n\omega\varepsilon}{\Lambda^2 r} A_n J_n(\Lambda r) - \dfrac{j\beta}{\Lambda} B_n J_n'(\Lambda r)$	$H_r = -\dfrac{n\omega\varepsilon_0}{\Gamma^2 r} C_n K_n(\Gamma r) + \dfrac{j\beta}{\Gamma} D_n K_n'(\Gamma r)$
$H_\phi = -\dfrac{j\omega\varepsilon}{\Lambda} A_n J_n'(\Lambda r) - \dfrac{n\beta}{\Lambda^2 r} B_n J_n(\Lambda r)$	$H_\phi = \dfrac{j\omega\varepsilon_0}{\Gamma} C_n K_n'(\Gamma r) + \dfrac{n\beta}{\Gamma^2 r} D_n K_n(\Gamma r)$

$$\Lambda^2 = \varepsilon \frac{\omega^2}{c^2} - \beta^2 \quad \text{and} \quad \Gamma^2 = \beta^2 - \frac{\omega^2}{c^2}\ ; \quad A_n, B_n, C_n, D_n \quad \text{are normalized amplitude; and the}$$

prime indicates differentiation with respect to the arguments Λr or Γr.

Imposition of the boundary conditions at $r = R$ leads to equations for determining the relative amplitudes of the coefficients, and also the eigenvalue equation. The eigenvalue equation is

$$\left[\frac{\varepsilon J'_n(u_1)}{u_1 J_n(u_1)} - \frac{K'_n(u_2)}{u_2 K_n(u_2)} \right] \left[\frac{J'_n(u_1)}{u_1 J_n(u_1)} + \frac{K'_n(u_2)}{u_2 K_n(u_2)} \right] = \left[\frac{n\beta}{k_0} \frac{(u_2^2 + u_1^2)}{u_1^2 u_2^2} \right]^2 \qquad (3.7.18)$$

where $u_1 = \Lambda R, u_2 = \Gamma R$. When $n = 0$, the right-hand side vanishes, and each factor on the left-hand side must equal zero. These two factors give the eigenvalue equations for the axially symmetric TM and TE modes:

$$\frac{\varepsilon J'_0(u_1)}{u_1 J_0(u_1)} = \frac{K'_0(u_2)}{u_2 K_0(u_2)} \qquad \text{TM modes} \qquad (3.7.19)$$

$$\frac{J'_0(u_1)}{u_1 J_0(u_1)} = -\frac{K'_0(u_2)}{u_2 K_0(u_2)} \qquad \text{TE modes.} \qquad (3.7.20)$$

In addition, u_1 and u_2 are related by the equation

$$u_1^2 + u_2^2 = (\varepsilon - 1) \left(\frac{\omega}{c} R \right)^2. \qquad (3.7.21)$$

The ratio of β to k_0 as a function of $2R/\lambda_0$ for a polystyrene rod is given below for axially symmetric TM_1 and TE_1 modes and the HE_{11} dipole mode. Both the TM_1 and TE_1 modes are cut off for $2a < 0.163\lambda_0$, while the HE_{11} mode has no low-frequency cutoff.

Comments:

1. The problem of exciting surface waves differs somewhat from that of exciting a propagating mode in an ordinary closed-boundary guide, in that some of the power radiated by the source goes into the propagating field – not necessarily bounded to the dielectric.

2. The conclusion reached in (3.7.12) that there is smooth ``transition" to $\omega \to 0$ is not general for surface waves. In order to demonstrate this fact let us return to (3.7.19). It is possible to write the dispersion relation in the following form
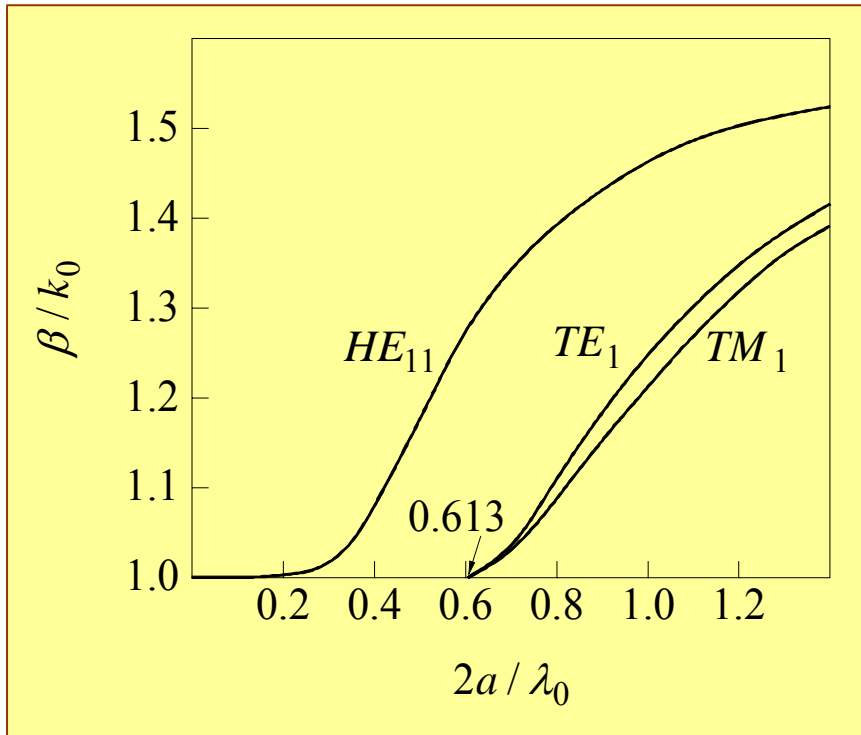
$$\frac{J_1\left(\sqrt{\psi_0^2 - \psi^2}\right)}{\sqrt{\psi_0^2 - \psi^2}\, J_0\left(\sqrt{\psi_0^2 - \psi_1^2}\right)} = \frac{1}{\varepsilon_r}\frac{1}{\psi}\frac{K_1(\psi)}{K_0(\psi)}. \tag{3.7.22}$$

wherein $\psi_0 = \dfrac{\omega}{c} R\sqrt{\varepsilon - 1}$ and $\psi = R\sqrt{k^2 - \omega^2 / c^2}$ as a function of the frequency for several phase velocities reads

$$\frac{1}{2} = \frac{1}{\varepsilon_r}\frac{1}{\psi}\frac{K_1(\psi)}{K_0(\psi)}. \tag{3.7.23}$$

The solution denoted by $\psi_c(\varepsilon_r)$ implies

$$\psi_c^2 = R^2\left(k^2 - \frac{\omega^2}{c^2}\right) \rightsquigarrow k^2 = \frac{\omega^2}{c^2} + \frac{\psi_c^2(\varepsilon_r)}{R^2} \tag{3.7.24}$$

and since for example for $\varepsilon_r = 3$, the solution is $\psi_c = 0.963$, we conclude that there is no solution which is consistent with the assumption $\psi \to 0$. Consequently, there is no solution at low frequencies.

3.8 Transients in Waveguides

In any waveguide, the phase velocity v_{ph}, is a function of frequency. As a consequence, all signals having a finite frequency spectrum will undergo dispersion when transmitted through a length of guide. The phase relationship between the frequency components of the original signal at the feeding point continually changes as the signal progresses along the guide. Any realistic analysis should take into account the frequency characteristics of the antenna or aperture that couples the signal into the guide as well as the characteristics of the circuit elements used to extract the signal at the receiving end. In this section we shall consider only the properties of the guide itself. The effect of losses and their variation will also be neglected. In practice, this does not lead to significant errors, because in most cases the frequency bandwidth of the signal is relatively narrow, and the mid-band frequency of operation is usually chosen far enough above the cutoff frequency so that the attenuation curve is approximately constant throughout the band.

Before some time, which we choose as the time origin $t = 0$, the disturbance in the guide is zero. When a current element is introduced into the guide, a disturbance or signal is generated. This signal is a solution of the time-dependent field equations. Let $\mathcal{E}(\mathbf{r},t), \mathcal{H}(\mathbf{r},t)$ be the time-dependent field vectors. For a unit impulse current element $\delta(t - t')$ applied at time $t = t'$ and located at the point (x', y', z'), the field vectors are a solution of

$$\nabla \times \boldsymbol{\mathcal{E}} = -\mu_0 \frac{\partial \boldsymbol{\mathcal{H}}}{\partial t}$$

$$\nabla \times \boldsymbol{\mathcal{H}} = \varepsilon_0 \frac{\partial \boldsymbol{\mathcal{E}}}{\partial t} + \mathbf{s}\delta(t - t')\delta(\mathbf{r} - \mathbf{r}') \tag{3.8.1}$$

where $\mathbf{t}$ is a unit vector giving the direction of the current element, and $\mathbf{r}$ designates the field point (x, y, z), while $\mathbf{r}'$ designates the source point or location. If the Laplace transform of these equations is taken, we get

$$\nabla \times \mathbf{E}(\mathbf{r}, s) = -\mu_0 s \mathbf{H}(\mathbf{r}, s)$$

$$\nabla \times \mathbf{H}(\mathbf{r}, s) = \varepsilon_0 s \mathbf{E}(\mathbf{r}, s) + \mathbf{s}e^{-st'}\delta(\mathbf{r} - \mathbf{r}') \tag{3.8.2}$$

where $\quad \mathbf{E}(\mathbf{r}, s) = \int_0^\infty \boldsymbol{\mathcal{E}}(\mathbf{r}, t)e^{-st}dt$

with a similar definition for $\mathbf{H}(\mathbf{r}, s)$. These equations are formally the same as those obtained by assuming a time dependence $e^{j\omega t}$, and the solution may be obtained by the methods we have previously discussed. All our previous solutions may be converted into solutions of (3.8.2) by replacing $j\omega$ by s and $e^{j\omega t}$ by $e^{-st'}$. The Laplace transform has the effect of suppressing the time variable. The solution to (3.8.2) constitutes the Laplace transform of the time-dependent Green's function. Inverting the transform yields the time-dependent Green's function. For an arbitrary spatial and time variation, the solution may be obtained by a super position integral.

If we restrict ourselves to a line current extending across the narrow dimension of a rectangular guide, the appropriate Green's function corresponding to $E_y(\vec{r})$

$$G(\mathbf{r}\,|\,\mathbf{r}',s) = \frac{-\mu_0}{a} \sum_{n=1}^{\infty} \phi_n(x)\phi_n(x') \frac{s\exp\left\{-st' - [(n\pi/a)^2 + s^2/c^2]^{1/2}\,|\,z - z'\,|\right\}}{\left[(n\pi/a)^2 + s^2/c^2\right]^{1/2}} \qquad (3.8.3)$$

where $\phi_n(x) = \sin(n\pi x/a)$. The inversion of this expression gives us the time-dependent Green's function corresponding to the disturbance set up in the waveguide by an impulse line current located at x', z'. A typical term from (3.8.3) gives

$$\frac{1}{2\pi j}\int_C \frac{\exp\left\{s(t-t') - \left[(n\pi/a)^2 + s^2/c^2\right]^{1/2}\,|\,z - z'\,|\right\}}{\left[(n\pi/a)^2 + s^2/c^2\right]^{1/2}}\,ds$$

$$= \begin{cases} cJ_0\left\{\dfrac{n\pi}{a}[c^2(t-t')^2 - (z-z')^2]^{1/2}\right\} & 0 < t - t' < \dfrac{|\,z - z'\,|}{c} \\[2ex] 0 & \text{otherwise} \end{cases} \qquad (3.8.4)$$

where J_0 is the Bessel function of the first kind. At any given distance $|\,z - z'\,|$ from the source, the disturbance is zero until a time $t = t' + |\,z - z'\,|/c$ is reached when the presence of the signal first becomes known to the observer at this position. *No information* reaches the observer in a time interval *less* than the time required to propagate a disturbance with

the velocity of light. The velocity of light is, therefore, the *wavefront velocity*.

The time derivative of the above function is

$$\frac{-c^3(n\pi/a)(t-t')}{[c^2(t-t')^2-(z-z')^2]^{1/2}} J_1\left\{\frac{n\pi}{a}[c^2(t-t')^2-(z-z')^2]^{1/2}\right\} \tag{3.8.5}$$

where J_1 is the Bessel function of the first kind and order 1. The solution for the time-dependent Green's function which is equal to $\mathcal{E}_y(\mathbf{r},t)$ becomes

$$\mathcal{G}(\mathbf{r}\,|\,\mathbf{r}',t-t') = \frac{1}{\varepsilon_0 a}\sum_{n=1}^{\infty}\frac{n\pi}{a}\phi_n(x)\phi_n(x')[c(t-t')]\frac{J_1\left\{(n\pi/a)[c^2(t-t')^2-(z-z')^2]^{1/2}\right\}}{[c^2(t-t')^2-(z-z')^2]^{1/2}} \tag{3.8.6}$$

for $t' < t < t'+|z-z'|/c$ and zero otherwise.

3.9 Waveguide Based Cavities

3.9.1 Power and Energy Considerations

The goal of this sub-section is to determine a general relation between power, energy and impedance at the input of an electromagnetic device. We shall consider the power in a volume V and an envelope S; through this envelope an average power P crosses

$$P = \frac{1}{2}\mathrm{Re}\left\{\oint \vec{E}\times\vec{H}^* \cdot d\vec{s}\right\}. \tag{3.9.1}$$

Thus based on the complex Poynting theorem

$$\frac{1}{2}\oint(\vec{E}\times\vec{H}^*)\cdot d\vec{s} = -2j\omega\int_V dV\left[\frac{1}{4}\vec{B}\cdot\vec{H}^* - \frac{1}{4}\vec{E}\cdot\vec{D}^*\right] - \frac{1}{2}\int_V \vec{E}\cdot\vec{J}^* dV. \tag{3.9.2}$$

Assuming linear medium characterized by $\mu = \mu' - j\mu''$, $\varepsilon = \varepsilon' - j\varepsilon''$ and σ we can separate the real and imaginary part of this theorem

$$\mathrm{Re}\left\{\frac{1}{2}\oint\oint \vec{E}\times\vec{H}^* \cdot d\vec{s}\right\} = -2\omega\int_V dV\left[\frac{1}{4}\mu''\,|H|^2 + \frac{1}{4}\varepsilon''\,|E|^2\right] - \frac{1}{2}\int dV\,\sigma\,|E|^2$$

$$\mathrm{Im}\left\{\frac{1}{2}\oint\oint \vec{E}\times\vec{H}^* \cdot d\vec{s}\right\} = -2\omega\int_V dV\left[\frac{\mu'}{4}\,|\vec{H}|^2 - \frac{\varepsilon'}{4}\,|\vec{E}|^2\right]. \tag{3.9.3}$$

Several comments are in place

1. The terms proportional to $\omega\mu''$ or $\omega\varepsilon''$ can be interpreted as loss.

2. The reactive energy flow into the volume V equals exactly 2ω the reactive energy difference $(W_M - W_E)$ stored in the volume.

3. In terms of a lumped parameters (RLC): if the current at the entrance is denoted by I and the voltage V, we may write the complex power at the input as

$$\frac{1}{2}VI^* = \frac{1}{2}ZII^* = \frac{1}{2}II^*\left[R + j\omega L + \frac{1}{j\omega C}\right], \tag{3.9.4}$$

where $P_L = R|I|^2/2$ represents all losses in the system, $W_M = L|I|^2/4$ represents the average magnetic energy stored in the system whereas $W_E = C|V|^2/4$ represents the average electric energy stored in the system hence

$$\frac{1}{2}VI^* = \frac{1}{2}Z|I|^2 = P_L + 2j\omega(W_M - W_E) \tag{3.9.5}$$

or

$$Z = \frac{P_L + 2j\omega[W_M - W_E]}{\frac{1}{2}|I|^2}. \tag{3.9.6}$$

This can be conceived as a generalization of the impedance concept.

3.9.2 Rectangular Waveguide Cavity
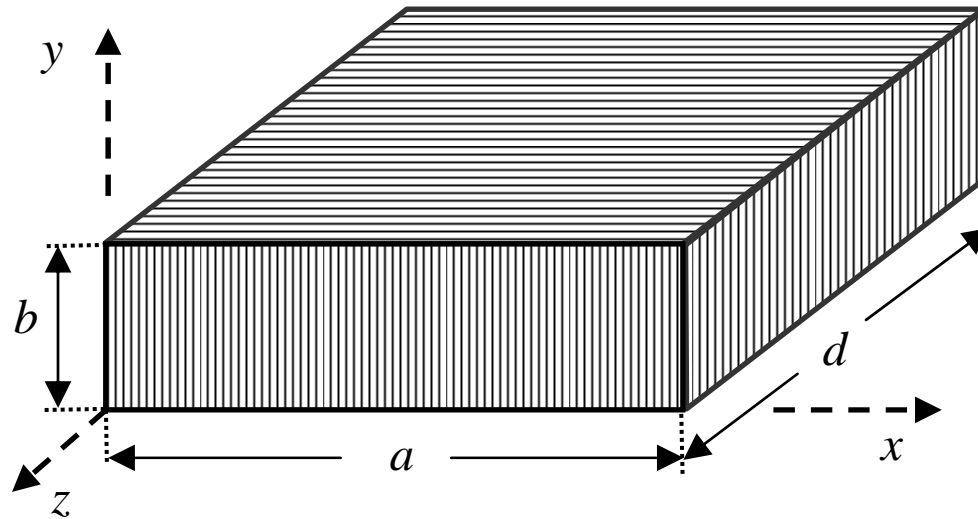
Consider a rectangular waveguide shortened at $z = 0$ and $z = d$. Without shortening plates the wavenumber is given by

$$\beta_{nm} = \left[\varepsilon_r \mu_r \frac{\omega^2}{c^2} - \left(\frac{\pi n}{a} \right)^2 - \left(\frac{\pi m}{b} \right)^2 \right]^{1/2}.$$

(3.9.7)

Because of the shortening planes

$$\beta_{nm} = \frac{\pi l}{d}$$

(3.9.8)

thus the resonance frequencies are given by

$$f_{n,m,l} = \frac{c}{2\pi} \frac{1}{\sqrt{\varepsilon_r \mu_r}} \left[\left(\frac{\pi n}{a} \right)^2 + \left(\frac{\pi m}{b} \right)^2 + \left(\frac{\pi l}{d} \right)^2 \right]^{1/2}. \qquad (3.9.9)$$

We shall examine next electromagnetic field characteristics in a cavity. In particular we shall calculate the quality factor of a TE_{101}. Choosing $d > a > b$, this is the lowest mode. It has the following field (non-zero) components

$$H_z = \left[Ae^{-j\beta z} + Be^{j\beta z} \right] \cos \left(\frac{\pi x}{a} \right)$$

$$H_x = \frac{j\beta a}{\pi} \left[Ae^{-j\beta z} - Be^{j\beta z} \right] \sin \left(\frac{\pi x}{a} \right) \qquad (3.9.10)$$

$$E_y = -\frac{j\omega a}{c\pi} \sqrt{\varepsilon_r \mu_r} \eta_0 \left[Ae^{-j\beta z} + Be^{j\beta z} \right] \sin \left(\frac{\pi x}{a} \right)$$

Bearing in mind that E_y vanishes at $z = 0$ we obtain $A + B = 0$ and applying the same condition at $z = d$ we get $Ae^{-j\beta d} - Be^{j\beta d} = 0 \;\Rightarrow\; -2jA\sin(\beta d) = 0$ therefore for a non trivial solution β has to satisfy $\beta d = \pi l$ which is just (3.9.8).

Consequently, the mode TE_{101} is described by

$$H_z(x,z;\omega) = -2jA\cos\left(\frac{\pi x}{a}\right)\sin\left(\frac{\pi z}{d}\right)$$

$$H_x(x,z;\omega) = 2jA\frac{a}{d}\sin\left(\frac{\pi x}{a}\right)\cos\left(\frac{\pi z}{d}\right) \qquad (3.9.11)$$

$$E_y(x,z;\omega) = -2A\frac{a}{\pi}\eta\left[\left(\frac{\pi a}{d}\right)^2+\frac{\pi^2}{d^2}\right]^{1/2}\sin\left(\frac{\pi x}{a}\right)\sin\left(\frac{\pi z}{d}\right)$$

The electric and the magnetic energy stored in the system

$$W_E = \frac{1}{4}\varepsilon_o\int_0^a dx\int_0^b dy\int_0^d dz|E_y|^2 = \frac{1}{4}\varepsilon_o|2A|^2\frac{a^2}{\pi^2}\eta^2\left[\frac{\pi^2}{a^2}+\frac{\pi^2}{d^2}\right]\frac{a\,d}{2\,2}b = W_M$$

Clearly at resonance the electric energy equals the magnetic energy stored in the system therefore the total average energy stored in the cavity is

$$W_T = 2W_E = \frac{1}{2}\mu_o(bad)\left[1+\frac{a^2}{d^2}\right]|A|^2. \qquad (3.9.12)$$

Next we shall calculate the loss. The surface current is given by $\vec{J}_s = \vec{n}\times\vec{H}$ therefore the dissipated power is given by

$$P_{\text{loss}} = \frac{1}{2}\int da\,\delta\,\frac{J^2}{\sigma} = \frac{1}{2}\int da\,\delta\left(\frac{J_s}{\delta}\right)^2 \frac{1}{\sigma} = \frac{1}{2}\int da\,\frac{|H_x|^2}{\delta\sigma} = \frac{R_s}{2}\int da\,|H_x|^2$$

$$= |A|^2\,R_s\left(2a^3b + 2d^3b + ad^3 + da^3\right)/d^2 \tag{3.9.13}$$

Consequently, the quality factor

$$Q = \frac{\omega W_T}{P_{\text{loss}}} = \frac{2\omega W_E}{P_{\text{loss}}} = \frac{\eta}{R_s}\frac{\left[(\pi/a)^2 + (\pi/d)^2\right]^{3/2}(ad)^3}{2\pi^2(2a^3b + 2d^3b + a^3d + d^3a)}. \tag{3.9.14}$$

As an example consider the following parameters

$$\sigma_{\text{Cu}} \sim 5.8\times 10^7\,[\text{Ohm/m}],\ a = b = d = 3\,[\text{cm}] \to f = 7.0\,[\text{GHz}],\ T = 1/f \simeq 0.14\,[\text{nsec}]$$

$$R_s \sim 0.022\,\Omega,\ Q \sim 12700,\ \tau = 2Q/\omega_0 = Q/\pi f \simeq 0.58\,[\text{msec}].$$

In the case of dielectric losses

$$P_{\text{loss},d} = \frac{1}{2}\omega\varepsilon''\int_V dV\,|E|^2 \ \Rightarrow\ Q_d = \frac{2\omega W_E}{P_{\text{loss},d}} = \frac{\varepsilon'}{\varepsilon''} \Rightarrow \boxed{\frac{1}{Q_{\text{eff}}} = \frac{1}{Q_d} + \frac{1}{Q}} \tag{3.9.15}$$

since the total power loss is the sum of the two mechanisms.

Exercise 3.18: Check whether (3.9.13) is correct. In particular check if H_z does not contribute to the relevant surface current. Calculate the impedance in (3.9.6).

3.9.3 Cylindrical Resonator

In this subsection we briefly repeat the previous exercise in cylindrical geometry. Consider a cylindrical waveguide of radius R. with two shorting planes at $z = 0$ and $z = d$. We shall examine in this case the TE_{11} mode

$$H_z = J_1\left(p'_{11} \frac{r}{R} \right) \cos\phi \left[Ae^{-j\beta z} + Be^{j\beta z} \right] \qquad (3.9.16)$$

wherein $p'_{11} = 1.841$. Determine all the other field components!! As in the previous subsection

$$\left. \begin{aligned} E_r(z = 0, d) &= 0 \\ E_\phi(z = 0, d) &= 0 \end{aligned} \right\} \Rightarrow -2jA\sin(\beta d) \Rightarrow \beta d = \ell\pi \Rightarrow \beta = \pi\ell/d. \qquad (3.9.17)$$

thus

$$\frac{\omega}{c} = \left[\left(\frac{\pi}{d} \right)^2 + \left(\frac{p'_{11}}{R} \right)^2 \right]^{1/2}. \qquad (3.9.18)$$

191
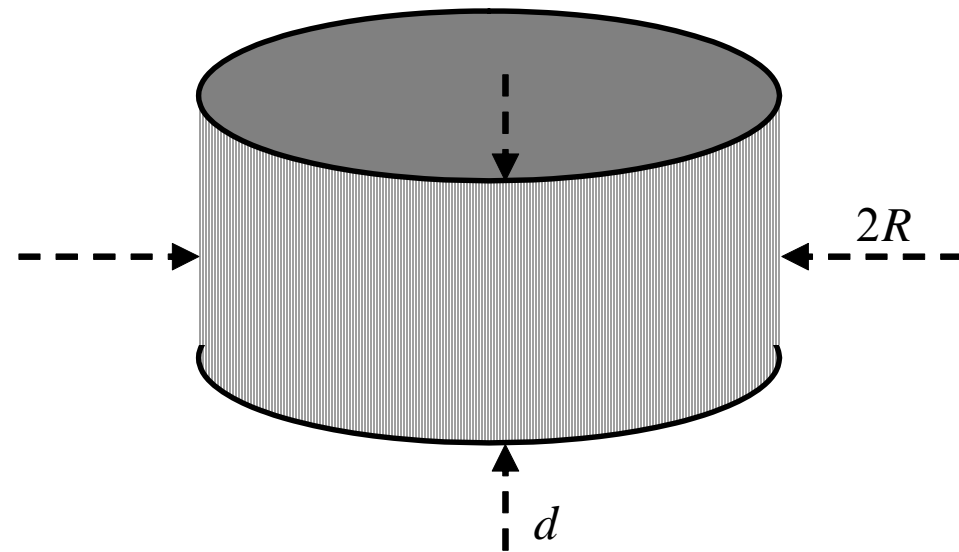
Exercise 3.19: Prove that the quality factor for a TE mode is given by

$$Q_{nml}^{(TE)} = \frac{1}{\frac{\omega}{c}\delta_s} \frac{\left[1-\left(\dfrac{n}{p'_{nm}}\right)^2\right]\left[\left(p'_{nm}\right)^2+\left(\dfrac{\pi l}{d}R\right)^2\right]^{3/2}}{\left(p'_{nm}\right)^2+2\dfrac{R}{d}\left(\dfrac{\pi l}{d}R\right)^2+\left(1-2\dfrac{R}{d}\right)\left(\dfrac{nl\pi R}{p'_{nm}d}\right)^2} \qquad (3.9.19)$$

For a TM mode the quality factor is given by

$$Q_{nml}^{(TM)} = \frac{1}{\frac{\omega_0}{c}\delta_s}\begin{cases} \dfrac{\left[p_{nm}^2+\left(\dfrac{\pi l}{d}R\right)^2\right]^{1/2}}{1+2\dfrac{R}{d}} & l>0 \\[4ex] \dfrac{p_{nm}}{1+\dfrac{R}{d}} & l=0 \end{cases} \qquad (3.9.20)$$

Exercise 3.20: Retrieve the result in (3.9.19)--(3.9.20). Compare to a rectangular cavity of the same volume or same surface.

3.9.4 Open Resonator – Circular Geometry

In many cases the cavity relies on evanescent waves that decay in one direction and they do not carry any power in that direction. One example is illustrated below: A cylindrical waveguide of radius R with a short-circuiting plane at z=0, a dielectric (ε_r) of thickness d.

Exercise 3.21: Determine the resonant frequency and the quality factor for a TM$_{nm}$ mode. Repeat the exercise for TE$_{nm}$ mode. Consider both metallic and dielectric loss.

3.9.5 Exciting a Cavity

Coaxial
line
(a)

Coaxial
line
(b)

Cavity

Waveguide   Aperture

(c)
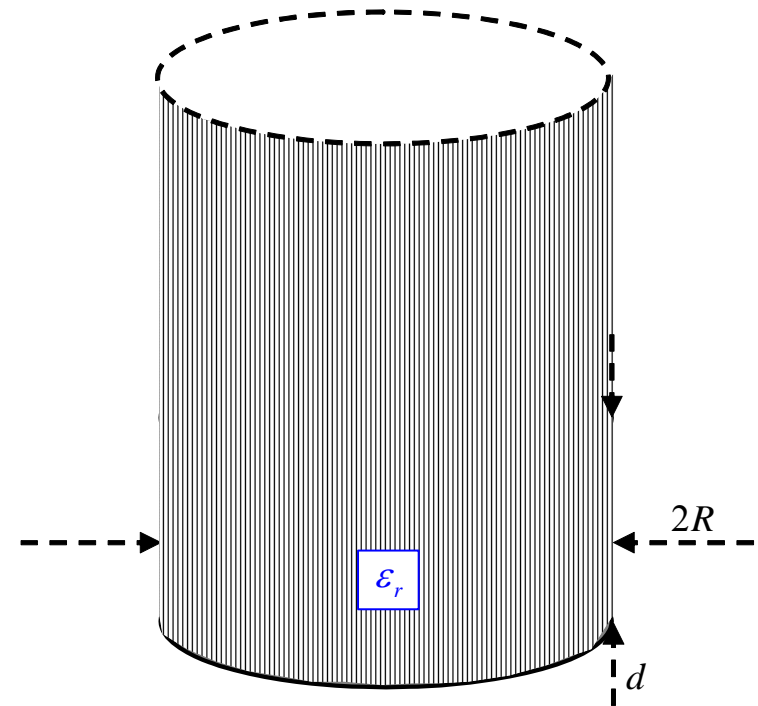
There are two main methods to excite cavities: with coaxial line (electric or magnetic coupling) or with a waveguide through an aperture.

In what follows, we shall consider a simple example of excitation of a cavity by a waveguide through a small (circular) aperture of radius r_0 as illustrated in lower frame. Ignoring loss processes the input impedance is given by the parallel impedance of the aperture

$$\overline{Z}_{in} = \frac{(j\overline{X}_L)(j\tan\beta d)}{j\overline{X}_L + j\tan(\beta d)}.$$

(3.9.21)

To include propagation loss (still assuming ideal aperture) the input impedance is

$$\overline{Z}_{in} = \frac{j\overline{X}_L \tanh(\alpha d + j\beta d)}{j\overline{X}_L + \tanh(\alpha d + j\beta d)}.$$

$2r_0$ b $\overline{Z}_c = 1$ $j\overline{X}_L$

d z d

$z = 0$ $z = d$

(a)   (b)

19
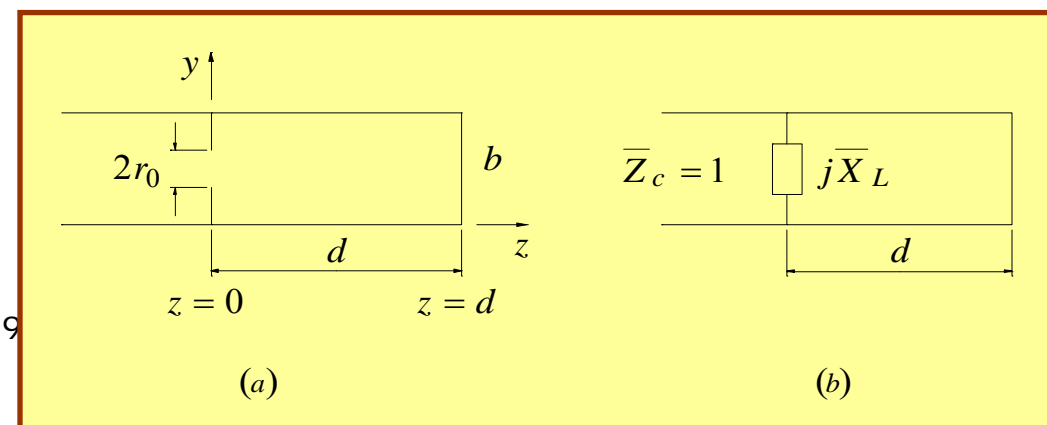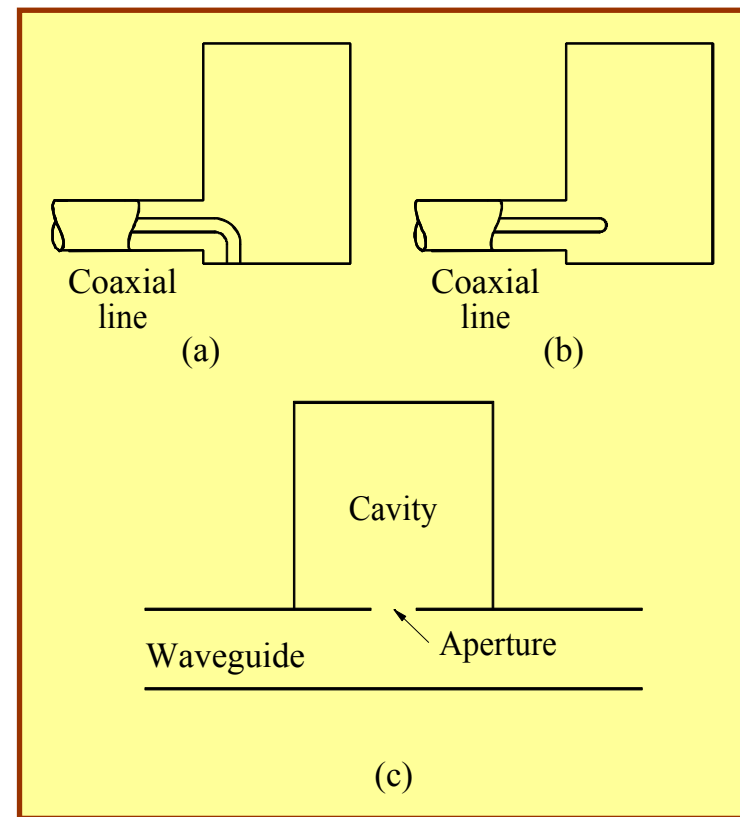
In case of a TE_{10} the normalized impedance of the aperture is $\overline{X}_L = \dfrac{8}{3\pi}\left(\dfrac{\pi r_0^2}{ab}\right)\beta r_0$

revealing that this is proportional to the areas ratio. For low loss

$$\overline{Z}_{in} \simeq \frac{(j\overline{X}_L)\,j\tan(\beta L)}{j\overline{X}_L + j\tan\beta\ell + \tanh(\alpha d)} \tag{3.9.23}$$

and the condition for resonance

$$\mathcal{D}(\omega) \equiv \overline{X}_L + \tan\beta\ell = 0 \tag{3.9.24}$$

implies that at resonance $(\omega = \omega_0)$

$$\overline{Z}_{in}(\omega = \omega_0) \simeq \frac{\overline{X}_L^2}{\alpha d}. \tag{3.9.25}$$

In the vicinity of the resonance

$$\overline{Z}_{in}(\omega) \simeq \frac{\overline{X}_L^2}{\alpha d + j\left.\dfrac{\partial\mathcal{D}}{\partial\omega}\right|_{\omega=\omega_0}(\omega-\omega_0)} \simeq \frac{\overline{Z}_{in}(\omega=\omega_0)}{1+\left(\dfrac{j}{\alpha d}\right)\left.\dfrac{\partial\mathcal{D}}{\partial\omega}\right|_{\omega=\omega_0}(\omega-\omega_0)} \tag{3.9.26}$$

Since for an RLC circuit the impedance in the vicinity of the resonance is $\overline{Z}_{in}(\omega) \simeq \overline{Z}_{in}(\omega=\omega_0)\left[1 + j(\omega-\omega_0)/\Delta\omega\right]^{-1}$ we conclude by analogy that the bandwidth is $\Delta\omega = \alpha d/\mathcal{D}'(\omega=\omega_0)$ implying that the quality factor $Q = \omega_0/\Delta\omega = \omega_0\mathcal{D}'(\omega=\omega_0)/\alpha d$.

Comment: It is interesting to note that $\mathcal{D}'(\omega = \omega_0)$ depends on the group velocity since $\overline{X}_L = U\beta d$

$$\mathcal{D}'(\omega = \omega_0) = \frac{\partial}{\partial\omega}[U\beta d + \tan(\beta d)] = \frac{\partial\beta}{\partial\omega}d\left[U + \frac{1}{\cos^2\beta d}\right]_{\omega=\omega_0}$$

$$= \frac{d}{V_{gr}}\left[U + 1 + \tan^2(\beta d)\right]_{\omega=\omega_0} = \frac{d}{V_{gr}}[U + 1 + (U\beta d)^2]$$

(3.9.27)

where $U = \frac{8}{3\pi}\left(\frac{\pi r_0^2}{ab}\right)\frac{r_0}{d}$ implying that the quality factor is inversely proportional to the group velocity in the waveguide consisting the cavity $Q \propto \mathcal{D}'(\omega = \omega_0) \propto 1/V_{gr}$.

3.10 Wedge in a Waveguide

3.10.1 Metallic Wedge

The goal of this section is to analyze a wave guide of a circular cross-section but which lacks a slice as illustrated below
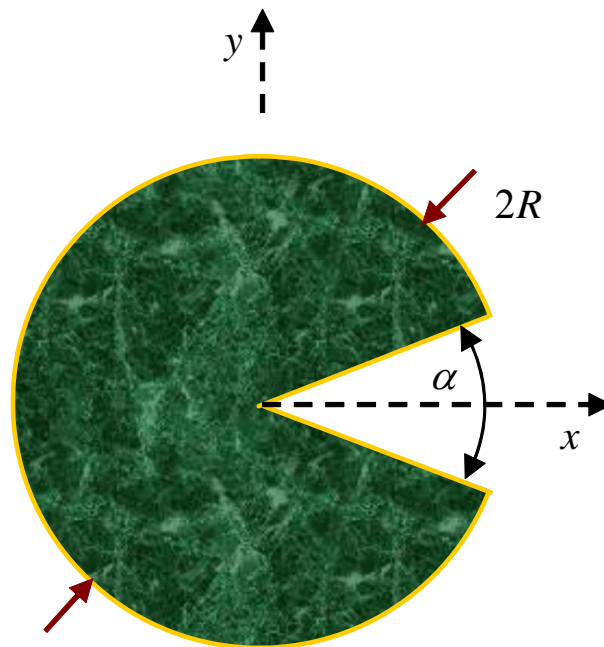
In order to keep the problem relatively simple, we shall limit the discussion to the evaluation of the cut-off frequency. For this purpose we recall that in Section 2.1 we

found that

$$\vec{E}_\perp = -\frac{jk_z}{k_\perp^2}\nabla_\perp E_z + \frac{j\omega\mu}{k_\perp^2}\vec{1}_z \times \nabla_\perp H_z$$

$$\vec{H}_\perp = -\frac{jk_z}{k_\perp^2}\nabla_\perp H_z - \frac{j\omega\varepsilon}{k_\perp^2}\vec{1}_z \times \nabla_\perp E_z \qquad (3.10.1)$$

$$k_\perp^2 = \omega^2\varepsilon\mu - k^2$$
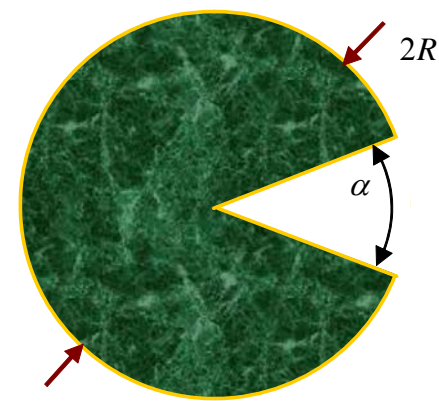
And both longitudinal components satisfy the wave equation. Limitint the analysis to the cut-off frequencies $k_z = 0$ these equations simplify

$$\vec{E}_\perp = -\frac{1}{j\omega\varepsilon}\vec{1}_z \times \nabla_\perp H_z \Rightarrow \begin{cases} E_r = \dfrac{1}{j\omega\varepsilon}\dfrac{1}{r}\dfrac{\partial}{\partial\phi}H_z \\[3mm] E_\phi = -\dfrac{1}{j\omega\varepsilon}\dfrac{\partial}{\partial r}H_z \end{cases}$$

$$\vec{H}_\perp = +\frac{1}{j\omega\mu}\vec{1}_z \times \nabla_\perp E_z \Rightarrow \begin{cases} H_r = \dfrac{-1}{j\omega\mu}\dfrac{1}{r}\dfrac{\partial}{\partial\phi}E_z \\[3mm] H_\phi = \dfrac{1}{j\omega\mu}\dfrac{\partial}{\partial r}E_z \end{cases} \qquad (3.10.2)$$

and the wave equation simplifies
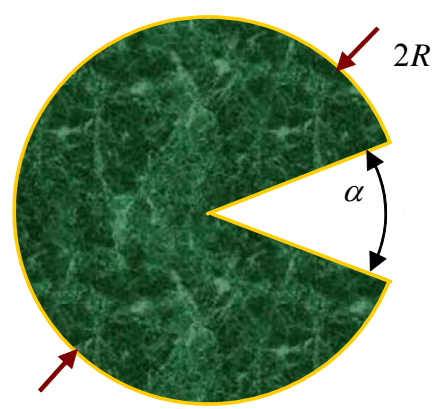
$$\left(\frac{1}{r}\frac{\partial}{\partial r}r\frac{\partial}{\partial r}+\frac{1}{r^2}\frac{\partial^2}{\partial\phi^2}+\omega^2\mu\varepsilon\right)\binom{E_z}{H_z}=0 \qquad (3.10.3)$$

Obviously, the solution of this set of equations describe a resonator whereby the field does not vary in the z-direction.

For the TM modes the solution is of the form

$$E_z(r,\phi)\propto J_v(qr)\left[A\cos(v\phi)+B\sin(v\phi)\right] \qquad (3.10.4)$$

subject to the boundary conditions

$$E_z(r=R,\alpha/2<\phi<2\pi-\alpha/2)=0$$

$$E_z(r,\phi=\alpha/2)=0 \qquad (3.10.5)$$

$$E_z(r,\phi=2\pi-\alpha/2)=0$$

The first condition implies that

$$J_v(qR)=0 \qquad (3.10.6)$$

wherein q is yet to be determined and from the other two conditions we will specify v:

$$E_z(r,\phi=\alpha/2)=0\Rightarrow A\cos(v\alpha/2)+B\sin(v\alpha/2)=0$$

$$E_z(r,\phi=2\pi-\alpha/2)=0\Rightarrow A\cos\left[v(2\pi-\alpha/2)\right]+B\sin\left[v(2\pi-\alpha/2)\right]=0 \qquad (3.10.7)$$

or explicitly
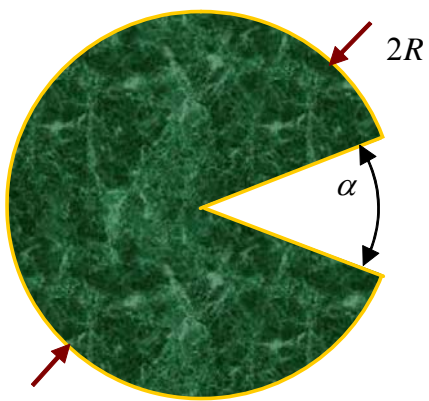
$$\begin{pmatrix} \cos(\nu\alpha/2) & \sin(\nu\alpha/2) \\ \cos[\nu(2\pi-\alpha/2)] & \sin[\nu(2\pi-\alpha/2)] \end{pmatrix}\begin{pmatrix} A \\ B \end{pmatrix}=0 \qquad (3.10.8)$$

For a non-trivial solution the determinant of the matrix is zero

$$\nu = \frac{\pi n}{2\pi-\alpha} = n\frac{1}{2-\alpha/\pi} \qquad (3.10.9)$$

wherein $n=1,2,3....\infty$. Now that we have determined ν we may proceed and establish the zeros of the Bessel function:

$$J_{n\frac{1}{2-\alpha/\pi}}(p)=0 \qquad (3.10.10)$$

As an example let us consider three Bessel functions in one case $\nu=1$ and for comparison we illustrate below $\alpha = \pi/5$ thus $\nu(n=1)=5/9$ and $\nu(n=2)=10/9$.

Obviously the Bessel function of a non-integer order has also zeros:

$p_{n,s}$	$s=1$	$s=2$	$s=3$
$\nu=1$	3.832	7.016	10.173
$\nu(n=1)=5/9$	3.220	6.366	9.509
$\nu(n=2)=10/9$	3.981	7.175	10.337
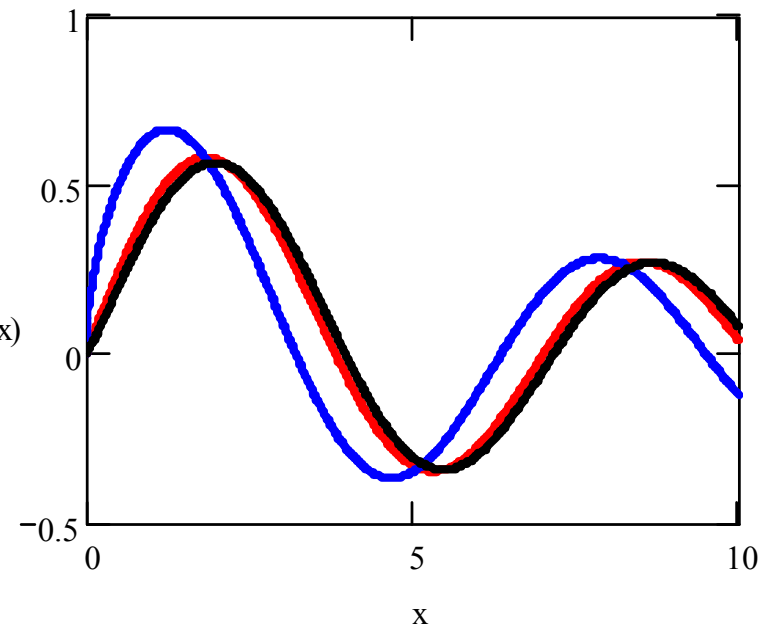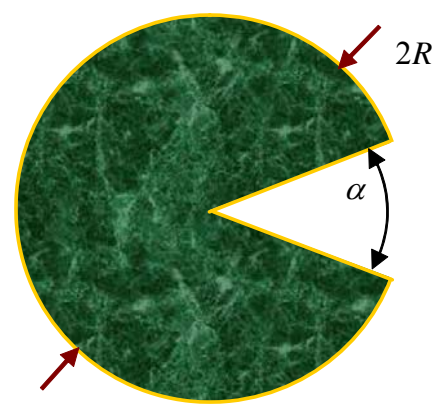
Explicitly

$$E_z(r,\phi) = \sum_{n,s=1}^{\infty} U_{n,s} J_{n\frac{1}{2-\alpha/\pi}}\left(p_{n,s}\frac{r}{R}\right)\sin\left(\pi n\frac{\phi-\alpha/2}{2\pi-\alpha}\right)$$

$$p_{n,s}: \quad J_{n\frac{1}{2-\alpha/\pi}}(p) = 0$$

(3.10.11)

and the cut-off frequencies are determined by

$$\omega_{co} = \frac{c}{R} p_{n,s}$$

The top frame in the right reveals the contours of constant E_z for $s=1$ and $n=1$. The central frame illustrates the case $s=1$ and $n=2$ whereas the lower frame corresponds to $s=2$ and $n=1$.

201

Ez

E
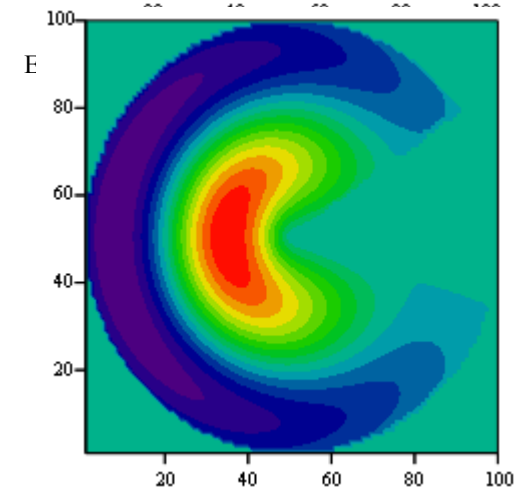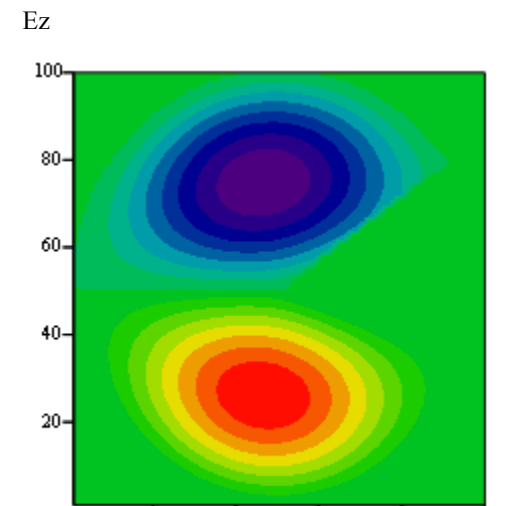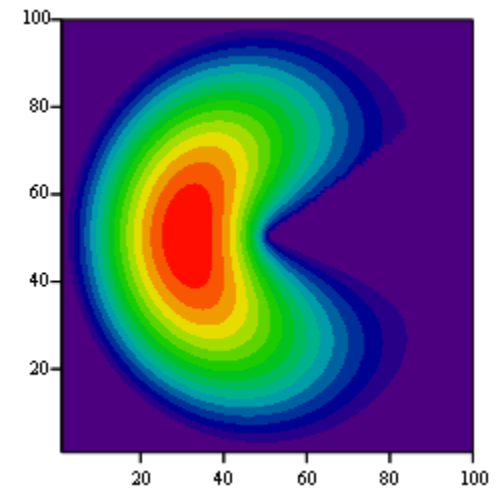
Ez3

A similar approach may be followed for the TE modes

$$H_z(r,\phi) \propto J_\nu(qr)\left[A\cos(\nu\phi) + B\sin(\nu\phi)\right] \qquad (3.10.13)$$

subject to the boundary conditions

$$E_\phi(r = R, \alpha/2 < \phi < 2\pi - \alpha/2) = 0$$

$$E_r(r, \phi = \alpha/2) = 0 \qquad (3.10.14)$$

$$E_r(r, \phi = 2\pi - \alpha/2) = 0$$

The first condition [Eq. (3.10.2)] implies that

$$\left[\frac{d}{dr}J_\nu(qr)\right]_{r=R} = 0 \qquad (3.10.15)$$

wherein q is yet to be determined and from the other two conditions we specify ν:

$$E_r(r, \phi = \alpha/2) = 0 \Rightarrow -A\sin(\nu\alpha/2) + B\cos(\nu\alpha/2) = 0$$

$$E_r(r, \phi = 2\pi - \alpha/2) = 0 \Rightarrow -A\sin\left[\nu(2\pi - \alpha/2)\right] + B\cos\left[\nu(2\pi - \alpha/2)\right] = 0 \qquad (3.10.16)$$

or explicitly

$$\begin{pmatrix} -\sin(\nu\alpha/2) & \cos(\nu\alpha/2) \\ -\sin\left[\nu(2\pi - \alpha/2)\right] & \cos\left[\nu(2\pi - \alpha/2)\right] \end{pmatrix}\begin{pmatrix} A \\ B \end{pmatrix} = 0 \qquad (3.10.17)$$

For a non-trivial solution the determinant of the matrix is zero

$$v = \frac{\pi n}{2\pi - \alpha} = n\frac{1}{2 - \alpha/\pi} \tag{3.10.18}$$

wherein $n = 1, 2, 3....\infty$. Now that we have determined v we may proceed and establish the zeros of the Bessel function:

$$J'_{n\frac{1}{2-\alpha/\pi}}(p) = 0 \tag{3.10.19}$$

From here the approach is virtually identical

$$H_z(r,\phi) = \sum_{n,s=1}^{\infty} U_{n,s} J_{n\frac{1}{2-\alpha/\pi}}\left(p'_{n,s}\frac{r}{R}\right)\cos\left(\pi n\frac{\phi - \alpha/2}{2\pi - \alpha}\right) \tag{3.10.20}$$

$$p'_{n,s} : J'_{n\frac{1}{2-\alpha/\pi}}(p) = 0$$

Exercise 3.22: Draw the contours of constant H_z. Compare the field distribution of the TE and TM modes. For both modes compare the magnetic and electric energy per-unit length.

3.10.2 Dielectric Wedge

The goal of this section is to analyze a waveguide of a circular cross-section but which has a material (μ_r, ε_r) slice as illustrated below

As in the metallic case we keep the problem relatively simple, and limit the discussion to the evaluation of the cut-off frequency. As a result, we can separate the analysis of the TE and TM modes. So let us start with the TM mode.

Vacuum	Slice
$\left(\dfrac{1}{r}\dfrac{\partial}{\partial r} r \dfrac{\partial}{\partial r} + \dfrac{1}{r^2}\dfrac{\partial^2}{\partial \phi^2} + \dfrac{\omega^2}{c^2}\right) E_z = 0$	$\left(\dfrac{1}{r}\dfrac{\partial}{\partial r} r \dfrac{\partial}{\partial r} + \dfrac{1}{r^2}\dfrac{\partial^2}{\partial \phi^2} + \dfrac{\omega^2}{c^2}\mu_r\varepsilon_r\right) E_z = 0$
$H_r = \dfrac{-1}{j\omega\mu_0}\dfrac{1}{r}\dfrac{\partial}{\partial \phi} E_z$	$H_r = \dfrac{-1}{j\omega\mu_0\mu_r}\dfrac{1}{r}\dfrac{\partial}{\partial \phi} E_z$
$H_\phi = \dfrac{1}{j\omega\mu_0}\dfrac{\partial}{\partial r} E_z$	$H_\phi = \dfrac{1}{j\omega\mu_0\mu_r}\dfrac{\partial}{\partial r} E_z$

A differential approach (separation of variables) is not applicable since the radial

variation needs to be the same in both regions but if this is the case the function does not satisfy the wave equation. We must seek an integral approach. For determining the cut-off frequencies associated with the TM-like modes we need to solve

$$\left(\frac{1}{r}\frac{\partial}{\partial r}r\frac{\partial}{\partial r}+\frac{1}{r^2}\frac{\partial^2}{\partial\phi^2}+\frac{\omega^2}{c^2}\right)E_z=-\frac{\omega^2}{c^2}f(\phi)E_z \tag{3.10.21}$$

wherein $f(\phi)$ is a function which equals $\mu_r\varepsilon_r-1$ in the region(s) with material and zero otherwise. A solution which satisfies the boundary conditions

$$E_z(r,\phi)=\sum_{n=-\infty}^{\infty}\sum_{s=1}^{\infty}\mathcal{E}_{n,s}J_n\left(p_{n,s}\frac{r}{R}\right)\exp(jn\phi) \tag{3.10.22}$$

substituting in (3.10.21) we get

$$\mathcal{E}_{n,s}\chi_{n,n}^{s,s}\left(-\frac{p_{n,s}^2}{R^2}+\frac{\omega^2}{c^2}\right)=-\frac{\omega^2}{c^2}\sum_{m=-\infty}^{\infty}\sum_{\sigma=1}^{\infty}\mathcal{E}_{m,\sigma}\chi_{m,n}^{\sigma,s}F_{n',m}$$

$$\chi_{n,n'}^{s,s'}\equiv\int_0^1 dx\,xJ_{n'}\left(p_{n',s'}x\right)J_n\left(p_{n,s}x\right),\ \chi_{n,n}^{s,s'}=\delta_{s,s'}\int_0^1 dx\,xJ_n\left(p_{n,s}x\right)J_n\left(p_{n,s}x\right) \tag{3.10.23}$$

$$F_{n',m}=\frac{1}{2\pi}\int_{-\pi}^{\pi}d\phi f(\phi)\exp\left[-j(n'-m)\phi\right]$$

Rewriting

$$\left(\frac{\omega}{c}R\right)^2 \sum_{m=-\infty}^{\infty} \sum_{\sigma=1}^{\infty} \mathcal{E}_{m,\sigma} \chi_{m,n}^{\sigma,s} \left[F_{n,m} + \delta_{n,m}\delta_{\sigma,s} \right] = \mathcal{E}_{n,s} \chi_{n,n}^{s,s} p_{n,s}^2 \qquad (3.10.24)$$

and defining the matrices

$$C_{\{n,s\},\{m,\sigma\}} = \frac{\chi_{m,n}^{\sigma,s}}{\chi_{n,n}^{s,s} p_{n,s}^2} \left[F_{n,m} + \delta_{n,m}\delta_{\sigma,s} \right] \qquad (3.10.25)$$

thus defining $\bar{\omega} = \omega R / c$.

$$\sum_{\{m,\sigma\}} C_{\{n,s\},\{m,\sigma\}} \mathcal{E}_{\{m,\sigma\}} = \bar{\omega}^{-2} \sum_{\{m,\sigma\}} I_{\{n,s\},\{m,\sigma\}} \mathcal{E}_{\{m,\sigma\}} \qquad (3.10.26)$$

implying that the (square of the) cut-off frequencies are the inverse of the eigen-values of the matrix $\mathbf{C}$

$$\left| \mathbf{C} - \bar{\omega}^{-2}\mathbf{I} \right| = 0. \qquad (3.10.27)$$

Exercise 3.23: Calculate the first cut-off frequency of a waveguide with dielectric slice identical with the metallic slice. Compare the two results. Examine the convergence of the solution.

Exercise 3.24: Repeat Exercise 3.23 for the TE mode including the formulation.

3.11 Appendix

3.11.1 Solution to Exercise 3.8

Analyze (numerically) the dependence of the normalized reactance on three parameters; the angular frequency (ω), its location (d) and its radius (R).
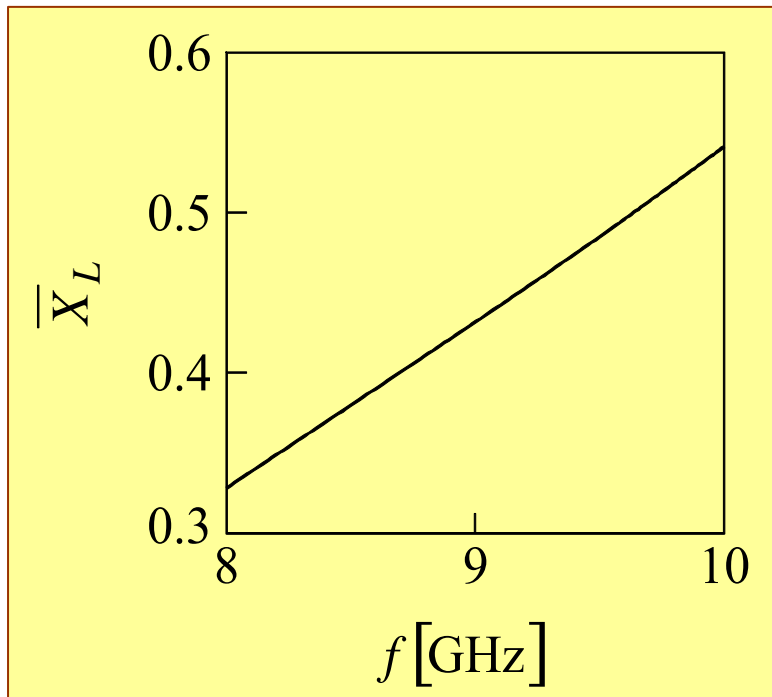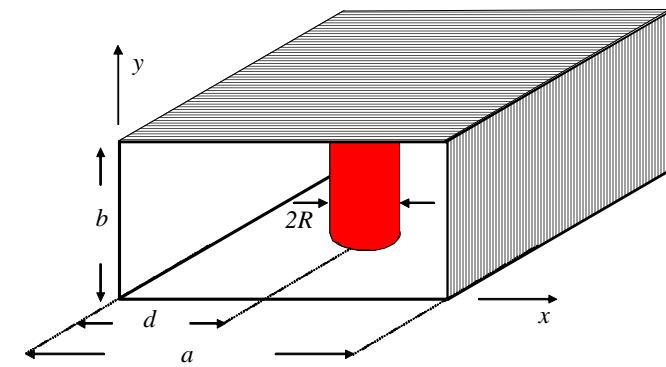
The normalized reactance of a cylindrical post located in a rectangular waveguide as a function of f. The normalized reactance given by Eq. (3.4.20) is shown to increase with frequency, which implies an *inductive* behavior. [$a = 2.5$ cm, $b = 1$ cm, $\varepsilon_r = 1$, $d = a / 2 = 1.25$ mm, $R = a / 20$, $n = 2, 3, \cdots 200$].
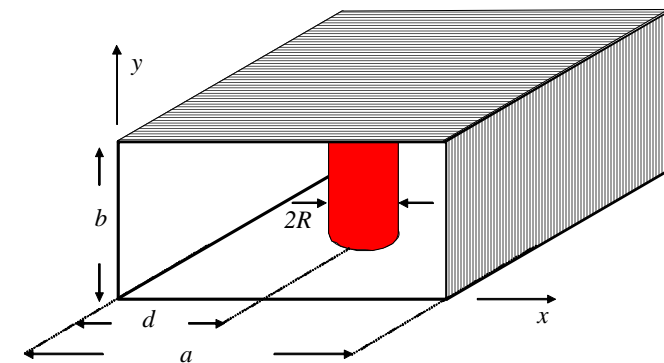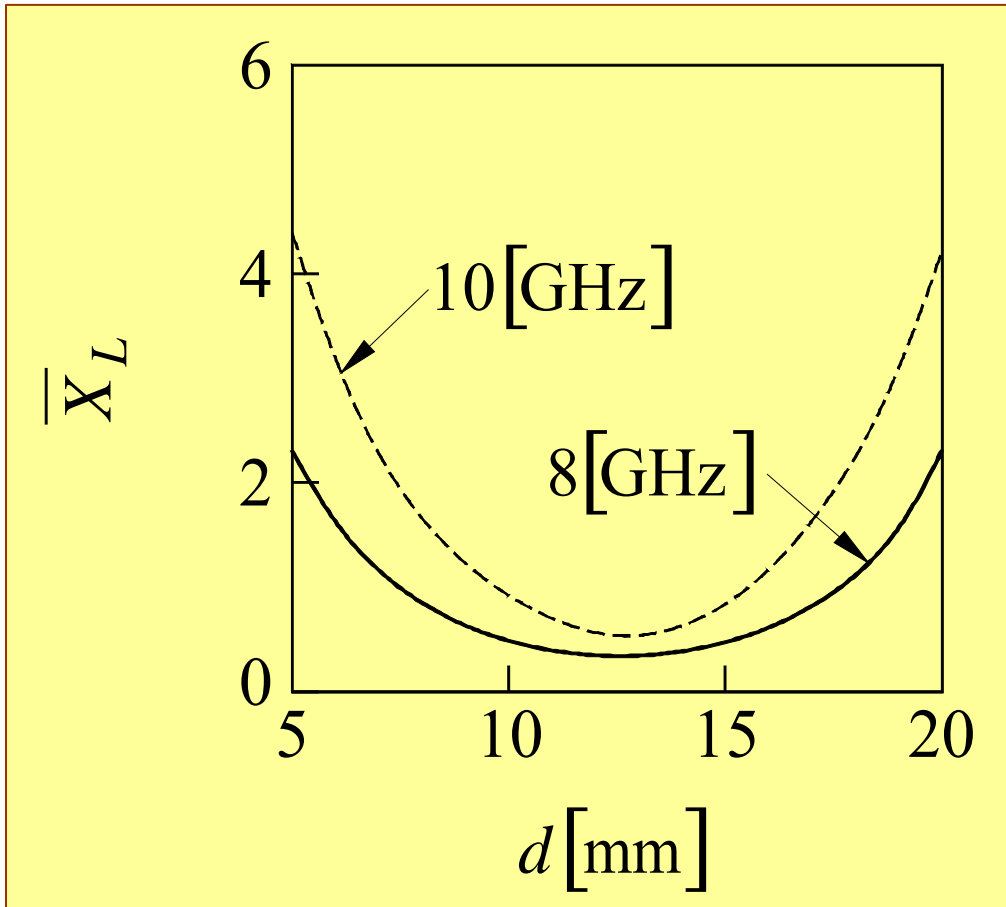
The normalized reactance of a cylindrical post located in a rectangular waveguide as a function of d. The solid line and the dotted line correspond to $f = 8$ GHz and $f = 10$ GHz, respectively. A minima in the normallized reactance is observed at the middle of the rectangular waveguide, whereas close to the edges the normalized reactance increases. [$a = 2.5$ cm, $b = 1$ cm, $\varepsilon_r = 1$, $R = a / 20$, $n = 2, 3, \cdots 200$].
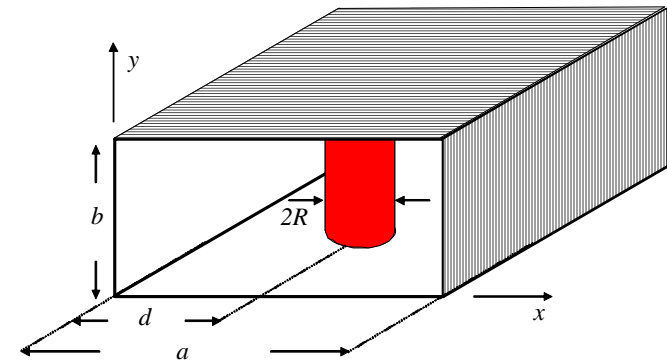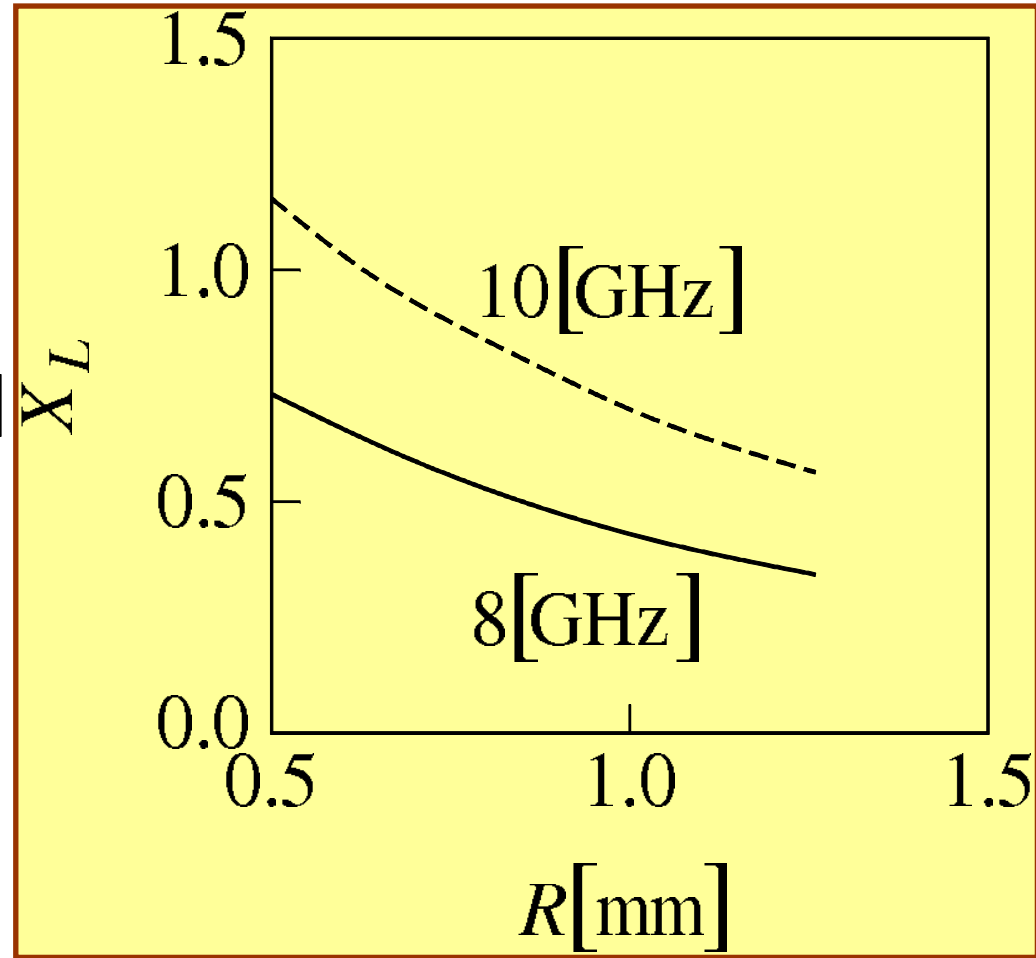
The normalized reactance of a cylindrical post located in a rectangular waveguide as a function of R. The solid line and the dotted line correspond to $f = 8$ GHz and $f = 10$ GHz. In this figure the post is assumed to be located at the middle of the waveguide. [$a = 2.5$ cm, $b = 1$ cm, $\varepsilon_r = 1$, $d = a/2 = 125$ mm, $n = 2, 3, \cdots 200$].
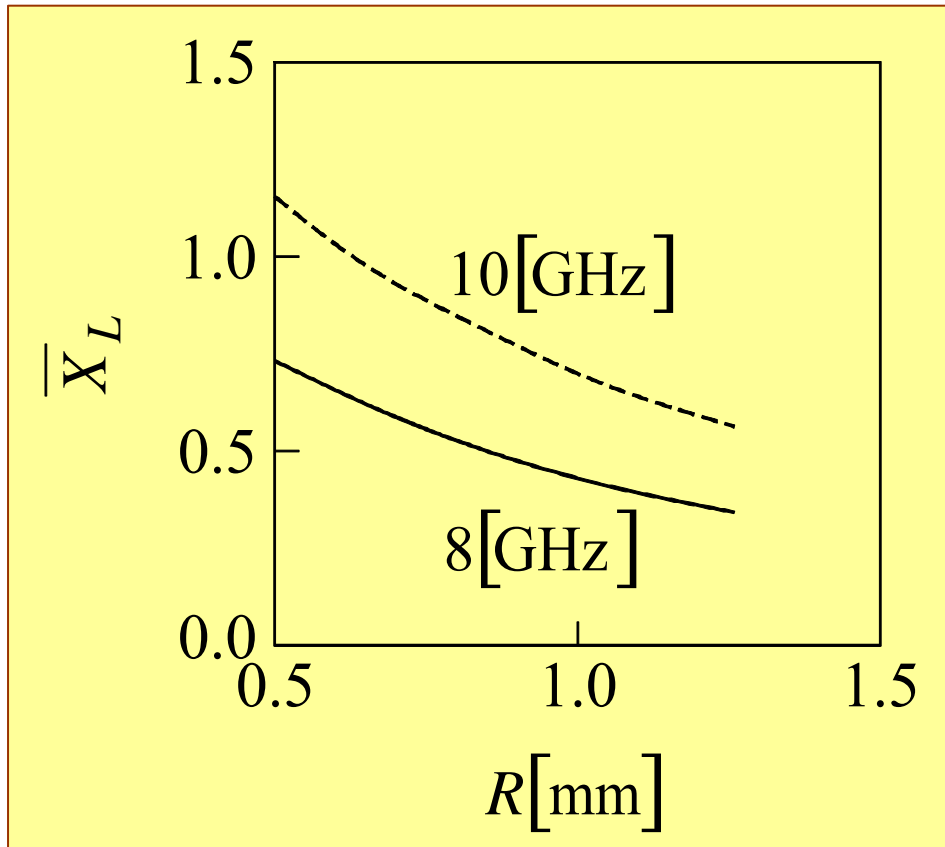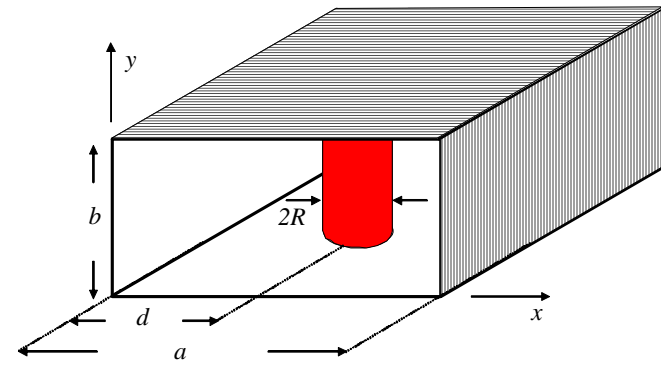
209

The normalized reactance of a cylindrical post located in a rectangular waveguide as a function of R. The solid line and the dotted line correspond to $f = 8$ GHz and $f = 10$ GHz, In this figure the post is assumed to be located close to one of the edges of the waveguide. [$a = 2.5$ cm, $b = 1$ cm, $\varepsilon_r = 1$, $d = 5$ mm, $n = 2,3,\cdots 200$].

Chapter 4
Matrix Formulations

4.1 Impedance Matrix

Consider an N port systems that is characterized at a given frequency by set of complex numbers Z_{ij} ~ i.e. $2N^2$ parameters

$$\begin{pmatrix} V_1 \\ V_2 \\ \vdots \\ V_N \end{pmatrix} = \begin{pmatrix} Z_{11} & \cdots & Z_{1N} \\ \vdots & & \\ \vdots & & \\ Z_{N1} & \cdots & Z_{NN} \end{pmatrix} \begin{pmatrix} I_1 \\ \vdots \\ \vdots \\ I_N \end{pmatrix} \tag{4.1.1}$$

or, explicitly, $Z_{ij} = \left. \dfrac{V_i}{I_j} \right|_{I_{k \neq j} = 0}$.
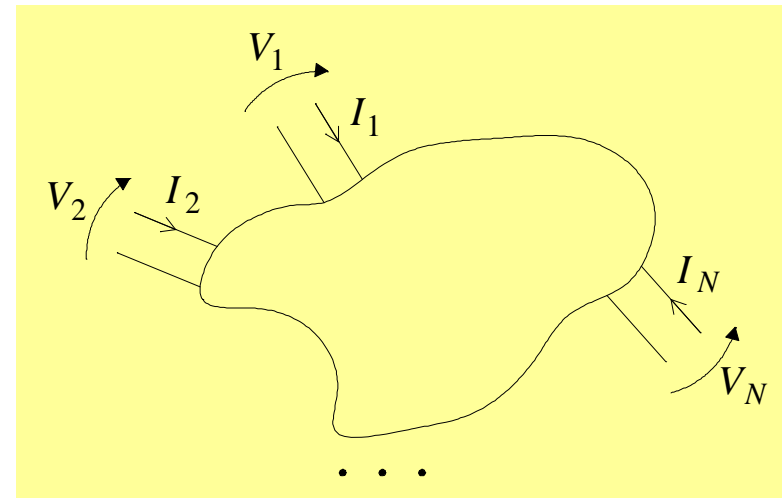
In a similar way we can define the admittance matrix

$$
\begin{pmatrix} I_1 \\ I_2 \\ \vdots \\ \vdots \\ I_N \end{pmatrix} = \begin{pmatrix} Y_{11} & \cdots & Y_{1N} \\ Y_{21} & \cdots & Y_{2N} \\ \vdots & & \\ \vdots & & \\ Y_{N1} & \cdots & Y_{NN} \end{pmatrix} \begin{pmatrix} V_1 \\ V_2 \\ \vdots \\ \vdots \\ V_N \end{pmatrix}.
\tag{4.1.3}
$$

Example: For the sake of simplicity, let us determine the Z matrix of a section of transmission line.

This two port system is characterized by

$$
\begin{pmatrix} V_1 \\ V_2 \end{pmatrix} = \begin{pmatrix} Z_{11} & Z_{12} \\ Z_{21} & Z_{22} \end{pmatrix} \begin{pmatrix} I_1 \\ I_2 \end{pmatrix}
\tag{4.1.4}
$$

and for example the first term is

$$
Z_{11} = \left. \frac{V_1}{I_1} \right|_{I_2 = 0}
\tag{4.1.5}
$$

wherein $I_2 = -I(z = \ell)$. Without loss of generality, the voltage and current wave are given by

212
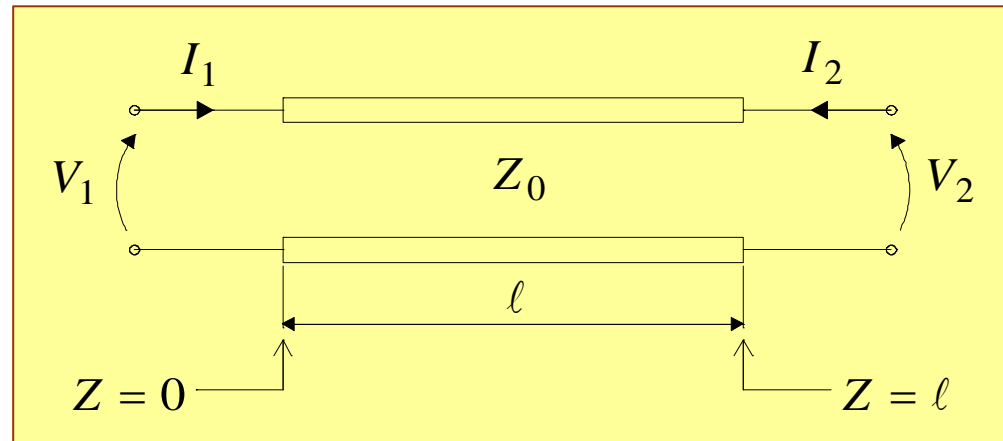
$$V(z) = V_+ e^{-j\beta z} + V_- e^{j\beta z}$$

$$I(z) = \left[V_+ e^{-j\beta z} - V_- e^{j\beta z} \right] \frac{1}{Z_o} \tag{4.1.6}$$

respectively. At the ``input'', i.e. at $z = 0$

$$V_1 = V_+ + V_- \qquad I_1 = \frac{1}{Z_o}(V_+ - V_-). \tag{4.1.7}$$

Based on (4.1.5) we explicitly have

$$Z_{11} = Z_o \left. \frac{V_+ + V_-}{V_+ - V_-} \right|_{I(\ell)=0} \tag{4.1.8}$$

wherein the condition $I(\ell) = 0$ implies

$$I(\ell) = \frac{1}{Z_o} \left[V_+ e^{-j\beta\ell} - V_- e^{j\beta\ell} \right] = 0 \rightsquigarrow V_- = V_+ e^{-2j\beta\ell} \tag{4.1.9}$$

hence

$$Z_{11} = Z_o \frac{1 + e^{-2j\beta\ell}}{1 - e^{-2j\beta\ell}} = Z_o \frac{\cos(\beta\ell)}{j\sin\beta\ell} = -jZ_o \operatorname{ctan}(\beta\ell) \tag{4.1.10}$$

$$Z_{11} = -jZ_o \operatorname{ctan}(\beta\ell). \tag{4.1.11}$$

In a similar way we may establish the other parameters of the matrix. For example,

$$Z_{12} = \frac{V_1}{I_2}\bigg|_{I_1=0} = Z_0 \frac{V_+ + V_-}{(-)\left[V_+ e^{-j\beta\ell} - V_- e^{j\beta\ell}\right]} \tag{4.1.12}$$

and since $I_1 = \dfrac{1}{Z_o}\left[V_+ - V_-\right] \rightsquigarrow V_+ = V_-$ we get

$$Z_{12} = -Z_0 \frac{2}{e^{-j\beta\ell} - e^{j\beta\ell}} = \frac{-jZ_0}{\sin(\beta\ell)} \tag{4.1.13}$$

In a similar way $Z_{21} = Z_{12}$ and $Z_{22} = Z_{11}$ implying

$$\underline{Z} = \begin{bmatrix} -jZ_o \operatorname{ctan}(\theta) & \dfrac{-jZ_o}{\sin\theta} \\ \dfrac{-jZ_o}{\sin\theta} & -jZ_o \operatorname{ctan}(\theta) \end{bmatrix}. \tag{4.1.14}$$

4.2 Scattering Matrix

In many cases it is more convenient to measure the amplitudes of the reflected and transmitted waves
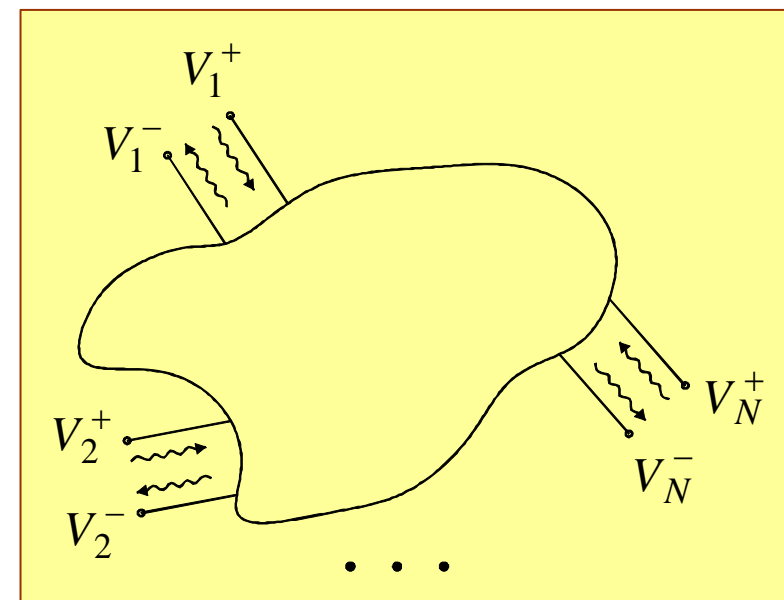
$$
\begin{pmatrix} \bar{v}_1^- \\ \bar{v}_2^- \\ \vdots \\ \vdots \\ \bar{v}_N^- \end{pmatrix}
=
\begin{pmatrix} S_{11} & \cdots & S_{1N} \\ \vdots & & \\ \vdots & & \\ S_{N1} & \cdots & S_{NN} \end{pmatrix}
\begin{pmatrix} \bar{v}_1^+ \\ \bar{v}_2^+ \\ \vdots \\ \vdots \\ \bar{v}_N^+ \end{pmatrix}
\tag{4.2.1}
$$

$$
\bar{v}_1^+ \equiv \frac{v_1^+}{\sqrt{Z_o}} \qquad \bar{v}_1^- \equiv \frac{v_1^-}{\sqrt{Z_o}}
\tag{4.2.2}
$$

the reason for this normalization becomes evident since

$$
P = \frac{1}{2Z_o}\left|V^+\right|^2 = \frac{V^+(V^+)^*}{2Z_o} = \frac{1}{2}\bar{v}^+(\bar{v}^+)^*.
\tag{4.2.3}
$$

The S matrix elements are defined by

$$S_{ij} = \frac{\overline{v}_i^-}{\overline{v}_j^+}\Bigg|_{\overline{v}_{k \neq j}^+ = 0} \quad .$$

(4.2.4)

In order to achieve $\overline{v}_k^+ = 0$ the port is loaded with a matched impedance, namely
    the diagonal term S_{ii} represents the reflection coefficient at the ith port when all the other ports are matched.
    Describing linear systems, both S and Z matrices are interrelated. Firstly it is convenient to define

$$\overline{Z}_{ij} = \frac{Z_{ij}}{Z_o}, \quad \overline{v} = \frac{v}{\sqrt{Z_o}} \quad \text{and} \quad \overline{I} = I\sqrt{Z_o} \quad \text{consequently}$$

$\overline{v} = \overline{v}^+ + \overline{v}^-$ and $\overline{I} = \overline{v}^+ - \overline{v}^-$.
    Using now the definition of the $\overline{Z}$ matrix

$$\overline{v} = \overline{v}^+ + \overline{v}^- = \overline{Z}\left[\overline{v}^+ - \overline{v}^-\right]$$

(4.2.5)

216
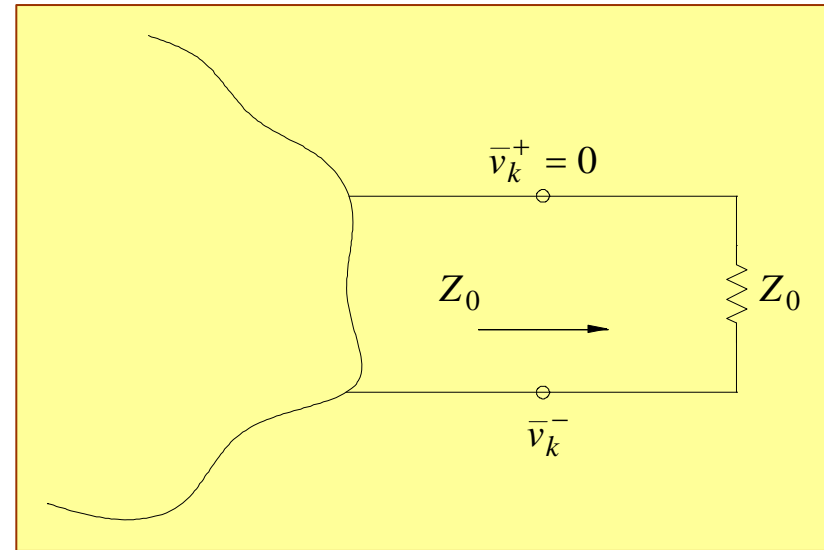
$$[I - \overline{\overline{Z}}]\overline{v}^{+} = -[I + \overline{\overline{Z}}]\overline{v}^{-} \tag{4.2.6}$$

thus since $\overline{v}^{-} = \underline{\underline{S}}\,\overline{v}^{+}$

$$\boxed{S = (\overline{\overline{Z}} + I)^{-1}(\overline{\overline{Z}} - I).} \tag{4.2.7}$$

Properties of the S matrix:

Property #1: If the system is reciprocal S is symmetrical

$$S_{ij} = S_{ji} \qquad \text{or} \qquad S = S^{t}. \tag{4.2.8}$$

This is true provided that at all ports the power is given by $\dfrac{1}{2}|\overline{v}_{n}|^{2}$ i.e. characterization impedance at all ports is the same. In order to prove this statement we recall that based on Lorentz reciprocity theorem (in absence of sources)

$$\oint_{s}\left[\vec{E}_{1} \times \vec{H}_{2} - \vec{E}_{2} \times \vec{H}_{1}\right] \cdot \vec{n}ds = 0 \Rightarrow \int_{i} E_{i} \times H_{j}d\vec{a} = \int_{j} E_{j} \times H_{i}d\vec{a} \tag{4.2.9}$$

and since the electric field is associated with the voltage whereas the local magnetic field is linked to the current $E_{1} \sim V_{1}, H_{2} \sim I_{2}$ thus

$$\overline{v}_{i}I_{j} = v_{j}I_{j}. \tag{4.2.10}$$

Bearing in mind that $I_i = \Sigma_j Y_{ij} v_j$ and $I_j = \Sigma_i Y_{ji} v_i$ we conclude that

$$\overline{v}_i \overline{v}_j Y_{ij} = \overline{v}_i \overline{v}_j Y_{ji} \Rightarrow Y_{ij} = Y_{ji} \Rightarrow Z_{ij} = Z_{ji} \qquad (4.2.11)$$

Namely both the admitance and impedance matrices are symmetric aobviously since $S = (Z + I)^{-1}(Z - 1)$ if Z is symmetrical so is S

$$\boxed{S_{ij} = S_{ji}.} \qquad (4.2.12)$$

Property #2. For a lossless system, S is unitary namely

$$S^{-1} = (S^*)^T \qquad (S^*)^+ S = I. \qquad (4.2.13)$$

For prooving this statement we bear in mind that power conservation implies

$$\left[\overline{v}^+\right]^T \left[\overline{v}^+\right]^* - \left[\overline{v}^-\right]^T \left[\overline{v}^-\right]^* = 0 \Rightarrow \left[\overline{v}^+\right]^T \underline{\underline{I}} \left[\overline{v}^+\right]^* - \left\{S\overline{v}^+\right\}^T \left\{S\overline{v}^+\right\}^* = 0$$

$$\left[\overline{v}^+\right]^T \underline{\underline{I}} \left[\overline{v}^+\right]^* - \left[\overline{v}^+\right]^T \underline{S}^t S^* \left[\overline{v}^+\right]^* = 0 \Rightarrow \left[\overline{v}^+\right]^T \left\{\underline{\underline{I}} - \underline{S}^t \underline{S}^*\right\}\left[\overline{v}^+\right]^* = 0 \qquad (4.2.14)$$

Example: Consider a two ports system with a load Z_L at the output

$$\begin{bmatrix} \bar{v_1}^- \\ \bar{v_2}^- \end{bmatrix} = \begin{pmatrix} S_{11} & S_{12} \\ S_{21} & S_{22} \end{pmatrix} \begin{bmatrix} \bar{v_1}^+ \\ \bar{v_2}^+ \end{bmatrix} \tag{4.2.15}$$

whereas the load

$$S_L = \rho_L = \frac{Z_L - Z_o}{Z_L + Z_o} = \frac{\bar{v_2}^+}{\bar{v_2}^-}. \tag{4.2.16}$$

Combining the two entails

$$\bar{v_1}^- = S_{11}\bar{v_1}^+ + S_{12}\bar{v_2}^+ = S_{11}\bar{v_1}^+ + S_{12}S_L\bar{v_2}^-$$

$$\bar{v_2}^- = S_{21}\bar{v_1}^+ + S_{22}S_L\bar{v_2}^- \rightarrow \bar{v_2}^-(1 - S_{22}S_L) = S_{21}\bar{v_1}^+ \tag{4.2.17}$$

Thus the reflection coefficient

$$\rho_{in} = S_{in} = \frac{v_1^-}{v_1^+} = S_{11} + \frac{S_{12}S_{21}S_L}{1 - S_L S_{22}}. \tag{4.2.18}$$
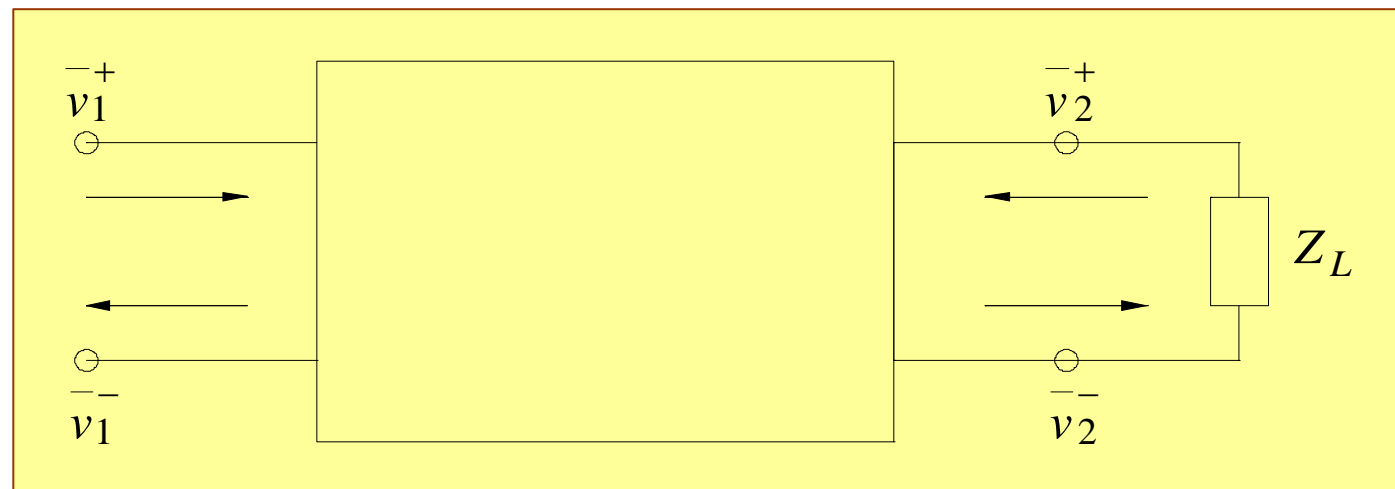
4.3 Transmission Matrix

$$\begin{pmatrix} v_1 \\ I_1 \end{pmatrix} = \begin{pmatrix} A & B \\ C & D \end{pmatrix} \begin{pmatrix} v_2 \\ I_2 \end{pmatrix} \tag{4.3.1}$$

$$\begin{aligned} v_1 &= Z_{11}I_1 - Z_{12}I_2 \\ v_2 &= Z_{21}I_1 - Z_{22}I_2 \end{aligned} \tag{4.3.2}$$

Thus

$$\begin{pmatrix} v_1 \\ I_1 \end{pmatrix} = \begin{pmatrix} \dfrac{Z_{11}}{Z_{12}} & \dfrac{Z_{11}Z_{22} - Z_{12}^2}{Z_{12}} \\[2ex] \dfrac{1}{Z_{12}} & \dfrac{Z_{22}}{Z_{12}} \end{pmatrix} \begin{pmatrix} v_1 \\ I_1 \end{pmatrix} \tag{4.3.3}$$

$$\text{Det}\{ABCD\} \equiv 1 \tag{4.3.4}$$
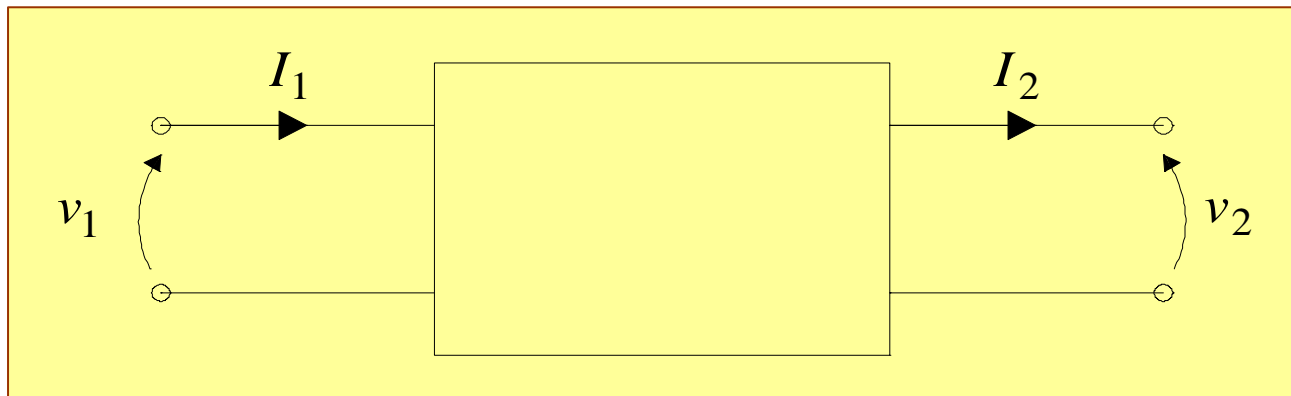
4.4 Wave-Amplitude Transmission Matrix

$$
\begin{pmatrix} \bar{v}_1^- \\ \bar{v}_1^+ \end{pmatrix} = \begin{pmatrix} T_{11} & T_{12} \\ T_{21} & T_{22} \end{pmatrix} \begin{pmatrix} \bar{v}_2^+ \\ \bar{v}_2^- \end{pmatrix}
\tag{4.4.1}
$$

Relation to S matrix

$$
T_{11} = S_{12} - \frac{S_{11}S_{22}}{S_{21}}, \; T_{12} = \frac{S_{11}}{S_{21}}, \; T_{21} = -\frac{S_{22}}{S_{21}}, \; T_{22} = \frac{1}{S_{21}}
\tag{4.4.2}
$$

In a reciprocal system S is symmetrical and $S_{12} = S_{21}$. Therefore

$$
\mathrm{Det}(T) = \frac{S_{12}}{S_{21}} = 1
\tag{4.4.3}
$$
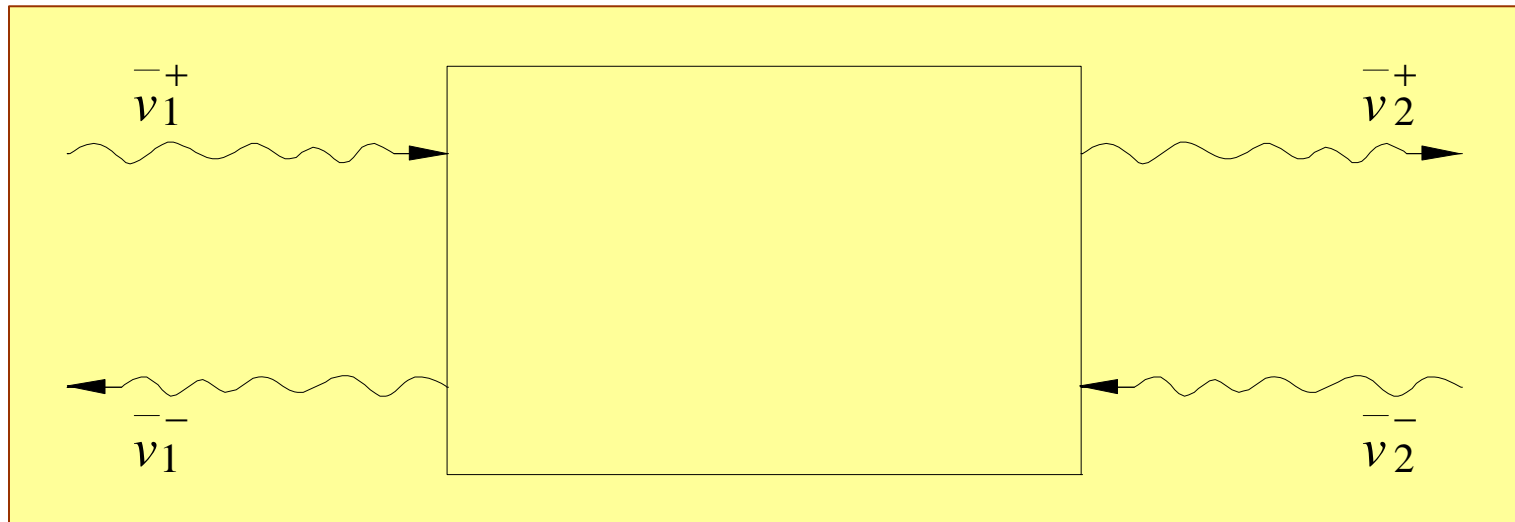
Example: Scattering and transmission matrices of a section of transmission line

$$\begin{pmatrix} v_1^- \\ v_2^- \end{pmatrix} = \begin{pmatrix} S_{11} & S_{12} \\ S_{21} & S_{22} \end{pmatrix} \begin{pmatrix} v_1^+ \\ v_2^+ \end{pmatrix} \tag{4.4.4}$$

$$S_{11} = \left.\frac{v_1^-}{v_1^+}\right|_{v_2^+=0} = 0,\ S_{22} = \left.\frac{v_2^-}{v_2^+}\right|_{v_1^+=0} = 0,\ S_{12} = \left.\frac{v_1^-}{v_2^+}\right|_{v_1^+=0} = e^{-j\beta\ell},\ S_{21} = \left.\frac{v_2^-}{v_1^+}\right|_{v_2^+=0} = e^{-j\beta\ell} \tag{4.4.5}$$

$$S = \begin{pmatrix} 0 & e^{-j\beta\ell} \\ e^{-j\beta\ell} & 0 \end{pmatrix} \rightsquigarrow T = \begin{pmatrix} e^{-j\beta\ell} & 0 \\ 0 & e^{-j\beta\ell} \end{pmatrix} \tag{4.4.6}$$
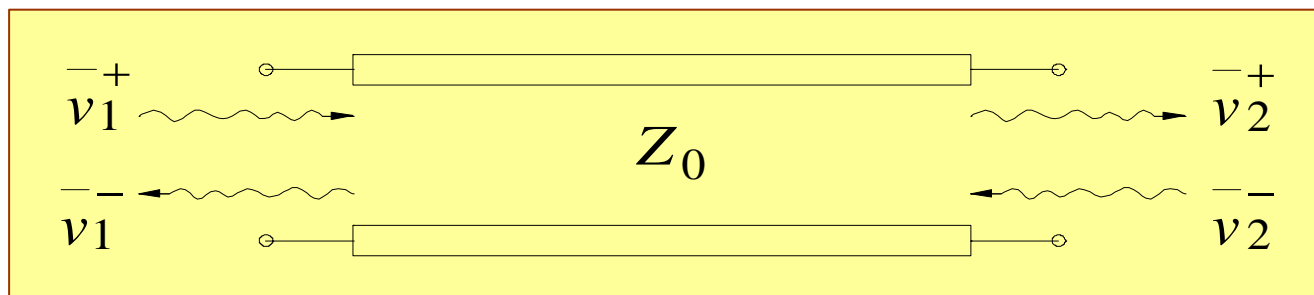
4.5 Loss Matrix

Based on the result in Eq.(4.2.14)

$$Q = I - (S^*)^T S \tag{4.5.1}$$

and since the dissipated power is

$$P_{\text{dis}} = \frac{1}{2} \left\{ \left[\overline{v}^+ \right]^T \left\{ I - (S^*)^T S \right\} \overline{v}^+ \right\} \tag{4.5.2}$$

the matrix defined above determines this dissipated power

$$P_{\text{dis}} = \frac{1}{2} \left\{ \left[\overline{v}^+ \right]^T \underline{\underline{Q}} \, \overline{v}^+ \right\}. \tag{4.5.3}$$

4.6 Directional Coupler

- 4 ports, lossless and reciprocal
- At least *one* symmetry plane
- Each port is matched when all
the
  other are loaded with Z_o
- The power entering (1) splits equally between (3) and (4). No power reaches (2).

input   direct

1   3

2   4

insulated   coupled
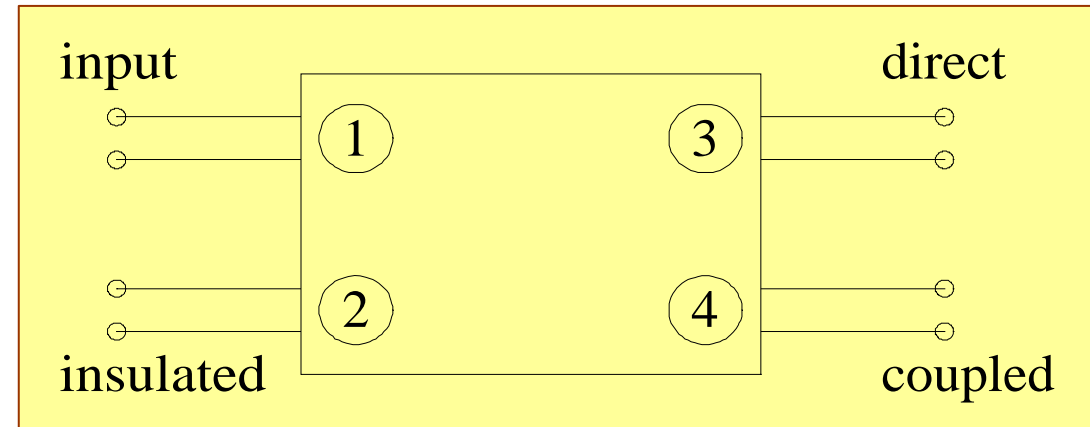
Performance parameters:

$$\text{Coupling} \quad : \quad C = 10\log\left(P_1 / P_4\right)$$

$$\text{Directivity} \quad : \quad D = 10\log\left(P_4 / P_2\right)$$

S matrix:

Isolation condition : $S_{12} = S_{21} = S_{34} = S_{43} = 0$

Matching condition : $S_{11} = S_{22} = S_{33} = S_{44} = 0$

Symmetrical condition : $S_{13} = S_{31},\ S_{23} = S_{32},\ S_{14} = S_{41},\ S_{24} = S_{42}$

$$S = \begin{pmatrix} 0 & 0 & S_{13} & S_{14} \\ 0 & 0 & S_{23} & S_{24} \\ S_{13} & S_{23} & 0 & 0 \\ S_{14} & S_{24} & 0 & 0 \end{pmatrix}_{224}$$

4.7 Coupling Concepts

We shall discuss several aspects of the coupling effect. Here we shall investigate coupling in transmission line configuration.

4.7.1 Double Strip Line: Parameters of the Line
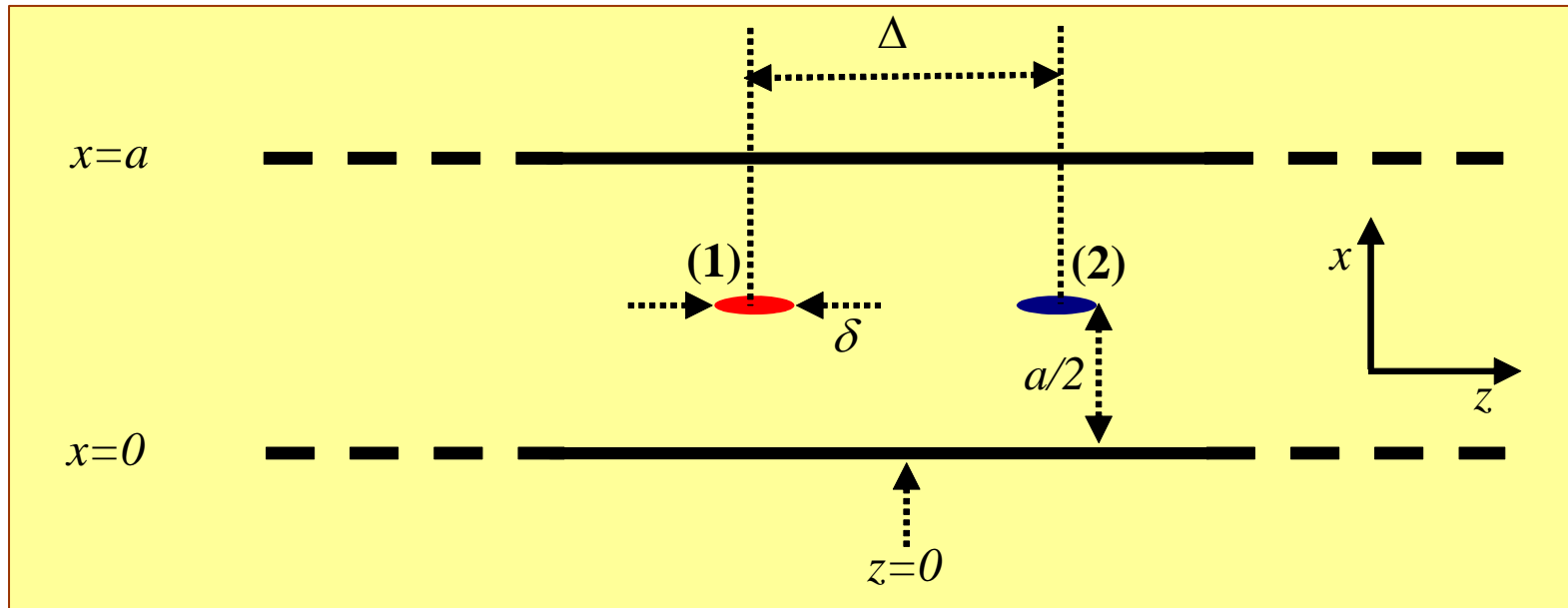
The basic configuration under consideration is illustrated above. Each one of the wires is charged thus the charge distribution in the system is assumed to be

$$\rho_1(x,z) = \lambda_1\delta\left(x-\frac{a}{2}\right)\delta\left(z-\frac{\Delta}{2}\right), \quad \rho_2(x,z) = \lambda_2\delta\left(x-\frac{a}{2}\right)\delta\left(z+\frac{\Delta}{2}\right)$$

For the electrostatic potential we may write the following expression

$$\Phi(x,z) = \sum_{n=1}^{\infty}\varphi_n(z)\sin\left(\frac{\pi n x}{a}\right)$$

Which satifies the boundary conditions on the two plates. This potential satisfies the Poisson equation i.e.,

$$\left(\frac{\partial^2}{\partial x^2}+\frac{\partial^2}{\partial z^2}\right)\varphi(x,z) = -\frac{1}{\varepsilon_o\varepsilon}\rho(x,z) \implies$$

$$\left[\frac{d^2}{dz^2}-\left(\frac{\pi n}{a}\right)^2\right]\varphi_n(z) = \frac{1}{\varepsilon_o\varepsilon}\frac{2}{a}\int dx\rho(x,z)\sin\left(\frac{\pi n x}{a}\right) \tag{4.7.1}$$

$$= -\frac{1}{\varepsilon_o\varepsilon}\frac{2}{a}\sum_v\lambda_v\delta\left(z-\frac{\Delta_v}{2}\right)\sin\left(\frac{\pi n}{2}\right)$$

where $v = 1,2$ and $\Delta_1 = \Delta, \Delta_2 = -\Delta$.

$$\varphi(x,z) = \frac{1}{2}\sum_{n=1}^{\infty}\sin\left(\frac{\pi n x}{a}\right)\text{sinc}\left(\frac{\pi n}{2}\right)\left[\lambda_1\exp\left(-\pi\frac{n}{a}\left|z+\frac{\Delta}{2}\right|\right)+\lambda_2\exp\left(-\pi\frac{n}{a}\left|z-\frac{\Delta}{2}\right|\right)\right] \quad (4.7.2)$$

For a strip of width δ we have

$$\varphi(x,z) = \frac{1}{2}\sum_{n=1}^{\infty}\sin\left(\frac{\pi n x}{a}\right)\text{sinc}\left(\frac{\pi}{2}n\right)\left\{\begin{array}{c}\dfrac{1}{\delta}\displaystyle\int_{-\frac{\Delta}{2}-\frac{\delta}{2}}^{-\frac{\Delta}{2}+\frac{\delta}{2}}d\xi\lambda_1(\xi)\exp\left[-\dfrac{\pi n}{a}|z-\xi|\right]\\[1em] +\dfrac{1}{\delta}\displaystyle\int_{\frac{\Delta}{2}-\frac{\delta}{2}}^{\frac{\Delta}{2}+\frac{\delta}{2}}d\xi\lambda_2(\xi)\exp\left[-\dfrac{\pi n}{a}|z-\xi|\right]\end{array}\right\} \quad (4.7.3)$$

Assuming that $\lambda_1(\xi)$ and $\lambda_2(\xi)$ are uniform

$$\varphi(x,z) = \frac{1}{2}\sum_{n=1}^{\infty}\sin\left(\frac{\pi n x}{a}\right)\text{sinc}\left(\frac{\pi}{2}n\right)$$

$$\times\left\{\frac{\lambda_1}{\delta}\int_{-\frac{\Delta}{2}-\frac{\delta}{2}}^{-\frac{\Delta}{2}+\frac{\delta}{2}}d\xi+\frac{\lambda_2}{\delta}\int_{\frac{\Delta}{2}-\frac{\delta}{2}}^{\frac{\Delta}{2}+\frac{\delta}{2}}d\xi\right\}\exp\left[-\frac{\pi n}{a}|z-\xi|\right] \quad (4.7.4)$$

Moreover, the potential is uniform on the strip

$$V_1 = \frac{1}{\delta} \int_{-\frac{\Delta}{2}-\frac{\delta}{2}}^{-\frac{\Delta}{2}+\frac{\delta}{2}} dz\, \varphi(x = \frac{a}{2}, z)$$

$$= \frac{\lambda_1}{2\delta} \sum_{n=1}^{\infty} \sin\left(\frac{\pi n}{2}\right) \mathrm{sinc}\left(\frac{\pi}{2}n\right) \int_{-\frac{\Delta}{2}-\frac{\delta}{2}}^{-\frac{\Delta}{2}+\frac{\delta}{2}} dz\, \frac{1}{\delta} \int_{-\frac{\Delta}{2}-\frac{\delta}{2}}^{-\frac{\Delta}{2}+\frac{\delta}{2}} d\xi \exp\left[-\frac{\pi n}{a}|z-\xi|\right] \qquad (4.7.5)$$

$$+ \frac{\lambda_2}{2\delta} \sum_{n=1}^{\infty} \sin\left(\frac{\pi n}{2}\right) \mathrm{sinc}\left(\frac{\pi}{2}n\right) \int_{-\frac{\Delta}{2}-\frac{\delta}{2}}^{-\frac{\Delta}{2}+\frac{\delta}{2}} dz\, \frac{1}{\delta} \int_{\frac{\Delta}{2}-\frac{\delta}{2}}^{\frac{\Delta}{2}+\frac{\delta}{2}} d\xi \exp\left[-\frac{\pi n}{a}|z-\xi|\right]$$

The integrals may be evaluated analytically therefore

$$U_{11} = \frac{1}{2}\frac{a}{\delta} \sum_{n=1}^{\infty} \left[\mathrm{sinc}\left(\frac{\pi n}{2}\right)\right]^2 \left[1 - \exp\left(-\frac{\pi n \delta}{2a}\right) \mathrm{sinhc}\left(\frac{\pi n \delta}{2a}\right)\right]$$

$$U_{12} = \frac{1}{2}\frac{a}{\delta} \sum_{n=1}^{\infty} \left[\mathrm{sinc}\left(\frac{\pi n}{2}\right)\right]^2 \left[\left(\frac{\pi n \delta}{2a}\right) \mathrm{sinhc}^2\left(\frac{\pi n \delta}{2a}\right)\right] \exp\left(-\pi\frac{n}{a}\Delta\right)$$

$$(4.7.6)$$

Similar considerations can be applied to the second strip hence $V_2 = U_{21}\lambda_1 + U_{22}\lambda_2$

and detailed calculation shows that $U_{21} = U_{12}$ and $U_{22} = U_{11}$. Note that the off diagonal term is proportional to

$$\sum \exp\left(-\pi n \frac{\Delta}{a}\right)()_n \qquad (4.7.7)$$

which indicates that the coupling drops rapidly. Furthermore, U_{11} are Δ independent! If the strips have different geometries $U_{11} \neq U_{22}$ but still $U_{12} = U_{21}$. In a matrix form:

$$\begin{pmatrix} V_1 \\ V_2 \end{pmatrix} = \begin{pmatrix} U_{11} & U_{12} \\ U_{21} & U_{22} \end{pmatrix} \begin{pmatrix} \lambda_1 \\ \lambda_2 \end{pmatrix} \Rightarrow \begin{pmatrix} \lambda_1 \\ \lambda_2 \end{pmatrix} = \begin{pmatrix} C_{11} & C_{12} \\ C_{12} & C_{22} \end{pmatrix} \begin{pmatrix} V_1 \\ V_2 \end{pmatrix} \qquad (4.7.8)$$

A similar approach can be applied for evaluation of the inductance

$$\begin{pmatrix} \Phi_1 \\ \Phi_2 \end{pmatrix} = \begin{pmatrix} L_{11} & L_{12} \\ L_{12} & L_{22} \end{pmatrix} \begin{pmatrix} I_1 \\ I_2 \end{pmatrix} \qquad (4.7.9)$$

Exercise 4.1: Analyze the coupling term.
Exercise 4.2: Calculate the inductance matrix and analyze the coupling term.
Exercise 4.3: Analyze the case when the two strips are not equally wide.
Exercise 4.4: Analyze the case when the two strips are not equally wide and are not in the same plane.

4.7.2 Equations of the System

The transmission line equations in this case read

$$\frac{d}{dz}V = -j\omega\underline{\underline{L}}I \rightsquigarrow \begin{pmatrix} \dfrac{dV_1}{dz} \\[2ex] \dfrac{dV_2}{dz} \end{pmatrix} = -j\omega \begin{pmatrix} L_{11} & L_{12} \\[1ex] L_{12} & L_{22} \end{pmatrix} \begin{pmatrix} I_1 \\[1ex] I_2 \end{pmatrix}$$

$$\frac{d}{dz}I = -j\omega\underline{\underline{C}}V \rightsquigarrow \begin{pmatrix} \dfrac{dI_1}{dz} \\[2ex] \dfrac{dI_2}{dz} \end{pmatrix} = -j\omega \begin{pmatrix} C_{11} & C_{12} \\[1ex] C_{12} & C_{22} \end{pmatrix} \begin{pmatrix} V_1 \\[1ex] V_2 \end{pmatrix}$$

(4.7.10)

It is convenient in this case to investigate the waves which propagate in this system

$$\frac{d^2}{dz^2}V = -j\omega\underline{\underline{L}}\frac{dI}{dz} = -j\omega\underline{\underline{L}}(-j\omega)\underline{\underline{C}}V = -\omega^2\underline{\underline{LC}}V \qquad (4.7.11)$$

Let us define the wavenumber matrix

$$\underline{\underline{K}}^2 \equiv \omega^2 \underline{\underline{LC}} = \begin{pmatrix} K_{11}^2 & K_{12}^2 \\ \\ K_{12}^2 & K_{22}^2 \end{pmatrix} \tag{4.7.12}$$

Assume a solution of the form $e^{-j\beta z}$

$$(-\beta^2 \underline{\underline{I}} + \underline{\underline{K}}^2)V = 0 \Rightarrow \left[\begin{pmatrix} -\beta^2 & 0 \\ \\ 0 & -\beta^2 \end{pmatrix} + \begin{pmatrix} K_{11}^2 & K_{12}^2 \\ \\ K_{12}^2 & K_{22}^2 \end{pmatrix} \right] \begin{pmatrix} V_1 \\ \\ V_2 \end{pmatrix} = 0 \tag{4.7.13}$$

Explicitly this reads

$$\begin{pmatrix} K_{11}^2 - \beta^2 & K_{12}^2 \\ \\ K_{12}^2 & K_{22}^2 - \beta^2 \end{pmatrix} \begin{pmatrix} V_1 \\ \\ V_2 \end{pmatrix} = 0 \Rightarrow (K_{11}^2 - \beta^2)(K_{22}^2 - \beta^2) - K_{12}^4 = 0 \tag{4.7.14}$$

Let us assume for simplicity sake that the two lines are identical i.e. $K_{11} = K_{22}$ hence

$$(K_{11}^2 - \beta^2)^2 - K_{12}^4 = 0 \rightsquigarrow \beta_{\pm}^2 = K_{11}^2 \pm K_{12}^2 \tag{4.7.15}$$

The eigen-vectors corresponding to β_+^2 may be derived from one of the two equations

eg., $(K_{11}^2 - \beta_+^2)V_1 + K_{12}^2 V_2 = 0$ threfore choosing $V_1 = 1$ we get $V_2 = -\dfrac{K_{11}^2 - \beta_+^2}{K_{12}^2} = 1$ implying

that the normalized egen-vector is

$$\overline{V}_+ = \begin{pmatrix} 1/\sqrt{2} \\ \\ 1/\sqrt{2} \end{pmatrix} \qquad (4.7.16)$$

And in a similar way, the normalized eigen-vector corresponding to β_-^2 is

$$\overline{V}_- = \begin{pmatrix} 1/\sqrt{2} \\ \\ -1/\sqrt{2} \end{pmatrix} \qquad (4.7.17)$$

The general solution has the form

$$V(z) = \overline{V}_+ \left[Ae^{-j\beta_+ z} + Be^{+j\beta_+ z} \right] + \overline{V}_- \left[Ce^{-j\beta_- z} + De^{+j\beta_- z} \right] \qquad (4.7.18)$$

4.7.3 Simple Coupling Process
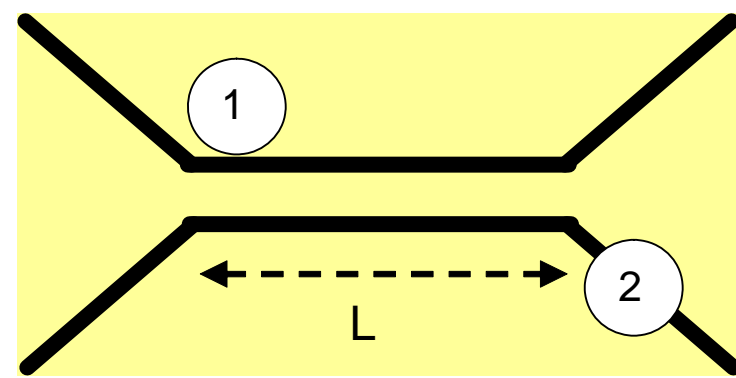
In this subsection we ignore reflections. The schematics of the system under consideration is illustrated in the right. Consider a solution of the form

$$V(z) = \overline{V}_+ A e^{-j\beta_+ z} + \overline{V}_- B e^{-j\beta_- z} \tag{4.7.19}$$

At $z = 0$ only the mode in the *first* line exists. The question is how the power varies with the length L.

$$
\begin{aligned}
V(z) &= \begin{pmatrix} 1/\sqrt{2} \\ 1/\sqrt{2} \end{pmatrix} A e^{-j\beta_+ z} + \begin{pmatrix} 1/\sqrt{2} \\ -1/\sqrt{2} \end{pmatrix} B e^{-j\beta_- z} \\
&= \begin{pmatrix} \left(1/\sqrt{2}\right) A e^{-j\beta_+ z} + \left(1/\sqrt{2}\right) B e^{-j\beta_- z} \\ \left(1/\sqrt{2}\right) A e^{-j\beta_+ z} - \left(1/\sqrt{2}\right) B e^{-j\beta_- z} \end{pmatrix}
\end{aligned}
\tag{4.7.20}
$$

In the absence of coupling $\beta_+ = \beta_- = K_{11}$
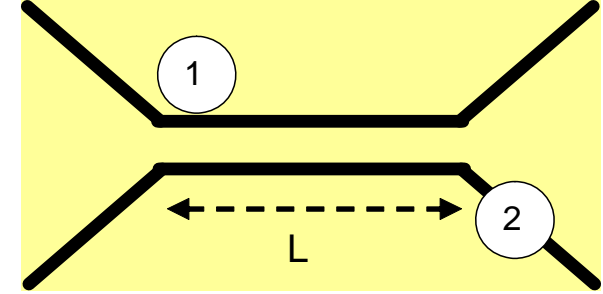
$$V(z) = C \begin{pmatrix} 1 \\ 0 \end{pmatrix} e^{-jK_{11}z} + D \begin{pmatrix} 0 \\ 1 \end{pmatrix} e^{-jK_{11}z} \tag{4.7.21}$$

Now since $V(z=0) = V_0$ for line 1 and $V(z=0) = 0$ for line 2 we get $C = V_0$ and $D = 0$ implying that the voltage on line 2 is always zero.

Let us reinstate the coupling process: the voltage along the transmission lines is given by

$$V(z=0) = \begin{pmatrix} V_0 \\ 0 \end{pmatrix} = \begin{pmatrix} A/\sqrt{2} + B/\sqrt{2} \\ A/\sqrt{2} - B/\sqrt{2} \end{pmatrix} \Rightarrow A = B = \frac{V_0}{\sqrt{2}} \tag{4.7.22}$$

hence

$$V(z) = \frac{V_o}{2} \begin{pmatrix} e^{-j\beta_+ z} + e^{-j\beta_- z} \\ e^{-j\beta_+ z} - e^{-j\beta_- z} \end{pmatrix} = \begin{pmatrix} V_o \exp\left[-j\frac{1}{2}(\beta_+ + \beta_-)z\right]\cos\left[\frac{1}{2}(\beta_+ - \beta_-)z\right] \\ V_o \exp\left[-j\frac{1}{2}(\beta_+ + \beta_-)z\right]j\sin\left[\frac{1}{2}(\beta_+ - \beta_-)z\right] \end{pmatrix}$$

In order to illustrate the coupling process, we examine the voltage on each one of the

lines
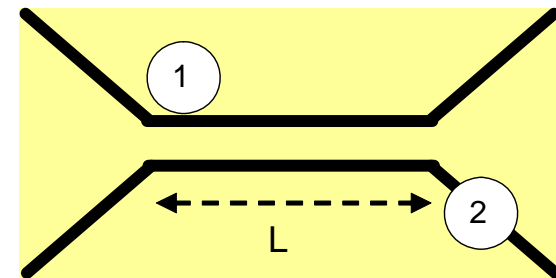
$$V_1 = \left| V_o \exp\left[-j\frac{1}{2}z(\beta_+ + \beta_-)z \right]\cos(\ ) \right| \simeq V_o \left| \cos\left[\frac{1}{2}(\beta_+ - \beta_-)z \right] \right| \qquad (4.7.23)$$

$$V_2 = \left| jV_o \exp\left[-j\frac{1}{2}z(\beta_+ + \beta_-)z \right]\sin(\ ) \right| \simeq V_o \left| \sin\left[\frac{1}{2}(\beta_+ - \beta_-)z \right] \right| \qquad (4.7.24)$$

Schematically these voltages are illustrated in the figure in the right. If we terminate the ``coupler'' at a length L such that

$$\frac{1}{2}(\beta_+ - \beta_-)L = \frac{\pi}{2} \qquad (4.7.25)$$

the voltage is maximum on line 2 and zero on line 1. Recall $\beta_\pm = \sqrt{K_{11}^2 \pm K_{12}^2}$. For simplicity we shall assume $K_{11}^2 \gg K_{12}^2$ hence

$$\beta_\pm = K_{11} \pm \frac{1}{2}\frac{K_{12}^2}{K_{11}}$$

and

235
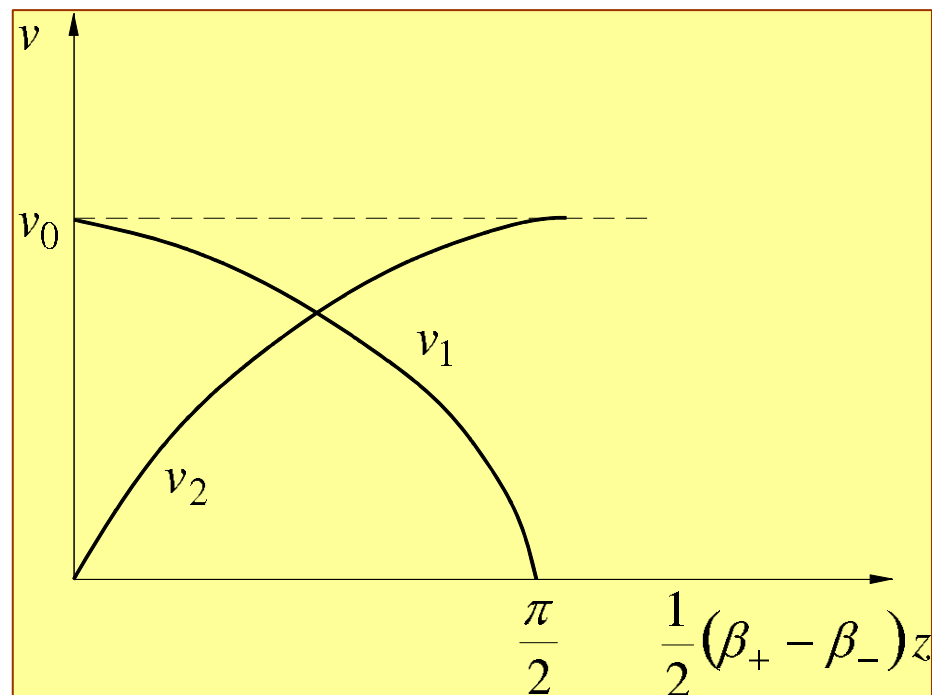
$$\frac{1}{2}(\beta_+ - \beta_-)L \simeq \frac{1}{2}\left[K_{11} + \frac{1}{2}\frac{K_{12}^2}{K_{11}} - \left(K_{11} - \frac{1}{2}\frac{K_{12}^2}{K_{11}}\right)\right]L = \frac{1}{2}\frac{K_{12}^2}{K_{11}}L$$

(4.7.27)

$$= \frac{\pi}{2} \quad \Rightarrow \quad L = \frac{\pi K_{11}}{K_{12}^2}$$
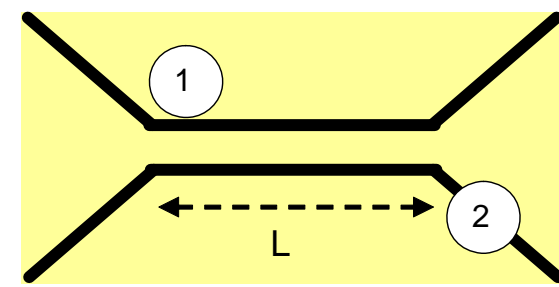
This clearly indicates that the coupling is directly related to the off diagonal term in the matrix $\underline{\underline{K}}^2$.

Exercise 4.5: Analyze L as a function of the geometry (separation Δ, width δ and planes separation a) in the previous section. Make sure that the result is independent of the number of harmonics.

Chapter 5
Nonlinear Components

5.1 Transmission Line with Resistive Nonlinear Load

Consider a transmission line with a non-linear load

$$V_L(t) = V_0 \tanh(I_L/I_0). \tag{5.1.1}$$

The voltage-wave has two components, V_+ propagating in the forward direction and V_- representing the reflected wave

$$V(z,t) = V_+\left(t - \frac{z}{v}\right) + V_-\left(t + \frac{z}{v}\right) \tag{5.1.2}$$

wherein v is the phase-velocity.

Z_0

Load

$z = 0$

237
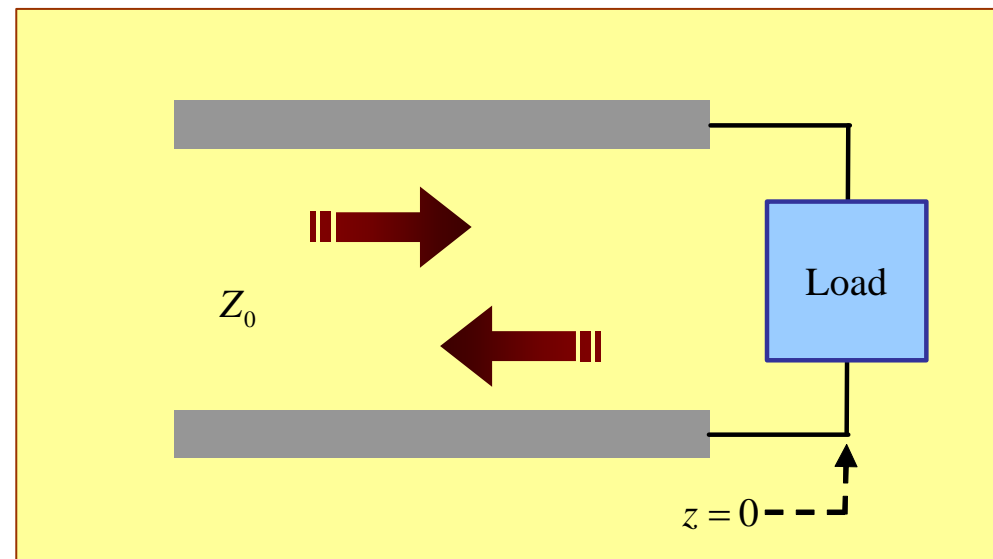
In a similar way the current $W_- = \int_{-\infty}^{\infty} dt \, \frac{1}{Z_0} V_-^2(t)$.

$$I(z,t) = \frac{1}{Z_0} \left[V_+ \left(t - \frac{z}{v} \right) - V_- \left(t + \frac{z}{v} \right) \right].$$ (5.1.3)

At the location of the load

$$V_L(t) = V(z = 0, t) = V_+(t) + V_-(t)$$

$$I_L(t) = I(z = 0, t) = \frac{1}{Z_0} [V_+(t) - V_-(t)]$$ (5.1.4)

thus after substituting in the constitutive relation

$$V_+(t) + V_-(t) = V_0 \tanh \left\{ \frac{1}{Z_0 I_0} [V_+(t) - V_-(t)] \right\}.$$ (5.1.5)

It is convenient to define

$$\overline{V}_\pm = \frac{V_\pm}{Z_0 I_0} \quad \text{and} \quad \overline{Z}_L = \frac{V_0}{Z_0 I_0}$$ (5.1.6)

hence

$$\overline{V}_+ + \overline{V}_- = \overline{Z}_L \tanh(\overline{V}_+ - \overline{V}_-).$$ (5.1.7)

Assuming that the incident wave is known $(\overline{V}_+)$ this expression determines the reflected wave. The figure above shows this reflected wave for several normalized impedance parameters.

Several comments about the plot are evident:

(i)   at the limit $\overline{Z}_L \to \infty$ for a finite solution, the reflected wave equals the incident one.

(ii)   At the other extreme, as $\overline{Z}_L \to 0$, the reflected wave is $\overline{V}_- = -\overline{V}_+$ therefore any solution is in between these two values.
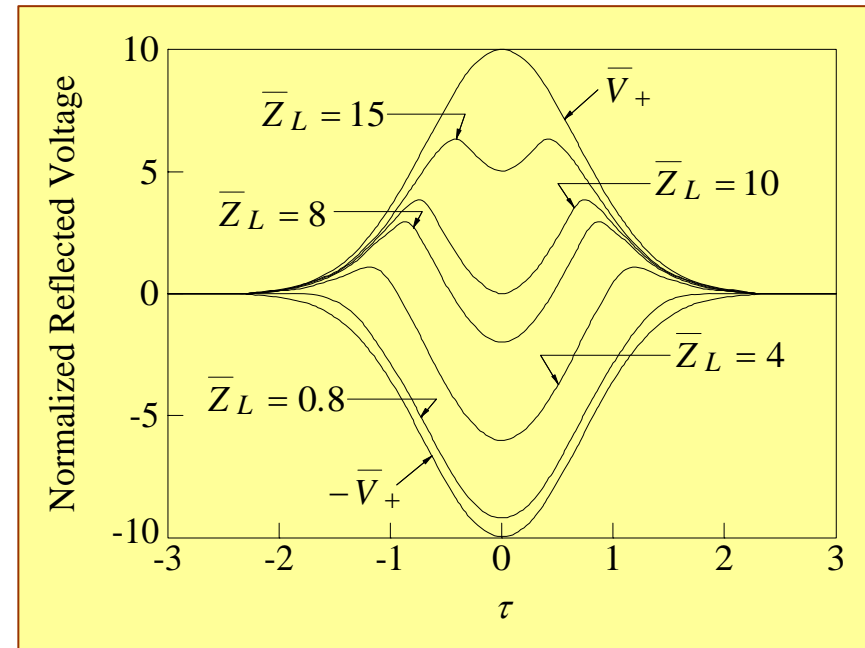
Another aspect of interest is the energy balance. The incident and reflected energy may be evaluated by

$$W_+ = \int_{-\infty}^{\infty} dt \frac{1}{Z_0} V_+^2(t), \ W_- = \int_{-\infty}^{\infty} dt \frac{1}{Z_0} V_-^2(t). \tag{5.1.8}$$

In a linear system the ratio of the two is

$$\rho_W \equiv \frac{W_-}{W_+} = \left(\frac{\overline{Z}_L - 1}{\overline{Z}_L + 1} \right)^2 \tag{5.1.9}$$

wherein $\overline{Z}_L = Z_L / Z_0$. The figure in the right illutrates ρ_W when the maximum value of the incident (Gaussian) wave is $V_+^{(max)} = 2, 5, 10$. This figure clearly reveals that there is full reflection when $\overline{Z}_L$ is zero or tends to infinity. Zero reflection occurs when

$$\overline{Z}_L = \overline{V}_+^{(max)} \Rightarrow \frac{V_0}{Z_0 I_0} = \frac{V_+^{(max)}}{Z_0 I_0} \Rightarrow V_+^{(max)} = V_0.$$
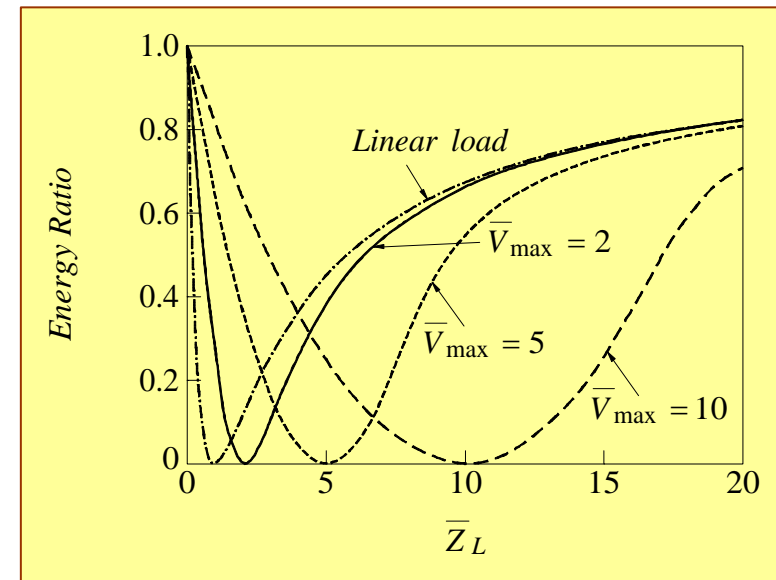
Chapter 6
Periodic Structures

In a variety of applications it is necessary to control the phase velocity of the wave or the propagation time. Periodic metallic or dielectric structures play an important role in implementation of these devices. The periodic geometry can be conceived as a set of obstacles delaying the propagation of the wave due to the multi-reflection process and, as will be shown during our discussion on Floquet's theorem, an infinite spectrum of spatial harmonics develops. A few of which cases these harmonics may propagate with a phase velocity larger or equal to c but the absolute majority have a smaller phase velocity.

In the first section we present the basic theorem of periodic structures namely, Floquet's theorem. This is followed by an investigation of closed periodic structures in Section 6.2 and open structures in the third. Smith-Purcell effect is considered as a particular case of a Green's function calculation for an open structure and a simple scattering problem is also considered. The chapter concludes by presenting a simple transient solution in a periodic structure.

6.1 The Floquet Theorem

A periodic function, $f(z)$, is a function whose value at a given point z is equal to its value at a point $z + L$ i.e.,

$$f(z) = f(z + L), \tag{6.1.1}$$

where L is the periodicity of the function. Any periodic function can be represented as a series of trigonometric functions $\exp(-j2\pi nz / L)$ and since this is an orthogonal and complete set of functions, it implies

$$f(z) = \sum_{n=-\infty}^{\infty} f_n e^{-j2\pi nz/L}. \tag{6.1.2}$$

The amplitudes f_n are determined by the value of the function $f(z)$ in a *single* cell. Specifically, we multiply (6.1.2) by $e^{j2\pi mz/L}$ and integrate over one cell i.e.,

$$\int_0^L dz f(z) e^{j2\pi mz/L} = \int_0^L dz e^{j2\pi mz/L} \sum_{n=-\infty}^{\infty} f_n e^{-j2\pi nz/L}. \tag{6.1.3}$$

Using the orthogonality of the trigonometric function we have

$$f_m = \frac{1}{L} \int_0^L dz f(z) e^{j2\pi mz/L}. \tag{6.1.4}$$

This presentation is called the Fourier series representation and it is valid for a *static* phenomenon in the sense that the value of $f(z)$ at the same relative location in two

different cells is identical. It can not describe a propagation phenomenon, thus it can not represent a *dynamic* system. In the latter case the function $f(z)$ has to satisfy

$$f(z) = \xi f(z+L), \tag{6.1.5}$$

which means that the value of the function is proportional to the value of the function in the adjacent cell up to a constant, ξ, whose absolute value has to be unity otherwise at $z \to \pm\infty$ the function diverges or is zero as can be concluded from

$$f(z) = \xi^n f(z+nL), \tag{6.1.6}$$

where n is an arbitrary integer. Consequently, the coefficient ξ can be represented as a phase term of the form $\xi = \exp(j\psi)$ hence

$$f(z) = e^{j\psi} f(z+L); \tag{6.1.7}$$

ψ is also referred to as the phase advance per cell. Without loss of generality one can redefine this phase to read $\psi = kL$. Since *a-priori* we do not know ψ, this definition does not change the information available. Nonetheless based on the Fourier series in (6.1.2) we can generalize the representation of a dynamic function in a periodic structure to

$$f(z) = \sum_{n=-\infty}^{\infty} f_n e^{-j2\pi nz/L} e^{-jkz}, \tag{6.1.8}$$

and realize that it satisfies

$$f(z) = e^{jkL} f(z+L), \tag{6.1.9}$$

which is identical with the expression in (6.1.7). The last two expressions are different representations of the so-called *Floquet's Theorem*. Later we shall mainly use the form presented in (6.1.8), however in order to illustrate the use of Floquet's theorem in its latter representation, we investigate next the propagation of a TM wave in a periodically loaded waveguide.

.
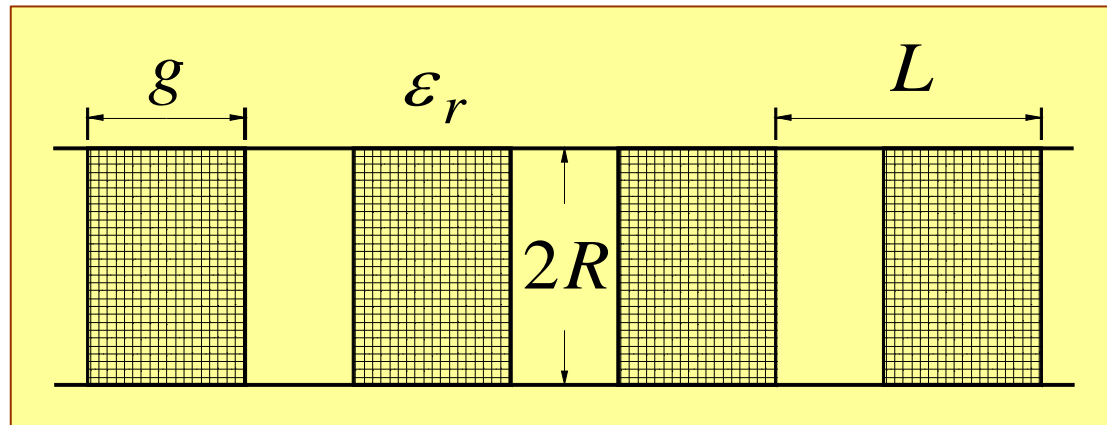
Let us consider a waveguide of radius R which is loaded with dielectric layers: a representative cell ($0 \leq z \leq L$) consists of a region, $0 \leq z \leq g$, filled with a dielectric, ε_r, and the remainder is vacuum -- see Figure 1. We shall determine the dispersion relation of this structure and for this purpose we write the solution of the magnetic vector

potential and electromagnetic field (steady state) in the dielectric ($0 \leq z \leq g$):

$$A_z(r,z) = \sum_{s=1}^{\infty} \mathrm{J}_0\left(p_s \frac{r}{R}\right)\left[A_s e^{-\Gamma_{d,s}z} + B_s e^{+\Gamma_{d,s}z}\right],$$

$$E_r(r,z) = \frac{c^2}{j\omega\varepsilon_{\mathrm{r}}}\sum_{s=1}^{\infty}\frac{p_s}{R}\Gamma_{d,s}\mathrm{J}_1\left(p_s \frac{r}{R}\right)\left[A_s e^{-\Gamma_{d,s}z} - B_s e^{+\Gamma_{d,s}z}\right],$$

$$E_z(r,z) = -\frac{c^2}{j\omega\varepsilon_{\mathrm{r}}}\sum_{s=1}^{\infty}\Gamma_{d,s}^2\mathrm{J}_0\left(p_s \frac{r}{R}\right)\left[A_s e^{-\Gamma_{d,s}z} + B_s e^{+\Gamma_{d,s}z}\right],$$

$$H_\varphi(r,z) = \frac{1}{\mu_0}\sum_{s=1}^{\infty}\frac{p_s}{R}\mathrm{J}_1\left(p_s \frac{r}{R}\right)\left[A_s e^{-\Gamma_{d,s}z} + B_s e^{+\Gamma_{d,s}z}\right], \qquad (6.1.10)$$

where $\Gamma_{d,s}^2 = (p_s / R)^2 - \varepsilon_{\mathrm{r}}(\omega/c)^2$. In a similar way, we have in the vacuum ($g < z < L$):

$$A_z(r,z) = \sum_{s=1}^{\infty} \mathrm{J}_0\left(p_s \frac{r}{R}\right)\left[C_s e^{-\Gamma_s(z-g)} + D_s e^{+\Gamma_s(z-g)}\right],$$

$$E_r(r,z) = \frac{c^2}{j\omega}\sum_{s=1}^{\infty} \frac{p_s}{R}\Gamma_s \mathrm{J}_1\left(p_s \frac{r}{R}\right)\left[C_s e^{-\Gamma_s(z-g)} - D_s e^{+\Gamma_s(z-g)}\right],$$

$$E_z(r,z) = -\frac{c^2}{j\omega}\sum_{s=1}^{\infty} \Gamma_s^2 \mathrm{J}_0\left(p_s \frac{r}{R}\right)\left[C_s e^{-\Gamma_s(z-g)} + D_s e^{+\Gamma_s(z-g)}\right],$$

$$H_\varphi(r,z) = \frac{1}{\mu_0}\sum_{s=1}^{\infty} \frac{p_s}{R} \mathrm{J}_1\left(p_s \frac{r}{R}\right)\left[C_s e^{-\Gamma_s(z-g)} + D_s e^{+\Gamma_s(z-g)}\right], \qquad (6.1.11)$$

with $\Gamma_s^2 = (p_s / R)^2 - (\omega/c)^2$. At this point we shall consider only the TM$_{01}$ mode ($s = 1$) thus the continuity of the *radial electric field* at $z = g$ implies

$$\frac{1}{\varepsilon_r}\Gamma_{d,1}\left[A_1 e^{-\Gamma_{d,1}g} - B_1 e^{+\Gamma_{d,1}g}\right] = \Gamma_1\left[C_1 - D_1\right], \qquad (6.1.12)$$

and in a similar way the continuity of the *azimuthal magnetic field* reads

$$A_1 e^{-\Gamma_{d,1}g} + B_1 e^{+\Gamma_{d,1}g} = C_1 + D_1. \qquad (6.1.13)$$

Last two equations express the relation between the amplitudes of the field in the dielectric and vacuum.

In the dielectric filled region of next cell ($L \le z \le L+g$) the field has a similar form

as in (6.1.10) i.e.,

$$A_z(r,z) = \sum_{s=1}^{\infty} J_0\left(p_s \frac{r}{R} \right) \left[A_s' e^{-\Gamma_{d,s}(z-L)} + B_s' e^{+\Gamma_{d,s}(z-L)} \right],$$

$$E_r(r,z) = \frac{c^2}{j\omega\varepsilon_r} \sum_{s=1}^{\infty} p_s R \Gamma_{d,s} J_1\left(p_s \frac{r}{R} \right) \left[A_s' e^{-\Gamma_{d,s}(z-L)} - B_s' e^{+\Gamma_{d,s}(z-L)} \right],$$

$$E_z(r,z) = -\frac{c^2}{j\omega\varepsilon_r} \sum_{s=1}^{\infty} \Gamma_{d,s}^2 J_0\left(p_s \frac{r}{R} \right) \left[A_s' e^{-\Gamma_{d,s}(z-L)} - B_s' e^{+\Gamma_{d,s}(z-L)} \right],$$

$$H_{\varphi}(r,z) = \frac{1}{\mu_0} \sum_{s=1}^{\infty} p_s R J_1\left(p_s \frac{r}{R} \right) \left[A_s' e^{-\Gamma_{d,s}(z-L)} + B_s' e^{+\Gamma_{d,s}(z-L)} \right] \qquad (6.1.14)$$

Accordingly, the boundary conditions at $z = L$ read

$$\frac{1}{\varepsilon_r} \Gamma_{d,1} \left[A_1' - B_1' \right] = \Gamma_1 \left[C_1 e^{-\Gamma_1(L-g)} - D_1 e^{\Gamma_1(L-g)} \right], \qquad (6.1.15)$$

and

$$A_1' + B_1' = C_1 e^{-\Gamma_1(L-g)} + D_1 e^{\Gamma_1(L-g)}. \qquad (6.1.16)$$

The relation between the amplitudes of the wave in the second cell ($L < z < 2L$) and the first cell can be represented in a matrix form

$$\mathbf{a}' = \mathbf{Ta}, \tag{6.1.17}$$

where the components of $\mathbf{a}'$ are A_1' and B_1' and similarly the components of a are A_1 and B_1. According to Floquet's theorem (6.1.9) the two vectors are expected to be related by

$$\mathbf{a}' = e^{-jkL}\mathbf{a}, \tag{6.1.18}$$

thus e^{-jkL} represents the eigen-values of the single cell transmission matrix T:

$$|\mathbf{T} - e^{-jkL}\mathbf{I}| = 0. \tag{6.1.19}$$

Explicitly this reads

$$e^{-2jkL} - e^{-jkL}(T_{11} + T_{22}) + T_{11}T_{22} - T_{12}T_{21} = 0. \tag{6.1.20}$$

For a passive system the determinant of the matrix $\mathbf{T}$ is unity (prove this statement!!), thus

$$e^{-2jkL} - e^{-jkL}(T_{11} + T_{22}) + 1 = 0. \tag{6.1.21}$$

The fact that the last term in this equation is unity indicates that if k is a solution of (6.1.21) $-k$ is also a solution. Consequently, we can write

$$\cos(kL) = \frac{1}{2}(T_{11} + T_{22}). \tag{6.1.22}$$

Note that this is an explicit expression for k as a function of the frequency and the other geometric parameters. In principle there are ranges of parameters where the right-hand

side is larger than unity and there is no real k which satisfies this relation. If only the frequency is varied then this result indicates that there are frequencies for which the solution of the dispersion relation is real thus a wave can propagate, or the solution is imaginary and the amplitude of the wave is zero. The frequency range for which the wave is allowed to propagate is called the *passband*. Explicitly, the right-hand side of (6.1.22) reads

$$\frac{1}{2}(T_{11} + T_{22}) = \frac{(Z_1 + Z_2)^2}{4Z_1 Z_2}\cosh(\psi + \chi) - \frac{(Z_1 - Z_2)^2}{4Z_1 Z_2}\cosh(\psi - \chi), \qquad (6.1.23)$$

where $\psi = \Gamma_1(L - g)$, $\chi = \Gamma_{d,1}g$, the characteristic impedances are

$$Z_1 = \frac{\eta_0 c \Gamma_{d,1}}{j\omega\varepsilon_r}, \qquad Z_2 = \frac{\eta_0 c \Gamma_1}{j\omega}, \qquad (6.1.24)$$

and $\eta_0 = 377\Omega$ is the impedance of the vacuum.

$f(GH_z)$

$f(GHz)$

kL/π

249
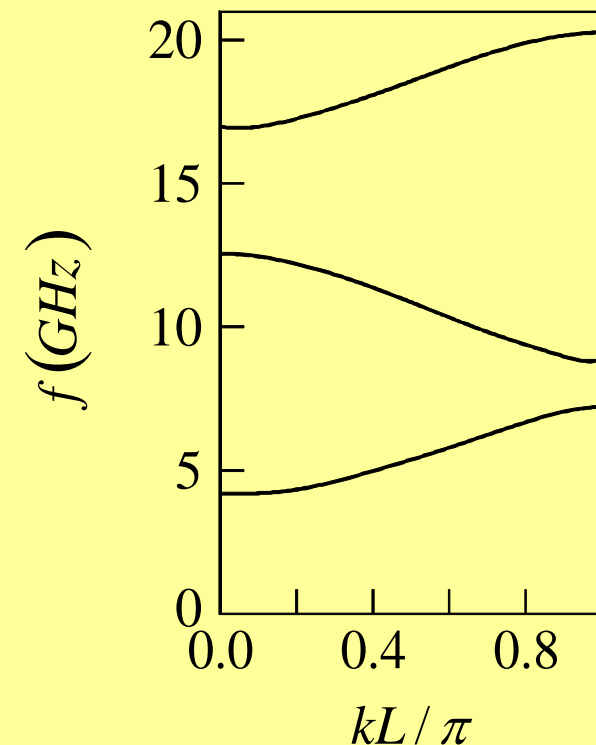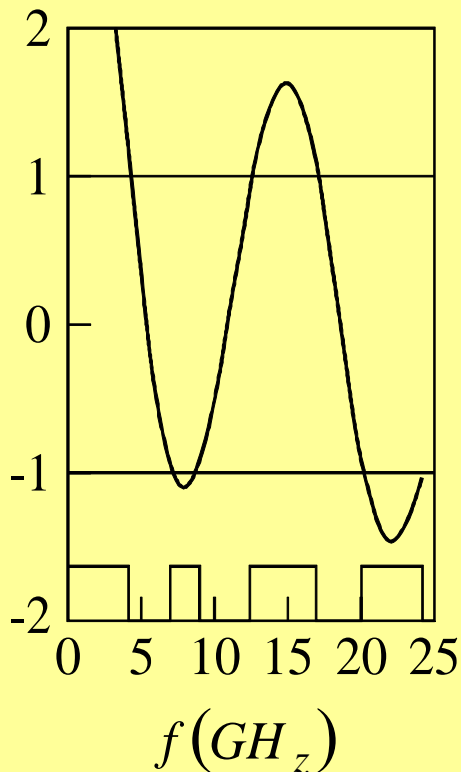
Figure 2 illustrates the right-hand side of (6.1.22) as a function of the frequency ($\varepsilon_{\mathrm{r}} = 10, R = 2$ cm, $L = 1$ cm and $g = L/2$). The blocks at the bottom, illustrate the forbidden frequencies, namely at these frequencies TM waves can not propagate. In Figure 3 the dispersion relation of the first three passbands is presented; these branches correspond only to the TM_{01} mode. Higher symmetric or asymmetric modes have additional contributions in this range of frequencies.

Comment 1. The expression in (6.1.22) is the dispersion relation of a TM_{01} mode in the periodic structure illustrated in Figure 1. From this simple example however we observe that *the dispersion relation of a periodic structure is itself periodic in k with a periodicity $2\pi/L$*. This is a general feature which can be deduced from (6.1.9). If the latter is satisfied for $k = k_0$ then (6.1.9) is satisfied also for $k = k_0 + 2\pi/L$ as shown next

$$f(z+L)e^{j(k_0+2\pi/L)L} = f(z+L)e^{jk_0L}e^{j2\pi},$$

$$= f(z+L)e^{jk_0L} = f(z). \qquad (6.1.25)$$

Consequently, since the dispersion relation is periodic in k, it is sufficient to represent its variation with k in the range $-\pi/L \le k \le \pi/L$; this k domain is also called the *first Brillouin zone*.

Comment 2. Bearing in mind the last comment, we can re-examine the expression in

(6.1.8) and realize that $f(z)$ is represented by a superposition of *spatial harmonics* $\exp(-jk_n z)$ where

$$k_n = k + \frac{2\pi}{L} n, \tag{6.1.26}$$

which all correspond to the solution of the dispersion relation of the system. According to this definition the phase velocity of each harmonic is

$$v_{ph,n} = \frac{\omega}{ck_n}, \tag{6.1.27}$$

and for a high harmonic index, n, this velocity decreases as n^{-1}. Furthermore, all harmonics with negative index correspond to backward propagating waves. In addition, note that the zero harmonic $(n = 0)$ has a positive group velocity for $\pi/L > k > 0$ and negative in the range $-\pi/L < k < 0$. This is a characteristic of *all* spatial harmonics. Since the group velocity is related to the energy velocity, one can conclude that although the the wave number of a particular space harmonic is positive, the power it carries may flow in the negative direction (if the group velocity is negative).

6.2 Closed Periodic Structure

Based on what was shown in the previous section one can determine the dispersion relation of a TM_{01} mode which propagates in a corrugated waveguide [Brillouin (1948)]. Its periodicity is L, the inner radius is denoted by R_{int} and the external by R_{ext}; the distance between two cavities (the drift region) is d. Using Floquet's Theorem (6.1.8) we can write for the magnetic potential in the inner cylinder ($0 < r < R_{int}$) the following expression

$$A_z(r,z) = \sum_{n=-\infty}^{\infty} A_n e^{-jk_{nz}z} I_0(\Gamma_n r), \qquad (6.2.1)$$

and accordingly, the electromagnetic field components read
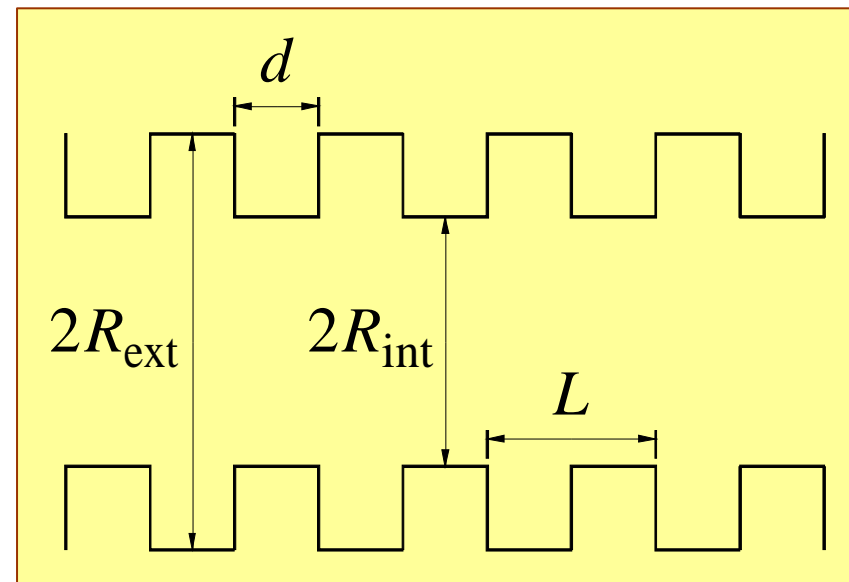
$$E_r(r,z) = \frac{c^2}{j\omega} \sum_{n=-\infty}^{\infty} (-jk_n\Gamma_n) A_n e^{-jk_{nz}z} \mathrm{I}_1(\Gamma_n r),$$

$$E_z(r,z) = \frac{c^2}{j\omega} \sum_{n=-\infty}^{\infty} (-\Gamma_n^2) A_n e^{-jk_{nz}z} \mathrm{I}_0(\Gamma_n r),$$

$$H_\varphi(r,z) = -\frac{1}{\mu_0} \sum_{n=-\infty}^{\infty} \Gamma_n A_n e^{-jk_{nz}z} \mathrm{I}_1(\Gamma_n r) \qquad (6.2.2)$$

In these expressions,

$$\Gamma_n^2 = k_n^2 - \frac{\omega^2}{c^2}, \qquad (6.2.3)$$

and $\mathrm{I}_0(x), \mathrm{I}_1(x)$ are the zero and first order modified Bessel functions of the first kind respectively. This choice of the radial functional variation is dictated by the condition of convergence of the electromagnetic field on axis.

In each individual groove (superscript σ) the electromagnetic field can be derived from the following magnetic vector potential:

$$A_z^{(\sigma)}(r,z) = \sum_{\nu=0}^{\infty} B_\nu^{(\sigma)} \cos\left[q_\nu(z - z_\sigma - d)\right] t_{0,\nu}(r), \qquad (6.2.4)$$

where $q_\nu = \pi\nu/(L-d)$,

$$t_{0,\nu}(r) = \mathrm{I}_0(\Lambda_\nu r)\mathrm{K}_0(\Lambda_\nu R_{\mathrm{ext}}) - \mathrm{K}_0(\Lambda_\nu r)\mathrm{I}_0(\Lambda_\nu R_{\mathrm{ext}}), \qquad (6.2.5)$$

and $\Lambda_v^2 = q_v^2 - (\omega / c)^2$. The electromagnetic field reads

$$E_r^{(\sigma)}(r,z) = \frac{c^2}{j\omega} \sum_{v=0}^{\infty} (-q_v) \Lambda_v B_v^{(\sigma)} \sin[q_v(z - z_\sigma - d)] t_{1,v}(r),$$

$$E_z^{(\sigma)}(r,z) = \frac{c^2}{j\omega} \sum_{v=0}^{\infty} (-\Lambda_v^2) B_v^{(\sigma)} \cos[q_v(z - z_\sigma - d)] t_{0,v}(r),$$

$$H_\varphi^{(\sigma)}(r,z) = -\frac{1}{\mu_0} \sum_{v=0}^{\infty} \Lambda_v B_v^{(\sigma)} \cos[q_v(z - z_\sigma - d)] t_{1,v}(r), \qquad (6.2.6)$$

In these expressions $t_{1,v}(r)$ is the derivative of $t_{0,v}(r)$ defined by

$$t_{1,v}(r) = I_1(\Lambda_v r) K_0(\Lambda_v R_{ext}) + K_1(\Lambda_v r) I_0(\Lambda_v R_{ext}), \qquad (6.2.7)$$

and except at $r = R_{int}$ all the boundary conditions are satisfied.

6.2.1 Dispersion Relation

Our next step is to impose the continuity of the boundary conditions at the interface $(r = R_{int})$. The continuity of the *longitudinal* component of the electric field $[E_z(r = R_{int}, -\infty < z < \infty)]$ reads

$$\frac{c^2}{j\omega}\sum_{n=-\infty}^{\infty}(-\Gamma_n^2)A_n e^{-jk_{n^z}}I_0(\Gamma_n R_{\text{int}})$$

$$= \begin{cases} 0 & \text{for } z_\sigma < z < z_\sigma + d, \\[2em] -\dfrac{c^2}{j\omega}\displaystyle\sum_{v=0}^{\infty}\Lambda_v^2 B_v^{(\sigma)}\cos[q_v(z-z_\sigma-d)]t_{0,v}(R_{\text{int}}) & \text{for } z_\sigma + d < z < z_\sigma + L, \end{cases} \qquad (6.2.8)$$

and the *azimuthal* magnetic field $[H_\varphi(r=R_{\text{int}}, z_\sigma + d < z < z_\sigma + L)]$ reads

$$-\frac{1}{\mu_0}\sum_{n=-\infty}^{\infty}\Gamma_n A_n e^{-jk_{n^z}}I_1(\Gamma_n R_{\text{int}}) = -\frac{1}{\mu_0}\sum_{v=0}^{\infty}\Lambda_v B_v^{(\sigma)}\cos[q_v(z-z_\sigma-d)]t_{1,v}(R_{\text{int}}). \quad (6.2.9)$$

From these boundary conditions the dispersion relation of the structure can be developed. For this purpose we analyze the solution in the grooves having Floquet's theorem in mind. The latter implies that the longitudinal electric field in the σ's groove has to satisfy the following relation:

$$\sum_{v=0}^{\infty}\Lambda_v^2 B_v^{(\sigma)}\cos[q_v(z-z_\sigma-d)]t_{0,v}(r) = \sum_{v=0}^{\infty}\Lambda_v^2 B_v^{(\sigma+1)}e^{jkL}\cos[q_v(z+L-z_{\sigma+1}-d)]t_{0,v}(r).$$

$$\text{(6.2.10)}$$

But by definition $z_{\sigma+1} - z_{\sigma} = L$ therefore, the last expression implies that

$$B_{\nu}^{(\sigma)} \overline{B}_{\nu} e^{-jkz_{\sigma}}. \qquad \text{(6.2.11)}$$

This result permits us to restrict the investigation to a *single cell* and without loss of generality we chose $z_{\sigma=0} = 0$ since if we know B_{ν} in one cell, the relation in (6.2.11) determines the value of this amplitude in all other cells. With this result in mind we multiply (6.2.8) by $e^{jk_m z}$ and integrate over one cell; the result is

$$\sum_{n=-\infty}^{\infty} \Gamma_n^2 A_n \delta_{n,m} L \mathrm{I}_0(\Gamma_n R_{\mathrm{int}}) \sum_{\nu=0}^{\infty} \Lambda_{\nu}^2 B_{\nu} t_{0,\nu}(R_{\mathrm{int}}) \int_d^L dz\, e^{jk_m z} \cos[q_{\nu}(z-d)], \qquad \text{(6.2.12)}$$

here $\delta_{n,m}$ is the Kroniker delta function which equals 1 if $n = m$ and zero otherwise. We also used the orthogonality of the Fourier spatial harmonics. We follow a similar procedure when imposing the continuity of the magnetic field with one difference, (6.2.9) is defined only in the groove aperture thus we shall utilize the orthogonality of the trigonometric function $\cos[q_{\nu}(z-d)]$. Accordingly, (6.2.9) is multiplied by $\cos[q_{\mu}(z-d)]$ and we integrate over $d < z < L$; the result is

$$\sum_{n=-\infty}^{\infty} \Gamma_n A_n \mathrm{I}_1(\Gamma_n R_{\mathrm{int}}) \int_d^L dz \cos\left[q_{\mu}(z-d)\right] e^{-jk_n z} = \sum_{\nu=0}^{\infty} \Lambda_{\nu} B_{\nu} t_{1,\nu}(R_{\mathrm{int}})(L-d) g_{\mu} \delta_{\nu,\mu},$$

$$\text{(6.2.13)}$$

where $g_0 = 1$ and $g_{\mu \neq 0} = 0.5$ otherwise. It is convenient to define the quantity

$$\mathcal{L}_{n,v}(k) = \frac{1}{L-d} \int_d^L dz \cos\left[q_v(z-d)\right] e^{jk_n z},$$ (6.2.14)

which allows us to write (6.2.12) as

$$A_n = \frac{1}{\Gamma_n^2 I_0(\Gamma_n R_{\text{int}})} \frac{L-d}{L} \sum_{v=0}^{\infty} \Lambda_v^2 t_{0,v}(R_{\text{int}}) \mathcal{L}_{n,v}(k) B_v,$$ (6.2.15)

and (6.2.13) as

$$B_v = \frac{1}{\Lambda_v t_{1,v}(R_{\text{int}}) g_v} \sum_{n=-\infty}^{\infty} A_n \Gamma_n I_1(\Gamma_n R_{\text{int}}) \mathcal{L}_{n,v}^*(k).$$ (6.2.16)

These are two equations for two unknown sets of amplitudes (A_n, B_v) and the dispersion relation can be represented in two equivalent ways: One possibility is to substitute (6.2.16) in (6.2.15) and get

$$\sum_{m=-\infty}^{\infty} \left[\delta_{n,m} - \frac{L-d}{L} \frac{\Gamma_m I_1(\Gamma_m R_{\text{int}})}{\Gamma_n^2 I_0(\Gamma_n R_{\text{int}})} \sum_{v=0}^{\infty} \frac{t_{0,v}(R_{\text{int}}) \Lambda_v}{t_{1,v}(R_{\text{int}}) g_v} \mathcal{L}_{n,v} \mathcal{L}_{m,v}^* \right] A_m = 0,$$ (6.2.17)

whereas the other possibility is to substitute (6.2.15) in (6.2.16) and obtain

$$\sum_{\mu=0}^{\infty}\left[\delta_{\nu,\mu} - \frac{L-d}{L}\frac{\Lambda_{\mu}^{2}t_{0,\mu}(R_{\text{int}})}{\Lambda_{\nu}t_{1,\nu}(R_{\text{int}})g_{\nu}}\sum_{n=-\infty}^{\infty}\frac{\text{I}_{1}(\Gamma_{n}R_{\text{int}})}{\Gamma_{n}\text{I}_{0}(\Gamma_{n}R_{\text{int}})}\mathcal{L}_{n,\nu}^{*}\mathcal{L}_{n,\mu}\right]B_{\mu}\,\overline{0}. \tag{6.2.18}$$

In both cases the dispersion relation is calculated from the requirement that the determinant of the matrix which multiplies the vector of amplitudes, is zero.

Although the two methods are equivalent, we found that the latter expression is by far more efficient for practical calculation because of the number of modes required to represent adequately the field in the groove compared to the number of spatial harmonics required to represent the field in the inner section. In the case of single mode operation we found that 1 to 3 modes are sufficient for description of the field in the grooves and about 40 spatial harmonics are generally used in the inner section. As indicated by these numbers it will be much easier to calculate the determinant of a 3×3 matrix rather than 40×40 one; we shall quantify this statement later. At this point we shall discuss the design of a disk-loaded structure assuming that the number modes in the grooves and harmonics in the inner space are sufficient.

Let assume that we want to determine the geometry of a disk-loaded structure which enables a wave at 10 GHz to be in resonance with electrons with $\beta = 0.9$ and the phase advance per cell is assumed to be $kL = 2\pi/3$. These two conditions determine the period of the structure. In our case $L = 9$ mm. There are three additional geometric parameters to be determined: $R_{\text{ext}}, R_{\text{int}}$ and d. The last two have

a dominant effect on the width of the passband and for the lowest mode, the passband increases with increasing R_{int} and decreases with increasing d. The passband, $\Delta\omega$, of a mode sets a limit on the maximum group velocity as can be seen bearing in mind that the half width of the *first Brillouin zone* is $\Delta k = \pi/L$. Consequently, $v_{gr} = \Delta\omega/\Delta k < \Delta\omega L/\pi$. A solution of the dispersion relation in (6.2.18) is illustrated the geometry chosen is: $L = 9\,\text{mm}$, $R_{int} = 8\,\text{mm}$ and $d = 2\,\text{mm}$ and from the condition of phase advance per cell of 120° at 10 GHz, we determined, using the dispersion relation, the value of the external radius to be $R_{ext} = 13.96$ mm.

Graph axes: vertical $f\,(GHz)$ from 8 to 11; horizontal kL/π from 0.0 to 0.8.
$R_{ext} = 14mm$
$R_{int} = 8mm$
$L = 9mm$
$d = 2mm$
$kL = 2\pi/3$
Beam Line $\beta = 0.9$
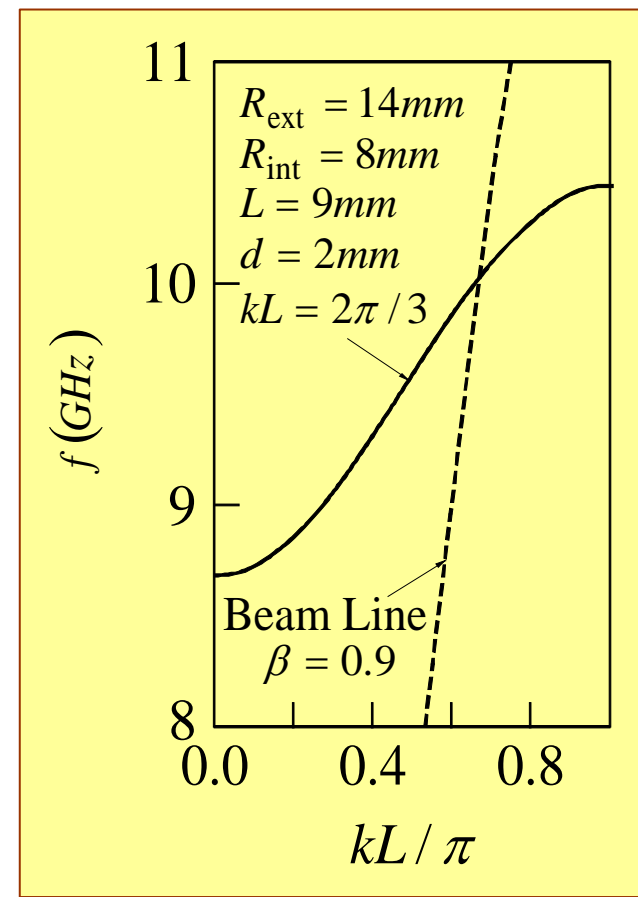
6.2.2 Modes in the groove

Therefore, before we conclude this subsection, we shall quantify the effect of higher modes. The first mode in the groove ($\nu = 0$) represents a TEM mode which propagates in the radial direction. Other modes ($\text{TM}_{0,\nu>0}$) are either propagating or evanescent. The amplitudes of the magnetic and electric field (E_z) of the TEM mode are constant at the groove aperture thus the choice of using a single mode in the groove is equivalent to the

average process at the boundary -- approach usually adopted in the literature. The Figure illustrates the dependence of upper and lower cut-off frequency on the number of harmonics used in the calculation; the number of modes in the grooves is a parameter. For the geometry presented above, the number of harmonics required is 20 or larger; typically about 40 harmonics are being used. The effect of the $\nu = 1$ mode is negligible in this case as seen for both upper and lower cut-off frequencies. The effect of the higher mode introduces a correction on the order of 1% which for most practical purposes is sufficient.
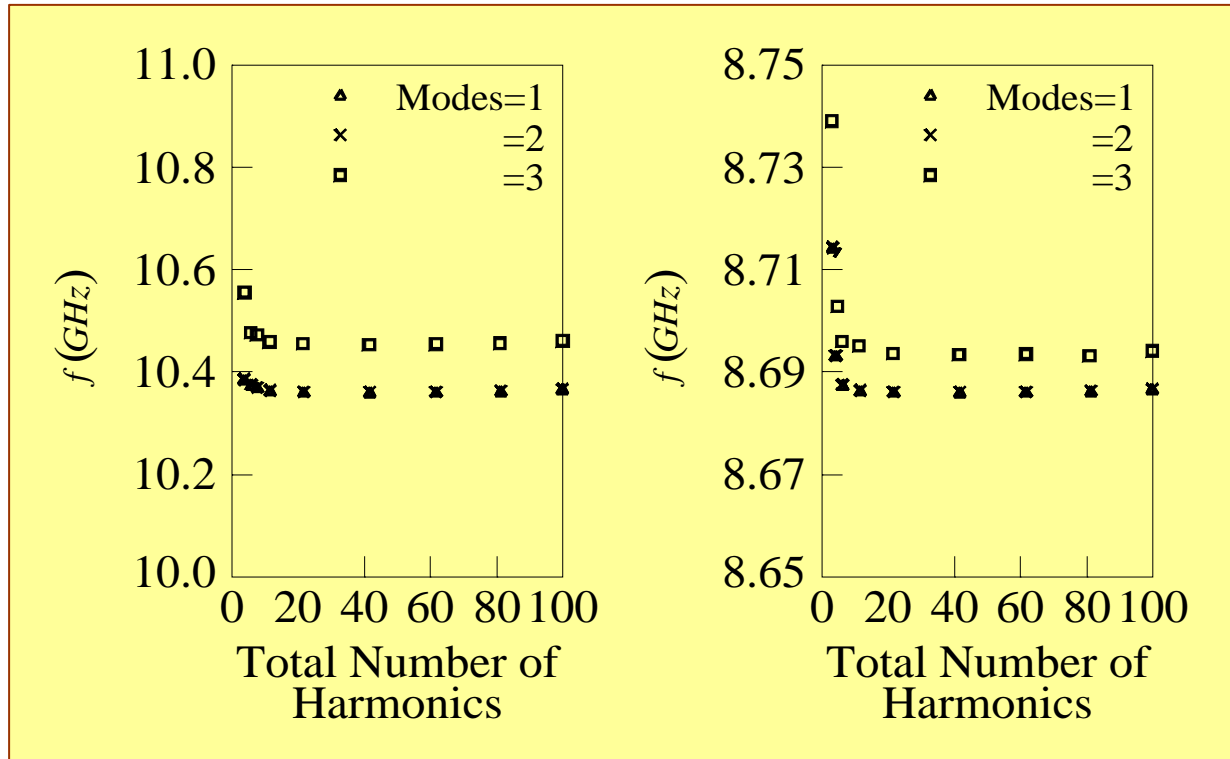
6.2.3 Spatial Harmonics Coupling

Contrary to uniform dielectric structures, here each mode consists of a superposition of an infinite number of spatial harmonics. These harmonics are all coupled by the conditions imposed on the electromagnetic field by the geometry at $r = R_{\text{int}}$. We shall limit the investigation to the accuracy associated with a single mode taken in the groove, therefore according to (6.2.15), we have

$$A_n = -\frac{1}{\Gamma_n^2 I_0(\Gamma_n R_{\text{int}})} \frac{\omega^2}{c^2} t_{0,0}(R_{\text{int}}) \mathcal{L}_{n,0}(k) B_0, \qquad (6.2.19)$$

and in this particular case

$$\mathcal{L}_{n,0}(k) = \frac{L-d}{L} \text{sinc}\left[\frac{1}{2} k_n(L-d)\right] \exp\left[j\frac{1}{2} k_n(L+d)\right]. \qquad (6.2.20)$$

Let us compare the first few spatial harmonics relative to the zero harmonic. For this purpose we take $f = 10$ GHz, $v_0 = 0.9c, R_{\text{int}} = 8$ mm, $L = 9$ mm and $d = 2$ mm. The ratio of the first two amplitudes is

$$\left|\frac{A_{-1}}{A_0}\right| = 8 \times 10^{-3}, \left|\frac{A_1}{A_0}\right| = 3 \times 10^{-6}, \left|\frac{A_{-2}}{A_0}\right| = 2 \times 10^{-6}, \left|\frac{A_2}{A_0}\right| = 1 \times 10^{-8} \qquad (6.2.21)$$

This result indicates that *on axis*, the amplitude of the interacting harmonic is dominant. At the *interface* with the grooves ($r = R_{int}$) the ratio between the contribution of the zero and nth harmonic is much closer to unity and it can be checked that it reads

$$\frac{|E_{z,n}(r = R_{int})|}{|E_{z,0}(r = R_{int})|} = \frac{|\text{sinc}(k_n(L-d)/2)|}{|\text{sinc}(k_0(L-d)/2)|}, \qquad (6.2.22)$$

which is a virtually unity.

A more instructive picture is obtained by examining the average power flowing in one time and spatial period of the system:

$$P = 2\pi \int_0^{R_{int}} dr\, r \frac{1}{L} \int_0^L dz \left[\frac{1}{2} E_r(r,z) H_\varphi^*(r,z) \right]. \qquad (6.2.23)$$

According to the definition in (6.2.2) we have

$$P = \frac{\pi}{\eta_0} \sum_{n=-\infty}^{\infty} |cA_n|^2 \frac{ck_n}{\omega} \int_0^{\Gamma_n R_{int}} dx\, x I_1^2(x); \qquad (6.2.24)$$

the integral can be calculated analytically [Abramowitz and Stegun (1968) p.484] and it reads

$$U(\xi) \equiv \int_0^{\xi} dx \, x \mathrm{I}_1^2(x) \overline{\xi} \mathrm{I}_0(\xi) \mathrm{I}_1(\xi) + \frac{1}{2} \xi^2 [\mathrm{I}_1^2(\xi) - \mathrm{I}_0^2(\xi)]. \tag{6.2.25}$$

Based on these definitions we can calculate the average power carried by each harmonic as

$$P_n = \frac{\pi}{\eta_0} |cA_n|^2 \frac{ck_n}{\omega} U(\Gamma_n R_{\text{int}}), \tag{6.2.26}$$

and the result is listed below

$$\frac{P_{-2}}{P_0} = -3 \times 10^{-3}, \quad \frac{P_{-1}}{P_0} = -0.16, \quad \frac{P_1}{P_0} = 1 \times 10^{-4}, \quad \frac{P_2}{P_0} = 3 \times 10^{-3} \tag{6.2.27}$$

Although there is a total flow of power along (the positive) direction of the z axis, a substantial amount of power is actually flowing backwards. In this numerical example for all practical purposes we can consider only the lowest two harmonics and write the total power which flows, normalized to the power in the zero harmonic. Thus if the latter is unity, then the power in the forward is $1 - 0.16 = 0.84$. This result indicates that if we have a finite length structure with finite reflections from the input end, then in this periodic structure we have an inherent feedback even if the output end is perfectly matched.

6.3 Open Periodic Structure

In this section an analysis similar to that in Section 6.2 is applied to an open periodic structure. As we shall see the number of modes which may develop in such a structure is *small* and therefore mode competition is minimized.

We shall consider a system in which the wave propagates along the periodic structure which consists of a disk-loaded wire, as illustrated in Figure 5 whose periodicity is L, the inner radius is denoted by R_{int}, the external by R_{ext} and the distance between two cavities is d. Floquet's theorem as formulated in (6.1.8) allows us to write for the magnetic potential in the external region ($\infty > r \geq R_{ext}$) the following expression

$$A_z(r,z) = \sum_{n=-\infty}^{\infty} A_n e^{-jk_n z} K_0(\Gamma_n r), \qquad (6.3.1)$$

and accordingly, the electromagnetic field components read
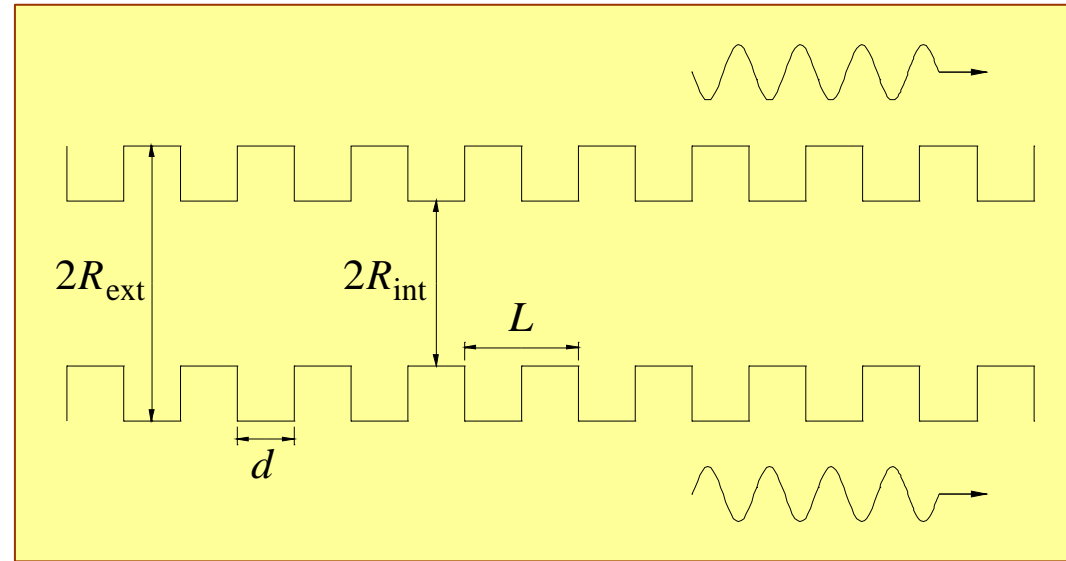
$$E_r(r,z) = \frac{c^2}{j\omega} \sum_{n=-\infty}^{\infty} (jk_n\Gamma_n) A_n e^{-jk_{nz}z} K_1(\Gamma_n r),$$

$$E_z(r,z) = \frac{c^2}{j\omega} \sum_{n=-\infty}^{\infty} (-\Gamma_n^2) A_n e^{-jk_{nz}z} K_0(\Gamma_n r), \qquad (6.3.2)$$

$$H_\varphi(r,z) = -\frac{1}{\mu_0} \sum_{n=-\infty}^{\infty} (-\Gamma_n) A_n e^{-jk_{nz}z} K_1(\Gamma_n r)$$

In these expressions $K_0(x), K_1(x)$ are the zero and first order modified Bessel functions of the second kind respectively and $\Gamma_n^2 = k_n^2 - (\omega/c)^2$. This choice of the radial functional variation is dictated by the condition of convergence of the electromagnetic field far away from the structure.

In each individual groove the electromagnetic field can be derived from the following magnetic vector potential:

$$A_z^{(\sigma)}(r,z) = \sum_{\nu=0}^{\infty} B_\nu^{(\sigma)} \cos[q_\nu(z - z_\sigma - d)] t_{0,\nu}(r), \qquad (6.3.3)$$

where $q_\nu = \pi\nu/(L-d)$,

$$t_{0,\nu}(r) = I_0(\Lambda_\nu r) K_0(\Lambda_\nu R_{\text{int}}) - K_0(\Lambda_\nu r) I_0(\Lambda_\nu R_{\text{int}}), \qquad (6.3.4)$$

and $\Lambda_\nu^2 = q_\nu^2 - (\omega/c)^2$. The electromagnetic field reads

$$E_r^{(\sigma)}(r,z) = \frac{c^2}{j\omega} \sum_{v=0}^{\infty} (-q_v) \Lambda_v B_v^{(\sigma)} \sin[q_v(z - z_\sigma - d)] t_{1,v}(r),$$

$$E_z^{(\sigma)}(r,z) = \frac{c^2}{j\omega} \sum_{v=0}^{\infty} (-\Lambda_v^2) B_v^{(\sigma)} \cos[q_v(z - z_\sigma - d)] t_{0,v}(r),$$

$$H_\varphi^{(\sigma)}(r,z) = -\frac{1}{\mu_0} \sum_{v=0}^{\infty} \Lambda_v B_v^{(\sigma)} \cos[q_v(z - z_\sigma - d)] t_{1,v}(r). \tag{6.3.5}$$

The index σ labels the ``cavity'' and in these expressions we used

$$t_{1,v}(r) = I_1(\Lambda_v r) K_0(\Lambda_v R_{int}) + K_1(\Lambda_v r) I_0(\Lambda_v R_{int}). \tag{6.3.6}$$

The solution above satisfies all boundary conditions with the exception of $r = R_{ext}$.

6.3.1 Dispersion Relation

Our next step is to impose the continuity of the boundary conditions at the interface $(r = R_{ext})$. Continuity of the longitudinal component of the electric field implies $E_z(r = R_{ext}, -\infty < z < \infty)$, reads

$$\frac{c^2}{j\omega} \sum_{n=-\infty}^{\infty} (-\Gamma_n^2) A_n e^{-jk_{nz}} \mathrm{K}_0(\Gamma_n R_{\mathrm{ext}}) =$$

$$\begin{cases} 0 & \text{for } z_\sigma < z < z_\sigma + d, \\ \\ -\dfrac{c^2}{j\omega} \sum_{\nu=0}^{\infty} \Lambda_\nu^2 B_\nu^{(\sigma)} \cos[q_\nu(z - z_\sigma - d)] t_{0,\nu}(R_{\mathrm{ext}}) & \text{for } z_\sigma + d < z < z_\sigma + L, \end{cases} \qquad (6.3.7)$$

and the azimuthal magnetic field, $H_\varphi(r = R_{\mathrm{ext}}, z_\sigma + d < z < z_\sigma + L)$, reads

$$\frac{1}{\mu_0} \sum_{n=-\infty}^{\infty} \Gamma_n A_n e^{-jk_{nz}} \mathrm{K}_1(\Gamma_n R_{\mathrm{ext}}) = \frac{1}{\mu_0} \sum_{\nu=0}^{\infty} \Lambda_\nu B_\nu^{(\sigma)} \cos[q_\nu(z - z_\sigma - d)] t_{1,\nu}(R_{\mathrm{ext}}). \quad (6.3.8)$$

Following the same arguments as in Section 6.2.1 it can be shown that $B_\nu^{(\sigma)} = B_\nu e^{-jkz_\sigma}$ and consequently we can limit the discussion to a single cell. We multiply (6.3.7) by $e^{jk_{mz}}$ and integrate over one cell; the result being

$$\sum_{n=-\infty}^{\infty} \Gamma_n^2 A_n \delta_{n,m} L \mathrm{K}_0(\Gamma_n R_{\mathrm{ext}}) \sum_{\nu=0}^{\infty} \Lambda_\nu^2 B_\nu t_{0,\nu}(R_{\mathrm{ext}}) \int_d^L dz\, e^{jk_{mz}} \cos[q_\nu(z - d)]. \qquad (6.3.9)$$

267

We follow a similar procedure when imposing the continuity of the magnetic field; the difference in this case is that (6.3.8) is defined only in the groove's aperture thus we shall utilize the orthogonality of the trigonometric function $\cos[q_\nu(z-d)]$. Accordingly, (6.3.8) is multiplied by $\cos[q_\mu(z-d)]$ and we integrate over $d < z < L$; the result is

$$\sum_{n=-\infty}^{\infty} \Gamma_n A_n K_1(\Gamma_n R_{\text{ext}}) \int_d^L dz \cos[q_\mu(z-d)] e^{-jk_n z} = \sum_{\nu=0}^{\infty} \Lambda_\nu B_\nu t_{1,\nu}(R_{\text{ext}})(L-d)g_\mu \delta_{\nu,\mu}.$$

(6.3.10)

In this expression $g_0 = 1$ and $g_{n\neq0} = 0.5$. It is convenient to define the quantity

$$\mathcal{L}_{n,\nu}(k) = \frac{1}{L-d} \int_d^L dz \cos[q_\nu(z-d)] e^{jk_n z},$$

(6.3.11)

by whose means, (6.3.9) reads

$$A_n = \frac{1}{\Gamma_n^2 K_0(\Gamma_n R_{\text{ext}})} \frac{L-d}{L} \sum_{\nu=0}^{\infty} \Lambda_\nu^2 t_{0,\nu}(R_{\text{ext}}) \mathcal{L}_{n,\nu}(k) B_\nu,$$

(6.3.12)

whereas (6.3.10)

$$B_\nu = \frac{1}{\Lambda_\nu t_{1,\nu}(R_{\text{ext}})g_\nu} \sum_{n=-\infty}^{\infty} A_n \Gamma_n K_1(\Gamma_n R_{\text{ext}}) \mathcal{L}_{n,\nu}^*(k).$$

(6.3.13)

These are two equations for two unknown sets of amplitudes (A_n, B_ν). The

dispersion relation can be represented in two equivalent ways: One possibility is to substitute (6.3.13) in (6.3.12) and obtain one equation for the amplitudes of the various harmonics

$$\sum_{m=-\infty}^{\infty} \left[\delta_{n,m} + \frac{L-d}{L} \frac{\Gamma_m K_1(\Gamma_m R_{\text{ext}})}{\Gamma_n^2 K_0(\Gamma_n R_{\text{ext}})} \sum_{v=0}^{\infty} \frac{t_{0,v}(R_{\text{ext}})\Lambda_v}{t_{1,v}(R_{\text{ext}})g_v} \mathcal{L}_{n,v} \mathcal{L}_{m,v}^* \right] A_m = 0. \qquad (6.3.14)$$

The other possibility is to substitute (6.3.12) in (6.3.13) and obtain one equation for the amplitudes of the various modes in the groove

$$\sum_{\mu=0}^{\infty} \left[\delta_{v,\mu} + \frac{L-d}{L} \frac{\Lambda_\mu^2 t_{0,\mu}(R_{\text{ext}})}{\Lambda_v t_{1,v}(R_{\text{ext}})g_v} \sum_{n=-\infty}^{\infty} \frac{K_1(\Gamma_n R_{\text{ext}})}{\Gamma_n K_0(\Gamma_n R_{\text{ext}})} \mathcal{L}_{n,v}^* \mathcal{L}_{n,\mu} \right] B_\mu = 0. \qquad (6.3.15)$$

In both cases the dispersion relation is calculated from the requirement that the determinant of the matrix which multiplies the vector of amplitudes, is zero. As in the closed structure the two methods are equivalent, but the last expression is by far more efficient for practical calculation.

There is one substantial difference between open and closed periodic structures. In the latter case, the radiation is guided by the waveguide and there is an infinite discrete spectrum of frequencies which can propagate along the system. In open structures, modes can propagate provided that the projection of the wavenumbers of *all harmonics* in the first Brillouin zone corresponds to waves whose phase velocity is smaller than c; in other

words, no radiation propagates outwards (radially). The figure illustrates the two regions of interest: in the shadowed region no solutions are permissible and in the remainder the solution is possible with an adequate choice of the geometric parameters. It is evident from this picture that waves at frequencies higher than

$$f \geq \frac{1}{2}\frac{c}{L},$$

can not be supported by a disk-loaded wire, regardless of the geometrical details of the cavity. With this regard, an open structure forms a low pass filter. Figure 3.1 illustrates the dispersion relation of such a system for $L = 3$ mm, $d = 1$ mm, $R_{int} = 15$ mm and $R_{ext} = 21$ mm. For comparison, in the same frequency range (0--50 GHz) there are 6 symmetric TM modes which can propagate in a closed system of the same geometry; obviously there are many others at higher frequencies.
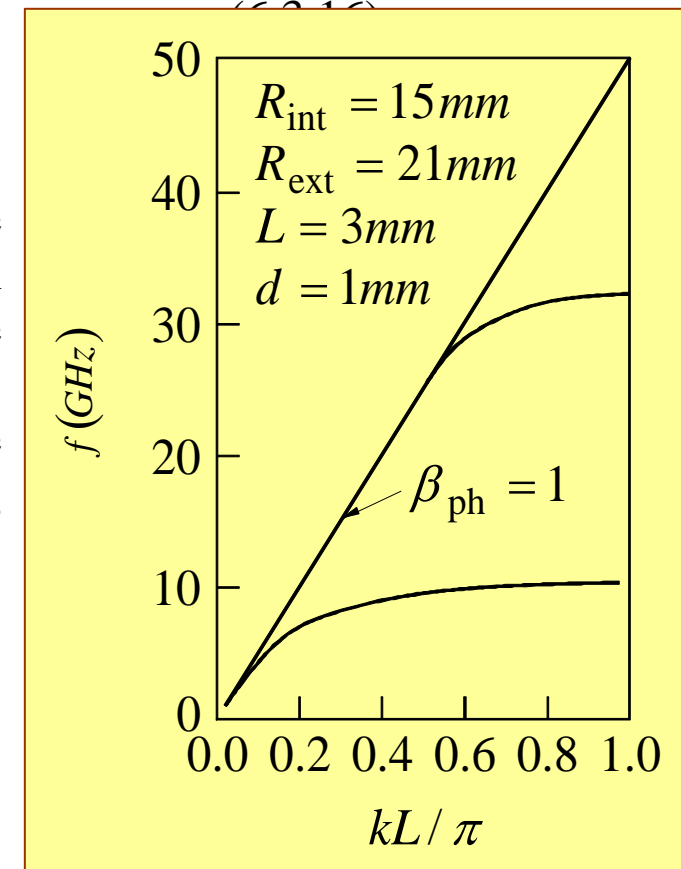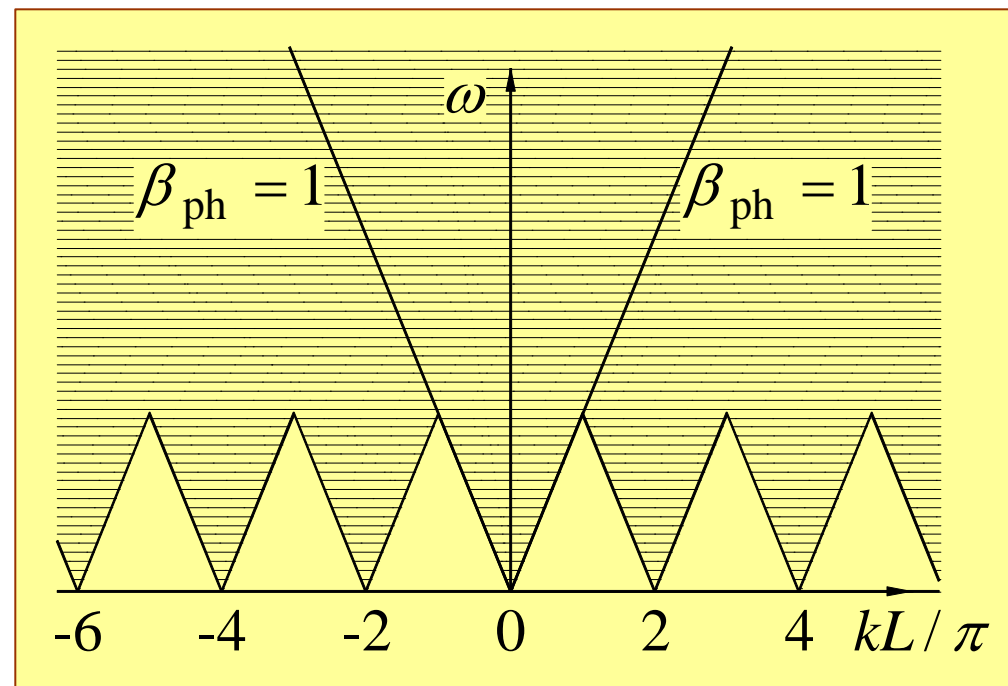
6.4 Transients

In order to illustrate the effect of the periodicity on the propagation of a wave packet we shall consider at $t = 0$ the same wavepacket $a(z)$, in vacuum and in a periodic structure. The propagation in vacuum will be represented by a dispersion relation $k^2 = \omega^2 / c^2$, therefore a scalar wave function $\Psi(z,t)$ is given by

$$\Psi(z,t) = \int_{-\infty}^{\infty} dk \psi(k) e^{-jkz} \frac{1}{2} \left[e^{jkct} + e^{-jkct} \right]. \tag{6.4.1}$$

Since at $t = 0$ this function equals $a(z)$, the amplitudes $\psi(k)$ can be readily determined using the inverse Fourier transform hence

$$\psi(k) = \frac{1}{2\pi} \int_{-\infty}^{\infty} dz a(z) e^{jkz}. \tag{6.4.2}$$

Substituting back into (4.1) we find that

$$\Psi(z,t) = \frac{1}{2} \left[a(z - ct) + a(z + ct) \right], \tag{6.4.3}$$

which basically indicates that the pulse moves at the speed of light in both directions and asymptotically, it preserves its shape. In a periodic structure the description of the wavepacket is complicated by the dispersion relation which in its lowest order approximation (e.g., first TM symmetric mode in a waveguide) can be expressed as

$$\omega(k) = \bar{\omega} - \delta\omega\cos(kL), \tag{6.4.4}$$

where $\bar{\omega} = (\omega_0 + \omega_\pi)/2$ is the average frequency between the low $(kL = 0)$ cut-off denoted by ω_0 and the high $(kL = \pi)$ cut-off denoted by ω_π. The quantity $\delta\omega = (\omega_\pi - \omega_0)/2$ is half the passband width and L is the period of the structure. Contrary to the previous case k here denotes the wavenumber in the first Brillouin zone. In the framework of this approximation we can use Floquet's representation to write

$$\Psi(z,t) = \mathrm{Re}\left[\sum_{n=-\infty}^{\infty} \int_{-\pi/L}^{\pi/L} dk \psi_n(k) e^{j\omega(k)t - jk_n z} \right], \tag{6.4.5}$$

where $k_n = k + 2\pi n/L$. The amplitudes $\psi_n(k)$ are determined by the value of the function at $t = 0$ hence

$$\psi_n(k) = 12\pi \int_{-\infty}^{\infty} dz a(z) e^{jk_n z}. \tag{6.4.6}$$

Substituting back into (6.4.5) we have

$$\Psi(z,t) = \mathrm{Re}\left[\frac{1}{2\pi} \int_{-\infty}^{\infty} d\zeta a(\zeta) \sum_{n=-\infty}^{\infty} \int_{-\pi/L}^{\pi/L} dk e^{jt[\bar{\omega} - \delta\omega\cos(kL)] - jk_n(z-\zeta)} \right]. \tag{6.4.7}$$

At this point we can take advantage of

$$e^{\frac{1}{2}\zeta(\tau - 1/\tau)} \equiv \sum_{\nu=-\infty}^{\infty} \tau^{\nu} J_{\nu}(\zeta), \tag{6.4.8}$$

and simplify the last equation to read

$$\Psi(z,t) = \text{Re}\left[\frac{1}{2\pi}\int_{-\infty}^{\infty}d\zeta a(\zeta)\sum_{n=-\infty}^{\infty}\int_{-\pi/L}^{\pi/L}dk e^{j\overline{\omega}t} \times \sum_{\nu=-\infty}^{\infty} J_{\nu}(\delta\omega t)e^{j(kL-\pi/2)\nu}e^{-jk_{n}(z-\zeta)}\right],$$

$$\tag{6.4.9}$$

which after the evaluation of the integrals and summation (over n) reads

$$\Psi(z,t) = \sum_{\nu=-\infty}^{\infty} a(z-\nu L)J_{\nu}(\delta\omega t)\cos(\overline{\omega}t - \pi\nu/2). \tag{6.4.10}$$

The figure illustrates the propagation of two wavepackets in vacuum (dashed line) and in a periodic structure. The latter is characterized by $\overline{\omega} = 2\pi \times 10$ GHz, $\delta\omega = \overline{\omega}/30$ and a spatial periodicity of $L = 1$ cm. At $t = 0$ the distribution is a Gaussian, $a(z) = \exp[-(z/L)^2]$. In each one of the frames $\Psi(z,t)$ was plotted at a different time as a function of z. Characteristic to all the frames is the relatively large peak following the front of the pulse.

It is evident that although the front of the pulse propagates at the speed of light (as in vacuum) the main pulse propagates slower. In fact, a substantial fraction of the energy remains at the origin even a long time after $t = 0$. For the parameters used, the amplitude of the signal at the origin $(z = 0)$ is dominated by the zero order Bessel function i.e., $J_0(\delta\omega t)$ therefore the energy is drained on a time scale which is determined by the asymptotic behavior of the Bessel function namely $\propto 1/\sqrt{\delta\omega t}$. Clearly the wider the passband the faster the energy is drained from the origin.
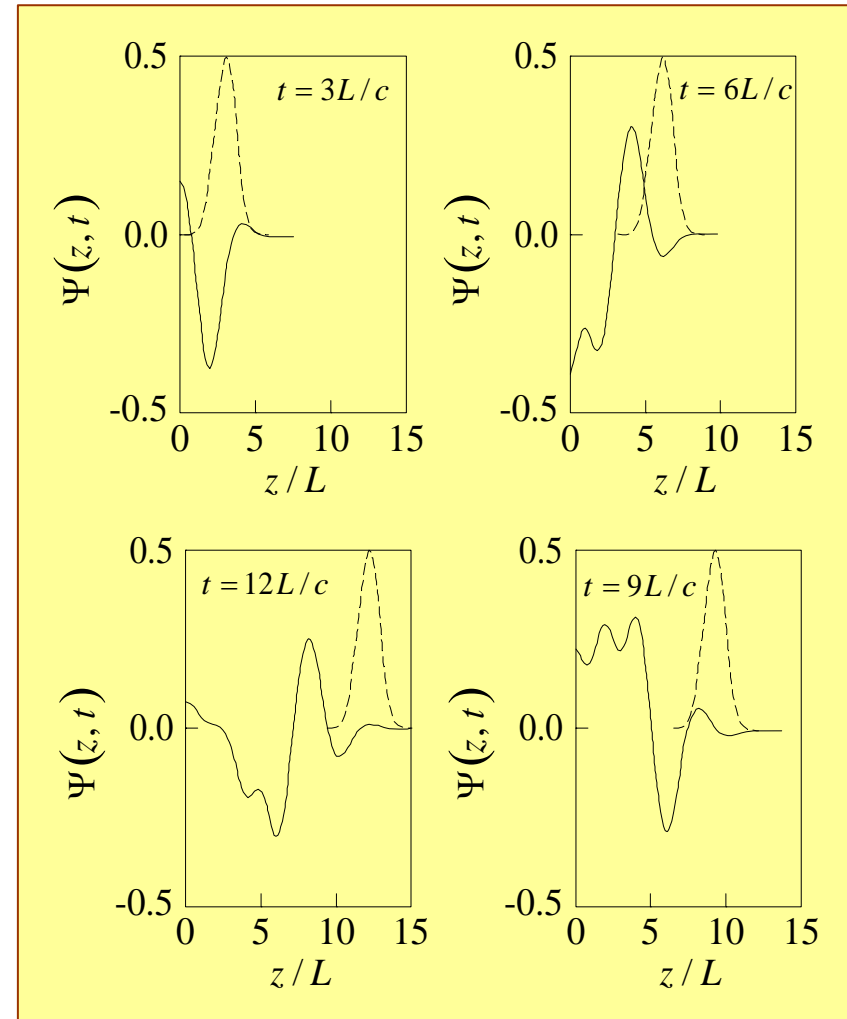
Exercise 6.1: Based on the solution for $A_z(r,z)$ in Section 6.1 determine the Floquet representation of the magnetic vector potential (TM_{01}). In other words write

$$A_z(r,z) = \text{J}_0\left(p_1\frac{r}{R}\right)\sum_n a_n(k)e^{-jk_n z}$$

and determine $a_n(k)$.

Exercise 6.2: Find all the waves which can propagate between $f = 0$ to 20 GHz, including asymmetric modes for the system described in Section 6.1. Repeat this exercise for the branches of the TE modes.

Exercise 6.3: Analyze the coupling of spatial harmonics for the system in Section 6.3 in a similar way as in Section 6.2.2.

Exercise 6.4: Repeat the calculation of the propagation of a transient in a periodic structure (Section 6.4) but this time for a TEM-like mode. [Hint: take $\omega = \omega_\pi \sim (kh)$.]

Chapter 7

Generation of radiation

Throughout these notes it was always assumed that somewhere there is a radiation source providing us with the necessary energy. In what follows we shall skim through the fundamentals of generation of radiation. Our discussion will be limited to ``vacuum'' devices, this is to say that the energy is extracted from free electrons in vacuum. Employed on medium ($<$1kW) and high ($>$1kW) power devices, the concepts to be discussed rely solely on energy and momentum conservation. Another very important family of devices relying on electrons moving in ``solid state'', will not be discussed here.

7.1 Single-Particle Interaction

On its own, an electron cannot transfer energy via a linear process to a monochromatic electromagnetic wave in vacuum if the interaction extends over a very long region. Non-linear processes may facilitate energy exchange in vacuum, but this kind of mechanism is rarely used since most systems require a linear response at the output. Therefore throughout this text we shall consider primarily linear processes and in this introductory chapter we shall limit the discussion to *single*-particle schemes. *Collective* effects, where the current is sufficiently high to affect the electromagnetic field, are also important but cannot be covered at this stage and they are the essence of a different course.

7.1.1 Infinite Length of Interaction

Far away from its source, in vacuum, an electromagnetic wave forms a plane wave which is characterized by a wavenumber whose magnitude equals the angular frequency, ω, of the source divided by $c = 299,792,458 \mathrm{m} s^{-1}$, the phase velocity of the plane wave in vacuum, and its direction of propagation is perpendicular to both the electric and magnetic field. For the sake of simplicity let us assume that such a wave propagates in the z direction and the component of the electric field is parallel to the x axis i.e.,

$$E_x(z,t) = E_0 \cos\left[\omega\left(t - \frac{z}{c}\right)\right]. \qquad (7.1.1)$$

If a charged particle moves at v parallel to z axis, then the electric field this charge experiences (neglecting the effect of the charge on the wave) is given by

$$E_x(z(t),t) = E_0 \cos\left[\omega\left(t - \frac{z(t)}{c}\right)\right]. \qquad (7.1.2)$$

A crude estimate for the particle's trajectory is

$$z(t) \simeq vt, \qquad (7.1.3)$$

therefore if the charge moves in the presence of this wave from $t \to -\infty$ to $t \to \infty$ then the average electric field it experiences is *zero*,

$$\int_{-\infty}^{\infty} dt \cos\left[\omega t\left(1 - \frac{v}{c}\right)\right] = 0, \qquad (7.1.4)$$

even if the particle is highly relativistic. The lack of interaction can be illustrated in a clearer way by superimposing the dispersion relation of the wave and the particle on the same diagram. Firstly, the relation between energy and momentum for an electron is given by

$$E = c\sqrt{p^2 + (mc)^2}, \qquad (7.1.5)$$

where $m = 9.1094 \times 10^{-31}$ Kg is the rest mass of the electron. Secondly, the corresponding

relation for a photon in free space is

$$E = cp. \tag{7.1.6}$$

For the interaction to take place the electron has to change its initial state, subscript i, denoted by (E_i, p_i) along the dispersion relation to the final, subscript f, denoted by (E_f, p_f) in such a way that the resulting photon in case of emission or absorbed photon for absorption, has exactly the same difference of energy and momentum i.e.,

$$E_i = E_f + E_{ph}, \tag{7.1.7}$$

and

$$p_i = p_f + p_{ph}. \tag{7.1.8}$$

In vacuum this is impossible, as can be shown by substituting (7.1.5)--(7.1.6) in (7.1.7)--(7.1.8). We can also reach the same conclusion by examining Fig. 1.1 The expression, $E = cp$, which describes the photon's dispersion relation, is parallel to the *asymptote* of the electron's dispersion relation. Thus, if we start from one point on the latter, a line parallel to $E = cp$ will never intersect (7.1.5) again. In other words, energy and momentum can not be conserved simultaneously in vacuum.

279
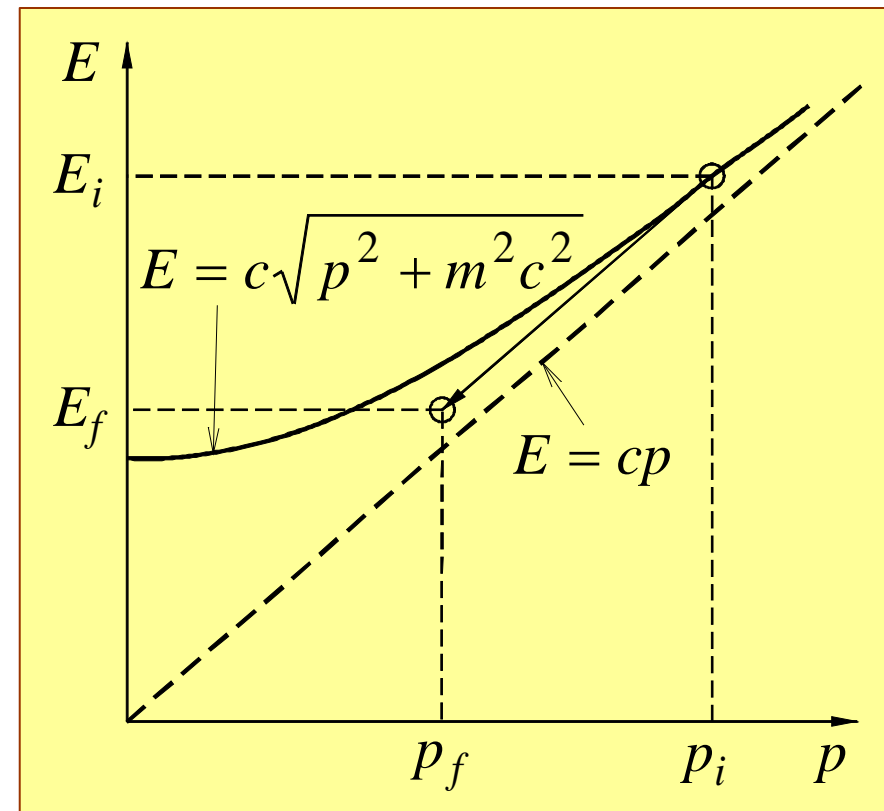
7.1.2 Finite Length of Interaction

If we go back to (7.1.4) we observe that if the electron spends only a finite time in the interaction region then it can experience a net electric field. Let us denote by $-T$ the time the electron enters the interaction region and by T the exit time. The average electric field experienced by the electron (subject to the same assumptions indicated above) is

$$\langle E \rangle = E_0 \frac{1}{2T} \int_{-T}^{T} dt \cos\left[\omega t \left(1 - vc\right)\right],$$

$$= E_0 \operatorname{sinc}\left[\omega T \left(1 - \frac{v}{c}\right)\right]; \qquad (7.1.9)$$

here $\operatorname{sinc}(x) = \sin(x)/x$. That is to say that if the time the electron spends in the interaction region, is small on the scale of the radiation period $T_0 = 2\pi/\omega$ then the net electric field it experiences, is not zero. From the perspective of the conservation laws, the interaction is possible since although the energy conservation remains unchanged i.e.,

$$E_i = E_f + \hbar\omega, \qquad (7.1.10)$$

the constraint on momentum conservation was released somewhat and it reads

$$|\,p_{\mathrm i} - p_{\mathrm f} - \hbar\frac{\omega}{c}\,| < \hbar c T, \qquad (7.1.11)$$

which clearly is less stringent than in (7.1.8) as also illustrated in the figure; $\hbar = 1.05457 \times 10^{-34}$ Jsec is the Planck constant. The operation of the klystron to be discussed subsequently relies on the interaction of an electron with a wave in a region which is shorter than the radiation wavelength.
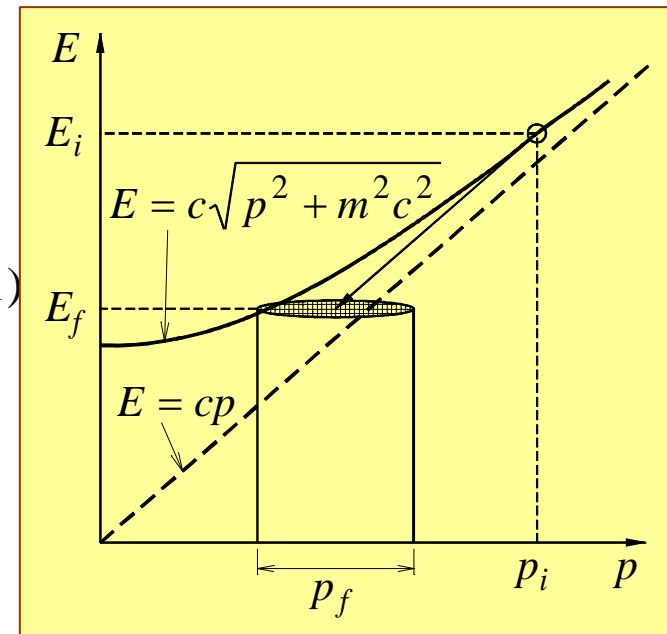
7.1.3 Finite Length Pulse

Another case where energy transfer is possible in vacuum is when the pulse duration is short. In order to examine this case we consider, instead of a periodic wave whose duration is infinite, a short pulse of a typical duration τ. In order to visualize the configuration, consider a field given by

$$E_x(z,t) = E_0 e^{-(t - z/c)^2/\tau^2}. \qquad (7.1.12)$$

A particle following the same trajectory as in (7.1.3) will clearly experience an average electric field which is non-zero even when the interaction duration is infinite. This is possible since the spectrum of the radiation field is broad -- in contrast to Sect. 7.1.1 where it was peaked -- therefore again the constraint of the conservation laws is less stringent:

281
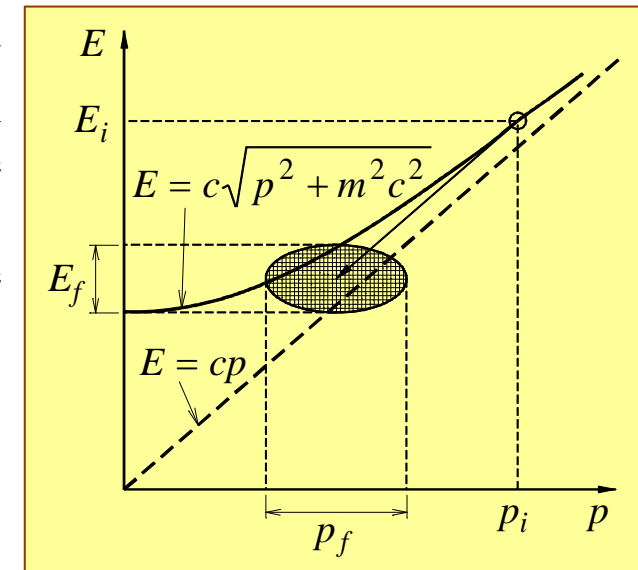
$$| E_{\mathrm{i}} - E_{\mathrm{f}} | < \frac{\hbar}{\tau}, \qquad (7.1.13)$$

and

$$| p_{\mathrm{i}} - p_{\mathrm{f}} | < \frac{\hbar}{c\tau}. \qquad (7.1.14)$$

Schematics of this mechanism is illustrated in the figure. It should be also pointed out that in this section we consider primarily the kinematics of the interaction and we pay no attention to the dynamics. In other words, we examined whether the conservation laws can be satisfied without details regarding the field configuration.

7.1.4 Cerenkov Interaction

It was previously indicated that since the dispersion relation of the photon is parallel to the asymptote of the electron's dispersion relation, the interaction is not possible in an infinite domain. However, it is possible to change the ``slope'' of the photon, namely to change its phase velocity -- see Figure. The easiest way to do so is by ``loading'' the medium where the wave propagates with a material whose dielectric coefficient is larger than one. Denoting the
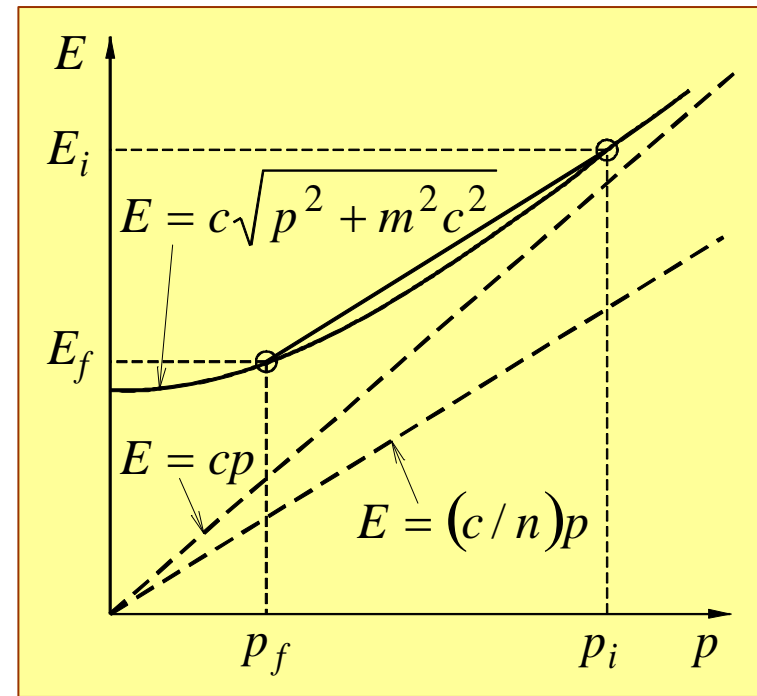
refraction coefficient by n, the dispersion relation of the photon is given by

$$E_{\mathrm{ph}} = \frac{c}{n} p_{\mathrm{ph}}, \qquad (7.1.15)$$

while the dispersion relation of the electron remains unchanged. Substituting in the expressions for the energy and the momentum conservation laws we find that the condition for the interaction to occur is

$$\frac{c}{n} = v, \qquad (7.1.16)$$

where it was assumed that the electron's recoil is relatively small i.e., $\hbar\omega / mc^2 \ll 1$. The result in (7.1.16) indicates that for the interaction to occur, the phase velocity of a plane wave in the medium has to equal the velocity of the particle. This is the so-called Cerenkov condition. Although dielectric loading is conceptually simple, it is not always practical because of electric charges which accumulate on the surface and of a relatively low breakdown threshold which is critical in high-power devices. For these reasons the phase velocity is typically slowed down using metallic structures with periodic boundaries. The operation of traveling wave tubes (or backward wave oscillators) relies on this concept.

7.1.5 Compton Scattering: Static Fields

It is not only a structure with periodic boundaries which facilitates the interaction between electrons and electromagnetic waves but also periodic fields. For example, if a magneto-static field of periodicity L is applied on the electron in the interaction region, then this field serves as a momentum ``reservoir'' which can supply momentum quanta of $n\hbar(2\pi/L)$ where $n = 0, \pm 1, \pm 2, ...$; see Figure. The energy conservation law remains unchanged i.e.,

$$E_i = E_f + E_{ph}, \tag{7.1.17}$$

but the momentum is balanced by the applied static field

$$p_i = p_f + p_{ph} + \hbar \frac{2\pi}{L} n. \tag{7.1.18}$$

For a relativistic particle ($\beta \simeq 1$) and when the electron's recoil is assumed to be small, these two expressions determine the so-called resonance condition which reads

$$\omega \simeq 2\gamma^2 \left(\frac{2\pi c}{L} n \right), \tag{7.1.19}$$

where $\gamma \equiv [1-(v/c)^2]^{-1/2}$. Note that the frequency of the emitted photon depends on the
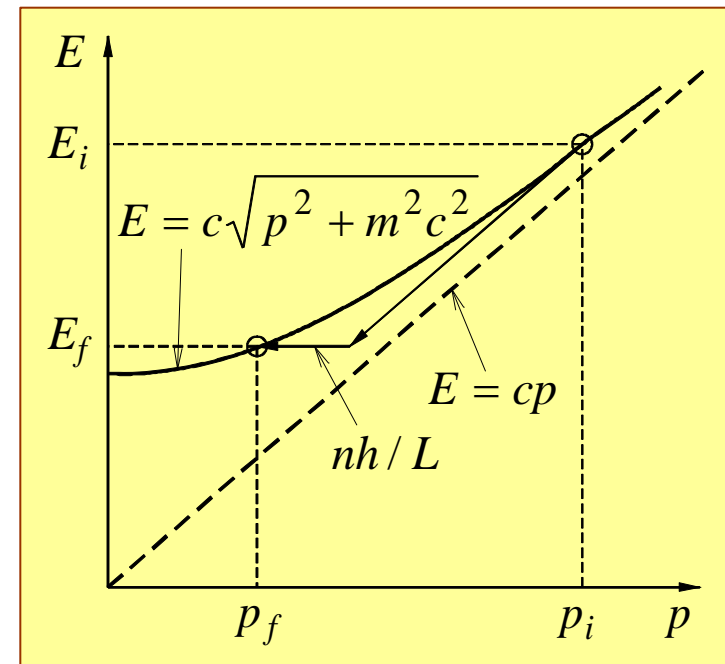
velocity of the electron which means that by varying the velocity we can change the operating frequency. A radiation source which possesses this feature is a tunable source. Identical result is achieved if we assume a periodic electrostatic field and both field configurations are employed in the so-called ``free electron lasers''.

7.1.6 Compton Scattering: Dynamic Fields

Static electric or magnetic field can be conceived as limiting cases of a dynamic field of zero or vanishingly small frequency and we indicated above that they facilitate the interaction between an electron and a wave. Consequently we may expect that the interaction of an electron with a wave will occur in the presence of another wave. Indeed, if we have an initial wave of frequency ω_1 and the emitted wave is at a frequency ω_2 the conservation laws read

$$E_{\mathrm{i}} + \hbar\omega_1 = E_{\mathrm{f}} + \hbar\omega_2, \tag{7.1.20}$$

and

$$p_{\mathrm{i}} = p_{\mathrm{f}} + \hbar\frac{\omega_1}{c} + \hbar\frac{\omega_2}{c}. \tag{7.1.21}$$

Following the same procedure as above we find that the ratio between the frequencies of the two waves is

$$\frac{\omega_2}{\omega_1} \simeq 4\gamma^2, \qquad\qquad (7.1.22)$$

which is by a factor of 2 larger than in the static case. The figure illustrates this process.
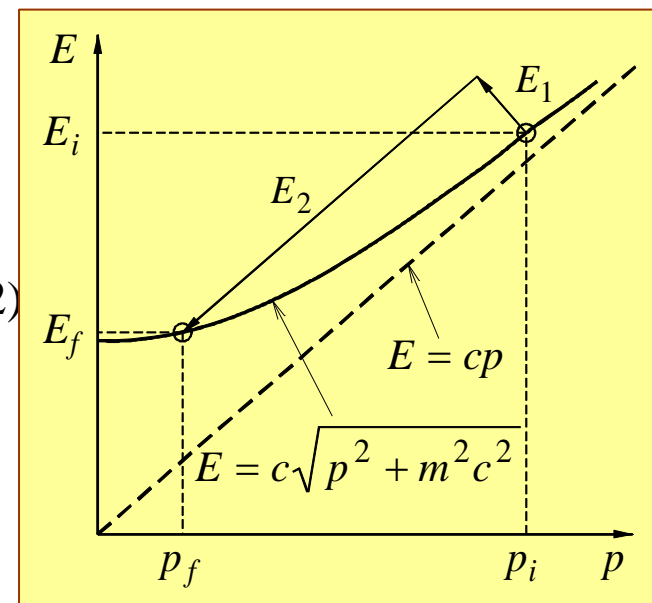
7.1.7 Uniform Magnetic Field

A periodic magnetic field can provide quanta of momentum necessary to satisfy the conservation law. It does not affect the average energy of the particle. An opposite situation occurs when the electron moves in a uniform magnetic field (B): there is no change in the momentum of the particle whereas its energy is given by

$$E = c\sqrt{p^2 + (mc)^2 - 2n\hbar e B}, \qquad\qquad (7.1.23)$$

where $e = 1.6022 \times 10^{-19}$ C is the charge of the electron and $n = 0, \pm 1, \pm 2....$

For most practical purposes the energy associated with the magnetic field is much smaller than the energy of the electron therefore we can approximate

$$E_{\mathrm{i}} - n_1 \hbar \frac{ec^2 B}{E_{\mathrm{i}}} = E_{\mathrm{f}} - n_2 \hbar \frac{ec^2 B}{E_{\mathrm{f}}} + E_{\mathrm{ph}}, \qquad (7.1.24)$$

and the momentum conservation remains unchanged i.e.,

$$p_{\mathrm{i}} = p_{\mathrm{f}} + p_{\mathrm{ph}}. \qquad (7.1.25)$$

From these two equations we find that the frequency of the emitted photon is

$$\omega = 2\gamma \frac{eB}{m} = 2\gamma^2 \left(\frac{eB}{m\gamma} \right). \qquad (7.1.26)$$

The figure on the right shows:

$$E = c\sqrt{p^2 + m^2 c^2 - 2neBh/2\pi}$$

with axes E and p, levels $n-1$, n, $n+1$, marked points E_i, E_f, p_f, p_i, and dashed line $E = cp$.

The last term is known as the relativistic cyclotron angular frequency, $\omega_{c,rel} \equiv eB/m\gamma$.

The figure illustrates schematically this type of interaction. It indicates that the dispersion line of the electron is split by the magnetic field in many lines (index n) and the interaction is possible since the electron can move from one line to another. Gyrotron's operation relies on this mechanism and it will be discussed briefly in the next section.

1.8 Synchronism Condition

All the processes in which the interaction of an electron with a monochromatic wave extends to large regions, have one thing in common: the velocity of the electron has to
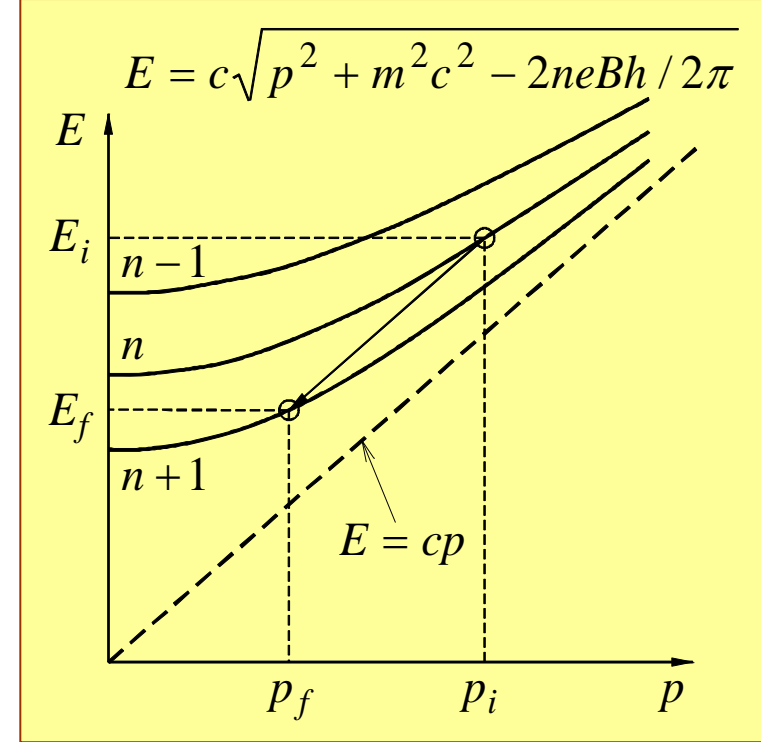
equal the *effective* phase velocity of the pondermotive wave along the electron's main trajectory, namely

$$v = v_{ph,eff}. \tag{7.1.27}$$

Here by pondermotive wave we mean the effective wave along the longitudinal trajectory of the particle which accounts for transverse or longitudinal oscillation. In the Cerenkov case we indicated that the phase velocity is c/n and there is no transverse motion therefore the condition for interaction implies $n = c/v$ where n is the refraction coefficient of the medium. In the presence of a periodic static field the wavenumber of the pondermotive wave is $\omega/c + 2\pi/L$ therefore

$$v_{ph,eff} = \frac{\omega}{\omega/c + 2\pi/L}, \tag{7.1.28}$$

and for a dynamic field

$$v_{ph,eff} = \frac{\omega_2 - \omega_1}{k_2 + k_1}, \tag{7.1.29}$$

where $k_{1,2} = \omega_{1,2}/c$ are the wavenumbers of the two waves involved. Finally, in a uniform magnetic field only the effective frequency varies

$$v_{ph,eff} = \frac{\omega - \omega_{c,rel}}{k}. \tag{7.1.30}$$

The reader can check now that within the framework of this formulation we obtain

(7.1.19) from (7.1.28), in the case of the dynamic field we have from (7.1.29) the $4\gamma^2$ term as in (7.1.22) and finally (7.1.30) leads to the gyrotron's operation frequency presented in (7.1.26).

7.2 Radiation Sources: Brief Overview

There are numerous types of radiation sources driven by electron beams. Our purpose in this section is to continue the general discussion from the previous section and briefly describe the operation principles of one ``member" of each class of what we consider the main classes of radiation sources. A few comments on experimental work will be made and for further details the reader is referred to recent review studies. The discussion continues with the classification of the major radiation sources according to several criteria which we found to be instructive.

7.2.1 The Klystron

The klystron was one of the first radiation sources to be developed. It is a device in which the interaction between the particle and the wave is localized to the close vicinity of a gap of a cavity, as illustrated in the Figure.
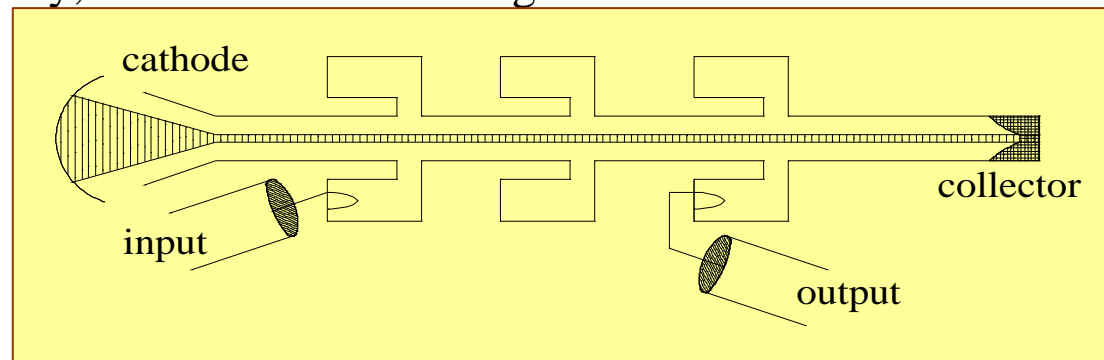
Electrons move along a drift tube and its geometry is chosen in such a way that at the frequency of interest it does not allow the electromagnetic wave to propagate. The latter is confined to cavities attached to the drift tube. The wave which feeds the first cavity modulates the velocity of the otherwise uniform beam. This means that after the cavity, half of the electrons have a velocity larger than the average beam velocity whereas the second half has a smaller velocity. According to the change in the (non-r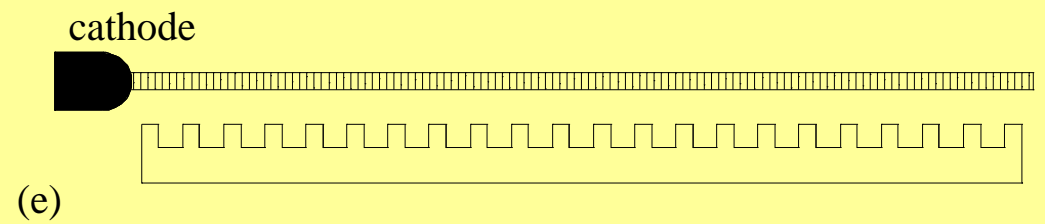elativistic) velocity of the electrons the beam becomes bunched down the stream since accelerated electrons from one period of the electromagnetic wave catch up with the slow electrons from the previous period. When this bunch enters the gap of another cavity it may generate radiation very efficiently. In practice, several intermediary cavities are necessary to achieve good modulation.

7.2.2 The Traveling Wave Tube

The traveling wave tube (TWT) is a Cerenkov device, namely the phase velocity of the interacting wave is smaller than c and the interaction is distributed along many wavelengths. Generally speaking, as the beam and the wave advance, the beam gets modulated by the electric field of the wave and in turn, the modulated beam increases the amplitude of the electric field. In this process both the beam modulation and the radiation field grow exponentially in space.

(a) cathode input output collector

(b) cathode input output output

(c) cathode input output

(d) cathode

(e) cathode
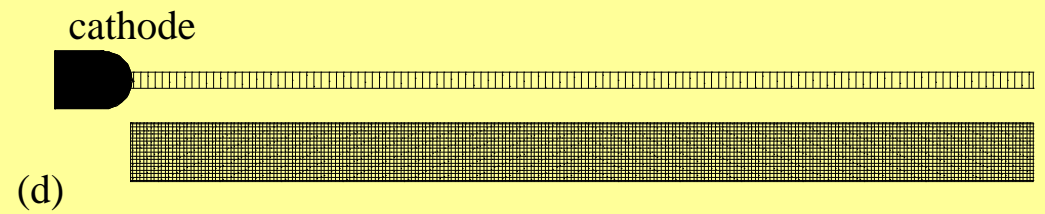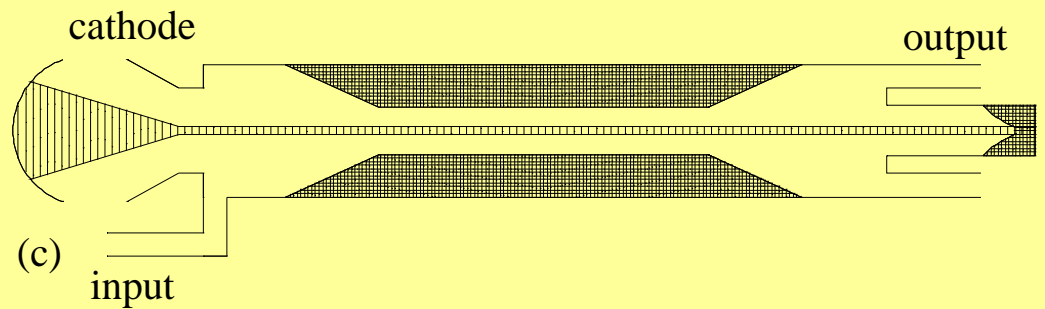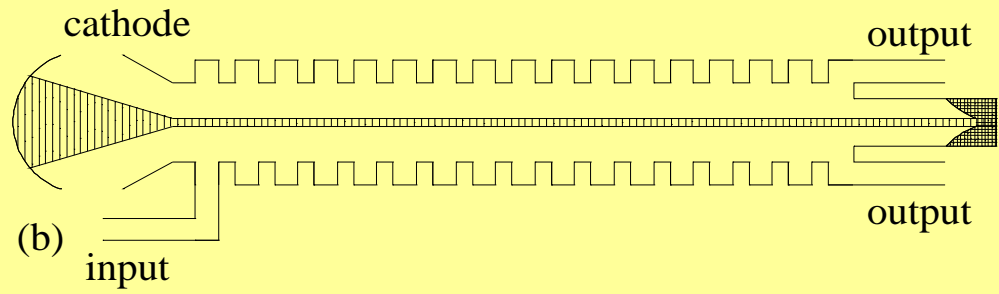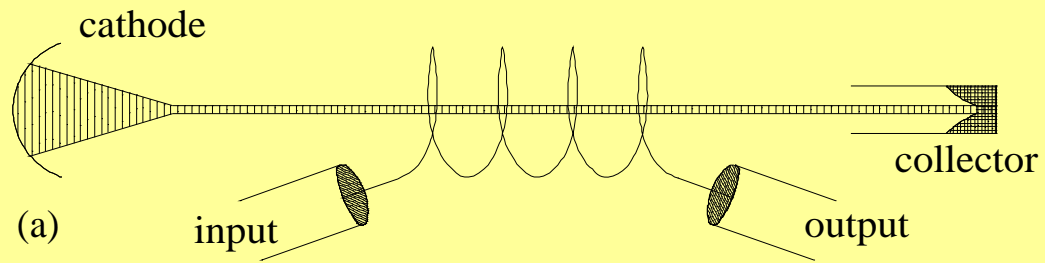
In the interaction process the electron oscillates primarily along the major axis (z direction) and the interaction is with the parallel component of the electric field. Correspondingly, the interaction occurs here with the transverse magnetic (TM) mode.

7.2.3 The Gyrotron

The gyrotron relies on the interaction between an annular beam, gyrating around the axis of symmetry due to an applied uniform magnetic field, and a transverse electric (TE) mode. The concept of generating coherent radiation from electrons gyrating in a magnetic field was proposed independently by three different researchers in the late fifties, and it has attracted substantial attention due to its potential to generate millimeter and submillimeter radiation.

In this device electrons move in the azimuthal direction and they get bunched by the corresponding azimuthal electric field. As in the case of the TWT the bunches act back on the field and amplify it. In contrast to traveling wave tubes or klystrons in which the beam typically interacts with the lowest mode, in the gyrotron the interaction is with high modes therefore various suppression techniques are employed in order to obtain coherent operation with a single mode.

The operation frequency is determined by the applied magnetic field, the energy of the electrons and, in cases of high mode operation, also by the radius of the waveguide:

$$\omega = \omega_c \gamma + \gamma \beta \sqrt{\omega_c^2 + \omega_{co}^2},$$ (7.2.1)

where $\beta = v/c$, $\omega_c = eB/m$ and ω_{co} is the cutoff frequency of the mode. The operating frequency in this case can reach very high values: for a magnetic field of 1T and $\gamma \simeq 2.5$ the operation frequency is of the order of 150 GHz or higher according to the mode with which the electrons interact.
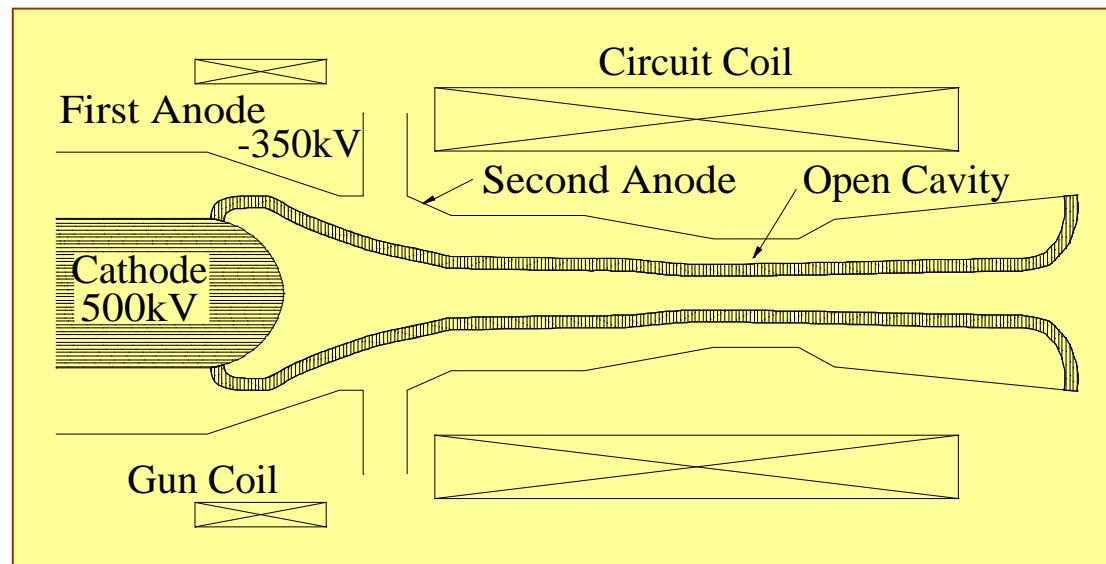
Since the interaction of the electrons is with an azimuthal electric field, it is necessary to provide the electrons with maximum momentum in this direction. The parameter which is used as a measure of the injected momentum is the ratio of the

transverse to longitudinal momentum $\alpha \equiv v_\perp / v_z$. This transverse motion is acquired by the electrons in the gun region as can be deduced from the schematics illustrated in the Figure. In relativistic devices this ratio is typically smaller than unity whereas in non-relativistic devices it can be somewhat larger than one.

Beam location is also very important. In the TWT case the interaction is with the lowest symmetric TM mode. Specifically the electrons usually form a pencil beam and they interact with the longitudinal electric field which has a maximum on axis. We indicated that gyrotrons operate with high TE modes and the higher the mode, the higher the number of nulls the azimuthal electric field has along the radial direction. Between each two nulls there is a peak value of this field. It is crucial to have the annular beam on one of these peaks for an efficient interaction to take place.

7.2.4 The Free Electron Laser

As the gyrotron, it is a fast-wave device in the sense that the interacting electromagnetic wave has a phase velocity larger or equal to c but instead of a uniform magnetic field it has a periodic magnetic field. The ``conventional'' free electron laser (FEL) has a magnetic field perpendicular to the main component of the beam velocity. As a result, the electrons undergo a helical motion which is suitable for interaction with either a TE or a TEM mode. The oscillation of electrons is in the transverse direction but the bunching is longitudinal and in this last regard the process is similar to the one in the

traveling wave tube. However, its major advantage is the fact that it does not require a metallic (or other type of) structure for the interaction to take place. Consequently, it has the potential to either generate very high power at which the contact of radiation with metallic walls would create very serious problems, or produce radiation at UV, XUV or X-ray where there are no other coherent radiation sources. The Figure illustrates the basic configuration.
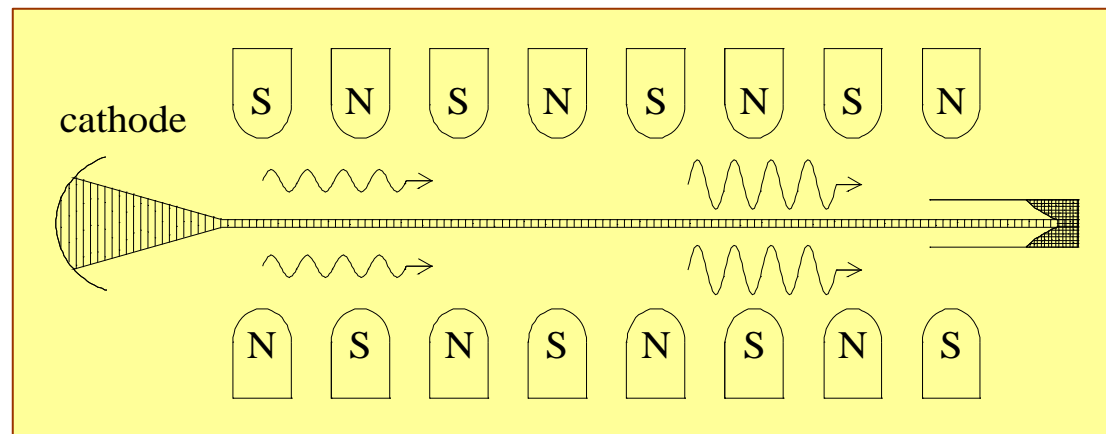
7.2.5 The Magnetron

The magnetron was invented at the beginning of the 20th century but because of its complexity there is no analytical model, as yet, which can describe its operation adequately as a whole. In recent years great progress has been made in the understanding of the various processes with the aid of particle in cell (PIC) codes. Its operation combines potential and kinetic energy conversion. The Figure illustrates the basic configuration. Electrons are generated on the cathode (inner surface) and since a perpendicular magnetic field is applied they form a flow which rotates azimuthally. The magnetic field and the voltage applied on the anode are chosen in such a way that, in equilibrium, the average velocity of the electrons equals the phase velocity of the wave supported by the periodic structure at the frequency of interest.

A simplistic picture of the interaction can be conceived in the following way: electrons which lose energy to the wave via the Cerenkov type interaction, move in upward trajectories -- closer to the anode. Consequently, two processes occur. Firstly, the closer the electron is to the periodic surface the stronger the radiation field and therefore
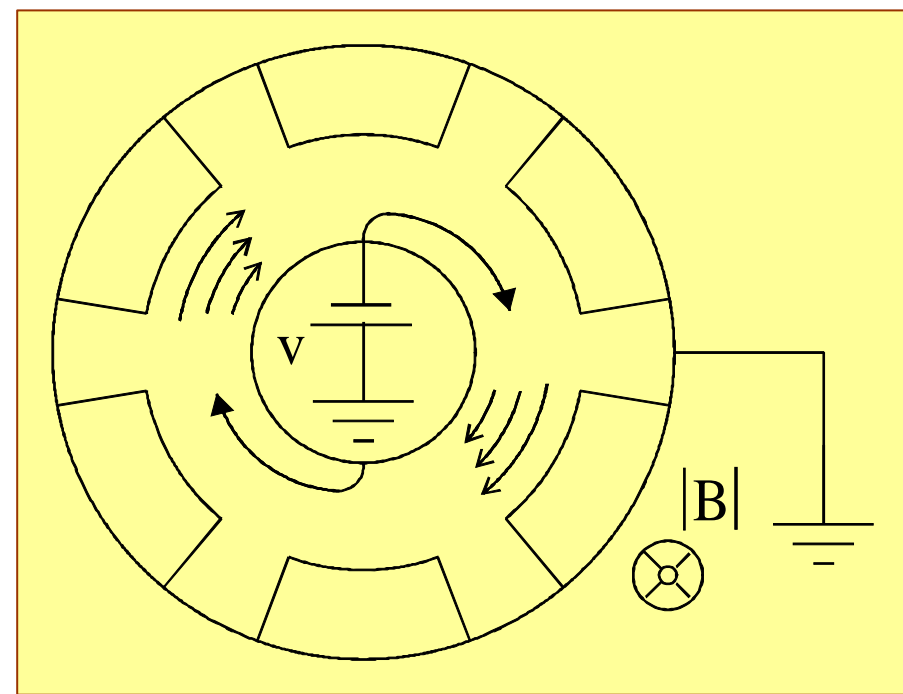
the deceleration is larger, causing a further motion upwards. Secondly, as it moves upwards its (dc) potential energy varies. Again, this is converted into electromagnetic energy.

Two major differences between the magnetron and other radiation sources mentioned above, are evident: *(i)* in the magnetron the beam generation, acceleration and collection occur all in the same region where the interaction takes place. *(ii)* The potential energy associated with the presence of the charge in the gap plays an important role in the interaction; the other device where this is important is the vircator which will be briefly discussed next.

7.3 Generation of radiation in a waveguide

In this subsection we consider the electromagnetic field associated with the symmetric transverse magnetic (TM) mode in a dielectric filled waveguide. As in the previous subsection, the source of thiss field is a particle moving at a velocity v_0, however, the main difference is that the solution has a constraint since on the waveguide's wall ($r = R$) the tangential electric field vanishes. Therefore, we shall calculate the Green function in the frequency domain subject to the condition $G(r = R, z \,|\, r', z') = 0$. We assume a solution of the form

$$G(r, z \,|\, r', z') = \sum_{s=1}^{\infty} G_s(z \,|\, r', z') \mathrm{J}_0 \left(p_s \frac{r}{R} \right), \qquad (7.3.1)$$

substitute in (2.4.11) and use the orthogonality of the Bessel functions we find that

$$G_s(z \,|\, r', z') = \mathrm{J}_0 \left(p_s \frac{r'}{R} \right) \frac{1}{\dfrac{1}{2} R^2 \mathrm{J}_1^2(p_s)} g_s(z \,|\, z'), \qquad (7.3.2)$$

where $g_s(z \,|\, z')$ satisfies

$$\left[\frac{d^2}{dz^2} - \Gamma_s^2 \right] g_s(z \,|\, z') = -\frac{1}{2\pi} \delta(z - z'), \qquad (7.3.3)$$

and

299

$$\Gamma_s^2 = \frac{p_s^2}{R^2} - \varepsilon_r \frac{\omega^2}{c^2}. \tag{7.3.4}$$

For $z > z'$ the solution of (7.3.3) is

$$g_s(z \mid z') = A_+ e^{-\Gamma_s(z-z')}, \tag{7.3.5}$$

and for $z < z'$ the solution is

$$g_s(z \mid z') = A_- e^{\Gamma_s(z-z')}. \tag{7.3.6}$$

Green's function is continuous at $z = z'$ i.e.,

$$A_+ = A_-, \tag{7.3.7}$$

and its first derivative is discontinuous. The discontinuity is determined by integrating (7.3.3)from $z = z' - 0$ to $z = z' + 0$ i.e.,

$$\left[\frac{d}{dz} g_s(z \mid z') \right]_{z=z'+0} - \left[\frac{d}{dz} g_s(z \mid z') \right]_{z=z'-0} = -\frac{1}{2\pi}. \tag{7.3.8}$$

Substituting the two solutions introduced above, and using (7.3.7)we obtain

$$g_s(z \mid z') = \frac{1}{4\pi\Gamma_s} e^{-\Gamma_s |z-z'|}. \tag{7.3.9}$$

Finally, the explicit expression for the Green's function corresponding to azimuthally symmetric TM modes in a circular waveguide is given by

$$G(r,z\,|\,r^{'},z^{'}) = \sum_{s=1}^{\infty} \frac{J_0(p_s r / R)J_0(p_s r^{'} / R)}{\frac{1}{2}R^2 J_1^2(p_s)}\frac{1}{4\pi\Gamma_s}e^{-\Gamma_s|z-z^{'}|}. \tag{7.3.10}$$

In this expression it was tacitly assumed that $\omega > 0$ and Γ_s [defined in (7.3.4)] is non-zero.

With Green's function established, we can calculate the magnetic vector potential as generated by the current distribution described in (2.4.10); the result is

$$A_z(r,z,\omega) = 2\pi\mu_0 \int_0^R dr\, r \int_{-\infty}^{\infty} dz^{'} G(r,z\,|\,r^{'},z^{'})J_z(r^{'},z^{'})$$

$$= -\frac{e\mu_0}{8\pi^2}\sum_{s=1}^{\infty}\frac{J_0(p_s r / R)}{\frac{1}{2}R^2 J_1^2(p_s)}\frac{2}{\Gamma_s^2 + \omega^2 / v_0^2}e^{-j(\omega/v_0)z}. \tag{7.3.11}$$

It will be instructive to examine this expression in the time domain; the Fourier transform is

$$A_z(r,z,t) = -\frac{e}{2\pi^2\varepsilon_0 R^2}\frac{\beta^2}{1-n^2\beta^2}$$

$$\times \sum_{s=1}^{\infty}\frac{J_0(p_s r / R)}{J_1^2(p_s)}\int_{-\infty}^{\infty}d\omega\frac{e^{j\omega(t-z/v_0)}}{\omega^2 + \Omega_s^2}, \tag{7.3.12}$$

where

$$\Omega_s^2 = \left(\frac{p_s c}{R}\right)^2 \frac{\beta^2}{1 - n^2 \beta^2}. \tag{7.3.13}$$

The problem has been now simplified to the evaluation of the integral

$$F_s(\tau = t - z/v_0) \equiv \int_{-\infty}^{\infty} d\omega \frac{e^{j\omega\tau}}{\omega^2 + \Omega_s^2}, \tag{7.3.14}$$

which in turn is equivalent to the solution of the following differential equation

$$\left[\frac{d^2}{d\tau^2} - \Omega_s^2\right] F_s(\tau) = -2\pi\delta(\tau). \tag{2.4.39}$$

If the particle's velocity is smaller than the phase velocity of a plane wave in the medium ($n\beta < 1$) then $\Omega_s^2 > 0$ and the solution for $\tau > 0$ is

$$F_s(\tau > 0) = A_+ e^{-\Omega_s \tau}, \tag{7.3.15}$$

or

$$F_s(\tau < 0) = A_- e^{\Omega_s \tau}. \tag{7.3.16}$$

As previously, in the case of Green's function, $F_s(\tau)$ has to be continuous at $\tau = 0$ and its derivative is discontinuous:

$$\left(\frac{d}{d\tau}F_s(\tau)\right)_{\tau=0^+} - \left(\frac{d}{d\tau}F_s(\tau)\right)_{\tau=0^-} = -2\pi. \tag{7.3.17}$$

When the velocity of the particle is smaller than c/n (i.e., $n\beta < 1$) the characteristic frequency Ω_s is real, therefore

$$F_s(\tau) = \frac{\pi}{\Omega_s} e^{-\Omega_s|\tau|}, \tag{7.3.18}$$

and

$$A_z(r,z,t) = -\frac{e}{2\pi\varepsilon_0 R^2} \frac{\beta^2}{1-\beta^2 n^2} \sum_{s=1}^{\infty} \frac{J_0(p_s r/R)}{J_1^2(p_s)\Omega_s} e^{-\Omega_s|t-z/v_0|}. \tag{7.3.19}$$

This expression represents a superposition of evanescent modes attached to the particle. It is important to emphasize that since the phase velocity of a plane wave in the medium is larger than the velocity of the particle there is an electromagnetic field in front ($\tau < 0$) of the particle. The situation is different in the opposite case, $\beta > 1/n$, since $\Omega_s^2 < 0$. In this case the waves are slower than the particle and there is no electromagnetic field in front of the particle i.e.,

$$F_s(\tau < 0) = 0. \tag{7.3.20}$$

By virtue of the continuity at $\tau = 0$ we have for $\tau > 0$

$$F_s(\tau > 0) = A_+ \sin\left(|\Omega_s|\tau\right). \tag{7.3.21}$$

Substituting these two expressions in (2.4.42) we obtain

$$F_s(\tau) = -\frac{2\pi}{|\Omega_s|}\sin\left(|\Omega_s|\tau\right)h(\tau),$$ (7.3.22)

and the magnetic vector potential reads

$$A_z(r,z,t) = -\frac{e}{\pi\varepsilon_0 R^2}\frac{\beta^2}{n^2\beta^2-1}$$

$$\times\sum_{s=1}\frac{J_0(p_s r/R)}{J_1^2(p_s)|\Omega_s|}\sin\left[|\Omega_s|\left(t-\frac{z}{v_0}\right)\right]h\left(t-\frac{z}{v_0}\right),$$ (7.3.23)

where $h(\xi)$ is the Heaviside step function. This expression indicates that when the velocity of the particle is larger than c/n, there is an entire superposition of *propagating* waves traveling behind the particle. Furthermore, all the waves have the same phase velocity which is identical with the velocity of the particle, v_0. It is important to bear in mind that this result was obtained after tacitly assuming that ε_r is frequency independent which generally is not the case, therefore the summation is limited to a finite number of modes. The modes which contribute are determined by the Cerenkov condition $n(\omega = \Omega_s)\beta > 1$.

After we established the magnetic vector potential, let us now calculate the average power which trails behind the particle. Firstly, the azimuthal magnetic field is given by

$$H_\varphi(r,z,t) = -\frac{1}{\mu_0}\frac{\partial}{\partial r}A_z(r,z,t)$$

$$= \frac{1}{\mu_0}\sum_{s=1}A_s\frac{p_s}{R}\mathrm{J}_1\left(p_s\frac{r}{R}\right)$$

$$\times\sin\left[|\Omega_s|\left(t-\frac{z}{v_0}\right)\right]h\left(t-\frac{z}{v_0}\right), \tag{7.3.24}$$

where

$$A_s = -\frac{e}{\pi\varepsilon_0 R^2}\frac{\beta^2}{n^2\beta^2-1}\frac{1}{\mathrm{J}_1^2(p_s)|\Omega_s|}. \tag{7.3.25}$$

Secondly, the radial electric field is determined by the electric scalar potential which in turn is calculated using the Lorentz gauge and it reads

$$E_r(r,z,t) = -\frac{\partial}{\partial r}\Phi(r,z,t)$$

$$= \frac{c^2}{\varepsilon_r v_0}\sum_{s=1} A_s \frac{p_s}{R}\mathrm{J}_1\!\left(p_s\frac{r}{R}\right)$$

$$\times \sin\!\left[|\Omega_s|\left(t-\frac{z}{v_0}\right)\right] h\!\left(t-\frac{z}{v_0}\right). \qquad (7.3.26)$$

With these expressions we can calculate the average electromagnetic power trailing the particle. It is given by

$$P = \frac{e^2\beta c}{2\pi\varepsilon_0\varepsilon_r R^2}\frac{1}{\varepsilon_r\beta^2-1}\sum_{s=1}\frac{1}{\mathrm{J}_1^2(p_s)}. \qquad (7.3.27)$$

Note that for ultra relativistic particle ($\beta \to 1$) the power is independent of the particle's energy. In order to have a measure of the radiation emitted consider a very narrow bunch of $N \sim 10^{11}$ electrons injected in a waveguide whose radius is 9.2 mm. The waveguide is filled with a material whose dielectric coefficient is $\varepsilon_r\,\overline{2}.6$ and all electrons have the same energy 450 keV. If we were able to keep their velocity constant, then 23 MW of power at 11.4 GHz (first mode, $s=1$) will trail the bunch. Further examining this expression we note that the average power is quadratic with the frequency i.e.,

$$P \equiv \sum_{s=1} P_s = \frac{(Ne)^2}{2\pi\varepsilon_0\varepsilon_r\beta c} \sum_{s=1} \frac{|\Omega_s|^2}{[p_s J_1(p_s)]^2}. \tag{7.3.28}$$

In addition, based on the definition of the Fourier transform of the current density in (2.4.10), we conclude that the current which this macro-particle excites in the sth mode is $I_s \overline{e} N \Omega_s / 2\pi$. With this expression, the radiation impedance of the first mode ($s = 1$) is

$$R_{C,1} = \frac{P_1}{\frac{1}{2}|I_1|^2} = \eta_0 \frac{4\pi}{\varepsilon_r \beta [p_1 J_1(p_1)]^2}. \tag{7.3.29}$$

For a relativistic particle, $\beta \simeq 1$, a dielectric medium $\varepsilon_r = 2.6$ the radiation impedance corresponding to the first mode is $\simeq 1200\Omega$ which is one order of magnitude larger than that of a dipole in free space or between two plates. Note that this impedance is independent of the geometry of the waveguide and for an ultra-relativistic particle it is independent of the particle's energy.

7.4 Generation of radiation in a cavity

In order to examine transient phenomena associated with reflected waves we shall calculate the electromagnetic energy in a cavity as a single (point) charge traverses the structure. Consider a lossless cylindrical cavity of radius R and length d. A charged particle (e) moves along the axis at a constant velocity v_0. Consequently, the longitudinal component of the current density is the only non-zero term, thus

$$J_z(\mathbf{r},t) = -ev_0 \frac{1}{2\pi r} \delta(r)\delta(z - v_0 t). \tag{7.4.1}$$

It excites the longitudinal magnetic vector potential $A_z(\mathbf{r},t)$ which for an azimuthally symmetric system satisfies

$$\left[\frac{1}{r}\frac{\partial}{\partial r} r \frac{1}{\partial r} + \frac{\partial^2}{\partial z^2} - \frac{1}{c^2}\frac{\partial^2}{\partial t^2} \right] A_z(r,z,t) = -\mu_0 J_z(r,z,t). \tag{7.4.2}$$

In this section we shall consider only the internal problem, ignoring the electromagnetic phenomena outside the cavity. The boundary conditions on the internal walls of the cavity impose that $E_z(r = R, z, t) = 0$, $E_r(r, z = 0, t) = 0$ and $E_r(r, z = d, t) = 0$ therefore the magnetic vector potential reads

$$A_z(r,z,t) = \sum_{s=1,n=0}^{\infty} A_{s,n}(t) \mathrm{J}_0\left(p_s \frac{r}{R} \right) \cos\left(\frac{\pi n}{d} z \right). \tag{7.4.3}$$

Using the orthogonality of the trigonometric and Bessel functions we find that the amplitude $A_{s,n}(t)$ satisfies

$$\left[\frac{d^2}{dt^2}+\Omega_{s,n}^2\right]A_{s,n}(t)=-\frac{ev_0}{2\pi\varepsilon_0}\frac{1}{\frac{1}{2}R^2J_1^2(p_s)}\frac{1}{g_nd}$$

$$\times\cos\left(\frac{\pi n}{d}v_0t\right)\left[h(t)-h\left(t-\frac{v_0}{d}\right)\right],\tag{7.4.4}$$

where

$$g_n\begin{cases}1 & \text{for } n=0,\\0.5 & \text{otherwise,}\end{cases}\tag{7.4.5}$$

and

$$\Omega_{s,n}=c\sqrt{\left(\frac{p_s}{R}\right)^2+\left(\frac{\pi n}{d}\right)^2},\tag{7.4.6}$$

are the eigen-frequencies of the cavity. Before the particle enters the cavity ($t<0$), no field exists, therefore

$$A_{s,n}(t<0)=0.\tag{7.4.7}$$

For the time the particle is in the cavity namely, $0<t<d/v_0$, the solution of (7.4.4)

consists of the homogeneous and the excitation term:

$$A_{s,n}\left(0 < t < \frac{d}{v_0}\right) = B_1 \cos(\Omega_{s,n}t)B_2 \sin(\Omega_{s,n}t)$$

$$+\alpha_{s,n} \cos(\omega_n t), \tag{7.4.8}$$

where

$$\alpha_{s,n} = -\frac{ev_0}{2\pi\varepsilon_0} \frac{1}{\frac{1}{2}R^2 J_1^2(p_s)} \frac{1}{g_n d} \frac{1}{\Omega_{s,n}^2 - \omega_n^2}, \tag{7.4.9}$$

and

$$\omega_n = \frac{\pi n}{d} v_0. \tag{7.4.10}$$

Since both the magnetic and the electric field are zero at $t = 0$, the function $A_{s,n}(t)$ and its first derivative are zero at $t = 0$ hence

$$B_1 \alpha_{s,n} = 0, \tag{7.4.11}$$

and

$$B_2 = 0. \tag{7.4.12}$$

Consequently, the amplitude of the magnetic vector potential $[A_{s,n}(t)]$ reads

$$A_{s,n}(t) = \alpha_{s,n}\left[\cos(\omega_n t) - \cos(\Omega_{s,n}t)\right]. \tag{7.4.13}$$

Beyond $t = d / v_0$, the particle is out of the structure thus the source term in (7.4.4) is zero and the solution reads

$$A_{s,n}\left(t > \frac{d}{v_0}\right) = C_1 \cos\left[\Omega_{s,n}\left(t - \frac{d}{v_0}\right)\right]$$

$$+ C_2 \sin\left[\Omega_{s,n}\left(t - \frac{d}{v_0}\right)\right]. \tag{7.4.14}$$

As in the previous case, at $t = d / v_0$ both $A_{s,n}(t > d / v_0)$ and its derivative, have to be continuous:

$$\alpha_{s,n}\left[(-1)^n - \cos\left(\Omega_{s,n}\frac{d}{v_0}\right)\right] = C_1, \tag{7.4.15}$$

$$\alpha_{s,n}\Omega_{s,n}\sin\left(\Omega_{s,n}\frac{d}{v_0}\right) = C_2\Omega_{s,n}. \tag{7.4.16}$$

For this time period, the explicit expression for the magnetic vector potential is

$$A_{s,n}\left(t > \frac{d}{v_0}\right) = \alpha_{s,n}\left[(-1)^n - \cos\left(\Omega_{s,n}\frac{d}{v_0}\right)\right]\cos\left[\Omega_{s,n}\left(t - \frac{d}{v_0}\right)\right]$$

$$+\alpha_{s,n}\sin\left(\Omega_{s,n}dv_0\right)\sin\left[\Omega_{s,n}\left(t - \frac{d}{v_0}\right)\right], \qquad (7.4.17)$$

The expressions in (7.4.7), (7.4.13), (7.4.17) describe the magnetic vector potential in the cavity at all times. The Figure illustrates schematically this solution.

During the period the electron spends in the cavity, there are two frequencies which are excited: the eigen-frequency of the cavity $\Omega_{s,n}$ and the ``resonances'' associated with the motion of the particle, ω_n. The latter set corresponds to the case when the phase velocity, $v_{ph}\bar{\omega}/k$, equals the velocity v_0. Since the boundary conditions impose $k\bar{\pi}n/d$ and the resonance implies

$$v_0 = v_{ph} = c\left(\frac{\omega^2}{c^2}\frac{d}{\pi n}\right),$$
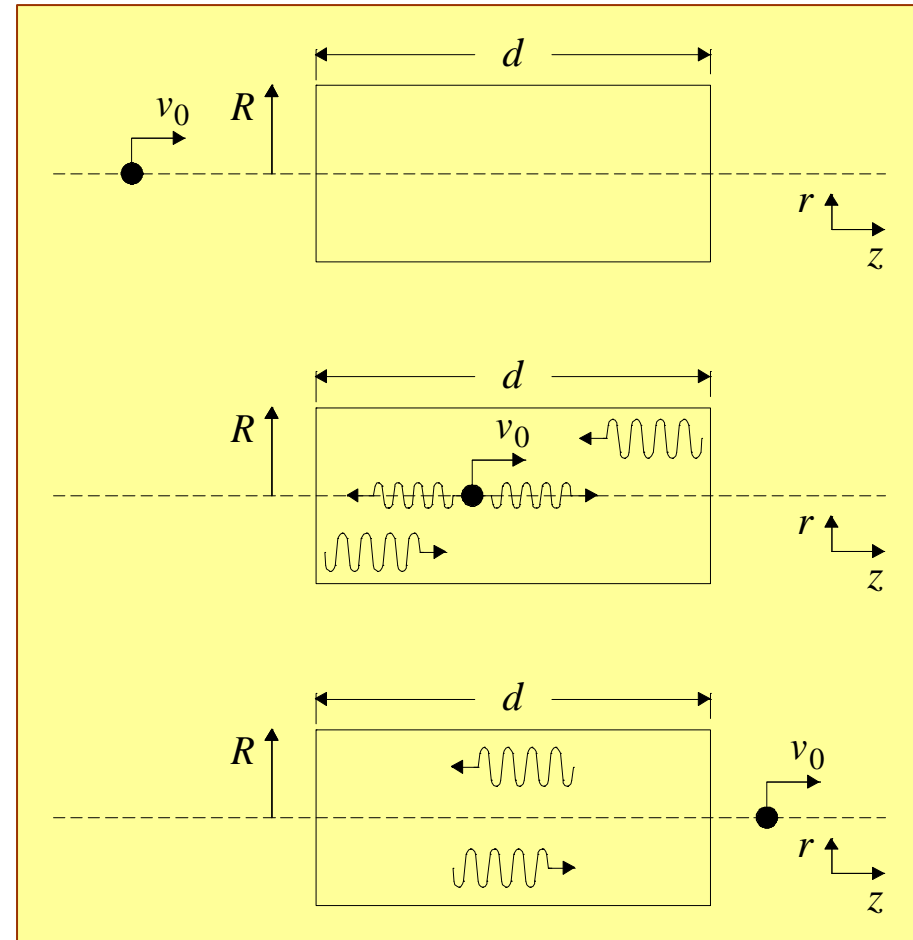
thus we can immediately deduce the resonance frequencies ω_n as given in (7.4.10).

Now that the magnetic vector potential has been determined, we consider the effect of the field generated in the cavity on the moving particle. The relevant component is

$$A_z\left(r,z,0<t<\frac{d}{v_0}\right)=\sum_{s=1,n=0}\alpha_{s,n}\mathrm{J}_0\left(p_s\frac{r}{R}\right)\times\cos\left(\frac{\pi}{nd}z\right)\left[\cos\left(\omega_n t\right)-\cos(\Omega_{s,n}t)\right].\quad(7.4.19)$$

Note that the upper limit in the double summation was omitted since in practice this limit is determined by the actual dimensions of the particle, which so far was considered infinitesimally small. In order to quantify this statement we realize that the summation is over all eigenmodes which have a wavenumber much longer than the particle's dimension i.e., $\Omega_{s,n}R_{\mathrm{b}}/c<1$.

According to Maxwell's equations, the longitudinal electric field is

$$\varepsilon_0\frac{\partial}{\partial t}E_z(\mathbf{r},t)=-J_z(\mathbf{r},t)+\frac{1}{r}\frac{\partial}{\partial r}rH_\varphi(\mathbf{r},t).\qquad(7.4.20)$$

Furthermore, the field which acts on the particle does not include the self field, therefore we omit the current density term. Using the expression for the magnetic vector potential [(2.1.36)], we have

$$E_z(\mathbf{r},t)=-c^2\int dt\frac{1}{r}\frac{\partial}{\partial r}r\frac{\partial}{\partial r}A_z(\mathbf{r},t),\qquad(7.4.21)$$

or explicitly,

$$E_z\left(r,z,0<t<\frac{d}{v_0}\right)=\sum_{s=1,n=0}\alpha_{s,n}\left(\frac{cp_s}{R}\right)^2 \mathrm{J}_0\left(p_s\frac{r}{R}\right)\times\cos(\frac{\pi n}{d}z)\left[\frac{\sin(\omega_n t)}{\omega_n}-\frac{\sin(\Omega_{s,n}t)}{\Omega_{s,n}}\right].$$

$$\text{(7.4.22)}$$

In a lossless and closed cavity the total power flow is zero, therefore Poynting's theorem in its integral form reads

$$\frac{dW}{dt}=-2\pi\int_0^R dr\,r\int_0^d dz E_z(r,z,t)\mathrm{J}_z(r,z,t).$$

$$\text{(7.4.23)}$$

Thus substituting the current density [(7.4.1)] we obtain

$$W=ev_0\int_0^{d/v_0}dt E_z(r,z=v_0 t,t),$$

$$\text{(7.4.24)}$$

which has the following explicit form

$$W=ev_0\sum_{s=1,n=0}\alpha_{s,n}\left(\frac{cp_s}{R}\right)^2\int_0^{d/v_0}dt\cos(\omega_n t)\times\left[\frac{\sin(\omega_n t)}{\omega_n}-\frac{\sin(\Omega_{s,n}t)}{\Omega_{s,n}}\right].$$

$$\text{(7.4.25)}$$

The time integral in this expression can be evaluated analytically. As can be readily deduced, the first term represents the non-homogeneous part of the solution and its contribution is identically zero whereas the second's reads

$$W=-ev_0\sum_{s=1,n=0}\alpha_{s,n}\left(\frac{cp_s}{R}\right)^2\frac{1-(-1)^n\cos(\Omega_{s,n}d/v_0)}{\Omega_{s,n}^2-\omega_n^2}.$$

$$\text{(7.4.26)}$$

Substituting the explicit expression for $\alpha_{s,n}$ we have

$$\overline{W} \equiv W \left(\frac{e^2}{4\pi\varepsilon_0 d} \right)^{-1}$$

$$= \sum_{s=1,n=0} \left(\frac{2p_s}{J_1(p_s)} \right)^2 \frac{1}{g_n} \times \frac{1}{\left[p_s^2 + (\pi nR / d\gamma)^2 \right]^2} \left[1 - (-1)^n \cos\left(\frac{\Omega_{s,n}}{v_0} d \right) \right] . (7.4.27)$$

In the Figure we illustrate two typical terms from the expression above as a function of the particle's momentum. The (normalized) energy stored at 10.7 GHz (corresponding to $s=1, n=1$) is shown in the left frame and we observe that for $\gamma\beta = 2.5$ the energy reaches its asymptotic value $[\overline{W}(s=1, n=1) \simeq 4]$. This is in contrast to the energy stored in the 35.5 GHz ($s=3, n=3$) wave which at the same momentum reaches virtually zero level; the asymptotic value $[\overline{W}(s=3, n=3) \simeq 0.5]$ is reached for a much higher momentum ($\gamma\beta = 15$).